

# **The Curing and Pressurisation Behaviour of Bone Cement During Acetabular Cup Implantation in Cemented Hip Replacements**

Alexander Thomas Boote

A thesis submitted for the degree of  
Doctor of Philosophy

Newcastle University, School of Engineering

September, 2021



## Abstract

Total hip replacement is the second most frequently performed arthroplasty surgery in the UK according to the National Joint Registry. It consists of resection of damaged bone and cartilage and implantation of an artificial acetabular cup and femoral head. These components are commonly fixed to the bone using polymethyl methacrylate (PMMA) bone cement which acts as a grout. A strong interface between the bone cement and bone relies on close mechanical interlocking. To achieve this, a load is applied to the cement to force it into the porous trabecular bone. The implant is then inserted into the pressurised cement and a load is applied to the acetabular cup until it is correctly positioned.

The work that follows in this thesis was based on the hypothesis that the pressure achieved during surgery at the bone cement-acetabulum interface is suboptimal and may contribute to the development of radiolucent lines and therefore, early loosening. It was also hypothesised that, as PMMA bone cement is a polymerising plastic, the application of deformation whilst it is setting may result in the generation of residual stresses, weakening the cement. The results confirmed the initial hypotheses and hence provided evidence for the requirement of a new surgical device. A new device was designed, manufactured, and tested. It was found that it performed better than the device currently in use. A patent has been filed and work is planned to further validate the novel cementing device.

## Acknowledgements

Firstly, I am grateful for the funding provided by the EPSRC and Zimmer Biomet which made this research possible. I would like to thank all my supervisors. The advice given by Robert Bigsby regarding the consideration that must be given to the commercial elements of total hip arthroplasty and the equipment facilitated through him from Zimmer Biomet was a great help. The clinical knowledge provided by Kenneth Rankin and David Deehan helped direct this research, ensuring its relevance in both a scientific and a clinical setting. David Swailes never failed to suggest potential improvements to the research which ultimately resulted in higher quality findings. Thank you to my primary supervisor, Philip Hyde, for providing me with this opportunity and for providing me with both the guidance and the trust to become an independent researcher. It has been a pleasure to discuss this work with you and I look forward to working with you in the future.

I have been a part of the family at Newcastle University for seven years now and it is difficult to separate my undergraduate degree and my PhD, so I want to thank the many wonderful people I have met during this time. Thank you to Adam Richardson, Mike Foster, Chris Brown, and Paul Scott for the assistance in the laboratory and for always been there for a cracking chat. Thank you to Stuart Baker and Shay Naylor for manufacturing the components used in this research. Thank you to all the lecturers who helped me become a proficient Biomechanical Engineer. Thank you to all my friends whom I met during my undergraduate, I am so lucky to have your continued support. Thank you to everyone whom I worked alongside during my PhD, your advice, wisdom, and friendship made anything seem achievable. Thank you, Kathryn Chamberlain who is an excellent guide, friend, and mentor. Thank you, Lewis Woollin, the parallels in our life were inexplicable and I was extremely lucky to have had you as a partner in my PhD journey. And thank you, Jake Sheriff; the coffee and rants kept me sane, especially in the last couple of years of my PhD. I know I can count on each of you any situation, and I am extremely grateful for that.

Thank you to Carlos Nisbet and Tom Patel for always listening to me ramble on about both my research and my woes. You always listened and provided valuable insights.

Thank you to my sister, for always believing in me; to my Dad, for never failing to answer honestly when I ask “why?”; and to Rosalie for supporting my throughout my PhD.

This thesis is dedicated to my Mum, Rosaleen Boote. I wouldn’t have been able to do this without the hundreds of hours you spent on the phone to me, assuring me that everything will work out. You are the reason for my optimism and determination. Thank you for your endless love and understanding.

# Contents

<b>Chapter 1. Background and Literature Review .....</b>	<b>1</b>
1.1 Introduction .....	1
1.2 The Natural Hip .....	2
1.2.1 Anatomy .....	2
1.2.2 Loading of the Natural Hip.....	3
1.3 Total Hip Replacement History .....	5
1.3.1 Pre-Charnley .....	5
1.3.2 Development of PMMA Bone Cement .....	6
1.3.3 Cementless Fixation .....	7
1.4 Joint Registries .....	8
1.4.1 Patient Age, Sex and Initial Diagnosis .....	8
1.4.2 Fixation Method and Bearing Material .....	9
1.4.3 Brand Combination .....	12
1.4.4 First Revision.....	13
1.4.5 Revision Components.....	14
1.4.6 Deficiencies .....	15
1.5 PMMA Bone Cement .....	16
1.5.1 Composition .....	16
1.5.2 Classification .....	16
1.5.3 Brands.....	17
1.5.4 Curing Characteristics .....	18
1.5.5 Residual Stress.....	24
1.5.6 Mechanical Properties .....	27

1.5.7 Allergies .....	30
1.5.8 Additives .....	30
1.6 Cemented Acetabular Arthroplasty .....	33
1.6.1 Bone Cement-Bone Interface .....	33
1.6.2 Surgical Preparation .....	37
1.6.3 Cement Mixing Techniques .....	40
1.6.4 Pressurisation .....	42
1.6.5 Acetabular Cup .....	49
1.7 Aims and Objectives .....	54
<b>Chapter 2. Rheological Characterisation of PMMA Bone Cements.....</b>	<b>55</b>
2.1 Introduction .....	55
2.2 Materials.....	58
2.3 Methods.....	59
2.4 Results.....	60
2.4.1 Viscosity – Brand.....	60
2.4.2 Viscosity – Temperature .....	61
2.4.3 Viscosity – Frequency.....	62
2.4.4 Phase Angle – Brand.....	63
2.4.5 Phase Angle – Temperature .....	64
2.4.6 Phase Angle – Frequency.....	65
2.4.7 Cement Curing Timings.....	66
2.4.8 Elastic Component of the Complex Modulus .....	66
2.5 Discussion .....	67
2.5.1 Viscosity .....	67
2.6 Phase Angle.....	69

2.6.2 Curing Times .....	71
2.6.3 Clinical Relevance and Other Thoughts .....	72
2.6.4 Future Work.....	72
2.7 Conclusions .....	73
<b>Chapter 3. Does Deformation During the Working Phase Significantly Weaken PMMA Bone Cement? .....</b>	<b>74</b>
3.1 Disclaimer.....	74
3.2 Introduction .....	74
3.2.1 Objectives .....	75
3.3 Materials .....	75
3.4 Methods .....	77
3.5 Results .....	79
3.5.1 Force-Stroke Plots .....	79
3.5.2 Porosity .....	80
3.5.3 Ultimate Tensile Strength.....	82
3.6 Discussion.....	83
3.6.1 Porosity .....	83
3.6.2 Ultimate Tensile Strength.....	84
3.6.3 Clinical Relevance and Other Thoughts.....	85
3.6.4 Future Work.....	85
3.7 Summary.....	86
<b>Chapter 4. Does Vacuum Mixing Affect Diameter Shrinkage of a PMMA Cement Mantle During <i>In Vitro</i> Cemented Acetabular Cup Implantation? .....</b>	<b>87</b>
4.1 Disclaimer.....	87
4.2 Introduction .....	87
4.2.1 Background and Motivation .....	87

4.2.2 Objectives .....	88
4.3 Materials.....	88
4.4 Methods.....	90
4.5 Results.....	94
4.6 Discussion .....	96
4.6.1 Clinical relevance.....	97
4.6.2 Study Limitations.....	97
4.6.3 Future Work .....	98
4.7 Summary .....	98

**Chapter 5. Does the Addition of a Flange to the Acetabular Cup Improve the Pressures Generated at the Acetabulum Surface During Mock Cemented Acetabular Cup Implantation? .....** 99

5.1 Disclaimer .....	99
5.2 Introduction .....	99
5.2.1 Background and Motivation .....	99
5.2.2 Objectives .....	100
5.3 Materials.....	100
5.4 Methods.....	102
5.5 Results.....	104
5.5.1 Pressurisation .....	106
5.5.2 Cup Insertion.....	107
5.6 Discussion .....	109
5.6.1 Pressurisation .....	110
5.6.2 Cup Insertion.....	111
5.6.3 Broader Context .....	113
5.6.4 Clinical relevance.....	114
5.6.5 Study Limitations.....	114

5.6.6 Future Work.....	115
5.7 Summary.....	115
<b>Chapter 6. Designing a Novel Pressuriser to Improve Cement Fixation .....</b>	<b>116</b>
6.1 Introduction .....	116
6.2 Motivation .....	116
6.3 Novel Pressuriser #1 .....	119
6.3.1 Material.....	120
6.3.2 Dimensions .....	121
6.3.3 Manufacturing .....	123
6.3.4 Preliminary Testing .....	124
6.4 Novel Pressuriser #2 .....	125
6.4.1 Dimensions .....	125
6.4.2 Preliminary Testing .....	126
6.5 Discussion.....	126
<b>Chapter 7. Does use of the Novel Acetabular Pressuriser Significantly Improve the Nature of the Pressures Generated at the Surface of a Mock Acetabulum During Pressurisation and the Acetabular Cup Implantation? .....</b>	<b>127</b>
7.1 Disclaimer.....	127
7.2 Introduction .....	127
7.2.1 Background and Motivation .....	127
7.2.2 Objectives .....	128
7.3 Materials .....	128
7.4 Methods <sup>249</sup> .....	131
7.5 Results .....	133
7.5.1 Pressurisation.....	134
7.5.2 Cup Insertion .....	136
7.6 Discussion.....	137

7.6.1 Pressure Magnitude.....	138
7.6.2 Pressure Change.....	138
7.6.3 Pressure Differential .....	140
7.6.4 Summary .....	140
7.6.5 Study Limitations.....	141
7.6.6 Clinical Relevance and Future Work .....	141
7.7 Summary .....	141
<b>Chapter 8. General Discussion and Conclusion .....</b>	<b>143</b>
8.1 Overview of Experiments .....	143
8.2 Summary .....	143
8.3 Key Results and Limitations .....	146
8.3.1 Chapter 2 – Rheological Characterisation of PMMA Bone Cements .....	147
8.3.2 Chapter 3 – Does Deformation During the Working Phase Significantly Weaken PMMA Bone Cement?.....	147
8.3.3 Chapter 4 – Does Vacuum Mixing Affect Diameter Shrinkage of a PMMA Cement Mantle During In Vitro Cemented Acetabular Cup Implantation?.....	148
8.3.4 Chapter 5 – Does the Addition of a Flange to the Acetabular Cup Improve the Pressures Generated at the Acetabulum Surface During Mock Cemented Acetabular Cup Implantation? .....	149
8.3.5 Chapter 7 – Does use of the Novel Acetabular Pressuriser Significantly Improve the Nature of the Pressures Generated at the Surface of a Mock Acetabulum During Pressurisation and the Acetabular Cup Implantation? .....	149
8.4 Conclusion .....	150
8.5 Further Work.....	152
<b>Chapter 9. References.....</b>	<b>154</b>

## List of Figures

Figure 1.1 Types of motion allowed by the hip joint .....	2
Figure 1.2 The bone and ligament structure of the natural hip.....	3
Figure 1.3 The anatomy of the upper leg and hip (left: posterior view, right: anterior) .....	3
Figure 1.4 From the NJR: Fixation by year of primary hip replacement. <sup>2</sup> .....	9
Figure 1.5 From the NJR: Cemented primary hip replacement bearing surface by year. <sup>2</sup> .....	10
Figure 1.6 From the NJR: KM estimates of cumulative revision in cemented primary hip replacements by bearing. Blue italics in the numbers at risk table signify that fewer than 250 cases remained at risk at these time points. <sup>2</sup> .....	12
Figure 1.7 From the NJR: KM estimates of cumulative re-revision by primary fixation in linked primary hip replacements. Blue italics in the numbers at risk table signify that fewer than 250 cases remained at risk at these time points. <sup>2</sup> .....	15
Figure 1.8 External Packaging of CMW 2 bone cement (DePuy). .....	17
Figure 1.9 External Packaging for Simplex P (Stryker). ....	18
Figure 1.10 External Packaging for Optipac 60 mixing system loaded with Refobacin R (Zimmer Biomet). ....	18
Figure 1.11 Basic geometries for a rotational rheometer: (left) concentric cylinder; (middle) cone and plate; (right) parallel plate. ....	21
Figure 1.12 Schematic of the divergence of zero-shear viscosity, $\eta_0$ , and equilibrium modulus, $Ge$ . The LST is marked by $p_c$ .....	23
Figure 1.13 Authors allergic reaction to bone cement.....	30
Figure 1.14 Acetabulum zones described by DeLee and Charnley. <sup>127, 129</sup> .....	34
Figure 1.15 The mechanism of late aseptic loosening of cemented acetabular components, showing the penetration of HDP progressing around the acetabular cup. <sup>140</sup> .....	36
Figure 1.16 Drawing showing use of the acetabular compactor designed by Oh <i>et al.</i> <sup>189</sup> .....	44
Figure 1.17 (left) Representation of the cement mantle produced by the DePuy T-handle pressuriser. (centre) Representation of the cement mantle produced by the Exeter pressuriser. (right) Representation of the cement mantle produced by the plunger T-handle pressuriser... <sup>45</sup>	45
Figure 1.18 (left) Insertion of the acetabular cup causes bone cement to be driven out of the acetabulum, around the cup margins. (right) Pressuriser seals acetabular margin and develops extrusion pressure in the cement. ....	46
Figure 1.19 Cross-sectional drawings of the new pressuriser (A) before and (B) after the advancement of the central plunger designed by Bernowski <i>et al.</i> <sup>193</sup> .....	47
Figure 1.20 Final design of the low-friction arthroplasty designed by Charnley showing the femoral stem and the acetabular cup. <sup>1</sup> .....	49

Figure 2.1 Various geometries available for rheological characterisation: (left) cup and bob configuration, (middle) cone and plate configuration, and (right) parallel plate configuration. <sup>76</sup>	58
Figure 2.2 Labelled image of the experimental set-up during one of the rheological tests....	59
Figure 2.3 Time-viscosity plot for each brand of cement at 23°C with a deformation rate of 1Hz. Three repeats were used for each testing condition. ....	61
Figure 2.4 Time-viscosity plot for each temperature using Simplex P with a deformation rate of 1Hz. Three repeats were used for each testing condition. ....	62
Figure 2.5 Time-viscosity plot for each frequency of deformation using Simplex P at a temperature of 23°C. Three repeats were used for each testing condition. ....	63
Figure 2.6 Time-tan( $\delta$ ) plot for each brand of cement at 23°C with a deformation rate of 1Hz. Three repeats were used for each testing condition. ....	64
Figure 2.7 Time-tan( $\delta$ ) plot for each temperature using Simplex P with a deformation rate of 1Hz. Three repeats were used for each testing condition. ....	65
Figure 2.8 Time-tan( $\delta$ ) for each frequency of deformation using Simplex P at a temperature of 23°C. Three repeats were used for each testing condition. ....	66
Figure 2.9 A graph showing the evolution and dependence of the elastic component of the complex modulus on the experiment temperature through time for Simplex P bone cement, deformed at 1Hz. Three repeats were used for each testing condition. ....	67
Figure 3.1 Optipac Cement Delivery System (Zimmer Biomet, Warsaw) .....	75
Figure 3.2 Simplex P Bone Cement packaging (Stryker, Michigan).....	76
Figure 3.3 Hivac bowl used for mixing the Simplex P bone cement (Summit Medical). ....	76
Figure 3.4 Technical drawings of the PE moulds used to produce the dog bone samples. ....	76
Figure 3.5 Universal tester fitted with centralised metal grips used to hold the bone cement specimens. ....	77
Figure 3.6 Failed specimens sectioned a few millimetres away from the fracture site for SEM analysis.....	77
Figure 3.7 A typical example of an SEM image taken at 1000X magnification of one of the pores present on the fracture surface of a failed dog bone sample. ....	79
Figure 3.8 Typical Force-Stroke plots for the test specimens. One sample showed slip in the centralised grips and the other did not. ....	80
Figure 3.9 Typical Force-Time plots for the test specimens. One sample showed slip in the centralised grips and the other did not. ....	80
Figure 3.10 Boxplots showing how deformation affects the porosity of each cement (D = deformed during curing, ND = no deformation during curing) The number of repeats for each test can be seen in Table 3.1. The bars indicate the maximum and minimum results, the box illustrates the interquartile range and the line within the box shows the mean. ....	81

Figure 3.11 Boxplots showing the porosity of Simplex P cements (V = vacuum mixed during curing, NV = not vacuum mixed during curing). The number of repeats for each test can be seen in Table 3.1. The bars indicate the maximum and minimum results, the box illustrates the interquartile range and the line within the box shows the mean. ....	81
Figure 3.12 Typical SEM images of the porosity at the fracture site for all cement samples. All images are given within the appendix (Appendix C). ....	82
Figure 3.13 Boxplots showing how deformation affects the UTS of each cement when they are vacuum mixed and non-vacuum mixed (D = deformed during curing, ND = no deformation during curing). The number of repeats for each test can be seen in Table 3.1. The bars indicate the maximum and minimum results, the box illustrates the interquartile range and the line within the box shows the mean. ....	83
Figure 3.14 Boxplots showing how the brand of cement affects the UTS of vacuum mixed cement (R = Refobacin R and S = Simplex P). The number of repeats for each test can be seen in Table 3.1. The bars indicate the maximum and minimum results, the box illustrates the interquartile range and the line within the box shows the mean. ....	83
Figure 4.1 Technical drawing of the model acetabulum used for cement pressurisation experiments (blanking bolts cover holes for a different experiment). ....	89
Figure 4.2 Technical drawing of the Depuy Smartseal Pressuriser used for cement pressurisation for all experiments. ....	89
Figure 4.3 Technical drawing of the flanged acetabular cup used for the experiments. ....	90
Figure 4.4 Mock acetabulum and Depuy pressuriser experimental set-up in the Shimadzu universal tester. ....	90
Figure 4.5 A 100 N force was applied to the Depuy Pressuriser with the bone cement sealed within the acetabulum model in the Shimadzu universal tester. ....	91
Figure 4.6 A 50 N force applied to the flanged acetabular cup in the Shimadzu universal tester. ....	92
Figure 4.7 Acetabular Zones as described by Delee and Charnley. <sup>127, 129</sup> ....	93
Figure 4.8 Boxplot displaying the significant difference in the external diameter due to the method of mixing. Five repeats were performed for each experiment. The bars indicate the maximum and minimum results, the box illustrates the interquartile range and the line within the box shows the mean. ....	94
Figure 4.9 Typical examples of SEM images taken to measure the bone cement porosity. The image on the left shows the vacuum mixed cement with minimal pores and the image on the right shows cement mixed by hand at atmospheric pressure with a significant number of pores. ....	95
Figure 5.1 Technical drawings with all relevant dimensions of the mock acetabulum (a) and the Depuy Smartseal pressuriser (b). ....	101
Figure 5.2. Technical drawings of a flanged (a) and unflanged (b) acetabular cup. ....	101

Figure 5.3 Mock acetabulum and Depuy pressuriser experimental set-up in the Shimadzu universal tester showing the sensor positions in relation to the rim and pole.....	102
Figure 5.4 A 100 N force was applied to the Depuy Pressuriser with the bone cement sealed within the acetabulum model in the Shimadzu universal tester.....	103
Figure 5.5 A 50 N force applied to the flanged acetabular cup in the Shimadzu universal tester. ....	104
Figure 5.6 A typical plot with an indication of how data is split up into fifths (pentiles) for further analysis.....	104
Figure 5.7. Four graphs showing examples of the pressure, temperature – time plot from each of the testing conditions. The pressure at various angles from the direction of forcing and the temperature through time are plotted. Pressurisation and cup insertion are indicated in (a) and are in similar positions in (b-d). The time and temperature of the cure point are also indicated. ....	105
Figure 5.8 QR code that contains a link ( <a href="https://youtu.be/dzs6CdNYWr0">youtu.be/dzs6CdNYWr0</a> ) to a YouTube video of an animated, annotated video of one of the experiments. Either scan QR code or enter URL to watch. ....	105
Figure 5.9 Boxplots of the average pressure for the unflanged, vacuum mixed condition. Each pair of boxplots represents the pressure at 0° and 75° for each pentile of cup insertion. Five repeats were performed for each testing condition. The bars indicate the maximum and minimum results, the box illustrates the interquartile range and the line within the box shows the mean. ....	109
Figure 5.10 A diagram showing that immediately upon insertion of the cup into the pressurised cement there will be a small contact area between them. This may result in a larger pressure generated at the pole of the acetabulum than at the rim.....	112
Figure 5.11 Reaction forces for a solid acetabular cement mantle according to Newton's third law. The normal (and measured) forces near the rim will be smaller than at the pole of the acetabulum if the cement behaves more like a solid.....	113
Figure 6.1 Graph showing how the brand of PMMA bone cement affects the value of $\tan(\delta)$ through time at 23°C with a frequency of deformation of 1 Hz. ....	117
Figure 6.2 Boxplots showing how deformation weakens PMMA bone cement for vacuum mixed Refobacin R and Simplex P and non-vacuum mixed Simplex P (ND = non-deformed, D = deformed). The number of repeats for each test can be seen in Table 3.1. The bars indicate the maximum and minimum results, the box illustrates the interquartile range and the line within the box shows the mean. ....	117
Figure 6.3 Typical example of a pressure-time plot when using a Depuy pressuriser and Simplex P bone cement to implant a flanged acetabular cup into a mock steel acetabulum. ....	118
Figure 6.4 The amount of pressure generated at the surface of the acetabulum is dependent upon how much of the cement and acetabular cup are in contact with each other. The indentation made in the cement after pressurisation with an improved novel pressuriser may result in a more uniform pressure across the acetabulum surface.....	118

Figure 6.5 Technical drawing of a Depuy acetabular pressuriser showing the single domed sealing surface. All values in mm.....119

Figure 6.6 A side by side comparison of a cross-section of the Depuy pressuriser and the novel pressuriser. A larger volume of cement is excavated at the pressurisation stage when using the novel pressuriser due to the excavating surface labelled in the diagram.....120

Figure 6.7 A number of bubbles can be seen on the backside of the novel pressuriser. As this is a non-functional surface it is not critical that it is free from imperfections. ....121

Figure 6.8 Technical drawing of the novel pressuriser, all values are in mm. Significant surfaces are labelled and discussed further below.....121

Figure 6.9 A diagram demonstrating two issues that arise when the offset between the sealing centroid and the excavating centroid is too large. The red hatched area indicates some of the excavating surface that is facing away from the acetabulum and the red solid area shows where some of the excavating surface overlaps with the acetabulum.....122

Figure 6.10 Technical drawing of the aluminium mould used to create the novel pressuriser, all values in mm. No dimensions for the internal cavity are given as it is simply the negative of the novel pressuriser. The bottom plate is on the left and the top plate on the right.....123

Figure 6.11 The first design of novel pressuriser with a smaller excavating surface of radius 25mm.....124

Figure 6.12 Wrinkles can be seen on the solidified acetabulum when the radius of the acetabular cup is larger than that of the excavating surface of the pressuriser.....125

Figure 6.13 A side-by-side comparison of the pressurisers with a radius smaller and larger than that of the acetabular cup to be inserted. The red arrows indicate the expected movement of cement upon implantation of the acetabular cup. With the smaller excavating radius, it is expected that the cement will crumple down towards the centre, this is evidenced by wrinkles seen on the cement mantle in figure 6.12. With a larger radius we expect the cement to move up and envelope the cup which is desirable. ....125

Figure 6.14 Technical drawing of the second iteration of novel pressuriser design, all values in mm.....126

Figure 7.1 Technical drawings with all relevant dimensions of the mock acetabulum. All dimensions are in mm.....129

Figure 7.2 Technical drawings of the Depuy pressuriser (right) and the novel pressuriser (left) with all relevant dimensions. All dimensions are in mm. ....129

Figure 7.3. Technical drawing of the flanged HXLPE acetabular cup. All measurements in mm. ....130

Figure 7.4 Mock acetabulum and Depuy pressuriser experimental set-up in the Shimadzu universal tester showing the sensor positions in relation to the rim and pole. ....131

Figure 7.5 A 100 N force was applied to the Depuy Pressuriser with the bone cement sealed within the acetabulum model in the Shimadzu universal tester. ....132

Figure 7.6 A force of 50 N is applied to the acetabular cup to force it into the bone cement in the Shimadzu universal tester.....	132
Figure 7.7 A typical plot with an indication of how data is split up into fifths (pentiles) for further analysis.....	133
Figure 7.8. Four graphs showing a typical example of the pressure, temperature – time plot from each of the testing conditions. The pressure at various angles from the direction of forcing and the temperature through time are plotted.....	134
Figure 7.9 The amount of pressure generated at the surface of the acetabulum is dependent upon how much of the cement and acetabular cup are in contact with each other. The impression made in the cement after pressurisation with the novel pressuriser may result in a larger, more uniform pressure across the acetabulum surface.....	138
Figure 7.10 A plot showing the full pressure and temperature - time plots even after the cure time. This shows how the solidification, and the subsequent heating and expansion of the mantle created unexpected pressure readings.....	139

## List of Tables

Table 1.1 From the NJR: KM estimates of cumulative revision (95% CI) by fixation and bearing, in primary hip replacements. Blue italics signify that fewer than 250 cases remained at risk at these time points and the number in brackets signifies the standard deviation. <sup>2</sup> .....	11
Table 1.2 From the NJR: KM estimates of cumulative revision (95% CI) of primary hip replacement by fixation, and stem/cup brand. Blue italics signify that fewer than 250 cases remained at risk at these time points and the number in brackets signifies the standard deviation. <sup>2</sup> .....	13
Table 2.1 Statistical results for each minute and each initial condition. A Y signifies that the brand of cement caused a significant difference in the viscosity. A * indicates that at least one of the data sets was not normal and therefore a Kruskal-Wallis test was used. Each statistical result used at least three measurements.....	60
Table 2.2 Statistical results detailing whether there is a significant difference in the viscosity due to the temperature of the experiment for each minute and each initial condition. A Y signifies that the temperature of the experiment caused a significant difference in the viscosity. A * indicates that at least one of the data sets was not normal and therefore a Kruskal-Wallis test was used. Each statistical result used at least three measurements.....	61
Table 2.3 Statistical results for each minute and each initial condition. A Y signifies that the frequency of deformation caused a significant difference in the viscosity. A * indicates that at least one of the data sets was not normal and therefore a Kruskal-Wallis test was used. Each statistical result used at least three measurements.....	62
Table 2.4 Statistical results for each minute and each initial condition. A Y signifies that the brand of cement caused a significant difference in $\tan(\delta)$ . A * indicates that at least one of the data sets was not normal and therefore a Kruskal-Wallis test was used. Each statistical result used at least three measurements.....	63
Table 2.5 Statistical results for each minute and each initial condition. A Y signifies that the temperature of the experiment caused a significant difference in $\tan(\delta)$ . A * indicates that at least one of the data sets was not normal and therefore a Kruskal-Wallis test was used. Each statistical result used at least three measurements.....	64
Table 2.6 Statistical results for each minute and each initial condition. A Y signifies that the frequency of deformation caused a significant difference in the $\tan(\delta)$ . A * indicates that at least one of the data sets was not normal and therefore a Kruskal-Wallis test was used. Each statistical result used at least three measurements.....	65
Table 2.7 The averages and means of the time till full cure for each temperature of experiment and each brand of cement. The frequency of deformation did not significantly affect the time till cure, this is due to the frequency sweep methodology. Each statistical result used at least three measurements. ....	66
Table 3.1 Number of samples tested per testing condition.....	78
Table 3.2. Pore number, porosity, force at failure and UTS of cement dog bone fracture samples. The number of repeats for each test can be seen in Table 3.1.....	82
Table 4.1 Results of bone cement mantle dimensions measured for vacuum mixed and hand mixed cements for a 52 mm mock acetabulum and 50 mm HXLPE cup. All mean values with	

+- standard deviations where appropriate, five repeats were performed for each experimental condition (student t-test as standard, \*for Mann-Whitney statistical tests)..... 95

Table 5.1 A table containing the average pressure and standard deviations in brackets for each testing condition, at each angle from the direction of loading, at each pentile during the pressurisation stage of the experiment. A \* indicates that the data set was non-normal. Five repeats were performed for each testing condition. .... 106

Table 5.2 A table containing statistical results comparing the pressures generated at the beginning of pressurisation to the pressures generate at the end. A \* indicates one or both sets of data being compared are non-normal. Five repeats were performed for each testing condition. .... 106

Table 5.3 A table containing the statistical results comparing the pressure at the pole of the acetabulum to the pressure at the rim during the pressurisation stage of cemented THA. Five repeats were performed for each testing condition. .... 107

Table 5.4 A table containing the average pressures and standard deviations in brackets for each testing condition, at each angle from the direction of loading at each pentile during the cup insertion phase of the experiment. Statistical differences between flanged and unflanged cups are indicated using [a]. A \* indicates that one or both data sets were non-normal. Five repeats were performed for each testing condition. .... 107

Table 5.5 A table containing the statistical results comparing the pressure at the beginning of cup insertion to the end of cup insertion. A \* indicates that one or both sets of data being compared are non-normal. Five repeats were performed for each testing condition..... 108

Table 5.6 A table containing the statistical results comparing the pressure at the pole of the mock acetabulum to the rim of the acetabulum at each pentile of cup insertion. A \* indicates that one or both sets of data being compared are non-normal. Five repeats were performed for each testing condition..... 108

Table 7.1 A table containing the average pressure and standard deviations in brackets for each testing condition, at each angle from the direction of loading, at each pentile during the pressurisation stage of the experiment. Statistical differences between the pressures generated due to which pressuriser was used are highlighted using [a]-[j] to indicate the relevant pair. A \* indicates that the data set was non-normal. Four repeats of each testing condition were performed. .... 134

Table 7.2 A table containing the statistical results comparing the pressure at the beginning of pressurisation to the end of pressurisation. A \* indicates that one or both sets of data being compared are non-normal. Four repeats of each testing condition were performed..... 135

Table 7.3 A table containing the statistical results comparing the pressure at the pole of the mock acetabulum to the rim of the acetabulum at each pentile of pressurisation. A \* indicates that one or both sets of data being compared are non-normal. Four repeats of each testing condition were performed. .... 135

Table 7.4 A table containing the average pressure and standard deviations in brackets for each testing condition, at each angle from the direction of loading, at each pentile during the cup insertion stage of the experiment. Statistical differences due to which pressuriser was used are highlighted using [a]-[c], indicating the relevant pair. A \* indicates that one or both data sets were non-normal. Four repeats of each testing condition were performed. .... 136

Table 7.5 A table containing the statistical results comparing the pressure at the beginning of cup insertion to the end of cup insertion. A \* indicates that one or both sets of data being compared are non-normal. Four repeats of each testing condition were performed. .... 137

Table 7.6 A table containing the statistical results comparing the pressure at the pole of the mock acetabulum to the rim of the acetabulum at each pentile of cup insertion. A \* indicates that one or both sets of data being compared are non-normal. Four repeats of each testing condition were performed..... 137

## Nomenclature

Term/Initialisation	Description/Definition
<b>Acetabular</b>	Relating to the Acetabulum, usually in reference to the cup shaped implant.
<b>Acetabulum</b>	The socket of the hip joint.
<b>Aseptic Loosening</b>	Loosening of an implant with no sign of infection, usually a result of osteolysis.
<b>ASTM</b>	American Society for Testing and Materials, an international standards organisation.
<b>Back Bleeding</b>	Bleeding in the pelvis that occurs after cementation which can result in the forcing of cement out of trabecular pores.
<b>Bone Cement-Bone Interface</b>	The interface between the cement and the bone which is created after implantation of prosthesis into a patient using cement.
<b>Bone Cement-Implant Interface</b>	The interface between the cement and the implant which is created after implantation of a prosthesis into a patient using cement.
<b>Bottoming out</b>	Term used for when an acetabular cup is inserted too far into PMMA cement and the pole (bottom) of the cup contacts the bone.
<b>BPO</b>	Benzoyl Peroxide, added to powdered PMMA as an initiator.
<b>Butterworth Filter</b>	A low pass filter with a flat pass band, ideal for the removal of noise from electrical signal.
<b>Cement Mantle</b>	The shape of hardened PMMA bone cement resulting from the implantation of a prosthesis.
<b>CMM</b>	Coordinate Measuring Machine. Used for the precise plotting of 3D coordinates.
<b>CoC</b>	Ceramic on Ceramic implant material combination.
<b>CoP</b>	Ceramic on Polymer implant material combination.
<b>CSA</b>	Cross Sectional Area.

<b>Cup Insertion</b>	The phase of total hip arthroplasty which involves the insertion of the acetabular cup into cement.
<b>Cure Time</b>	The time defined in the international standards as when the temperature of the curing PMMA bone cement is halfway between the maximum and the ambient temperature.
<b>Curing</b>	The process of PMMA bone cement polymerisation and eventual solidification.
<b>DMpT</b>	Dimethyl-p-toluidine, reduces the required energy for polymerisation reactions.
<b>Dog Bone Samples</b>	Testing samples shaped as dog bones usually used for mechanical testing.
<b>Dough Time</b>	The time defined in the standards as when PMMA bone cement no longer adheres to an unpowdered latex surgical glove.
<b>Elastic Component</b>	The elastic component of the complex modulus measured during rheological characterisation. Often used to determine how solid-like a material is. Sometimes referred to as the storage modulus.
<b>Equilibrium Modulus</b>	The parameter that determines how much of an applied strain will result in an indefinite stress.
<b>F</b>	Force.
<b>FEA</b>	Finite Element Analysis.
<b>Femur</b>	The bone that constitutes the upper leg, the head of which is the ball in the hip joint.
<b>Flanging Out</b>	Term used for when an acetabular cup is inserted too far into PMMA bone cement and the flange of the cup contacts the bone.
<b>Full Cure</b>	Rigidification, solidification, hardening of the PMMA bone cement.
<b>G'-G'' cross over</b>	The moment that the elastic modulus becomes as large as the viscous component during a polymerisation reaction. Also, can be seen as when $\tan(\delta) = 1$ .
<b>Hand Mixing</b>	Sometimes represented as NV or non-vacuumed. When the cement is mixed using a spatula in a bowl at atmospheric pressure.

<b>HXLPE</b>	Highly Cross-Linked Polyethylene.
<i>in vitro</i>	Within glass.
<i>in vivo</i>	Within the living.
<b>Interdigitation</b>	The penetration of digits of cement into the porous cancellous bone.
<b>Interstice</b>	A gap between two surfaces.
<b>ISO</b>	International Standardisation Organisation.
<b>KM Estimate</b>	Kaplan-Meier estimate, a calculation of the likelihood of survival which considers the measurements that have dropped out of the population.
<b>LST</b>	The Liquid-Solid Transition; used in this context as the moment that a curing material can store stresses indefinitely. May also be referred to as the moment of gelation.
<b>Mixing Phase</b>	The phase defined by a manufacturer when the powdered and liquid elements of PMMA bone cement are mixed.
<b>MMA</b>	Methyl Methacrylate.
<b>MoM</b>	Metal on Metal bearing combination.
<b>Moment of Gelation</b>	The moment that a curing material can store stresses indefinitely through the development of an equilibrium modulus.
<b>MoP</b>	Metal on Polymer bearing combination.
<b>MRSA</b>	Methicillin-Resistant Staphylococcus Aureus, a bacterium that is resistant to several commonly used antibiotics.
<b>MRSE</b>	Methicillin-Resistant Staphylococcus epidermidis, a bacterium that is resistant to several commonly used antibiotics.
<b>MWCNT</b>	Medium Weight Carbon Nanotubes
<b>ND</b>	PMMA bone cement that was not deformed during the waiting phase.
<b>Necrosis</b>	Death of body tissue.

<b>NJR</b>	National Joint Registry. Referring directly to the organisation set-up to collect information regarding joint replacements in the UK.
<b>Nyquist Criterion</b>	Criterion for selection of a frequency that is used in data filtering techniques. It is defined as half the sampling rate of the data being recorded.
<b>Osteolysis</b>	The breakdown of bone.
<b>Pa</b>	Pascals, a measurement of pressure defined as 1N/1m.
<b>PE</b>	Polyethylene.
<b>Pentile</b>	A fifth of the total duration of a phase.
<b>Phase Angle</b>	The angle that describes the lag of a response to an input. Used in the context of rheological characterisation: 0° means perfectly in sync and 90° means completely out of sync.
<b>PMMA</b>	Polymethyl Methacrylate.
<b>Polymerisation</b>	The chemical reaction which involves the addition of monomers to a long chain of other similar units.
<b>Porosity</b>	Defined as the total area or volume of pores divided by the total area or volume of the entire object. It may be represented as a fraction or a percentage.
<b>Pressure Change</b>	The change in pressure from the start to the end of a particular phase.
<b>Pressure Differential</b>	The difference in pressure from one location to another, usually the pole and the rim of the acetabulum.
<b>Pressurisation</b>	The phase of total hip arthroplasty which involves the pressurisation of cement in the body.
<b>Pressuriser</b>	The surgical device used to pressurise PMMA bone cement into the body, usually referring to the acetabular pressuriser.
<b>Primary Implant</b>	The prosthesis that is initially implanted into the body at primary surgery.
<b>PTFE</b>	Polytetrafluoroethylene.

<b>Radiographs</b>	Images captured using x-rays.
<b>Reaming</b>	The removal of bone and soft tissue using a reamer.
<b>Revision Implant</b>	The prosthesis that is implanted into the body to replace the primary implant at revision surgery.
<b>Rheology</b>	The science of the deformation of material.
<b>RLL</b>	Radio Lucent Line. Appears on radiographs as a darker area between the opaque cement mantle, bone or prosthesis.
<b>SA:V</b>	Surface area to volume ratio.
<b>SEM</b>	Scanning Electron Microscope/Microscopy. A Hitachi TM3030 was used in this project.
<b>Setting Phase</b>	The phase of PMMA bone cement curing after the working phase and before the cement is completely solidified.
<b>Setting Time</b>	The time defined in the standards when the cement reaches a temperature halfway between the ambient and the maximum temperature.
<b>Shear Thinning</b>	The phenomena where an increase in the rate of deformation results in a reduction in the viscosity of a fluid.
<b>Stress Locking</b>	The moment referred to arbitrarily in the literature where stresses can no longer relax. Similar to the moment of gelation or liquid solid transition.
<b>Stretch Pouring</b>	The process where a viscous liquid with a significant amount trapped air within is poured from a height through a thin stream so that the air will be released.
<b><math>\tan(\delta)</math></b>	The tangent of the phase angle, frequently used to examine the moment of gelation and the relationship between viscous and elastic components of the complex modulus.
<b>THA</b>	Total Hip Arthroplasty.
<b>THR</b>	Total Hip Replacement.
<b>UHMWPE</b>	Ultra-High Molecular Weight Polyethylene.
<b>Universal Tester</b>	Shimadzu AGS-X, used to apply a load or a strain to testing samples.

<b>UTS</b>	Ultimate Tensile Strength.
<b>V</b>	Vacuum Mixed Cement.
<b>Vacuum Mixing</b>	The PMMA bone cement is mixed under a partial vacuum, usually around 0.4 bar (absolute). Used to minimise the entrapment of air into the cement.
<b>Viscosity</b>	A measure of a materials resistance to flow.
<b>Viscous Component</b>	The viscous component of the complex modulus measured during rheological characterisation. Often used to determine how liquid-like a material is. Sometimes referred to as the loss modulus.
<b>Waiting Phase</b>	A phase defined by the manufacturer. Occurs between the end of the mixing phase and the dough time.
<b>Working Phase</b>	A phase defined by the manufacturer. Occurs between the dough time and the start of the setting phase.
<b>NV</b>	Non-vacuum mixed cement. See hand mixed cement.



# Chapter 1. Background and Literature Review

## 1.1 Introduction

Total hip arthroplasty (THA) involves the resection and reconstruction of the natural hip joint. It is frequently performed on elderly patients who suffer from severe arthritis, it is also increasingly being performed on younger patients who wish to continue an active lifestyle and participate in sports.<sup>1</sup> This is possible due to the incremental improvements made in the field over the last 60 years. As less destructive techniques and implants are developed, the risk of revision is decreased as is the risk of re-revision.<sup>2</sup> Despite this, a significant number of implants still fail, many fail due to aseptic loosening of the cup.<sup>2,3</sup> The cement-bone interface is the focus of this thesis. This literature review will primarily focus on PMMA bone cement, the filling agent used to secure the implant to the bone, and the many factors and variables that influence the longevity of the interface created between the cement and the bone after implantation of the acetabular cup, namely: thermal necrosis,<sup>4-12</sup> chemical necrosis,<sup>10, 11, 13, 14</sup> fluid imposition,<sup>15-19</sup> and cement shrinkage.<sup>6, 9-11, 20, 21</sup>

The key takeaways from this review are the sensitivity of PMMA bone cement to control variables, the poor quality of the studies relating to the pressure generated at the acetabulum bone interface due to a lack of published data and minimal control of variables, and the lack of detail in the publications produced by the National Joint Registry (NJR) with regards to the surgical equipment and brand of cement used.

## 1.2 The Natural Hip

The natural hip joint is a ball (femoral head) and socket (acetabulum) type joint. This joint allows flexion, extension, adduction, abduction and medial and lateral rotation of the femur in relation to the pelvis (Figure 1.1).

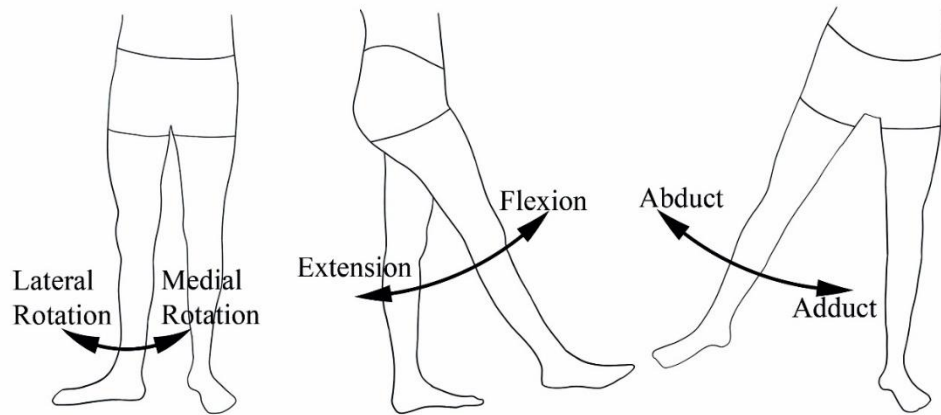


**Figure 1.1** Types of motion allowed by the hip joint.

### 1.2.1 Anatomy

The structure of the hip can be seen below (Figure 1.2). The femoral head is connected to the acetabulum by a ligament on the head of the femur. This ligament is connected to the transverse acetabular ligament which allows rotation of the femur inside the acetabulum fossa. The head of the femur and the lunate acetabulum surface is covered in cartilage which reduces the friction between the bones. The whole joint is encapsulated in ligaments: the iliofemoral and the ischiofemoral ligament, this forms a joint capsule that contains synovial fluid which lubricates the joint, reducing the friction in the joint.<sup>22</sup>

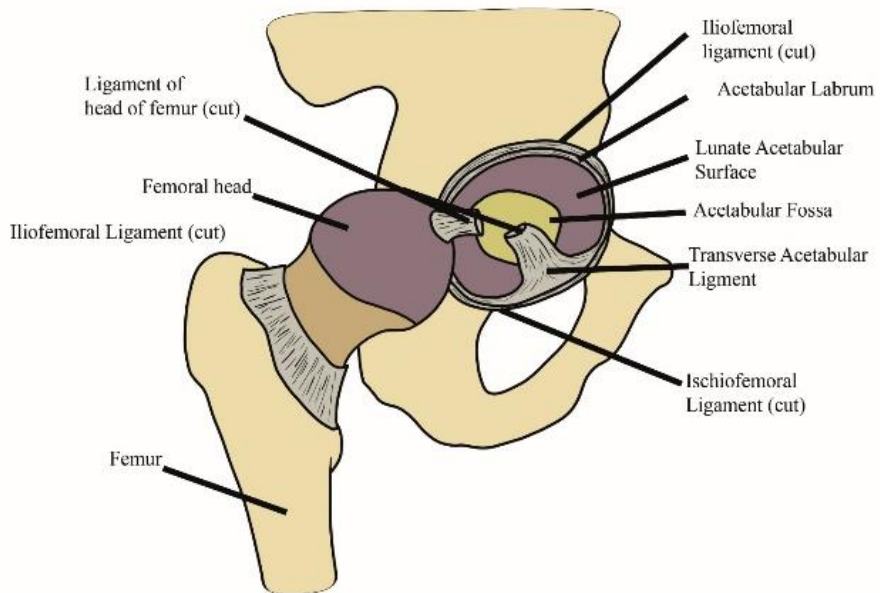


**Figure 1.2** The bone and ligament structure of the natural hip.

A simplified diagram of the muscles that stabilise or control movement of the hip joint can be seen below (Figure 1.3).

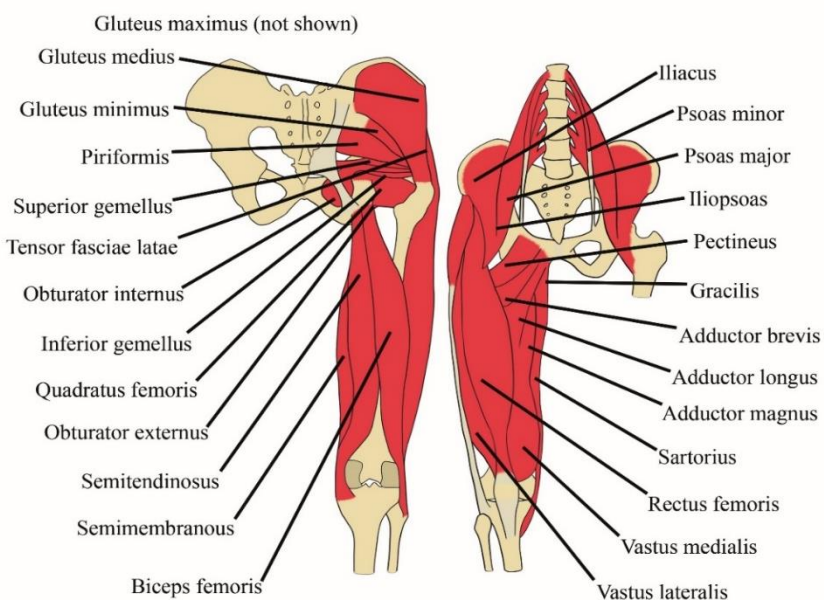


**Figure 1.3** The anatomy of the upper leg and hip (left: posterior view, right: anterior)

The muscles of the hip can be broken down into three main categories: the gluteal muscles, the inner hip muscles, and the thigh muscles.<sup>22</sup>

### 1.2.2 Loading of the Natural Hip

The loads transferred between the femur and the acetabulum are very large thus when artificial components are implanted these will also be under a large amount of stress.

In 1966, J. P. Paul emphasised that any device that is implanted must be strong enough to withstand these forces and also that degenerative changes in the function of a joint are likely caused by an abnormal incident or through repeated use at normal high loads.<sup>23 24</sup>

J. P. Paul measured the contact force between a subject's foot and the ground. He found that there were two peaks: one at the heel strike and one when the opposing foot was removed from the ground. The peak value of joint force for the hip was on average 3.9x bodyweight.<sup>23</sup>

Bergmann *et al.* reported the forces present in the hip during common activities such as walking (at various speeds), navigating stairs, sitting down and standing up, standing on each leg individually and when the knee is bent.<sup>25</sup> They measured the peak hip contact force and torsional implant moment, both reported as a percentage of bodyweight.

They found that the inter-individual variation between patients was large. The largest forces seen were during stair climbing (251% BW) and descending (<260% BW).

## 1.3 Total Hip Replacement History

The following section will give a brief, summarised history of the development of total hip replacement (THR) with a particular focus on bone cement.

### 1.3.1 Pre-Charnley

The intention of THA is to reduce pain, increase mobility and prevent catastrophic failure of damaged and diseased hip joints. In 1992, Coventry observed that the THA may be the “Operation of the Century” with other authors echoing this sentiment.<sup>26, 27</sup> This is a remarkable achievement considering a fact that Smith-Petersen phrased well: “The hip joint is a fulcrum exposed to the leverage of the strongest muscles in the body and to the trauma of weight bearing.”<sup>26, 28</sup>

The first attempt at THA was performed by Professor Themistocles Glück in Germany, 1891. He used ivory to replace the femoral heads of tuberculosis patients.<sup>29</sup> Unfortunately, despite publishing details on five implants from other joints he did not report the outcomes of the hip implant.<sup>30</sup> Smith-Petersen introduced his design of THA by criticising previous attempts of interposing skin and pig bladder submucosa between the femoral head and the acetabulum to recreate a hip joint. These achieved limited success due to three main reasons: patients commonly went into shock before the joint was exposed; secondly, the joint was defective due to a lack of proper instruments; finally, the interposed tissue would perish. In 1923, his solution was to use a glass mould to “guide nature’s repair”. Many moulds shattered due to the large forces present at the hip joint and fell out of favour.<sup>28</sup> In 1938, Wiles attempted to replace the femoral head and acetabulum with stainless steel components fixed to the bone using screws.<sup>26, 31, 32</sup> Although this innovation also resulted in unsatisfactory results, it set a precedent for future designs of THRs.

In 1961 John Charnley presented a new technique for hip arthroplasty. He wrote that work performed by Smith-Petersen and by Judet influenced his design. He discusses that the Smith-Petersen design could never be considered a mechanically stable ball and socket design as the metal hemisphere wasn’t fixed. The Judet system called “resection-reconstruction”, consisted of removing the femoral head and replacing it with a mushroom-shaped piece of methyl polymethyl methacrylate. Charnley comments that this is a more stable design as the components are fixed to the bone. He says that the observation of squeaking of the Judet design started his research. Squeaking is a result of friction between two surfaces, causing wear and eventual loosening of the femoral component which was only secured by a metal spike.<sup>1</sup>

His research into lubrication and frictional coefficients resulted in him using polytetra fluoroethylene for both components (PTFE). Initially, he lined the femoral head with PTFE and manufactured the acetabular cup from it, but necrosis of the femoral bone meant that the femoral component had to be replaced. He used a metallic prosthesis which was cemented into the femur so that the cement would “transfer the weight of the body from the metallic stem of the prosthesis uniformly to the cancellous bone of the interior of the neck and the upper end of the femur.”<sup>1, 33</sup> The extremely high wear rates of PTFE led to an immune reaction from the body leading to failure of the joint.<sup>34</sup> Charnley’s engineering associate, Harry Craven, had been experimenting with ultra-high molecular weight polyethylene (UHMWPE) and had found that

it had a very low wear rate and thus it became the material of choice for the acetabular cup.<sup>35</sup> The principles of this design still largely remain; low friction between articulating surfaces and a high area of contact between prosthesis and bone to ensure satisfactory transfer of forces.

### ***1.3.2 Development of PMMA Bone Cement***

At the start of the 20<sup>th</sup> century, Otto Röhm completed his thesis: “On the polymerization products of acrylic acid”. In 1907, based on this research, he started a company called Röhm & Haas and later developed a process for developing methyl methacrylate (MMA) on an industrial scale. In 1935 Bauer patented a process to develop dentures. Addition of BPO (Benzoyl Peroxide) as an initiator, the discovery that mixing ground PMMA with the MMA monomer created a pliable dough, and would improve the handling properties of the curing dough, led to the wide adoption of acrylic resins in cranioplasty and denture by the 1940s. However, a temperature of near 100°C was needed to cure the resin.<sup>36, 37</sup>

It was discovered that adding a co-initiator would mean the cement could be hardened at room temperature. The companies Degussa and Kulzer developed the first cement that would be the blueprint for all future cements in Paladure. Paladure contained dimethyl-p-toluidine (DMpT). This information was then made widely known after the end of World War two and several companies went on to develop their own mixtures for PMMA bone cement. Kuhn and D.C. Smith give a detailed history for CMW, Simplex P and Palacos R.<sup>36, 37</sup>

#### ***1.3.2.1 CMW Bone Cement***

Whilst setting, the pliable dough could be moulded to the intricate geometry of exposed trabecular in the femoral canal. Charnley used Nu-Life to secure femoral implants to broken femurs. In 1960 he stated that it was a grouting effect of the cement that fixes it to the bone.<sup>38</sup> This meant that pressurisation of the cement into the bone was crucial for securing fixation.<sup>36, 37</sup>

Charnley approached the Dental Manufacturing Company with several suggestions as to how they could improve Nu-Life for use as an implant bonding material. He worked directly with CMW Laboratories Ltd. to make these changes the key one being the addition of barium sulphate so that the cement would be radiopaque, making observations of the cement mantle on radiographs possible.<sup>39</sup>

#### ***1.3.2.2 Simplex P***

Simplex had been used for cranioplasty operations for years before being employed as a material for the fixation of implants to bone. Simplex Pentocryl, manufactured by Dental Filling Ltd., was recommended for use in arthroplasty and cranioplasty.

In 1962, a new MMA homopolymer was developed and BPO was encapsulated into the beads of the PMMA powder, which was then irradiated. Simplex has not changed much since its conception. Antibiotics have been added and other formulations have been developed but they stem from the same base.<sup>39</sup>

### ***1.3.2.3 Palacos R***

Paladon was a hot-cure plastic that was used for dental prosthetics and produced by Heraeus. Dr. Diener developed a faster curing Palacos R which contained zirconium dioxide so the bone cement would be visible on radiographs. This cement was recommended for covering skull defects and for bone surgery. Ethylene oxide was used for sterilisation as it would not change the nature of the cement.<sup>39</sup>

### ***1.3.3 Cementless Fixation***

Some of the earliest designs of cemented THR had high rates of failure and many observers claimed that cement was the cause of failure. Loosening was called “cement disease”.<sup>40</sup> These claims inspired designs that discarded cement entirely and achieved fixation using screws or other forms of mechanical fixation. These new designs had significantly worse outcomes than cemented hips. In the 80s, innovations saw the development of a material that would allow bone ingrowth, when applied to the surfaces of the femoral stem and acetabular cup bone could grow onto, or into the implant itself achieving some longevity similar to cemented hips.<sup>41</sup>

## 1.4 Joint Registries

Joint registries are an excellent tool for determination of which surgical techniques and devices, implants, and surgeons offer the best longevity for THRs. Long term follow-up studies are useful for identifying a successful innovation but can be too slow and limited in the control variables. A sufficiently detailed joint registry is the best tool for observing the long-term impact of innovations. The problem with many current joint registries is the lack of details provided in the annual reports. This thesis concentrates on PMMA bone cement, unless there is a specific study focusing on cementing techniques commissioned by the registry these properties are often not mentioned in the annual reports despite information on the cement used being collected at the time of surgery (Chapter 9.Appendix A). Bone cement is incredibly complex and improving one property may be detrimental to another, so long-term data regarding repercussions of changes are vital.

Several commonly referenced registries have been omitted due to limited use of cemented acetabular components or lack of recent publications: these include the American Joint Replacement Registry (AJRR), the Australian Orthopaedic Association National Joint Replacement Registry (AOANJRR) and the Swedish Hip Arthroplasty Register (SHAR). The NJR which covers England, Wales and Northern Island was considered the best registry for the focus of this literature review.<sup>2</sup>

The 17<sup>th</sup> NJR annual report, published in 2020, contains 1,191,253 records of hip arthroplasties from England, Wales, Northern Ireland, and the Isle of Man. Reports of follow-ups over 15 or 16 years after implantation are reported.

The primary measure of survivorship analysis, or implant longevity, used in the NJR, as well as most other registries, is called a Kaplan-Meier estimate. This value makes estimates of survival whilst considering when a patient is censored, which could happen for any number of reasons (lost to follow-up, death etc.). It is an estimate as it makes assumptions as to what would happen to the patient if they did not fall out of the study. It is essentially a survival function which in the case of joint arthroplasties is often inverted to give estimates of the percent of implants that fail.

As this thesis is focused on cemented acetabular components, the data for cemented THRs will be examined in more detail.

### 1.4.1 Patient Age, Sex and Initial Diagnosis

In the NJR, the mean age for a primary THR was  $68.1 \text{ years} \pm 11.4 \text{ years}$ . The median age was higher at 69 years with an interquartile range of 61-76 years. More interesting is the discrepancy in the mean age between methods of fixation. Resurfacing surgery was performed on the youngest patients at  $53.9 \text{ years} \pm 9.1 \text{ years}$ ; this is to preserve acetabular bone stock in young patients as revision of the component is likely,<sup>42</sup> reverse hybrid and hybrid hips were implanted at similar ages:  $69.7 \text{ years} \pm 9.8 \text{ years}$  and  $69.1 \text{ years} \pm 10.9 \text{ years}$  respectively. Most notable is the difference in the mean age of implantation for uncemented and cemented hips:  $64.4 \text{ years} \pm 11.3 \text{ years}$  and  $73.0 \text{ years} \pm 9.1 \text{ years}$ , respectively. This is expected as uncemented hips

preserve more bone stock than cemented hips and are therefore purported to be better for revision surgery.

A larger proportion of hip surgeries were performed on women with 40.1% of all patients being male. Men also received less cemented and more uncemented implants at 33.5% and 44.7% respectively.

Osteoarthritis was given as the reason for THRs in 91.5% of surgeries.

#### 1.4.2 Fixation Method and Bearing Material

There are currently five primary methods of fixation. These include cemented, uncemented, hybrid (where the femoral component is cemented and the acetabular component is uncemented), reverse hybrid (reverse of the methods of hybrid fixation for each component) and resurfacing. Of hips that were replaced in 2019, uncemented fixation is the most popular method of fixation according to the NJR, 34.9 % being fixed with this method but the proportion is decreasing each year. The second most popular is hybrid fixation with 34.7 % and is increasing in popularity. The third most prevalent is cemented fixation with 26.0 %. Reverse hybrid, resurfacing and “Unsure” have popularities of 2.3 %, 0.6% and 1.4 % respectively (Figure 1.4).

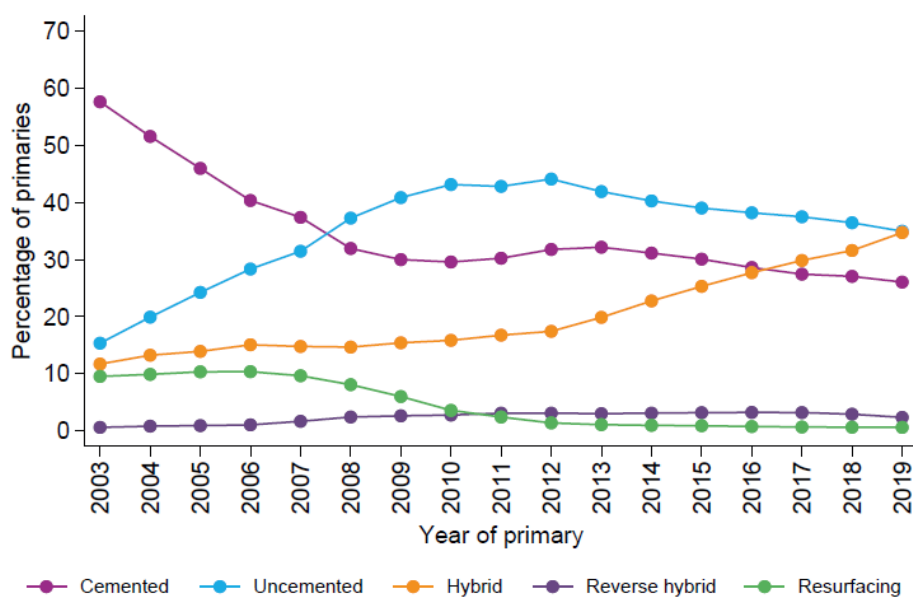


**Figure 1.4** From the NJR: Fixation by year of primary hip replacement.<sup>2</sup>

In 2004, 94.2 % of cemented total hip arthroplasties used metal on polymer (MoP) implants; 5.60 % used ceramic on polymer (CoP) and 0.19 % used metal on metal (MoM). As of 2019, 78.8 % used MoP implants and 20 % used CoP and less than 0.1 % used MoM implants (Figure 1.5). The cessation of MoM implant is due to the adverse effects metallic debris has on the surrounding tissue. The CoP hips were given to the youngest patients with a mean age of 64.5 years  $\pm$  10.4 years.

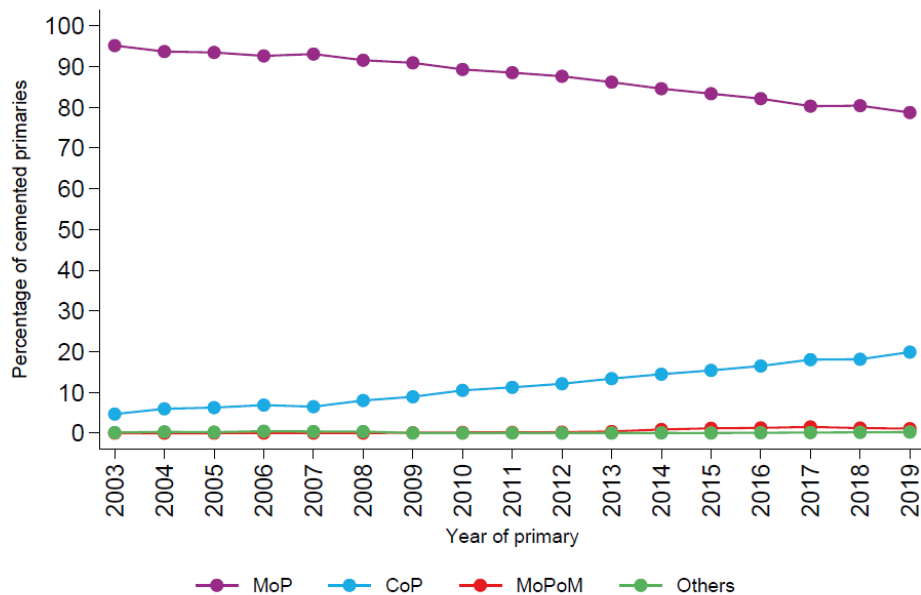


**Figure 1.5** From the NJR: Cemented primary hip replacement bearing surface by year.<sup>2</sup>

Cost and likelihood of revision are the main driving forces behind material selection for cemented THA's as the patients are older.

For all bearing material combinations, Cemented THA's have the best longevity at all time points after surgery. At 1-year post-operation, the KM estimate for cumulative revision for all cemented hips is 0.56, for uncemented hips, it is 0.97. At 15 years post-op cemented implants have a KM estimate for cumulative revision of 5.46, uncemented implants have an equivalent figure of 8.75. Cemented CoP hips have the best KM estimate for cumulative revision rate for the first 10 years post-op for all fixation and material combinations with a significant number of data points. However, hybrid Ceramic-on-Ceramic (CoC) and CoP hips have the best longevity at 15 years (Table 1.1).

**Table 1.1** From the NJR: KM estimates of cumulative revision (95% CI) by fixation and bearing, in primary hip replacements. Blue italics signify that fewer than 250 cases remained at risk at these time points and the number in brackets signifies the standard deviation.<sup>2</sup>

Fixation	Bearing surface	N	Time since primary					
			1 year	3 years	5 years	10 years	13 years	15 years
All cases*		1,191,253	0.81 (0.79-0.83)	1.52 (1.50-1.55)	2.24 (2.21-2.27)	4.56 (4.51-4.62)	6.30 (6.22-6.39)	7.53 (7.40-7.67)
All cemented		378,279	0.56 (0.53-0.58)	1.10 (1.07-1.14)	1.54 (1.50-1.59)	3.01 (2.93-3.09)	4.45 (4.32-4.58)	5.46 (5.27-5.66)
Cemented and	MoP	328,507	0.56 (0.54-0.59)	1.11 (1.07-1.15)	1.56 (1.51-1.61)	3.06 (2.98-3.14)	4.50 (4.37-4.64)	5.51 (5.31-5.72)
	MoM	411	0.74 (0.24-2.27)	1.79 (0.86-3.72)	2.62 (1.42-4.83)	5.94 (3.86-9.10)	8.26 (5.57-12.17)	11.13 (6.23-19.45)
	CoP	46,957	0.49 (0.43-0.56)	0.98 (0.89-1.08)	1.38 (1.26-1.50)	2.42 (2.21-2.65)	3.76 (3.38-4.19)	4.85 (4.22-5.58)
	MoPoM	2,197	1.27 (0.86-1.86)	1.98 (1.43-2.73)	2.75 (1.95-3.89)	3.93 (2.37-6.49)		
	Others	207**	1.10 (0.27-4.37)	1.10 (0.27-4.37)	1.10 (0.27-4.37)			
All uncemented		444,739	0.97 (0.94-1.00)	1.80 (1.76-1.84)	2.66 (2.61-2.71)	5.52 (5.42-5.62)	7.50 (7.33-7.67)	8.75 (8.49-9.01)
Uncemented and	MoP	173,611	1.04 (0.99-1.09)	1.68 (1.62-1.74)	2.13 (2.06-2.21)	3.82 (3.68-3.96)	5.48 (5.22-5.74)	6.64 (6.22-7.08)
	MoM	29,029	1.06 (0.95-1.18)	3.49 (3.28-3.71)	7.72 (7.41-8.03)	17.75 (17.30-18.22)	21.41 (20.86-21.97)	23.24 (22.49-24.02)
	CoP	108,161	0.83 (0.78-0.89)	1.41 (1.33-1.49)	1.84 (1.74-1.93)	3.07 (2.90-3.26)	3.95 (3.68-4.24)	5.01 (4.56-5.51)
	CoC	130,627	0.96 (0.91-1.01)	1.78 (1.71-1.85)	2.32 (2.24-2.41)	3.61 (3.48-3.74)	4.69 (4.46-4.94)	5.89 (5.24-6.17)
	CoM	2,152	0.56 (0.32-0.98)	2.75 (2.13-3.55)	4.81 (3.97-5.82)	7.95 (6.83-9.25)		
	MoPoM	724	1.88 (1.09-3.21)	2.75 (1.70-4.43)	2.75 (1.70-4.43)			
	CoPoM	319	1.34 (0.50-3.53)	2.67 (0.90-7.81)	2.67 (0.90-7.81)			
	Others	116**	3.45 (1.31-8.93)	7.15 (3.64-13.82)	8.32 (4.39-15.44)	19.33 (11.46-31.54)		
All hybrid		261,765	0.79 (0.76-0.83)	1.32 (1.27-1.37)	1.82 (1.76-1.88)	3.38 (3.27-3.50)	4.57 (4.39-4.75)	5.65 (5.34-5.99)
Hybrid and	MoP	149,561	0.84 (0.79-0.88)	1.36 (1.30-1.43)	1.83 (1.75-1.91)	3.22 (3.08-3.37)	4.35 (4.13-4.58)	5.44 (5.05-5.87)
	MoM	2,733	0.85 (0.56-1.27)	2.70 (2.14-3.41)	5.90 (5.03-6.93)	16.21 (14.71-17.84)	19.55 (17.83-21.42)	22.38 (20.07-24.91)
	CoP	79,343	0.75 (0.69-0.82)	1.21 (1.13-1.30)	1.56 (1.45-1.67)	2.48 (2.25-2.73)	3.44 (2.97-3.98)	4.68 (3.80-5.76)
	CoC	26,528	0.60 (0.52-0.70)	1.10 (0.98-1.24)	1.63 (1.47-1.80)	2.80 (2.56-3.05)	3.68 (3.35-4.06)	4.17 (3.66-4.74)
	MoPoM	2,761	1.30 (0.92-1.84)	1.98 (1.42-2.76)	2.40 (1.71-3.35)			
	CoPoM	670	1.01 (0.45-2.26)	1.53 (0.65-3.54)	1.53 (0.65-3.54)			
	Others	169**	1.87 (0.61-5.69)	2.86 (1.05-7.63)	2.86 (1.05-7.63)	2.86 (1.05-7.63)		
All reverse hybrid		31,207	0.87 (0.77-0.98)	1.54 (1.40-1.69)	2.07 (1.90-2.25)	3.60 (3.28-3.96)	5.54 (4.78-6.42)	7.52 (5.86-9.62)
Reverse hybrid and	MoP	21,273	0.90 (0.78-1.03)	1.52 (1.36-1.71)	2.00 (1.79-2.22)	3.67 (3.25-4.14)	5.50 (4.58-6.61)	7.44 (5.47-10.08)
	CoP	9,720	0.78 (0.62-0.98)	1.53 (1.29-1.81)	2.08 (1.79-2.42)	3.23 (2.75-3.79)	5.45 (4.16-7.12)	7.57 (4.83-11.77)
	Others	214**	2.45 (1.03-5.80)	3.30 (1.46-7.38)	10.24 (5.70-18.02)	21.64 (13.38-33.91)	21.64 (13.38-33.91)	
All resurfacing		39,065	1.21 (1.11-1.33)	2.99 (2.82-3.16)	5.27 (5.05-5.50)	10.66 (10.33-10.99)	13.16 (12.78-13.55)	14.84 (14.37-15.33)
Resurfacing and	MoM	38,919	1.21 (1.11-1.33)	2.99 (2.82-3.16)	5.27 (5.05-5.50)	10.66 (10.33-10.99)	13.16 (12.78-13.55)	14.84 (14.37-15.33)
	Others	146**	1.44 (0.36-5.65)					

It is clear why cemented MoP THA's are taken to be the gold standard. They have a predictable, good, long-term performance with around 70 years of clinical history. The material combination also has a significant impact on the estimate of cumulative revision in cemented revision surgery. MoM hips initially perform well but the number that fail increase significantly as time continues. CoP and MoP hips both perform well for all 16 years *in vivo* (Figure 1.6).

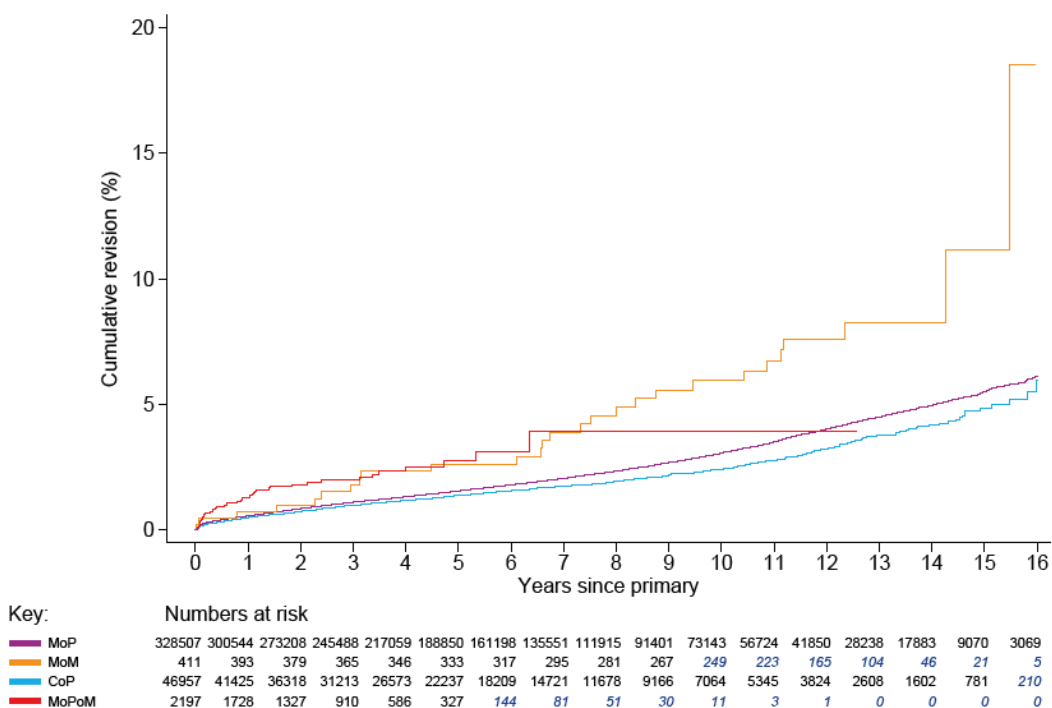


**Figure 1.6** From the NJR: KM estimates of cumulative revision in cemented primary hip replacements by bearing. Blue italics in the numbers at risk table signify that fewer than 250 cases remained at risk at these time points.<sup>2</sup>

#### 1.4.3 Brand Combination

The KM estimates of the cumulative revision rate for various brands can be seen below (Table 1.2). The top four most popular component combinations were selected for comparison. Additionally, as all of the top cemented combinations use an Exeter V40 stem<sup>43</sup>, the next most popular combination that didn't use the V40 stem was included. The most frequently implanted implant combination was the Exeter V40 stem with the Exeter Contemporary Flanged cup<sup>44</sup> with 84,353 recorded data points, second was the V40 stem with the Exeter X3 Rimfit cup<sup>45</sup> with 30,579 data points, the V40 stem and the Exeter Contemporary Hooded cup<sup>46</sup> was next with 28,049, the V40 stem with the Elite Plus Ogee Cup<sup>47</sup> had 25,181 data points. The next most popular implant combination that didn't use a V40 stem was the CPT stem<sup>48</sup> and the ZCA cup<sup>49</sup> which had 16,302 entries. All combinations had a cumulative rate of revision less than 1 % at 1-year post-operation. The most successful at 1-year was the V40 stem with the Ogee flanged cup which had a revision rate of 0.39 % and the least successful was the Exeter contemporary hooded with a revision rate of 0.93 %. At 5 years, which is the oldest clinical available for the V40 stem and the Exeter X3 Rimfit cup, the combination with the lowest rate of revision was still the V40-Elite Plus Ogee with 1.19 % revision rate and the worst was still the V40 stem with the Exeter Contemporary Hooded cup with a revision rate of 2.21 %. This trend continues to 15 years, the V40-Elite Plus Ogee had the lowest revision rate of 3.46 % and the worst performing was the V40 stem with the Exeter Contemporary Hooded cup with a revision rate of 7.51 %.

**Table 1.2** From the NJR: KM estimates of cumulative revision (95% CI) of primary hip replacement by fixation, and stem/cup brand. Blue italics signify that fewer than 250 cases remained at risk at these time points and the number in brackets signifies the standard deviation.<sup>2</sup>

Stem:cup brand	N	Median	Percentage (%) males	Time since primary							
		(IQR) age at primary		1 year	3 years	5 years	10 years	13 years	15 years		
<b>Cemented</b>											
C-Stem AMT											
Cemented Stem[St] : Charnley and Elite Plus LPW[C]	3,161	75 (71-79)	31	0.58 (0.37-0.92)	1.20 (0.86-1.66)	1.48 (1.10-2.00)	2.68 (1.98-3.61)				
C-Stem AMT	4,100	77 (72-81)	33	0.28 (0.16-0.51)	0.82 (0.56-1.20)	1.27 (0.90-1.78)	2.20 (1.57-3.06)				
C-Stem AMT	10,312	75 (69-80)	32	0.45 (0.34-0.61)	0.96 (0.76-1.21)	1.22 (0.95-1.57)	1.67 (1.21-2.31)				
C-Stem Cemented Stem[St] : Elite Plus Ogee[C]	5,544	72 (66-77)	40	0.41 (0.27-0.62)	0.92 (0.69-1.23)	1.24 (0.96-1.60)	2.79 (2.25-3.46)	4.22 (3.39-5.24)	4.43 (3.53-5.55)		
C-Stem Cemented Stem[St] : Marathon[C]	8,215	68 (60-75)	41	0.42 (0.30-0.59)	0.96 (0.75-1.23)	1.44 (1.15-1.80)	2.37 (1.82-3.08)				
CPT[St] : Elite Plus Ogee[C]	3,028	73 (67-79)	36	0.67 (0.43-1.03)	1.51 (1.12-2.02)	2.10 (1.63-2.70)	3.91 (3.11-4.91)	5.04 (3.90-6.52)	5.04 (3.90-6.52)		
CPT[St] : ZCA[C]	16,302	76 (71-81)	31	0.84 (0.70-0.99)	1.44 (1.25-1.65)	2.10 (1.85-2.37)	3.83 (3.39-4.32)	4.70 (4.07-5.41)	4.88 (4.18-5.70)		
Charnley Cemented Stem[St] : Charnley Cemented Cup[C]	4,593	72 (66-78)	38	0.31 (0.18-0.52)	1.13 (0.86-1.49)	1.80 (1.44-2.25)	3.52 (2.96-4.17)	5.17 (4.39-6.09)	6.60 (5.45-8.00)		
Charnley Cemented Stem[St] : Charnley Ogee[C]	10,427	73 (67-78)	38	0.38 (0.28-0.52)	1.22 (1.02-1.46)	1.89 (1.64-2.19)	3.79 (3.38-4.24)	5.14 (4.58-5.75)	5.82 (5.12-6.61)		
Charnley Cemented Stem[St] : Charnley and Elite Plus LPW[C]	6,829	74 (68-79)	29	0.37 (0.25-0.55)	0.75 (0.57-0.99)	1.17 (0.93-1.46)	2.54 (2.14-3.02)	3.53 (2.98-4.18)	4.45 (3.45-5.74)		
Exeter V40[St] : Cenator Cemented Cup[C]	2,521	75 (69-80)	32	0.64 (0.39-1.04)	1.39 (0.99-1.94)	2.06 (1.56-2.72)	2.82 (2.18-3.64)	4.82 (3.67-6.31)	6.09 (3.84-9.58)		
Exeter V40[St] : Charnley and Elite Plus LPW[C]	4,984	73 (68-78)	31	0.63 (0.45-0.90)	1.26 (0.98-1.63)	1.50 (1.17-1.90)	2.12 (1.65-2.72)	2.88 (2.17-3.80)	3.45 (2.31-5.12)		
Exeter V40[St] : Elite Plus Cemented Cup[C]	5,142	73 (67-79)	33	0.33 (0.21-0.54)	0.65 (0.46-0.92)	0.87 (0.64-1.18)	1.50 (1.13-1.99)	2.56 (1.82-3.59)	3.99 (2.49-6.36)		
Exeter V40[St] : Elite Plus Ogee[C]	25,181	74 (69-80)	35	0.39 (0.32-0.48)	0.85 (0.74-0.98)	1.19 (1.05-1.34)	2.23 (2.00-2.49)	2.89 (2.55-3.27)	3.46 (2.76-4.34)		
Exeter V40[St] : Exeter Contemporary Flanged[C]	84,353	74 (69-79)	34	0.51 (0.46-0.56)	0.97 (0.90-1.05)	1.34 (1.26-1.43)	2.42 (2.26-2.60)	3.40 (3.09-3.73)	4.57 (3.79-5.51)		
Exeter V40[St] : Exeter Contemporary Hooded[C]	28,049	75 (70-80)	32	0.93 (0.82-1.05)	1.65 (1.50-1.81)	2.21 (2.03-2.41)	4.19 (3.86-4.56)	6.53 (5.87-7.26)	7.51 (6.47-8.71)		
Exeter V40[St] : Exeter Duration[C]	16,880	73 (67-79)	32	0.59 (0.49-0.72)	1.18 (1.03-1.36)	1.62 (1.43-1.83)	3.84 (3.50-4.23)	5.75 (5.18-6.39)	6.79 (5.86-7.86)		
Exeter V40[St] : Exeter X3 Rimfit[C]	30,579	70 (63-77)	35	0.49 (0.41-0.57)	0.90 (0.79-1.03)	1.28 (1.12-1.46)					
Exeter V40[St] : Marathon[C]	6,870	71 (64-78)	36	0.44 (0.31-0.63)	0.94 (0.71-1.25)	1.35 (1.03-1.78)	2.00 (1.30-3.09)				
Exeter V40[St] : Opera[C]	2,811	74 (68-80)	32	0.40 (0.22-0.71)	0.85 (0.57-1.28)	1.25 (0.89-1.76)	3.30 (2.50-4.35)	5.45 (4.06-7.30)	10.41 (5.28-19.96)		
MS-30[St] : Low Profile Durasul Cup[C]	3,768	74 (68-80)	32	0.22 (0.11-0.44)	0.50 (0.31-0.81)	0.79 (0.53-1.18)	1.62 (1.12-2.35)	2.59 (1.57-4.23)	2.59 (1.57-4.23)		
Muller Straight Stem[St] : Low Profile Durasul Cup[C]	3,641	75 (70-80)	28	0.50 (0.32-0.80)	0.80 (0.55-1.17)	1.12 (0.80-1.58)	2.62 (1.93-3.56)	3.90 (2.72-5.57)	5.33 (2.96-9.50)		
Stanmore Modular Stem[St] : Stanmore-Arcom Cup[C]	5,414	75 (70-80)	29	0.45 (0.30-0.67)	1.07 (0.83-1.40)	1.54 (1.23-1.93)	2.48 (2.01-3.05)	4.17 (3.27-5.33)	4.48 (3.44-5.82)		

Note: Blank cells indicate that the number at risk at the time shown has fallen below ten and thus estimates have been omitted as they are highly unreliable. [St] = Stem; [C] = Cup; [SL] = Shell liner.

#### 1.4.4 First Revision

According to the NJR, around 2.94 % of 1,191,253 THA's received a revision. The NJR use revisions per prosthesis-years as a value for the rate of revision for different variables. It considers how long each implant survives so that an implant that fails soon after implantation will have a much higher number of revisions per 1,000 prosthesis-years than one that survives

on average for 20 years. For cemented hips, there were 1.09 revisions per 1,000 prosthesis-years due to aseptic loosening. Equivalent figures for dislocation/subluxation and infection were 0.84 and 0.68 revisions per 1,000 prosthesis-years. The most common cause of revision for uncemented hips was aseptic loosening, causing 1.40 revisions per 1,000 prosthesis-years, closely behind this was an “adverse reaction to particulate debris” with 1.25 revisions per 1,000 prosthesis-years.

The frequency of the above causes for revisions is dependent on the amount of time after implantation. Aseptic loosening causes little failure immediately after implantation and the frequency increases through time. Dislocation and subluxation occurred most frequently immediately after surgery with some cases after this with no obvious pattern, it is similar for infection. Finally, the incidence of lysis was low at first and increased over time.

#### ***1.4.5 Revision Components***

A key argument for uncemented THR is that they are easier to revise. The success of revised implants is only part of the story. For the surgeon to make an informed decision of what to implant at primary surgery, they must know how successfully that implant can be revised, this data is limited; however, graphs are reported that show the percentage cumulative re-revision rates after revision surgery by primary fixation method.

As can be seen below, reverse hybrid fixation sees a spike in the cumulative re-revision rate at 13 years; however, as the number of examples number in the single figures, this change is not considered significant. The likelihood of early re-revision for a resurfacing is less than other methods of fixation for the first 7-8 years after implantation.

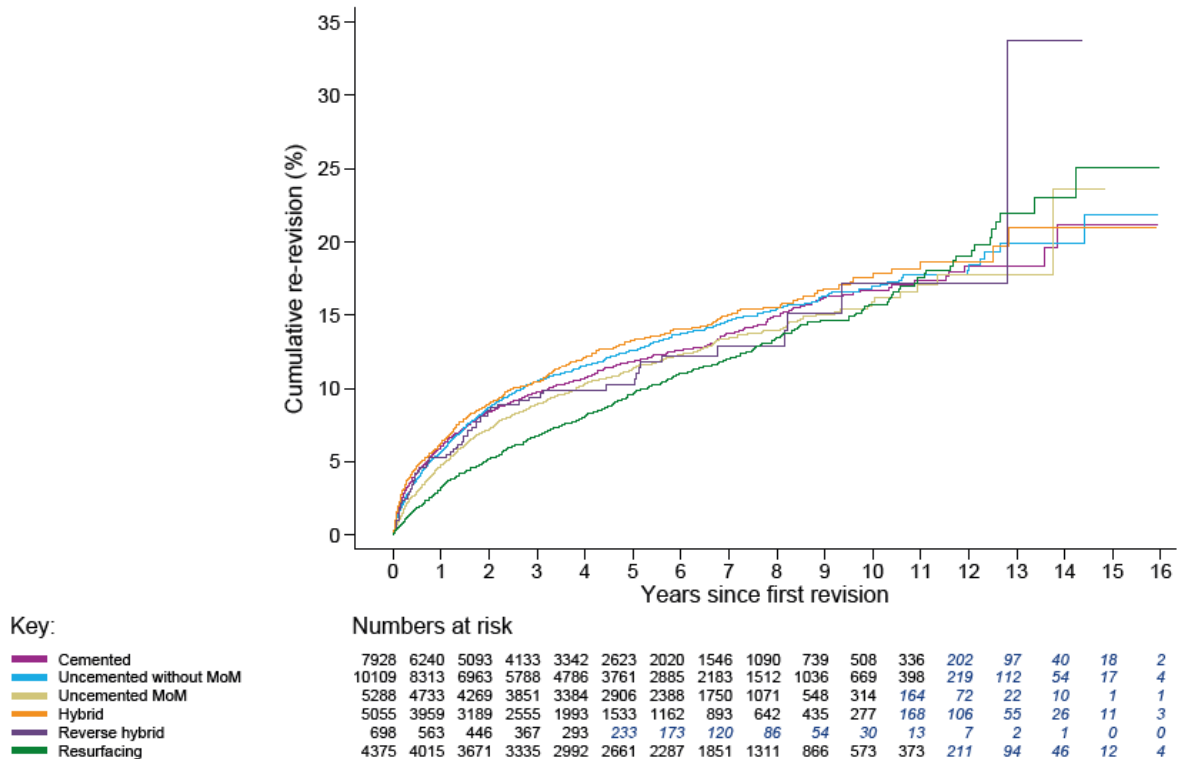


**Figure 1.7** From the NJR: KM estimates of cumulative re-revision by primary fixation in linked primary hip replacements. Blue italics in the numbers at risk table signify that fewer than 250 cases remained at risk at these time points.<sup>2</sup>

#### 1.4.6 Deficiencies

Although the NJR and other national joint registries provide some of the most valuable data for the analysis of implants, there is a severe deficiency in the depth of data provided in the annual reports. It is understandable that the data entry form that must be filled in and filed at the time of operation needs to be short enough so as to not cause operative personnel to avoid it – there are several surprising gaps in what data is provided, and importantly, reported on. Firstly, the type of bone cement used should attract as much attention as the implants; after all, it is implanted into the body. Secondly, innovations in the operative technique do not necessarily equate to an increase in the longevity of the implant. In order to optimise THR, a full inventory of the surgical procedure would ideally be provided. Although this may be costly on time and resources, it is not believed that it is unreasonable that there should be a log of all equipment used during the surgery, and from this, it would be possible to extrapolate the optimal surgical technique. This thesis focuses on the design of the acetabular pressuriser. If the design and size of the pressuriser used in surgery were logged, it would have been easier to detect and analyse problems (Appendix A).

## 1.5 PMMA Bone Cement

The development of cold-curing PMMA bone cement was vital in the success of cemented THR.

### 1.5.1 Composition

Bone cement usually comes as two components: a powder and a liquid which are mixed as a ratio of 2:1 with a deviation of  $\pm 5\%$ , in line with standards.<sup>39</sup> These components may be provided in separate packages to be mixed in a separate vessel, or supplied in a cement delivery system designed for storage, mixing, and delivery of the cement without any transfer between containers.<sup>50</sup> There are four frequently used components in the liquid: a monomer, an activator, a stabiliser, and a colourant. The powder usually contains a polymer and co-polymers, an initiator, a radiopacifier, antibiotics and sometimes a colouring pigment.<sup>36</sup>

The liquid component is primarily composed of MMA monomer, some cements use butyl-methacrylate (BuMA) instead of MMA. The addition of DMpT to the liquid component significantly reduces the required temperature to initiate polymerisation, acting as both an accelerator, as it decomposes the peroxide, and as a co-initiator.<sup>10, 36</sup> Addition of a stabiliser, usually hydroquinone, ensures that a polymerisation reaction is not activated before mixing of the powdered and liquid component by catching free radicals.<sup>10</sup> A colourant may be added so that the surgeon can easily distinguish between bone cement and anatomical features, such as chlorophyllin in Palacos R. The liquid component of most cements have very similar components and quantities.<sup>36</sup>

The powdered component of PMMA bone cement is primarily composed of pre-polymerised PMMA and copolymers. PMMA is a non-crystalline glassy polymer.<sup>51</sup> The powder may be ground PMMA or beads of cement, produced through suspension polymerisation, and sometimes a combination of the two.<sup>36, 39</sup> Much like the liquid component, an initiator is added to the powder in the form of BPO. The quantity of BPO determines the setting time and temperature, increasing the concentration of BPO speeds up polymerisation and therefore the cement will set quicker and at a higher temperature.<sup>39</sup> A radiopacifier is added so that the cement mantle can be observed on radiographs; this may be zirconium dioxide or barium sulphate. A colouring pigment is sometimes added to the powdered component. A powder-based antibiotic is usually added as liquid antibiotics have been shown to significantly weaken the resulting cement.<sup>52</sup> Gentamicin, cefuroxime, and tobramycin are the most frequently used and studied antibiotics.<sup>53</sup>

### 1.5.2 Classification

Different bone cements are required for different purposes. For cemented femoral implantation the cement is delivered in a retrograde fashion which requires the cement to be injected through a hole with a small diameter and therefore a cement with a doughy consistency is not appropriate. Fixation of the acetabular component can be done with a cement of a high viscosity due to the shallow nature of the reamed acetabulum. The viscosity is a commonly used classification system and consists of low, medium, and high viscosity cement. Most cements,

once mixed, start at a relatively low viscosity which increases through time due to polymerisation until the cement becomes rigid. At some point, all bone cements will be of medium and high viscosity, the classification system is more nuanced than it first appears.<sup>39</sup>

When low viscosity cement is mixed it has a very low viscosity. It is runny and sticky. This phase lasts for 3-4 minutes. Proceeding this, the cement has a short working phase (when the cement is no longer sticky but still pliable) and then there is a short time between the end of this phase and full hardening.<sup>39</sup>

Medium viscosity cements are not as runny as low viscosity cements immediately after mixing. The waiting phase tends to last less than 3 minutes. The cement then enters the working phase when it is no longer sticky. The viscosity of the cement only increases a small amount during this phase. After the working phase, there is usually a 1-3 minute wait until full cure.<sup>39</sup>

High viscosity cements have a high initial viscosity and a short sticky phase. The working phase is generally long and the viscosity in this phase increases gradually. The time between the end of the working phase and hardening is around 2 minutes.<sup>39</sup>

This is a helpful classification system for clinical personnel, but it is insufficient for material scientists. The viscosity of the substance is only one aspect of the flow behaviour of bone cement and therefore is not fully representative.

### 1.5.3 Brands

Unfortunately, the annual report of the NJR does not publish bone cement data despite its central role in the success or failure of the implant.<sup>54</sup> Bone cement is as much of an implant as the femoral and acetabular components as they are permanently *implanted* into the body. For this review, only cements used in this PhD are covered.

CMW 2 is manufactured by DePuy Synthesies and is considered a high viscosity bone cement. The agent added to make Simplex P radiopaque is barium sulphate. It is sold as two components: a sachet containing a powder and an ampule containing a liquid, a mixing vessel is not provided.



**Figure 1.8** External Packaging of CMW 2 bone cement (DePuy).

Simplex P is manufactured by Stryker. It has over 50 years of clinical history and is subject to many studies. It is classified as a medium viscosity bone cement. The agent added to make Simplex P radiopaque is barium sulphate. It is sold as two components: a sachet containing a powder and an ampule containing a liquid, a mixing vessel is not provided.



**Figure 1.9** External Packaging for Simplex P (Stryker).

Although Palacos R has been sold by many manufacturers it is primarily associated with Heraeus. It is another high viscosity cement with a long working time. Zirconium dioxide is used as a radiopacifier. It is sold as two components: a sachet containing a powder and an ampule containing a liquid, a mixing vessel is not provided.

Refobacin R is manufactured by Zimmer Biomet and is a high viscosity, antibiotic-loaded cement. The example below shows the cement preloaded in the Optipac vacuum system. It is a medium viscosity cement with a long working time.



**Figure 1.10** External Packaging for Optipac 60 mixing system loaded with Refobacin R (Zimmer Biomet).

#### 1.5.4 Curing Characteristics

The authors feels that current standards regarding curing characteristics are insufficient because they are aligned with the requirements of surgeons rather than those of material scientists as they are parochial and subjective. The international standards outline the method of determination of the doughing time as the time between when “the cement is mixed [...] until the mixture is able to separate cleanly from a gloved finger.” This is not sufficient as when the cement stops sticking to a glove allows room for a difference in opinion of what “sticky” is. Nor is the definition of the setting time of the cement, which is determined as the time it takes to reach “a temperature midway between ambient and maximum.”

For the next section, only a brief overview of the intrinsic factors of curing bone cement will be covered. The extrinsic factors such as mixing conditions and temperature will be discussed later.

#### **1.5.4.1 Cement Curing Phases**

There are four phases from mixing to full solidification: the mixing, waiting, working, and setting phase. The limits of these times are determined either by the manufacture or by tests outlined in ISO 5833:2002.<sup>55</sup> They are usually illustrated in working curve diagrams.<sup>36</sup>

The mixing phase starts when the powder and liquid are combined, and ends once the mixture has become homogenous, the mixing phase is not affected by temperature. The next phase is the waiting phase: this begins once the cement is homogenous and ends at the dough point. This is affected by temperature, the higher the temperature, the faster the diffusion of the monomer and the faster the solvation of the PMMA particles. Following this is the working phase, this is the time when the cement is pliable enough to be deformed and forced into the bone. There is no standardised definition of this phase. As this is the time the surgeon will implant the cement and the implant the time between the start and end of the working phase needs to be regular. The next phase is the waiting phase which ends when the cement reaches the setting time defined in the standards as when the temperature of the cement reaches halfway between the ambient and the maximum temperature.

#### **1.5.4.2 Thermal Properties and Polymerisation rate**

Thermal curves illustrate the rate of polymerisation.<sup>12</sup> Bone cement polymerises using free radical polymerisation which is an exothermic reaction. Each new monomer added to the polymer chain will generate some heat.

The thermal behaviour of bone cement during curing is important; Eriksson and Alberksson observed bone necrosis when bone was subjected to temperatures of 44°C – 47°C for 1 minute.<sup>56</sup> Lundskog found that if the bone was subjected to temperatures of 50°C for 1 minute or 47°C for 5 minutes the bone cells were resorbed and replaced with fat cells.<sup>57</sup>

Reports of the maximum temperature that bone cement reaches during curing vary. This may be accounted for by the broad range of control variables used for the studies. DiPisa *et al.*<sup>58</sup> and then Dunne and Orr<sup>12</sup> highlight studies showing that the thermal curve, and therefore the maximum temperature, is a function of the quantity of heat produced and the rate of heat production<sup>59</sup>, the thermal properties of the surrounding components<sup>60-62</sup> and the preparation of the cement.<sup>12, 63</sup> The maximum temperature reported for bone cement varied from 41°C to 110°C. Mayer reports a maximum temperature of 107°C for cement 10 mm thick and 60°C for cement 3 mm thick.<sup>64</sup> Revie *et al.* report a mean maximum temperature of 67.46°C.<sup>8</sup> Huiskies *et al.* reported far higher temperatures of 100°C – 110°C and say that cement thickness and the location that measurements were taken influenced the maximum temperature<sup>65</sup>. Sih *et al.* report maximum temperatures of 41°C for 1 mm thick cement, 50°C for 5mm thick cement and 60°C for 6 mm – 7 mm cement.<sup>66</sup> Li *et al.* also found a significant difference in the maximum temperatures generated due to the thickness of the cement “patty”.<sup>62</sup>

#### **1.5.4.3 Polymerisation Progress**

The progress of polymerisation can be measured using Differential Scanning Calorimetry (DSC). According to Freire, DSC is a technique that measures the apparent molar heat capacity

of a macromolecule as a function of temperature and uses this quantity to yield a complete thermodynamic characterisation of the transition occurring; in this case, polymerisation.<sup>67</sup>

Nzihou *et al.* reported DSC results for a standard bone cement formulation and found that the ambient temperature had a significant impact on the extent of polymerisation. The hotter the surrounding temperature the more monomer reacted. They report that at 20°C, 25°C, 30°C, and 40°C the degree of polymerisation was 0.24, 0.39, 0.43 and 0.6, respectively. This seems remarkably low considering the number of studies reporting that the concentration of residual monomer in the solidified bone cement is in the range of 2 – 6 %.

The dangers of MMA were reported by Charnley and have been further investigated since.<sup>68</sup> Unreacted MMA is toxic and has been shown to cause bone remodelling adjacent to the implantation area in canines.<sup>69</sup> Kuhn<sup>36</sup> translates two studies initially reported in German by Scheuermann and Rudiger *et al.* showing that the concentration of MMA monomer in bone cement decreases to approximately 0.5 % within 2 – 3 weeks<sup>70</sup>; this was confirmed in explanted cemented arthroplasties.<sup>71</sup>

#### **1.5.4.4 Stress Relaxation**

When most brands of cement are initially mixed, they form a liquid that flows in reaction to any applied stress and therefore, the stress is reduced to zero as we would expect from a mostly viscous material. However, it is important to determine whether PMMA bone cement can store stresses indefinitely and if so, when does this characteristic develop. Viscoelastic models have been proposed for PMMA, but most are focused on when pure PMMA is near the glass transition temperature.<sup>72</sup> PMMA bone cement contains many additives and therefore has a different molecular structure so these models may not be appropriate. Although the literature often does not discuss these models or the implications for the residual stresses at long times it appears that there is some consensus that the most accurate model includes a time-independent elastic component.<sup>73</sup> This means that although there will be significant stress relaxation, not all internal or external stresses will fully relax. Many factors affect the extent of relaxation including the environment, age of cement, the magnitude of initial strain and strain rate.<sup>74, 75</sup>

Eden *et al.* developed a theoretical model from experimental results that included two spring dashpots and a spring in parallel. This accurately matched the experimental results.<sup>73</sup>

Yetkinler *et al.* applied compressive strains of 1%, 2.5% and 5% to bone cement specimens at 37°C in an aqueous environment and monitored the diminishing load for 100h. The significant initial stress of around 6.5 MPa decayed to around 2.5 MPa within 1 – 10 hours, for the 1% applied strain, the same was also found for the other testing conditions.<sup>14</sup>

#### **1.5.4.5 Rheology**

The rheological behaviour of PMMA bone cement describes how the cement will flow and how the cement will react to an applied force.

There are many methods for measuring the rheological properties of a material. Capillary rheometers force the material through a small diameter and measure the flow rate and the load applied to the cement. A cup and bob geometry may be used, a bob is spun inside a cup filled

with the fluid being characterised, this is used most commonly with fluid of very low viscosity which would leak from a plate. The most frequently used geometries are cone and plate and parallel plates (Figure 1.11).<sup>76</sup> The cone and plate geometry tends to provide more reliable data as it ensures a constant shear rate along its radius. For bone cements, oscillatory deformation is preferable as the cement becomes very hard to deform in later stages so continuous rotation may cause the plates to separate from the sample. The gap between the plates should be at least 5 x larger than the largest cement particle, potentially 100  $\mu\text{m}$ .<sup>77</sup> All methods used the principle of applying a predetermined load or strain to a sample and measuring the response of the material. The testing geometry that should be used is dependent on the application and a rheological expert should be consulted on this point.

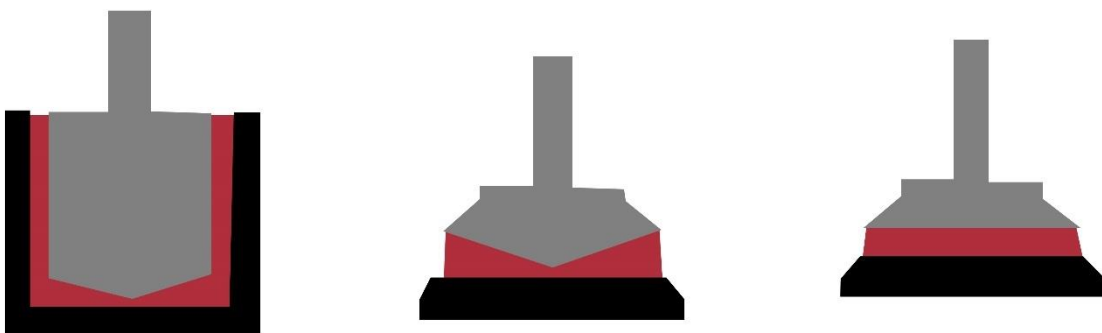


**Figure 1.11** Basic geometries for a rotational rheometer: (left) concentric cylinder; (middle) cone and plate; (right) parallel plate.

There are many properties that may be investigated when performing a rheological characterisation of a material. This thesis focuses on viscosity, the equilibrium modulus, the storage modulus, and the loss modulus. The viscosity is the most widely studied and understood parameter in rheological theory and it is a description of a materials resistance to deformation.<sup>78</sup> The equilibrium modulus describes how much of an applied strain is converted into a residual stress and is an important parameter when investigating materials that are setting such as polymerising plastics.<sup>79</sup> The storage modulus describes the instantaneous elastic response to an applied strain and loss modulus describes the delayed, viscous response to an applied strain.<sup>77</sup> Each of these measures are important but it depends on the application as to which are possible to measure and which are most relevant to the characteristics being investigated.

Rose and Farrah published a rheological characterisation of some commonly used bone cements and how the ambient temperature affects the cement viscosity. They used a parallel plate geometry, oscillatory deformation, and a gap size of 500  $\mu\text{m}$ . They characterised six cements at different temperatures. A higher temperature increased the rate of polymerisation and thus the viscosity increases at a faster rate. It is also clear from this that the temperature does not have a significant effect on the initial viscosity except in the case of Palacos R.<sup>77</sup> Boger *et al.* found a similar relationship between the cement viscosity profile and temperature using a double gap measurement system (similar to a cup and bob system but creates more surface area for the cement to interact with the top measurement plate).

Each of the cement brands have significantly different initial viscosities and develop differently. Farrar and Rose point out that this is intentional by the manufacturers as each of the cements have a different application. The viscosity of the cement when it is initially mixed has been found to be largely dependent on the size of the PMMA particles. Farrar and Rose tested this hypothesis by mixing the powdered PMMA and the liquid MMA without any DMpT, therefore preventing the initiation of the polymerisation reaction. The initial viscosity and rise are due to polymer bead solvation. Pascual *et al.* highlight that solvation of the PMMA beads and the diffusion of the liquid to the solid-state have effects on the curing characteristics and the initial viscosity. They also found that the setting time is significantly increased with larger average diameter of PMMA particle size.<sup>80</sup> Ferracane and Greener also found a larger proportion of smaller particles in lower viscosity cement.<sup>81</sup>

It has been found that increasing the rate of deformation of bone cement whilst it is curing decreases the viscosity. This phenomenon is known as shear thinning. Ferracane and Greener performed rheological characterisation of bone cement using a cone on plate rheometer at different strain rates.<sup>81</sup> At all times that the viscosity was measured an increased strain rate reduced the viscosity. It is widely agreed that shear thinning is typical behaviour of PMMA bone cement whilst curing.<sup>82-84</sup>

It is important to understand how the flow behaviour of curing bone cement is best described at each stage of polymerisation. Initially, some cements are best described as a viscous fluid, it will then enter a viscoelastic phase and finally, it will cure into a primarily elastic solid. These are key questions for PMMA bone cement:

1. What parameter governs when a material starts storing stresses indefinitely?
2. Is there a way to directly observe when this parameter becomes significant?
3. Is there a way to measure the consequences of this transition?

#### **1.5.4.6 Liquid-Solid Transition**

The parameter that describes how much of an applied strain will be retained as a residual stress is referred to as the equilibrium modulus by Horst H. Winter, who is one of the leading authorities in rheology.<sup>79</sup> However, no studies could be found regarding the equilibrium modulus of PMMA bone cement. Most of his work concerns cross-linking polymers and commercial PMMA does not crosslink without the addition of a crosslinking agent. Two-thirds of the initial bone cement mixture is pre-polymerised powder, the polymerisation reaction is due to the liquid monomer dissolving the polymer beads and polymerising between them. The rheology of this complex system has not been widely studied or analysed; however, Winter and Mours discuss *physical* gels which share rheological properties with chemically crosslinking systems<sup>85, 86</sup> as they are able to form extensive molecular or particular clusters by a variety of different mechanisms.<sup>79</sup> If PMMA bone cement acts as a chemical gel at the liquid-solid transition (LST) otherwise known as the moment of gelation, a few important phenomena are worth consideration. Firstly, at the LST the zero-shear viscosity will diverge to infinity and an

equilibrium modulus will develop (Figure 1.12). After this moment, any applied strains that are not allowed to recover will result in residual stress.

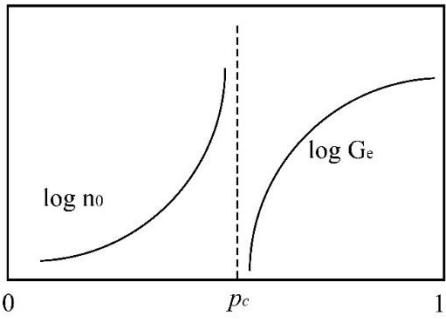


**Figure 1.12** Schematic of the divergence of zero-shear viscosity,  $\eta_0$ , and equilibrium modulus,  $G_e$ . The LST is marked by  $p_c$ .

If a step strain,  $\gamma_0$ , is applied to the bone cement mixture then some of the resulting stress,  $\tau$ , will not fully relax and will be proportional to the magnitude of strain applied multiplied by the equilibrium modulus,  $G_e$ :<sup>87</sup>

$$\lim_{t \rightarrow \infty} \tau = G_e \gamma_0$$

Therefore, it is important to identify when this LST occurs so that deformation after it can be minimised. Several authors have used rheological techniques to attempt to identify when this moment occurs.

Farrar and Rose detail the standard oscillatory rheological equations very clearly so I shall use the equations from there.<sup>77</sup> They consider an applied oscillatory stress and describe it in terms of the amplitude and frequency of the applied stress.

$$\sigma(t) = \sigma_0 \exp(i\omega t)$$

Where  $\sigma_0$  is the amplitude and  $\omega$  is the frequency and  $i = \sqrt{-1}$ . The material will thus react to this oscillating stress as an oscillating strain with a slight delay due to the viscous component.

$$\gamma(t) = \gamma_0 \exp(i(\omega t - \delta))$$

Where  $\gamma_0$  is the strain amplitude and  $\delta$  is the phase difference between the applied stress and resulting strain.

The “complex shear modulus” is defined as:

$$G^* = \frac{\sigma(t)}{\gamma(t)}$$

And according to rheological theory, this can be written as:

$$G^* = G' + iG'' = \frac{\sigma_0}{\gamma_0} (\cos(\delta) + i\sin(\delta))$$

It follows that:

$$\tan(\delta) = \frac{G''}{G'}$$

Where  $G'$  is the storage modulus and  $G''$  is the loss modulus. The complex modulus of PMMA bone cement can be described using a loss and a storage component. The instantaneous, elastic response of the material is described by the storage modulus,  $G'$  and the delayed, viscous response is described by the loss modulus,  $G''$ .

Farrar and Rose attempt to identify whether there is any rheological parameter that is more objective a measure of when the cement should be implanted. They tested for correlation between the time when the storage modulus becomes larger than the loss modulus and the dough point of the cement. They present interesting graphs showing the plots of  $G'$ ,  $G''$  and  $\tan(\delta)$  but they are without context as the dough point is not labelled. They report that the  $G'$ - $G''$  crossover correlates with the previously discussed dough times but provide no data regarding the dough times which reduces the confidence of the validity of their conclusions. Often it is taken that when  $G'$  becomes larger than  $G''$  the material is primarily elastic.<sup>77, 88</sup>.

Nicholas *et al.* also measured  $\tan(\delta)$  and viscosity of several commercially available bone cements. They do not report any significance of the  $G'$ ,  $G''$  cross-over but state that the viscous component,  $G''$  reaches a peak when the cement transitions from a viscous liquid to an elastic solid, but they do not say how they identified this moment.

There doesn't appear to be agreement regarding the behaviour of the viscosity of the cement when the  $G'$ ,  $G''$  crossover happens. The cements used in the Nicholas *et al.* study are mostly high viscosity cements and, in the Farrar and Rose, study most are low viscosity which partly explains the difference in the times that the cross over occurs. In the Farrar and Rose study, the cross over occurred near the end of polymerisation, apart from Palacos R, the high viscosity cement. In the Nicholas *et al.* study, the crossover occurs before measurements started.

A paper by Winter states that the  $G' - G''$  crossover cannot be used to detect the gel point because the frequency of measurement changes when the crossover occurs and is therefore not just a property of the material being tested but also a result of the methodology used. They instead present another method for measuring the LST, the relationship between  $\tan(\delta)$  and the frequency of deformation is described by a power law. This means that if we perform a multifrequency oscillatory experiment whilst the cement cures, we may be able to detect when the gel point occurs.<sup>79</sup>

A very brief conference paper by Spiegelberg discusses this in 1998 but seems to only have tested one cement with one repeat and reported limited information or data. No other papers could be found by the author or others that discuss this.<sup>89</sup>

There is difficulty when comparing rheological studies due to the sensitivity of the PMMA bone cement to environmental variables and the lack of international standards. The similarities in the data have been covered here but the scale of the results is significantly different. The overall profiles are similar between relevant articles for all variables.

### 1.5.5 Residual Stress

A residual stress in the same direction as an applied stress will lower the required applied stress for mechanical failure of the cement.<sup>90</sup> There are also implications for fatigue failure. It has

been shown that the larger the applied stress the lower the number of cycles to failure,<sup>91</sup> although it cannot be said that the magnitude of the residual stresses contributes to this.

Residual stresses can develop in many ways; however, these stresses can only exist indefinitely if the bone cement has developed an equilibrium modulus so that the stresses cannot fully relax.

### 1.5.5.1 Shrinkage Stress

Most of the literature regarding residual stresses in bone cement focus on the femoral side of THA. There are two causes of PMMA cement shrinkage.

Firstly, shrinkage occurs due to an increase in the molecular weight as MMA is polymerised into PMMA. Polymerisation of pure MMA into PMMA would result in a shrinkage of 21%. However, there is usually a 2:1 ratio of powder to liquid. The powder, as we have already discussed is mostly PMMA and so will not shrink due to an increase in molecular density. Haas *et al.* found that Simplex P shrunk by 2 – 5 %<sup>9</sup> and Rimnac *et al.* found that Palacos R shrank by 3%. Kuhn reports that bone cement in a liquid environment swells by 2 - 3%, potentially offsetting polymerisation shrinkage *in vivo*.<sup>39</sup>

Secondly, thermal shrinkage is observed in bone cement. Various studies have reported the maximum temperature that the cement reaches during polymerisation, these figures range from 40 – 120 °C. However, studies that use a cement mass between 3 – 7 mm thick reported temperatures around 60°C. Ahmed *et al.* investigated the coefficient of linear thermal expansion for cooling cement and found a value of  $7.22 \times 10^{-5} /{^\circ}\text{C}$  for temperatures between 1 and 43 °C and  $8.76 \times 10^{-5} /{^\circ}\text{C}$  for temperatures between 43 and 86 °C. Assuming the cement will cool from 60 °C to 37 °C *in vivo* and only using the larger coefficient of linear thermal expansion we get a total percentage shrinkage of 0.20 %.<sup>20</sup> This is significantly less than the expected shrinkage due to polymerisation.

Ahmed *et al.* reported that the onset of significant stresses at the femoral component surface coincided with the rapid increase in temperature, they conclude that thermal shrinkage generates most of the residual and transient stresses within the cement matrix. However, their experimental set-up consisted of strain gauges on a hollow metal cylinder, the high temperatures would have caused the metal cylinder to expand, creating tensile stresses which would rise and fall with the temperature. The stress at the cylinder then dropped to become compressive stresses as the cement cooled and tightened around the stem.<sup>20</sup>

Lennon and Prendergast measured the temperature of cement in a physical femoral model, identified cracks on a physical femoral model, and developed a Finite Element Analysis (FEA) model of the residual stresses generated using thermal data.<sup>92</sup> They use the “stress locking” theory, which states that all stressed before a certain point will be able to relax so are not considered significant and are ignored, in the model they define this moment as either at peak temperature or at the end of polymerisation (it is not stated why they decided that it would occur then). This “stress locking” point is equivalent to the LST. When the stress locking point occurred significantly affected the maximum residual stress, they estimate 1 – 2 MPa when “stress locking” occurs at the end of polymerisation but 4 – 7 MPa when it is set at peak temperature. They also report that the addition of porosity into the model increased the

maximum stresses by a factor of three. Many assumptions and estimations are made in this paper, most importantly: the moment of “stress locking” is chosen arbitrarily.<sup>92</sup>

Orr *et al.* developed a computational model using thick-walled cylinder theory, allowing calculation of the hoop stresses and they performed a simple preliminary fatigue experiment which confirmed that radial cracks are likely created from the cement-prosthesis interface due to shrinkage and fatigue. In a second experiment, cement was prepared under vacuum according to the manufacturer's instructions and then injected into a mould creating rings which were then fitted onto a mock femoral stem, heated and allowed to cool. The rings were then examined under a scanning electron microscope (SEM). They found that the rings which had been heated to at least 80°C had cracks that radiated primarily from the tapered stem. The authors cite a paper by Jasty *et al.* who reported cracks that extended radially from the cement-prosthesis interface post mortem at up to 17 years post-op.<sup>93</sup> They then used this data to develop a computational model. The authors suggest that cement cracks are present from the time of implantation of hip stems and prior to loading. Stresses are expected to be larger for cement mixed under vacuum and that this is due to the existence of pores within the matrix reducing the shrinkage of the external dimensions.<sup>94</sup>

Roques *et al.* performed an *in vitro* experiment in which they measured the stresses at the implant interface using strain gauges on a hollow stainless-steel tube. They also used a technique called acoustic emission to listen for the development of microcracks and creep as the cement cures. They found that the cement clearly shrank onto the stem rather than away as the stem was bonded to the cement when it was removed. This may not be true *in vivo* as the acetabular or femoral bone that the cement is implanted into will be warmer than the implant and therefore it is likely that the cement will polymerise faster there. They conclude that significant tensile residual stresses are generated due to shrinkage and are up to 10 MPa, which is 37% of the static tensile strength. The acoustic emission measurements also showed microcracks and sliding occurred during curing to relieve residual stresses.<sup>21</sup>

Hingston *et al.* investigated the effect of the viscosity of the cement on the thermal curve and on the residual stress generation. They found that the viscosity of the cement had no significant effect on either of the measured variables. They also measured the residual strains using a similar methodology to the other reported studies. They found a similar pattern of results. They found axial strains in the femur and stem 3 hours after the start of cement mixing only reduced a further 5.5 and 7.9 % at three days.<sup>95</sup>

Briscoe and New developed a 2D and a 3D FEA model to calculate the local residual stresses in the femoral cement mantle using the local degree of polymerisation to calculate the material properties. They report that the results have good agreement with the previously reported studies.<sup>96</sup>

None of these studies consider the fact that a force is maintained on the implants whilst the cement cures, this force may also be stored within the cement.

### **1.5.5.2 Flow Induced Residual Stress**

As previously discussed, at the LST the curing polymer will develop an equilibrium modulus and strains applied after this will be stored as stresses if they are not allowed to be recovered.

As part of the surgical procedure for cemented THA is application of a force on the implant until the cement is fully set, there will be significant residual stresses. Most literature regarding this phenomenon, known as “flow-induced residual stress” discusses the warping of thin-walled injection moulded parts.

Baaijens and Douven state that the application of force to a curing polymer will result in a strain that aligns the polymer chains.<sup>97</sup> The maximum entropy state is when the chains are randomly orientated so a residual stress will be present which tends away from the aligned polymer chains.<sup>98</sup> No studies could be found which investigated this potential source of cement mantle weakening. As most of the current literature focuses on injection moulding, thermoplastics are the primary focus, but a curing plastic would likely exhibit the same properties as seen in the rheological section. There are three phases during the injection moulding of a product: filling, packing and cooling. During the filling stage, the thermoplastic melt is forced into the mould. During the packing phase, a pressure is applied to fill the remainder of the cavity and to compensate for cooling shrinkage. Finally, the component is cooled and is then ejected. Residual stresses can develop due to the large deformations occurring at the filling stage and they can also develop due to the large pressures occurring at the packing phase.<sup>99</sup> These phases can be seen as equivalent to the cement delivery and implant insertion phases in cemented total joint arthroplasty and then the waiting phase where a force is applied to the component until full cure.

For many of these experiments, there is too much emphasis placed on computer simulations. Several significant assumptions have to be made regarding the properties of the cement. If any assumptions are incorrect then the final results are invalid. More emphasis should be placed on actual measurements of residual stresses or the effects of the stresses.

### **1.5.6 Mechanical Properties**

Once the joint replacement system has been implanted it will undergo a loading cycle. These loading cycles are often complex, the cement mantle will undergo all forms of loading whilst *in vivo*. Bergmann *et al.* reported that in 3.9 years of the implant being *in situ* it will undergo roughly ten million cycles so measuring the fatigue strength of bone cement is important.<sup>100</sup> They also report that peak loads during stumbling can be as high as 11 kN and whilst going upstairs the peak forces can be as high as 4.2 kN.<sup>100</sup> A quick calculation of the potential stress the cement mantle will experience when a patient stumbles with a 3 mm thick acetabular cement mantle which has been formed in an acetabulum which has been reamed to 60 mm gives a maximum stress of 15.2 MPa.

#### **1.5.6.1 Compression Testing**

ISO 5833:2002 outlines a methodology for the determination of the compressive properties of PMMA bone cement<sup>55</sup>. It requires the moulding of cylinders that are 6 mm in diameter with a height of 12 mm. The testing and curing of the cement should be done at  $(23 \pm 1)^\circ\text{C}$ . Remove the specimens from the mould and allow them to rest for  $(24 \pm 2)$  h after the time of mixing. They then measured the diameter and loaded the samples into the test machine. They applied a compressive load with a crosshead speed of 19.8 mm/min – 25.6 mm/min. Then divided the force at failure by the original diameter to obtain the average compressive strength.

Lee reports the average compressive strength of a large sample size by combining the reports from Saha and Pal<sup>101</sup>, Lewis<sup>11</sup> and Kuhn<sup>39</sup> and report that the average compressive strength of all PMMA bone cements tested is 93.0 MPa.<sup>102</sup>

#### **1.5.6.2 Bend Testing**

The standards require moulding of the cement into cuboid samples approximately 75 mm in length, 10 mm wide and 3.3 mm thick. All components must be kept at (23 ± 1) °C for 2 h before moulding and once moulded the cement is conditioned at (23 ± 1) °C for (24 ± 2) h before testing. The deflection of the specimen is measured for an applied load of 15 N and 50 N and the force at failure, to the nearest 0.5 N, is measured. The bending modulus is calculated using the following equation:

$$E = \frac{\Delta Fa}{4fbh^3} (3l^2 - 4a^2)$$

Where all lengths are in mm and forces in N, and  $\Delta F$  is the difference between deflections under loads of 15 N and 50 N;  $b$  is the average measured width of the specimens;  $h$  is the average measured thickness of the specimen;  $l$  is the distance between the outer loading points;  $\Delta F$  is the load range, and  $a$  is the distance between the inner and outer loading points. The bending strength is calculated using the following equation:

$$B = \frac{3Fa}{bh^2}$$

Where  $F$  is the force at break in N,  $b$  is the width of the specimen,  $h$  is the height and  $a$  is the distance between the inner and outer loading points.

A review of the literature by Lee found that the average bending strength for bone cement is 64.2 MPa.<sup>102</sup> Kuhn and Ege report the four-point bending modulus as 2915 MPa for Simplex P<sup>39</sup> Weber and Bargar report a value of 2290 MPa for Simplex P.<sup>103</sup>

#### **1.5.6.3 Tensile Testing**

The standards do not provide a testing methodology for obtaining the tensile strength of PMMA bone cement thus it is difficult to compare results. There are standards available for the tensile testing of plastics.<sup>104</sup> A report by Dunne<sup>105</sup> and another by Spierings<sup>106</sup> report results from basic tensile test experiments for a variety of cement formulations, although there is some variation due to the brand of cement, the ultimate tensile strength (UTS) was always between 30 – 60 MPa.

#### **1.5.6.4 Creep Testing**

The creep of bone cement describes how the cured cement deforms due to an applied load. As previously covered, bone cement is a viscoelastic substance. There will be an instantaneous deformation due to the elastic component and then a transient response which occurs over time due to the viscous component. After a period of time, when the load is removed, some of the deformation will recover, this is called primary creep, the strain that does not recover is called

secondary creep.<sup>105</sup> Several reports have found that cement does creep, although there are disagreements over whether this is advantageous so that the cement adjusts to the stress distribution at the cement-bone interface or whether it is disadvantageous as it may eventually lead to component loosening.<sup>39</sup>

#### 1.5.6.5 Fatigue Testing

Most systems fail after being implanted for a significant amount of time and once they have undergone a significant amount of loading cycles. Good fatigue performance is vital for PMMA bone cement.

As calculated earlier, according to measurements made by Bergmann *et al.* the cement may be subject to stresses as large as 15.2 MPa, this is below the ultimate failure stress, but it will still affect the cement, pre-existing cracks may grow, the cement may weaken, inter-matrix imperfections may align.<sup>25</sup> The fatigue performance of bone cement is highly sensitive to changes in conditions and formulations. This will be discussed in more detail in the relevant sections but here a study by Soltész is presented which compared the different methodologies found in the standards.<sup>107</sup>

The first described methodology is an adapted version of the four-point bending test described in ISO 5833: Implants for surgery — Acrylic resin cements.<sup>55</sup> Second is an adapted version of the tensile tests described in ISO 527: Plastics – Determination of tensile properties.<sup>104</sup> The specimens are dog bone-shaped and the load applied to them is purely tensile axial. The final version is ASTM F2118: Standard Test Method for Constant Amplitude of Force Controlled Fatigue Testing of Acrylic Bone Cement Materials (American Society for Testing and Materials).<sup>108</sup> This standard requires cylindrical specimens with a tapered centre to be manufactured. These samples are then loaded with fully reversible compressive and tensile loading. All these testing methodologies may continue until a predefined time, e.g., 10 million cycles; or they may continue until failure.

For all three methodologies, the ultimate strength must be determined as a reference value so that the cyclic fatigue load can be calculated. The force is applied at different rates: 90 N/min for the bending setup, 1650 N/min for the tensile setup and 950 N/min for the tension/compression setup.

For the actual testing, Soltész *et al.* used Simplex P and Palacos R bone cement. The bone cements give very similar results for the same testing methodologies. However, there is a significant difference between the bending results and the tensile and tensile/compression results. Soltész *et al.* explain that this may be a result of different stress distributions and specimen sizes.<sup>107</sup>

The loads and frequencies required for fatigue testing methodologies are lower than what many universal testers and standard load cells can reach accurately, this makes testing the fatigue performance of PMMA bone cement difficult if the appropriate equipment is not available. Due to the conditions that hip implants are usually subjected to *in vivo*, loads applied cyclically over a long period, fatigue testing is likely the most clinically relevant measurement.

### **1.5.7 Allergies**

There are many components in PMMA bone cement, and several can cause allergic reactions. These reactions can affect personnel that work with bone cement and, of course, the patient.

There are several primary elicitors of allergic reactions, within bone cement this could be gentamicin, BPO, MMA DMpT and hydroquinone.<sup>109,110</sup> These elicitors could result in eczema, delayed healing, recurrent effusion, pain or implant loosening.<sup>111-114</sup> The most recent NJR makes no mention of allergic reaction to bone cement or metal sensitivity.

In an unfortunate coincidence, I have an allergy to PMMA. I developed severe hand eczema in the second year of research and unfortunately, my general practitioner and dermatologist could not alleviate it. However, as I entered my third year I read an article that discussed bone cement as the cause of hand eczema in surgeons.<sup>111</sup> I tried to use extra gloves and better respiratory equipment to relieve this but it didn't work. The first national lockdown due to COVID-19 meant that I had to stop experiments and the eczema improved. In the summer of 2020, I resumed experiments, but the eczema came back rapidly and just as severe. Once the experiments were completed the hand eczema cleared up again (Figure 1.13).



**Figure 1.13** Authors allergic reaction to bone cement.

### **1.5.8 Additives**

Further particles and compounds may be added to improve the performance of bone cement.<sup>115</sup>

#### **1.5.8.1 Carbon Nanotubes**

The addition of carbon nanotubes, specifically multi-walled carbon nanotubes has been shown to increase the mechanical strength, specifically compressive strength, compressive modulus, bending strength, bending modulus and fatigue performance of bone cement at low concentrations. However, at higher concentrations, it was shown that there was a statistically

significant reduction in mechanical properties.<sup>116</sup> Osteoblastic cells adhered and proliferated on the surface of all the cements with MWCNT in them, suggesting that cements impregnated with MWCNT are biocompatible.<sup>117, 118</sup> It has also been shown that the addition of 1 wt% improved the osseointegration, promoting bone ingrowth.<sup>118</sup>

Ormsby *et al.* also investigated how the addition of MWCNT to PMMA bone cement affected the cure time and temperature. They found the setting time was significantly extended with the addition of MWCNT, they suggest this may be due to the MWCNT influencing the free radical polymerisation. Due to this, the rate of polymerisation was reduced, and the maximum temperature was reduced and thus the extent of thermal necrosis was reduced.<sup>6</sup> There is still a significant amount of research that must be performed regarding the addition of carbon nanotubes to PMMA bone cement before it should be used *in vivo*.

#### **1.5.8.2 Chitosan**

It has been shown that chitosan has antibacterial properties as well as being non-toxic and biodegradable.<sup>105, 119</sup> However, a study by Tunney *et al.* reports that the addition of chitosan did not prevent bacterial colonisation and decreased the release of gentamicin in antibacterial loaded bone cement. It also did not prevent biofilm formation. Not only were the antibacterial properties of bone cement not improved but the addition of chitosan decreased the mechanical properties of the bone cement.<sup>119</sup> A study by Khandaker *et al.* reported similar findings with no mechanical strength improvements and a decrease in fracture toughness.<sup>120</sup> Results reported by Dunne *et al.* also agree with these findings, they report a reduced release of gentamicin, no additional antimicrobial benefits and reduced compressive and bending strengths.<sup>105</sup> However, Endogan *et al.* reported that the addition of Chitosan did not influence the tensile strength and improved the compressive strength of bone cement. They also found that there was a significant reduction in the maximum temperature measured for bone cement with an average particle size between 50 and 150  $\mu\text{m}$ .<sup>121</sup>

#### **1.5.8.3 Vitamin E**

The polymerisation of PMMA produces free radicals which induce local inflammation and alter macrophage activity.<sup>11</sup> Vitamin E is known to act as a free radical catcher. It has also been shown to reduce the peak temperature reached due to polymerisation.<sup>122</sup> This combination of characteristics may reduce tissue necrosis which is a major cause of implant loosening.<sup>2</sup> As it acts as a radical catcher it is likely that the reaction will progress slower, this has been measured through *in vitro* experimentation which will mean a longer operation and a higher chance of complications.<sup>122</sup> It has also been shown to reduce the mechanical properties including tensile and compressive strength.<sup>122</sup>

#### **1.5.8.4 Silver**

Silver ions are known as a natural antibiotic. They deactivate enzymes which are vital for bacteria survival and replication.<sup>123</sup> Silver benzoate has been added to PMMA and silver compounds were released for over 28 days and inhibited 99.9% of bacteria for 2 days. The addition of 1% silver ions significantly reduced the mechanical strength.<sup>124</sup> The effect of the

addition of silver nanoparticles on bacterial growth was also tested. Bone cement with nanoparticles reduced the growth of normal bacteria as well as MRSA and MRSE whereas Gentamicin alone limited the growth of *S. epidermidis* but has a reduced effect on MRSA and MRSE.<sup>125</sup>

## 1.6 Cemented Acetabular Arthroplasty

According to the most recent NJR, the most common cause of failure of cemented THA's is aseptic loosening with 1.06 revisions per 1,000 prosthesis-years; osteolysis, often the precursor to aseptic loosening, caused 0.21 revisions per 1,000 prosthesis-years.<sup>2</sup> Despite excellent long and short-term results, many hips still fail due to osteolysis at the cement-bone interface. Failure at the cement bone interface in THR frequently occurs on the acetabular side.<sup>126</sup>

Clinical observations of the cement-bone interface will be reviewed in this section first, then the various aspects of the implantation of a cemented acetabular component into a patient will be considered.

### 1.6.1 Bone Cement-Bone Interface

There are two key interfaces in most arthroplasties: the cement-implant interface and the cement-bone interface. This thesis is focused on the latter.

#### 1.6.1.1 Radiolucent Lines

Radiolucent lines (RLLs) are dark lines between interfaces on the radiograph of THR (Figure 1.14).<sup>127</sup> They occur at the cement-bone interface of cemented THR. Barrack *et al.* published a 12-year radiographic review of 50 'second generation' hips. They reported that no femoral components were revised for aseptic loosening and only one was defined as loose. They report that 11 patients had undergone revision surgery due to a loose acetabular component and a further 11 had radiographic signs of loosening.<sup>126</sup> In an 11-year radiographic review, Mulroy and Harris report that of 105 hips, only three femoral components were loose, none were probably loose and 24 were graded as possibly loose; 42 % of acetabular components were radiographically loose.<sup>128</sup> The studies described above are widely accepted to be evidence that radiolucent lines are an indicator of early THA implant loosening. There is much debate in the literature regarding which RLLs are of concern. The location, size and whether they are progressive are the variables that have attracted the most attention. DeLee and Charnley described a system to define the location of RLLs. The acetabular cup was separated into three zones: zone I – superior/lateral third, zone II – the central third, and zone III – the inferior/medial third (Figure 1.14).<sup>127</sup> The studies described above are good evidence that although there is debate about which radiolucent lines are of concern radiolucent lines are reliable indicators of an increased likelihood of early implant failure.

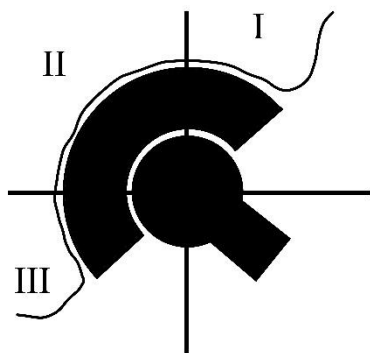


**Figure 1.14** Acetabulum zones described by DeLee and Charnley.<sup>127, 129</sup>

Kneif *et al.* investigated how the location of a RLL affected the risk of early implant migration. A review of the immediate post-operative and 6-month radiographs of 46 patients indicated that RLLs in zone III on the immediate post-operative radiograph and the 6-month radiograph are positively and significantly associated with implant migration. They found no significant correlation for RLLs on zone I or II.<sup>129</sup> Garcia-Cimbrelo *et al.* performed a more extensive study that included 452 hips, all of which used the Charnley low-friction arthroplasty. The average follow-up time was twenty years. The demarcation system used was initially described by Hodgkinson *et al.*<sup>130</sup> Radiographs taken at the most recent follow up showed that 5 % of acetabular cups with no demarcation on the immediate post-operative radiograph had migrated; 11 % of cups with demarcation in zone 1 had migrated, 35 % of the cups with demarcation in zones 1 and 2 were loose and 72 % of cups with demarcation in all zones had migrated.<sup>131</sup> In a review study Ritter *et al.* retrospectively reviewed 185 cemented Charnley total hip arthroplasties to determine whether there was a correlation between radiological findings and failure of THA components. The mean follow up was 11.7 years. They found that with radiological demarcation in zone I the incidence of loosening was 28.21 %, with no demarcation in this zone the risk of loosening was 0.69 %. They emphasise that careful cementing is crucial for a successful THA.<sup>132</sup> DeLee and Charnley also reported that radiological demarcation increased the risk of later implant loosening.<sup>127</sup>

Other authors have suggested that it is a *progressive* RLL which is indicative of later loosening. Iwaki *et al.* investigated the significance of RLLs on the femoral interface and found that it was only progressive lines that were significantly associated with later loosening of implants.<sup>133</sup> Strömbärg *et al.* reported that in a review of 61 loose stems, 23 loose acetabular cups and 42 controls, radiolucencies that developed within the first postoperative year were indicative of later loosening, however, an unchanged radiographic appearance meant the that risk of later loosening was small.<sup>134</sup>.

All the previous reports agree that the radiographic appearance of the cement-bone interface can be used to identify whether a THA is at risk of later loosening. The studies described used similarly rigorous control mechanisms to ensure that the findings are valid and therefore it is believed that the radiographic appearance of cemented THRs can be used to identify factors that may affect the longevity of THA implants. A survey performed by Lieberman *et al.* investigated the follow-up routines of surgeons and report that the average time until the first follow-up visit was 4.9 weeks after surgery with 63 % seeing their patients within 6 weeks.

They also report that 90 % of respondents saw patients one year after implantation.<sup>135</sup> There is concern regarding the efficacy of standard radiographs in identifying flaws in the cement mantle. Reading *et al.* performed simulated THA on cadaver femurs and used standard radiographs to identify flaws, they then sectioned the femurs and used faxitron radiography (a higher resolution than standard film) to determine the true number of flaws. They found that defects were found up to 100 times more frequently using the faxitron images than standard film.<sup>136</sup> Claus *et al.* implanted hips into cadavers and took radiographs of the implanted component, they then removed the components, created defects, reinserted the complex and then took radiographs. This was repeated two more times, each time the defect was enlarged. A blinded orthopaedist then assessed the radiographs to determine the presence and size of the defects. It was found that the sensitivity of the detection of osteolysis on a radiograph was 41.5 %. This sensitivity was significantly affected by the location of the defect. They concluded that overall an experienced orthopaedist identified only 73.6 % of the defects, however, once one is identified it is highly likely that it is a true defect.<sup>137</sup> Using radiographs to monitor patients after having total hip replacement surgery is the standard practice. Although Reading *et al.* and Claus *et al.* identifies concerns regarding whether radiographs are sufficient for detecting flaws at the bone cement – bone interface, they found that there is actual *more* flaws found when more sophisticated forms of measurement are used. It is believed that this conclusion does not call into question the findings that radiolucent lines at the bone cement – bone interface are positively associated with early loosening of components. Caution should be taken and further investigation into the relationship between RLLs and early component loosening using higher quality methods of observation would be welcomed; this would further confirm this fundamental assumption that almost all work to improve this interface has been based upon.

There is reason for concern regarding the cause of RLLs. Especially those that develop soon after implantation. As Charnley remarked, the fact that not all THR's develop RLLs implies that it is not an inherent defect due to the cement. There are no studies investigating whether a particular cement or implant is the primary cause. Therefore, it is believed that whether an implant develops a RLL is dependent on either the individual patient or the surgical technique. The work done Barrack *et al.*, Mulroy and Harris, DeLee and Charnley, Kneif *et al.*, Garcia-Cimbrello *et al.*, Ritter *et al.* and Iwaki *et al.* is fundamental to all subsequent work and it is felt that the rigorous methodology and large sample sizes mean that confidence can be placed in their conclusions. However, the lack of investigation into other variables such as the implant used, the surgeon, the operative and patient demographics<sup>127</sup> mean that a meta-analysis should be performed using the data available from these studies.

### **1.6.1.2 Explants**

To understand the mechanism of how RLLs develop it is important to look at what they are. This can be done by examining the tissue at the cement-bone interface at revision surgery or at autopsy. Goldring *et al.* published a study that performed histologic analysis on RLLs for 85 patients undergoing revision. The tissue found at the site of RLLs was organised into a synovial-like lining and there was an invariable presence of particulate implant material; including PE wear particles and PMMA particles; both surrounded by macrophage giant cells which are associated with tissue reformation. This would explain the bone resorption occurring at this interface and progressive loss of fixation.<sup>138</sup> Further to this, Han *et al.* reported that the extent

of UHMWPE wear is significantly correlated with the incidence and extent of osteolytic lesions.<sup>139</sup>

Schamzried *et al.* presented findings regarding the mechanism of loosening of acetabular components. The study involved analysis of 14 cemented polyethylene acetabular components from 11 patients at autopsy which had been *in situ* for between 4.8 and 17.5 years. They state that the final RLL invariably involves resorption of the trabecular bone from the cement-bone interface. They report no cement fragmentation or particulate PMMA near the transition zone, where healthy interface and soft tissue meet. Instead, they state that the transition zone is characterised by “a cutting wedge of bone resorption containing macrophages, small extracellular, and intracellular polyethylene particles within macrophages”; due to this, the authors believe that late aseptic loosening of the acetabular socket is biological in nature.

The authors detail a sequence of events that their data suggests takes place: polyethylene wear particles are generated at the articulating surfaces which become dispersed within the synovial fluid. The small particles can penetrate small gaps between the cement and the bone at the intraarticular edge of the cement-bone interface. These particles trigger an immune response and thus bone resorption. This resorption of bone at the very edge of the cement-bone interface allows more and larger particles to penetrate deeper into the interface (Figure 1.15). This progressive process eventually results in visible RLLs in zone I and zone III and eventual global radiolucency and aseptic loosening. This is evidenced in this article by the soft tissue layer being generally thickest at the articular margin and becoming thinner towards zone II.<sup>140</sup> However, this study did not consider RLLs that appear on the immediate post-op radiograph where there has been no time for the generation of PE wear debris.

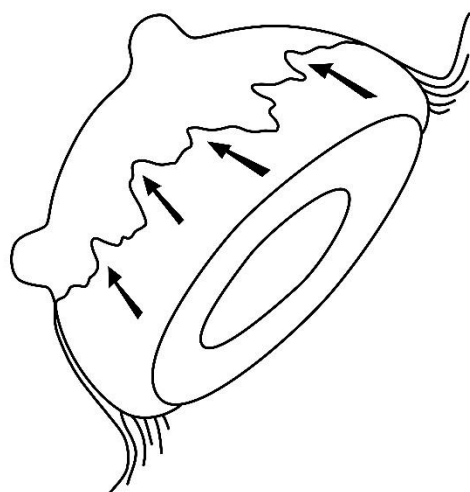


**Figure 1.15** The mechanism of late aseptic loosening of cemented acetabular components, showing the penetration of HDP progressing around the acetabular cup.<sup>140</sup>

It may be argued that because not all implants develop a RLL, progression of events can be prevented or slowed significantly. Delee and Charnley made this point and highlighted that of the 141 low friction arthroplasties followed up at 10.1 years, 69 % showed no demarcation, this means that it is not a fundamental defect of PMMA bone cement that causes RLLs but other variables.<sup>127</sup> It would also be advantageous if the wear debris generated at the articulating was

not biologically active, Liu *et al.* showed that particles smaller than 50 nm did not elicit a biological response.<sup>141</sup>

A review by Jiang *et al.* further details the biological pathways that occur in the body due to the production of wear debris. All evidence suggests that it is the imbalance between bone formation due to applied loads and bone resorption triggered due to foreign bodies (wear particles) which leads to progressive aseptic loosening of cemented components.<sup>142</sup> An investigation comparing the amount of PE wear and the extent of bone resorption that occurs due to the activity level of the patient would be of interest.

### ***1.6.2 Surgical Preparation***

Surgical preparation is a key factor in the operative technique.

#### ***1.6.2.1 Temperature of Components***

The pre-heating or cooling of components is not frequently discussed in reviews of modern operative techniques for cemented acetabular implantation.<sup>143-145</sup> However, it has been the subject of many studies.

Rodop *et al.* investigated the effects of pre-cooling the femoral stem on the maximum temperature of the bone cement. They found that pre-cooling the stem to less than -8°C resulted in a decrease of the maximum curing temperature of cement by approximately 7°C and does not affect the setting time.<sup>146</sup> Wykman *et al.* used water cooling in 19 patients to attempt to reduce the maximum temperature reached due to cement curing. They found that water cooling reduced the number of incidences where the PMMA bone cement temperature exceeded 44°C.<sup>147</sup> DiPisa *et al.* found that cooling the acetabular component to -84 °C, reduced the maximum temperature reached by the cement from 70 to 49 °C and also increased the setting time by 5.5 minutes.<sup>58</sup> In a chapter in the book “The Well Cemented Total Hip Arthroplasty” edited by Breusch, Spierings states that pre-chilling the cement increases the setting time of the cement so that the surgeon has more time to perform the procedure.<sup>148</sup> Koh *et al.* found significant variation in the setting time of the cement depending on how long it was allowed to equilibrate with the temperature of the operating theatre. They recommend having storage with temperature and humidity control for the cement, surgical instruments, and implants and to have clearly defined protocol to ensure standardisation of procedure and therefore reproducible setting times.<sup>149</sup>

Altering the temperature of the components may also affect the mechanical properties and the porosity within the cement. Palletier *et al.* investigated the effects of cement temperature on the pore distribution and the mechanical properties. They found that mechanical properties were improved, the radius of the pores increased, and the concentration of pores increased at the centre of the cement when the cement was cured at 50°C rather than room temperature. The authors advocated heating components.<sup>150</sup>

Iesaka *et al.* preheated the femoral component to 37°C and performed a mock *in vitro* cemented femoral implantation. They found an increased shear strength of the cement-prosthesis interface, fatigue properties were significantly improved and there was a >99% decrease in

interface porosity. The setting time decreased 12 % but the maximum cement polymerisation temperature increased by 6 °C.<sup>151</sup>

Bishop *et al.* investigated the effect of heating the femoral component so that polymerisation occurs faster at the prosthesis – cement interface to try and trigger the cement to shrink onto the stem and thus ensure a secure bond at this interface. They pre-heated the stem to 44 °C and implanted it using PMMA bone cement into a human cadaver kept at 37 °C. They found that the porosity at the prosthesis – cement interface was reduced and that the temperature recorded at the cement-bone interface showed a negligible increase.<sup>7</sup> Li *et al.* used a mathematical model to predict how pre-heating and pre-cooling would affect polymerisation. They found that pre-cooling the component significantly reduced the maximum curing temperatures, but it also increased time till full cure. If the prosthesis was heated, polymerisation starts at the cement-implant interface and progresses towards the bone. This may reduce the formation of voids at the cement – prosthesis interface.<sup>152</sup>

### **1.6.2.2 Surgical Approach**

The surgical approach to THA may affect the complication rate. Aggarwal *et al.* compared five commonly used surgical approaches and investigated any correlation with the incidence of complications. This study followed up on 3574 patients, all of whom had at least two years of follow up data available. They report that the posterior approach had a lower rate of complication.<sup>153</sup> Graves *et al.* investigated how surgical approach affected patient-reported function after primary THA. They compared the patient-reported function of a direct anterior approach with a posterior approach. The results were similar for both approaches, for the direct-anterior approach, there was a slight improvement in patient-reported functionality at 3 months but there was a greater blood loss during surgery.<sup>154</sup> Madsen *et al.* investigated the effect of the surgical approach on the gait mechanics of patients 6 months following surgery. The gait of most (85%) of the patients 6 months after surgery had not returned to normal. The authors state that the differences in gait due to the surgical approach were significant but the clinical significance and persistence of the difference past 6 months is unknown.<sup>155</sup>

### **1.6.2.3 Bone Removal and Cleaning**

In THA, the cartilage and cortical bone are removed from the acetabulum, exposing the trabecular bone. An acetabular reamer looks like a hemispherical cheese grater that is attached to the end of a drill. A commonly debated question is whether the subchondral bone plate should be removed in cemented THA. It has been identified as part of improved cementing techniques.<sup>156</sup> Reaming exposes more porous bone into which cement can be forced; however, removal may result in a weakening of the implant complex. Vasu *et al.* found that the tensile stresses were greatest near the superior roof. They state that due to this, the cup would grip the top of the femoral head.<sup>157</sup> Retention of the subchondral plate would provide more resistance to deformation. The main argument for removal is that it exposes more of the porous trabecular bone that the bone cement can penetrate into and thus achieve a better interlock. Poor interlock has frequently been identified as a contributor to the failure of THA.<sup>158</sup> Flivik *et al.* performed a randomised controlled trial using 50 patients diagnosed with primary osteoarthritis. The patients were split into two groups: one group would have the subchondral plate removed and

the other it would be preserved. They found that removal of the subchondral plate resulted in a better radiographic appearance and fewer RLLs. No other differences were found in clinical follow-ups.<sup>159</sup> Once the top layer of bone is removed, anchorage holes are drilled which expose more of the porous trabecular bone.<sup>44, 143</sup>

The Rim Cutter is a device that cuts a regular rim into the naturally irregular rim of the acetabulum. It was designed to assist the surgeon in the placement and alignment of the acetabular cup and make a regular gap between the rim of the cup and the acetabulum so that cement could be better pressurised. Conroy *et al.* performed a randomised control trial to assess the effect of using a rim cutter device. They measured a significant increase in the depth of cement penetration in zone I and an increase in the thickness of the cement mantle in zone II and zone III and a reduced incidence of the cup making contact with the acetabular bone bed.<sup>160</sup> Darmanis *et al.* compared the radiographs of 90 patients who underwent cement THA. They found that cups implanted alongside the use of the rim cutter had a more anatomically accurate centre of rotation, a thicker and more uniform cement mantle and a reduced incidence of RLLs.<sup>161</sup> Smith *et al.* investigated the effects of using the rim cutter on the pressures generated in the acetabulum and on the penetration of cement into the bone in an *in vitro* experiment. They found that the use of the rim cutter significantly increased the pressure at the pole of the acetabulum (zone II) and increased penetration of cement at the rim of the acetabulum (zones I and III).<sup>162</sup> Baker *et al.* performed a radiographic review of 150 patients who had received a cemented THA; the rim cutter was used in 75 operations and not in the other 75. They found that components that were implanted using the rim cutter technique had significantly more RLLs.<sup>163</sup> The efficacy of the rim cutter is still contested, if sufficient data were collected by the registries, a conclusion about the efficacy of the rim cutter could be reached.

Dorr *et al.* investigated the effect of several factors on the depth of cement penetration achieved using 16 tibiae from cadavers. Samples were prepared by exposing the cancellous bone and cleaning using either pulse lavage or a syringe and needle. Once the cement was fully cured the depth of cement penetration was measured using a radiograph. The authors found that pulse lavage resulted in more cement penetration when the cement was in a low viscosity state at 1 minute, this difference was statistically significant.<sup>164</sup> Lavage of the bone bed removes much of the remaining soft tissue on the acetabulum creating a higher quality interface between bone and cement. Halawa *et al.* investigated the effects of the surgical procedure on the shear strength of the cement-bone interface. They used cadaver femurs and found that thorough cleaning of the trabecular bone increases the shear strength of the interface.<sup>165</sup> Krause *et al.* used proximal tibias from human amputate limbs to investigate the effect of thorough brushing and high lavage. They found cleaning increased the fixation strength. They say that this is due to the cement being able to penetrate pores that would otherwise be blocked by cutting debris.<sup>166</sup> Majkowski *et al.* used bovine femurs to investigate the effects of cleaning the bone and found an increased cement penetration and strength when the bone is cleaned. Without cleaning the mean penetration was 0.2 mm and the shear strength was 1.9 MPa. With pressurised lavage, the penetration of cement was 4.8 – 7.9 mm and the strength was 26.5 MPa and 36.1 MPa.<sup>167</sup> In a review of Swedish national hip arthroplasty registry data Malchau *et al.* found that pulsatile lavage significantly reduced the risk of implant loosening.<sup>168</sup>

#### **1.6.2.4 Blood Management**

Majkowski *et al.* investigated the effect of bleeding on the cement-bone interface in an *in vitro* study. They found that the shear strength was reduced significantly in half of the interfaces due to the presence of bleeding although they found no significant difference in the cement penetration.<sup>16</sup> Juliusson *et al.* compared the depth of cement penetration *in vivo* using a small hole drilled for the purpose of the study. In 32 cases, they found that penetration increased approximately 100 % in the absence of blood flow.<sup>169</sup> Benjamin *et al.* investigated the effect of blood flow on the penetration of cement in an *in vitro* study which used Perspex cylinders to simulate the femoral shaft. The holes used to simulate the penetration of cement into bone were 1 mm in diameter. They conclude that bleeding may not just compromise the bone-cement interface but also the cement itself.<sup>17</sup>

Hypotensive anaesthesia has been highlighted as a way of enhancing the quality of the interlock at the cement-bone interface by reducing the flow of blood.<sup>170</sup>

#### **1.6.3 Cement Mixing Techniques**

As previously discussed, RLLs are a good indicator of failure and some authors have linked their development to surgical technique. Therefore, a full review of all cement preparation techniques will be presented here.

##### **1.6.3.1 Vacuum Mixing**

Pores present within the cement matrix act as crack nucleation sites, they also lower the cross-sectional area of the cement mantle and therefore create larger stresses. Vacuum mixing has been suggested to reduce the porosity. Lewis performed *in vitro* tests comparing the strength of hand mixed and vacuum mixed cements. The samples were prepared to ASTM F451-95 specification. The author found that the fatigue performance of bone cement is significantly improved when the cement is mixed under vacuum.<sup>171</sup> Lidgren *et al.* investigated the effect that vacuum mixing had on the fracture strength, maximum deflection, modulus of elasticity, and hardness. They found that all the above were improved when vacuum mixing is used compared to when the cement is hand mixed. They used ASTM standards for all mechanical testing.<sup>172</sup> Wang *et al.* performed *in vitro* testing of cements mixed under different vacuums from 0.05 bar to 1 bar (absolute). They found a statistically significant reduction in the number of voids and micropores with a decreased vacuum pressure. They also measured an increase in the density of the cement with decreasing pressure.<sup>173</sup> Wixon *et al.* mixed cement under a partial vacuum and found that the porosity of the cement was less than 1 % and the tensile and compressive strength were improved. The tensile fatigue life was also increased when the cement was vacuum mixed.<sup>174</sup> Mau *et al.* performed *in vitro* tests to investigate how different vacuum mixing systems affect porosity. They reported that the lower the number of opportunities for air entrapment the lower the porosity, in this respect Cemvac and Optivac cement mixing systems performed well.<sup>175</sup>

Coultrup *et al.* used computational modelling and found that cement porosity had very little effect on the fatigue performance of bone cement mantles. However, a thinner mantle and a cup that has been inserted further into the natural socket are both correlated with worse mechanical

performance.<sup>176</sup> In an *in vitro* study, Hansen and Jensen investigated the effect that the mixing method had on the mechanical properties of bone cement. They used the “proposed standards” but do not say which standards they use. They found that vacuum mixing did not have a significant effect on the ultimate compressive strength, four-point bending strength, and bending modulus.<sup>177</sup> Macaulay *et al.* compared the mean pore size and mean porosity of Simplex P when it is vacuum mixed or mixed at atmospheric pressure. They found no significant difference in mean pore size nor mean porosity due to mixing pressure.<sup>178</sup> Mitchell *et al.* reported that they found no difference in pushout strength or cycles to failure due to the method of mixing but found significantly more void area at the implant cement interface for Palacos R and Osteobond cements. Overall, they conclude that vacuum mixing does not significantly reduce interface porosity nor does it improve the mechanical properties.<sup>179</sup>

Using data from the Swedish national hip arthroplasty registry, Malchau *et al.* reported that the use of vacuum mixing increases the risk of revision for the first 4-5 years after operation but after this time the use of vacuum mixing significantly decreases the risk of revision when compared to hand mixing.<sup>168</sup> In a chapter in “The Well-Cemented Total Hip Arthroplasty” Jian-Sheng Wang summarises that overall, the addition of vacuum mixing to contemporary cement preparation techniques is positive.<sup>180</sup>

### **1.6.3.2 Centrifugation**

Davies *et al.* measured the effect that centrifuging cement had on the porosity and fatigue life of five cements. They conclude that the fatigue properties of cements are primarily determined by the chemical composition; and secondly, that every time the porosity of the cement was reduced successfully using centrifugation, the fatigue life also improved; however, centrifugation is not effective at reducing the porosity in high viscosity cements.<sup>181</sup>

The nature of the porosity of PMMA bone cement was measured by Macaulay *et al.*. They found that overall there was no difference in the mean pore size or mean porosity between hand mixed and centrifuged cement.<sup>178</sup>

Burke *et al.* report that centrifugation successfully reduced the porosity of the cement tested, it also improved the UTS by 24%, ultimate tensile strain by 54 % and an increase of 136 % for the fatigue life. They also report that there was no change in elastic modulus or the setting properties and the toxicity was not affected.<sup>182</sup>

Davies and Harris investigated how centrifugation of PMMA bone cement affected the diametrical shrinkage, hypothesising that if the porosity is reduced, the reduction in the external dimensions would have to account for the bulk and heat shrinkage. They also measured the fatigue life of the cements. They found that a reduction in porosity improves the fatigue strength and that there is no resulting reduction in the external dimensions.<sup>183</sup>

Hansen and Jensen investigated the effects of cement mixing method in an *in vitro* study. They found that centrifuging the cement improved the ultimate compressive strength. They also reported improved ultimate bending strength and stiffness for Palacos brands. They said that the experiments were performed with the “proposed standard”. They seem to be referring to ISO 5833.<sup>177</sup>

#### 1.6.4 Pressurisation

Askew *et al.* performed an *in vitro* study investigating the effect of cement penetration and the bone strength on the quality of the cement-bone interface. They performed tests on 71 human specimens. The pressure applied to the cement was reported to be 8, 16, 39, 76, and 172 kPa and the time from mixing to pressurisation was  $90 \pm 5$  seconds. The pressure was applied for either 5 or 30 seconds. The sample was loaded in tension until failure with a maximum stroke rate of 15 mm/min. The bone specimens were also compressively loaded to failure at a maximum stroke rate of 0.4 mm/min. The authors report that the duration of pressure applied was not a significant factor for the penetration of cement nor the fracture load. They also state that there is an optimal penetration depth of about 4 mm as there is no significant increase in the load capacity after this depth and the pressure required to achieve this penetration depth was 76 kPa for most cases. The strength of the cement-bone interface is also dependent on the bone strength.<sup>184</sup>

Factors affecting the strength of the cement-bone interface were investigated by Krause *et al.*. They obtained human bone samples from the proximal tibias of patients who had undergone amputation, various degrees of bone cleaning were performed from as cut, to high intensity pulsating lavage. When the cement was applied to the bone, approximately 3 minutes after mixing it was either gently finger packed or was applied using a pressurising system achieving a cement pressure of roughly 17 kPa. Once the cement had cured, the samples were placed into a test jig and loaded in tension at a maximum stroke rate of 254 mm/min. The shear strength of the interface was also tested with a maximum stroke rate of 12.7 mm/min. The authors report that the pressurised cement had a deeper penetration into bone than finger packed cement and that more penetration was achieved with a clean bone. The interface of the pressurised cement samples was significantly stronger in tension than those that were finger packed. The shear strength of the interface was improved when the bone was cleaned using lavage compared to the as cut samples for the finger packed cement.<sup>166</sup>

Markolf *et al.* performed *in vitro* experiments to measure how the magnitude of applied pressure affected the flow rate of PMMA bone cement. They found that even small increases in the applied pressure significantly increased the flow rate of cement through a 1.1 mm orifice.<sup>185</sup>

Walker *et al.* used various methods to investigate the penetration of cement into cancellous bone. A retrospective radiographic study of 45 radiograph sets was performed which measured the depth of cement penetration and measured any RLLs that had developed. However, it has been shown that radiographic observations are not reliable in detecting defects within cement mantles; therefore, the measurements in this study may not be reliable. They also performed *in vitro* tests. They used prepared human cancellous bone for testing. The pressure applied to the cement and the time of cement application was varied: 17, 34 and 52 kPa applied at 2, 4, and 6 minutes after mixing. This methodology reflects the timings and pressures used in surgery. The samples were placed under an increasing tensile load until failure at a maximum stroke rate of 60 mm/min. They do not provide a reason for this stroke rate. From the radiographic study, the authors report that the more penetration of cement the fewer RLLs develop. Although, as previously stated, this conclusion is weakened by the method of measurement. This is evidence that it is the surgical technique that is the primary factor in the development of RLLs. For the penetration tests the authors report that there was a correlation between the depth of cement penetration and the average pore diameter of the bone, the pressure applied and the time the

cement was applied. This is evidence that the patient characteristics determine whether RLLs will develop; a dense network of trabecular bone will mean that the cement will not penetrate as deep and therefore more RLLs will develop. It is also evidence that the pressurisation technique affects the strength of the interface. In the discussion, the authors highlight that there was significant scatter in the data and there was a low statistical correlation between an increasing cement depth and the resulting cement strength after the first millimetre of penetration was achieved. This is evidence that the strength of bone cement-bone interface can be improved through increasing the penetration of cement into bone; although the weak statistical correlation should be considered when using the conclusions from this study. They state that the optimal cement penetration range is between 3 – 4 mm; however, the data presented is limited, it is difficult to outline an “optimal penetration” as there are many factors including patient age, bone strength, activity level that all affect how strong the fixation will be.<sup>186</sup>

MacDonald *et al.* performed experiments on proximal femurs in dogs which investigating the effect of penetration of cement on the shear strength of the cement-bone interface. The dogs were anaesthetised and operated on. An increase in the depth of penetration of cement into bone increases the strength of the cement-bone bond and the strength is also dependent on the cement used.<sup>187</sup>

Juliusson *et al.* investigated how the magnitude of applied pressure and the time of cementation affected the depth of cement penetration in an *in vivo* study. In 32 total hip arthroplasties. The application of pressure to the cement was done for 20 seconds with a random schedule of pressures of 0.1 MPa, 0.2 MPa, and 0.3 MPa. The authors found that to achieve “optimal penetration of 3 – 5 mm<sup>188</sup>” at least 200 kPa of pressure must be generated in the cement.<sup>169</sup>

#### **1.6.4.1 Pressurisation Devices**

The previous section presented papers investigating the link between pressurisation, penetration of cement into bone and the resulting strength of the cement-bone interface. The overall agreement of these studies was that the cement should be pressurised to improve the quality of the cement-bone interface. This is because the interdigitation of PMMA bone cement into the bone is the only form of fixation at this interface. Therefore, it is important that upon application of a pressurisation device to the doughy cement during surgery a cement pressure sufficiently large enough to force the cement into the bone is crucial. How this pressure is generated is not as significant as the fact that it is generated. As will be discussed in the following paragraphs, most acetabular pressurisers generate a pressure through sealing the doughy cement in the acetabulum and, upon application of a load by the surgeon, reducing the volume where the cement is contained thereby increasing the pressure of the cement and forcing it into the exposed trabecular bone.

Oh *et al.* designed an acetabular cement compactor that aimed to pressurise the cement by sealing the acetabulum and reducing the volume within the sealed area. This was achieved through a device that, when pressed against the acetabulum rim, contains the cement by a silicone-based seal pressed against a rubber sheet, a trigger is pulled which extends a central plunger and thus pressurises the cement (Figure 1.16). The authors used a human cadaveric specimen fitted with five pressure transducers at: the ilium, roughly zone I, the ischium, zone

III, the keying hole and the “base” but it is not known where this may be. The pressure at all locations except the keying hole had an increased pressure when the compactor was used. Pressures ranged from 113 – 149 kPa using the compactor and 8 – 53 kPa for finger packing in all locations except the keying hole where pressures of 233 kPa were measured. The authors do not clarify whether these pressures are averages or maximums, but these figures are large if they are averages. They also measured the intrusion depth of cement: use of the cement compactor resulted in a statistically significant increase in the measured cement intrusion depth.<sup>189</sup>

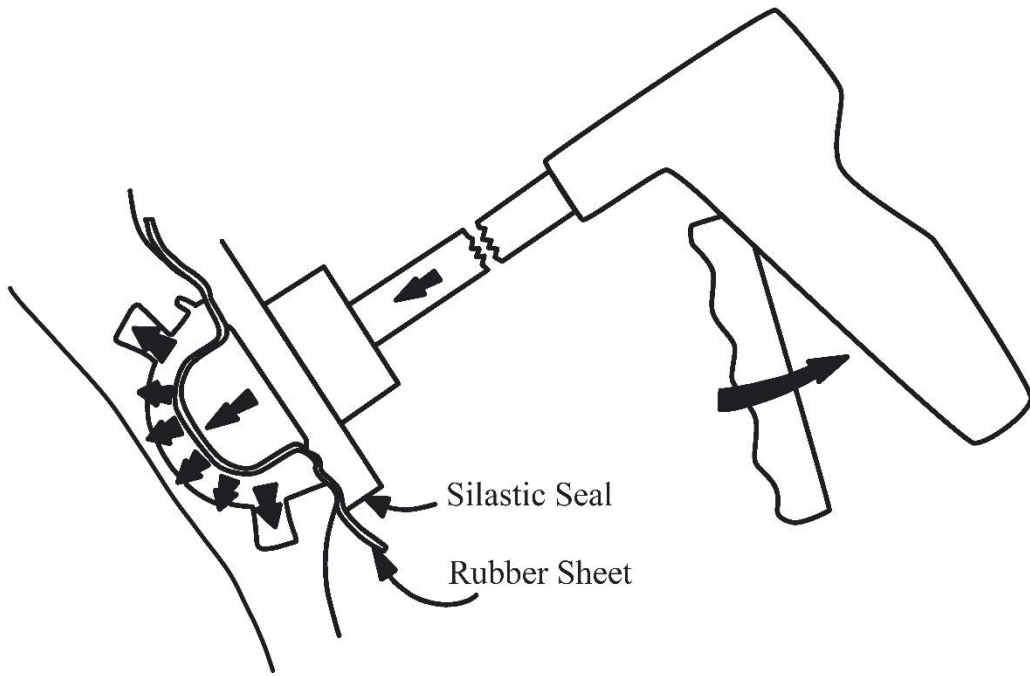


**Figure 1.16** Drawing showing use of the acetabular compactor designed by Oh *et al.*<sup>189</sup>

Wadia *et al.* investigated the pressures and intrusion achieved by several designs of pressuriser including one designed by the authors. Representations of the three designs of pressuriser tested can be seen below (Figure 1.17). The first two are representative of commonly used pressurisers – the Depuy pressuriser and the Exeter pressuriser. The third pressuriser is a novel design that was designed by two of the authors of the paper. It consists of a hollow cylinder to which the silicone head is attached, inside the cylinder is a central plunger when the pressuriser is placed against the acetabulum rim it seals the cement within the acetabulum, a load is then applied to the central plunger, forcing the silicone head to extend and reduce the volume within the acetabulum and thus pressurise the cement. A pressure transducer was mounted at the pole and a transverse ligament notch was cut into the rim of the mock acetabulum, but no details of dimensions are given. Holes of diameter 1.5 mm were drilled at regular intervals between the pole and the rim so that penetration of cement could be measured. The cement was vacuum mixed and inserted into the model by hand.

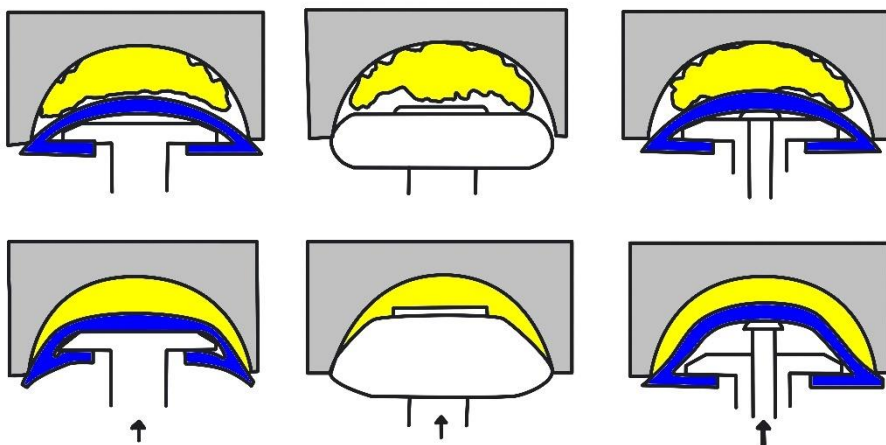


**Figure 1.17** (left) Representation of the cement mantle produced by the DePuy T-handle pressuriser. (centre) Representation of the cement mantle produced by the Exeter pressuriser. (right) Representation of the cement mantle produced by the plunger T-handle pressuriser.

The authors report that the cement mantle thickness produced using the pressuriser they designed was more consistent than the other designs of pressuriser, although the acetabular cup still needs to be inserted so mantle uniformity is not a key parameter for the pressuriser. Cement intrusion was consistent for the novel design of pressuriser but was often less than what was achieved with the other pressures but due to the presentation style, it is difficult to properly compare results. The authors do not provide pressure profiles for the Exeter style pressuriser but claim that the maximum pressures are consistently higher with their novel design of pressuriser. This study has numerous flaws, but most crucially, the load applied to the pressuriser is not controlled; therefore, many biases may be introduced and neither the pressures nor the intrusion depths can be reliably compared.<sup>190</sup> This is frequently the trade-off for more clinically relevant experiments.

Lee and Ling describe a device that is designed to “improve the extrusion of bone cement”. The device was designed to seal the acetabulum to prevent cement escape and thus allowing pressure to be applied to the cement, forcing it into the bone. It consists of a balloon that is connected to a piston and handle. When the handle is pulled the fluid is driven into the balloon and thus it inflates (Figure 1.18). However, there is no scientific data provided with which to properly assess the pressuriser. The authors conclude that the device improved the intrusion of cement into the bone and reduces lamentations caused by finger pressing. They also state that the pressuriser is made by Howmedica and has been in frequent use for two years.<sup>184, 191</sup>

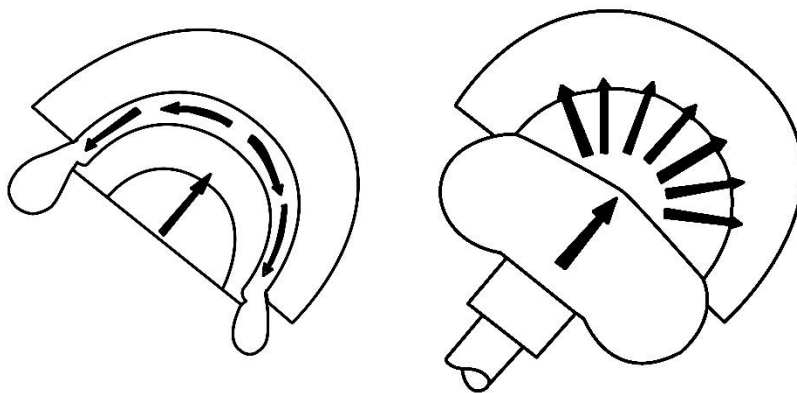


**Figure 1.18** (left) Insertion of the acetabular cup causes bone cement to be driven out of the acetabulum, around the cup margins. (right) Pressuriser seals acetabular margin and develops extrusion pressure in the cement.

Flivik *et al.* state that as the pressure required to achieve optimal cement penetration is so high (The authors previously measured that 200 kPa of pressure is required to achieve optimal penetration of cement into bone.<sup>169</sup>) keying holes should be sequentially filled to achieve the pressure and then cement added to the acetabular cavity to connect all the cemented holes and the packed together using a compressor. They performed the experiments on 14 patients receiving THA's. The patients were randomly assigned a pressurisation technique. They either used a conventional pressuriser (Richards, Smith-Nephew, Memphis, TN) which resembles a DePuy Pressuriser, or they used the injector and the sequential method. The authors provide the mean and peak pressures of each of the techniques. There were no significant differences in the pressures achieved due to the pressurisation technique used; however, sequential cementation resulted in significantly more penetration at the keying holes 0.65 mm vs 2.8 mm although it is not clear what caused this difference. For the sequential pressurisation technique, injection of cement into the holes and therefore pressurisation started 1 minute and 45 seconds after mixing. The compressor was applied at 2.5 minutes after mixing. The conventional pressuriser was applied 2.5 minutes after mixing. It is likely that these results are a result of the earlier application of cement, whilst it is in a lower viscosity state.<sup>192</sup>

Bernoski *et al.* developed a pressuriser with two notable features: a flap to seal the transverse ligament notch to minimise cement escape, and a central plunger that can be advanced to generate pressure within the cement in the acetabulum once it has been sealed (Figure 1.19). They performed *in vitro* testing of the new device using a Sawbone model acetabulum (Sawbones Europe, Malmö, Sweden) which was fitted with pressure transducers at the pole and at the rim. The cement was inserted into the model four minutes after mixing and a force of 210 N was applied to the device: a pressuriser without flap, a pressuriser with a flap, and an acetabular cup with a flange and cement spacers to prevent bottoming out. The authors only report the peak values for the pressure which do not adequately detail the pressurisation process. Both pressurisers maintain pressure better than when the cup alone is used. Statistical analysis showed that the pressuriser with a flap produced significantly higher pressures at the pole. At the rim, the pressuriser with flap produced the largest peak pressures, the pressuriser without flap produced the second-highest pressures and the cup alone produced the smallest peak

pressures, all differences were statistically significant. It is difficult to draw any conclusions from this test as no mean pressures were reported.<sup>193</sup>

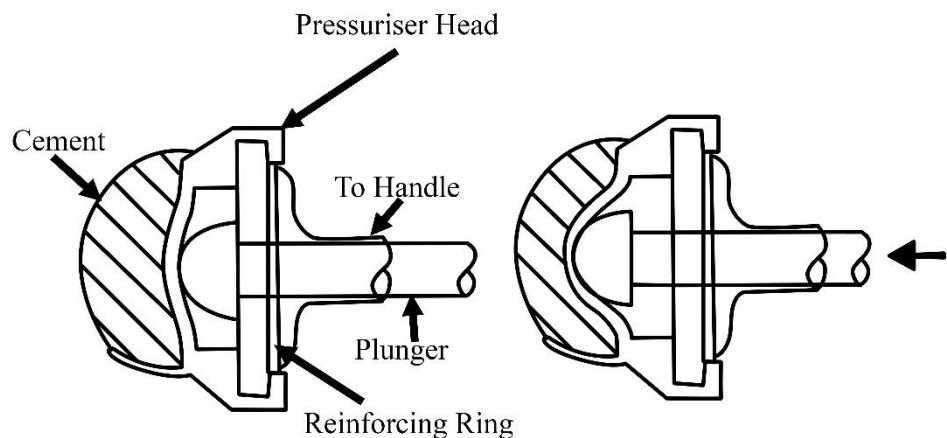


**Figure 1.19** Cross-sectional drawings of the new pressuriser (A) before and (B) after the advancement of the central plunger designed by Bernowski *et al.*<sup>193</sup>

Parsch *et al.* published a report which directly compared the pressures and the penetration of cement achieved when using the two commonly used types of pressuriser: the Bernowski (similar to Depuy) and the Exeter. The pelvises were fitted with a system that would simulate a back-bleeding pressure of 25 – 30 mmHg. Three pressure transducers were loaded in the DeLee – Charnley zones I, II and III. After the cement was mixed and inserted, a load of 60 N was applied to the pressuriser for approximately 2.5 to 3 minutes. The peak and sustained pressures were calculated from the raw data. Radiographs were taken to determine if there were any RLLs in between the cement and the bone. The depth of cement penetration was measured. The authors state that both pressurisers achieved the minimum requirements for optimal cement penetration. They also state that the sustained pressure “tended” to be higher for the Exeter pressuriser, but this difference was not statistically significant. The penetration achieved at all locations was between 2.00 mm and 3.62 mm but once again, there was no significant difference between the pressurisers tested.<sup>194</sup>

New *et al.* designed a pressuriser that would measure the pressures of the acetabular cement during the surgery. The device consisted of a DePuy pressuriser which had a pressure transducer mounted inside. The instrumented pressuriser was used by two surgeons performing THA, data was collected for 16 operations. There was no difference between the surgeons for the mean or the peak pressures. They conclude that these *in vivo* measurements for pressure are comparable to *in vitro* measurements; therefore giving validation to *in vitro* testing and showing that this instrumented device is suitable for achieving optimal cement pressurisation.<sup>195</sup> The author believes that more experiments are required to confirm this. The data presented indicates that this conclusion is valid. The pressure transducer was calibrated and was shown to be indicative of pressures generated at the pole of the acetabulum. More details of the calibration are required to have more confidence in the findings. Further experiments should be performed to test the conclusions as it is a fundamental assumption of instrumented pressurisers that the measured pressures are equivalent to cement pressures generated *in vivo*.

The limited literature investigating pressuriser designs is surprising as acetabular pressurisers are a consistent part of contemporary cementing techniques. Of the papers that are available, most do not have sufficient control over the variables, and many do not report the data in sufficient detail. It is difficult to objectively determine which acetabular pressuriser is the best to use, especially without registry data.

#### 1.6.4.2 *Vibration*

As seen previously, bone cement is subject to shear thinning, that is, increasing the rate of deformation reduces the viscosity. Application of vibration whilst the bone cement is being pressurised or whilst the acetabular cup is being inserted may result in more cement penetration or a higher quality of contact between the cement and bone.

Drew *et al.* performed *in vitro* experiments using a model femur with a reamed cavity and holes for cement penetration and a mock femoral stem. A force was applied to the femoral stem so that it would be inserted at a constant speed. In some of the tests, a vibration was also applied. The authors report that optimum cement penetration of 4 mm was achieved with an applied frequency of 19 Hz. Without vibration, the maximum force applied to the stem was 185 N and with frequency, the maximum force was approximately 125 N.<sup>196</sup>

In a letter to the editor of *The Lancet*, Thomas *et al.* reported that, in an *in vitro* study, increasing both the amplitude and the frequency of vibration applied to bone cement during implantation resulted in significant increases in the extent of cement flow. The scope of this experiment is limited but the results show that vibration during the application of cement in arthroplasty surgery has the potential to increase the quality of the cement-bone interface.<sup>197</sup>

In another study by Thomas *et al.*, they detail an *in vitro* and an *in vivo* experiment. Five blocks of bone were vibrated at 500 Hz at an acceleration of 50 m/s<sup>2</sup> for 20 seconds and 5 samples were left undisturbed during the application of bone cement. The samples were then analysed in an SEM. For the *in vivo* study, the authors exposed the cancellous bone of the tibial plateau in six dogs under general anaesthesia. Palacos E was used with high pressure (67 kPa), low pressure (6.7 kPa), and low pressure (6.7 kPa) with vibration. Standard radiographs were taken of the cement and then the bones were sliced using a band saw. These slices were then analysed under MFR and SEM. Analysis showed that the cement-bone interface for vibrated bone in the *in vitro* study was higher quality, in terms of both penetration and cement contact with bone. In the *in vivo* study, only minimal ingress of cement was achieved with low pressure cement application. High-pressure injection resulted in more cement penetration into bone. Low pressure with vibration resulted in a better interface than low pressure alone but it was not possible to distinguish between interfaces created with low pressure and vibration and interfaces created with high pressure.<sup>19</sup>

Wang *et al.* also investigated the effect of vibration on the quality and strength of the cement-bone interface in an *in vitro* experiment. The cement was inserted into the medullary canal and the vibration probe was inserted. The vibration applied had a frequency of 800 Hz, for 20 seconds but no amplitude is given. After vibration, the cement was pressurised, but no values are given regarding the magnitude of the pressure. No standards are cited for the pull-out (A) and push-out (B) tests and no stroke rate is given. Various fatigue tests were also performed but the detail is limited, three different tests were performed: using results for the strength of the

interface from the push-out tests (Ultimate strength (US) - 3159 N) the samples were loaded to 30, 50, and 70 % (C1, C2, and C3 respectively). The application of vibration before pressurisation increases the strength of the interface. The authors also state that images show an increase in the quality of the interface with a better filling effect in the vibrated specimens.<sup>198</sup>

Vibration to bone cement during application is an appealing surgical technique. Lowering the viscosity of bone cement would be beneficial for operations where the cement must flow through a small diameter before contacting the bone i.e. in vertebroplasty<sup>199, 200</sup>. If the viscosity is too small upon contacting the bone, leakage may occur.

### ***1.6.5 Acetabular Cup***

The design of the cemented acetabular cup has not changed significantly since it was first introduced in 1961 (Figure 1.20).

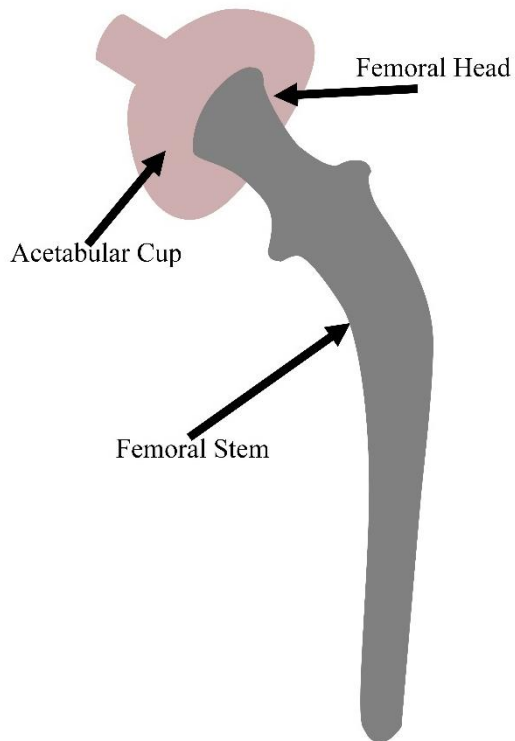


**Figure 1.20** Final design of the low-friction arthroplasty designed by Charnley showing the femoral stem and the acetabular cup.<sup>1</sup>

#### ***1.6.5.1 Material***

The acetabular cup was initially made from Polytetrafluoroethylene (PTFE). This material was selected due to its very low friction coefficient and the fact that it is bioinert. Charnley initially attempted to simply line both the acetabulum and femoral head with PTFE which would

preserve bone stock, however, the lack of stresses encountered by the bone resulted in bone resorption and subsequent implant failure.<sup>201</sup>

In 1962, Charnley started using high-density polyethylene (HDPE) after it was recommended by Harry Craven due to the high wear rate of PTFE. Although the coefficient of friction is larger for HDPE (roughly 5x) it is significantly more resistant to wear (500 – 1000x more resistant). Charnley also reported that despite his earlier claims, HMWPE was capable of boundary lubrication where the two materials are separated by a thin film of fluid.<sup>35, 201, 202</sup>

HDPE is a linear polymer with a molecular weight of up to 200,000 g/mol, whereas ultra-high molecular weight polyethylene (UHMWPE) has a viscosity average weight of 6,000,000 g/mol. It has been shown to have a higher ultimate strength, impact strength, and is more abrasion and wear-resistant than HDPE. The volumetric wear rate of HDPE has been shown to be 4.3x larger than UHMWPE.<sup>202</sup>

In the 1990s, it was shown that highly-crosslinked UHMWPE (HXLPE) acetabular cups showed an improved wear-resistance and a decreased occurrence of osteolysis.<sup>202-206</sup> The wear debris generated by HXLPE has been shown to be smaller and less bio reactive.<sup>207</sup>

Cross-linking by irradiation has been shown to increase the crystallinity of polyethylene by first breaking the chemical bonds of the polymer and allowing them to reform, increasing the number of crosslinks and the wear resistance. However, when the polymer chain is broken a free radical is produced. Some of these free radicals become trapped. Vitamin E has been added to the UHMWPE to act as a free-radical catcher. This new material has received FDA clearance and *in vitro* testing has shown improved fatigue performance.<sup>202, 208</sup>

#### **1.6.5.2 Acetabular Flange**

The addition of a flange to the pressure injection cup (PIJ) by Charnley was an early innovation to the design of the acetabular cup. Charnley states that a plain hemispherical cup is not optimal: it is unable to exert an injection pressure on the cement and the cup can wobble whilst the cement is still soft. If the flange of the acetabular cup is correctly trimmed it will contact the acetabular rim and thus stabilise it whilst the cement is still soft. He states that “the original ideas of the pressure injection socket was for the rim to make contact with the periphery of the acetabulum before the body of the socket touched the floor of the acetabulum” and that “the cement [...] would then be pressured by deflection of the semi-rigid rim.”<sup>201</sup>

Oh *et al.* investigated the effect of the type of flange on the pressure and penetration of PMMA bone cement into a mock acetabulum. They used 4 cups each with different flange designs – unflanged, three-scallop flange, multiple-scallop flange, continuous flange.<sup>209</sup> The flange, where present, extended from the cup by 2.5 mm. It is assumed that the insertion was position-controlled as the insertion load is reported. The cups were implanted into a polyethylene block with a 55 mm bore using an unnamed PMMA cement. Pressure sensors were fixed at 0° and 45° from the direction of loading. The results show that the continuous flange produced the largest intrusion depths, the largest insertion load and the largest pressures at the pole (0°) and the rim (45°).<sup>209</sup>

Shelly and Wroblewski performed *in vitro* experiments to compare the efficacy of the unflanged cup compared to an ogee-flanged cup in the pressurisation of cement in the acetabulum. The

mock acetabulum had a 5 mm orifice at the pole which led to a rheometer. The mouth of the hole was covered in a metal mesh with a similar pore size to cancellous bone. The rheometer was filled with paraffin and was arranged so that a constant back pressure of 25 mmHg was maintained, it was also attached to a mercury-filled column so that the pressure could be measured. A 78 N force was applied to the cup. They found that the unflanged cup produced minimal pressurisation and the small pressures it did generate were not maintained. The authors also state that it is difficult to keep the unflanged cup concentric and avoid bottoming out. The authors also conclude that a 78 N force is sufficient to generate a pressure of 170 mmHg or 22.7 kPa with the ogee-flanged cup.<sup>210</sup>

Beverland *et al.* implanted flanged, unflanged and custom acetabular cups into an irregular acetabulum model and measured how the cup design impacted the pressure at the pole of the acetabulum and the intrusion depth of PMMA cement at the pole and at the rim. The penetration at the pole of the acetabulum was larger than at the rim for the unflanged cup but was larger at the rim than the pole for the flanged cup. The irregular rim itself is an uncontrolled variable making a comparison between studies difficult. Custom acetabular components may provide benefits but when the acetabulum bone bed is sufficiently reamed then there is large conformity between regular acetabular cups and acetabulum bone.<sup>211</sup>

Hodgkinson *et al.* reviewed 302 cemented acetabular components followed for between 9 and 11 years after implantation and state that they have shown that the addition of a flange significantly reduces the incidence of demarcation at all time points after implantation and that this is due to a superior quality cement-bone interface.<sup>130</sup>

Parsch *et al.* performed cadaver experiments to investigate how the addition of a flange to the acetabular component affects the pressure and penetration of cement into the cadaver bone. Pressure transducers were fixed into acetabular zones I, II and III. A back-bleeding pressure was simulated using a saline bag lifted 1 m. Three minutes after mixing either an unflanged cup or an ogee-flanged cup was inserted into the cement. A load of between 60 and 100 N was applied to the cup by hand using a spring-loaded device. The authors found no significant difference in penetration depth due to whether the cup had a flange or not in any of the zones. They found that whilst a flange increased the peak pressures generated in the acetabulum, it did not increase the average pressure which has been shown to be more important for cement penetration. Given all the data, it may be possible to see a significant difference in the pressure differential between the pole (zone II) and the rim (zone I and III); however, this was not investigated. The authors conclude that cup insertion should not be the sole means of pressurisation.<sup>194</sup>

Ørskov *et al.* implanted flanged and unflanged Opera cups into mock ceramic acetabula and cadaveric acetabula and they measured the pressures and penetration of the cement and thickness of the cement mantle. Two and a half minutes after the commencement of mixing the cement was placed into the acetabulum and pressurised with a load of 80 N for 90 seconds using a conventional pressuriser, similar to the Depuy pressuriser. Ten of each kind of cup were implanted. Five minutes after the commencement of mixing the cup was implanted with the tester in position control, the stroke rate is not reported. Once correctly positioned, a force of 25 N was applied until full cure. In the cadaver study, 10 of each cup type were implanted into paired acetabula. The paper does not state whether pressurisation and cup insertion were performed using the universal tester or a surgeon in the cadaver study. The authors report that

there is no significant difference due to the cup used in either the pressures generated, or cement penetration achieved. The flanged cup did have a significantly thicker cement mantle both centrally and laterally than the unflanged cup. The authors conclude that the flanged cups do not generate a larger pressure than the unflanged cup during insertion and that the improved clinical outcomes of flanged cups may be due to the flange closing the gap between the cement and the bone at the rim of the acetabulum, they do not present any data for this conclusion.<sup>212</sup>

Bhattacharya *et al.* performed an *in vitro* study which compared the pressures generated when various designs of cups were implanted into a mock acetabulum fitted with three pressure sensors, all placed at the same angle from the direction of implantation. The three cups implanted were the Charnley Ogee flagged cup, Exeter low profile cup and the Exeter low profile cup with the flanged removed. A universal tester was used to apply a 70 N force for pressurisation and cup insertion. A conventional Depuy style pressuriser was used for pressurisation. The authors report that the flanged cups did not consistently nor significantly produce larger pressures than the unflanged cups and therefore flanged cups are not necessary to improve the cementation and survival of cemented acetabular components.<sup>213</sup>

### **1.6.5.3 Other Design Considerations**

The acetabular cup has a semi-circular metal wire which is used to identify the orientation of the acetabular cup. It has been shown that an acetabular cup with excessive anteversion or retroversion is more likely to fail than well placed cups.<sup>214, 215</sup> Charnley initially only used one semi-circular wire but it was shown that three radiographs are required to clearly identify the orientation of the cup in all three planes.<sup>214</sup> Derbyshire and Raut investigated the efficacy of using another configuration of wire which went in a semi-circle around the rim and then turned and followed the circumference of the cup through the pole which they named the “double-d wire marker”. They performed *in vitro* experiments and found that although the error for both was similar, and the “double-d” wire marker could also be used to determine whether rotation was anteversion or retroversion, the circular wire marker made more repeatable measurements<sup>216</sup>. Several popular modern cemented acetabular cups, such as the Exeter X3 Rimfit Acetabular Cup (Stryker) now use metal wires that go around the cup, near where the rim is situated as well as wires that go over the pole so that rotation in all three planes can be measured more easily.<sup>45</sup>

Several authors have reported data that raises concerns regarding thin cement mantles. Wroblewski *et al.* found that of 59 revised cemented sockets, 19 of them had wear on the external diameter of the cup and this was associated with a thin cement mantle.<sup>217</sup> In a 20 year follow up study, Kobayashi *et al.* reported that a thin cement mantle, particularly in Delee-Charnley zone I and II, and particularly in the rheumatoid group, was positively correlated with significant radiological demarcation.<sup>218</sup> Faris *et al.* performed a double-blinded study where 470 cemented acetabular implantations were performed. One group of patients received an acetabular cup with cement spacers integrated into the external diameter of the cup and the other had an identical cup with the spacers removed. It was believed that cement spacers would ensure a regular cement mantle thickness. They found that there was initially an increased likelihood of early loosening for the cups with cement spacers. However, the cups with polyethylene spacers had significantly thicker and more uniform mantles in all zones.<sup>219</sup>

Lichtinger and Müller reported a retrospective radiological study that included two groups of patients. One of the groups had a Charnley-Müller cup implanted which did not have cement spacers and the other group had a similar cup but with 3 mm cement spacers on the external diameter. They found that the addition of the cement spacers to the acetabular cup significantly reduced the number of underfilling defects on the radiograph. They conclude that the use of the acetabular cup with preformed cement spacers helps to improve the quality of the cement mantle.<sup>220</sup>

Goodman and Carter state that FEA models have predicted that there may be a mechanical component to the cause of failure, Goodman and Carter performed a radiographic review and conclude that their observations of RLLs in zone I and III concur with previous FEA studies that predict weaknesses in these areas.<sup>221</sup> Schmalzried *et al.* also discuss this and agree that a metal-backed acetabular component may reduce the amount of stress transferred to the cement-bone interface.<sup>140</sup> A 10-year follow up study performed by Chen *et al.* reviewed the clinical and radiographic results of 86 hip replacements that used a metal-backed acetabular component. They found that the overall incidence of radiographic loosening was significantly higher for metal-backed acetabular cups than those of non-metal-backed acetabular cups and thus the authors do not recommend the use of these cups and also close monitoring of patients who already have them implanted.<sup>222</sup>

It can be seen that the external face of the cemented acetabular cup has various design features. No literature containing information on the motivation behind these design aspects nor any published data regarding their efficacy could be found. Experiments should be performed to test the effect of these features on the pressures and penetrations achieved in the acetabulum during THA. Reviews could be performed to determine the effects of these design features on the development of RLLs on radiographs and the longevity of cemented implants.

## **1.7 Aims and Objectives**

Aim:

To investigate how curing PMMA bone cement behaves as it is being pressurised and use this knowledge to recommended changes to current cemented acetabular cup surgical techniques and equipment.

Objectives:

1. To determine the curing parameters of PMMA bone cement, specifically the moment of gelation and how this is affected by temperature, the brand and therefore viscosity of cement, and rate of deformation.
2. To determine how deformation of bone cement during curing affects the tensile strength of the solidified cement.
3. To compare the diametrical shrinkage of bone cement mantles when the cement is mixed under vacuum and mixed at atmospheric pressure and when a flanged or unflanged cup is implanted.
4. To determine whether the addition of a flange to the acetabular cup or the method of mixing affects the pressures generated at the acetabulum bone surface during cemented acetabular cup insertion.
5. To design, manufacture, and test a novel pressuriser designed with knowledge acquired from the literature and throughout this PhD.
6. To compare the pressures generated at the acetabulum bone surface during the cement pressurisation stage of cemented acetabular cup implantation when the acetabular cement pressuriser design is used and compare this with other state of the art pressuriser designs.

## Chapter 2. Rheological Characterisation of PMMA Bone Cements

### 2.1 Introduction

Studies investigating the curing behaviour of PMMA bone cement have been limited. The standards currently only specify the end of the mixing phase as when “the mixture is able to separate from an unpowdered latex surgical gloved finger”.<sup>55</sup> This parameter may be used by the surgeon to identify when the cement is ready to be implanted into the body, but it is a parochial and subjective measure that does not provide sufficient information for researchers and material scientists.

Newton's law of viscosity is defined as:<sup>223</sup>

$$\tau = \mu \frac{dy}{dx}$$

Where:  $\mu$  is the dynamic viscosity,  $\frac{dy}{dx}$  is the rate of deformation, and  $\tau$  is the resulting shear stress. Another way to describe this relationship is that the faster you deform a Newtonian fluid the more resistance there will be to that deformation.<sup>223</sup> In a purely viscous material, once deformation has stopped, the internal stresses will dissipate.<sup>224</sup> This is not true of an elastic material. Elastic behaviour is given by Hooke's law.<sup>224</sup>

$$\tau = E\gamma$$

Where:  $E$  is the elastic modulus,  $\gamma$  is the applied strain and  $\tau$  is the resulting stress. Another way to describe this is that the larger the magnitude of the applied strain, the larger the resulting stress. There is no temporal element to this behaviour, a stress generated due to an applied strain will continue if the strain is not removed.

Curing PMMA bone cement is a viscoelastic material. This is evident when considering how PMMA bone cement behaves from initial mixing to full cure. When it is first mixed, depending on the brand used, the cement is runny for low viscosity cements and pliable for high viscosity cements; in this phase, the flow behaviour is primarily governed by viscosity. As polymerisation continues, the cement becomes more resistant to an applied force, this is often described as the viscosity of the cement becoming larger, but this is not the only parameter that is changing. The cement also becomes more elastic. Eventually, the cement will fully cure, and the cement will become a stiff, primarily elastic solid.

It is important to determine whether PMMA bone cement can store stresses indefinitely and if so when this transition occurs. The commonly accepted viscoelastic model for PMMA bone cement includes a time-independent elastic component.<sup>73</sup> Meaning that stresses will not fully relax.<sup>14, 73, 75</sup>

When does curing cement store stresses generated due to an applied strain indefinitely?

Winter describes the transition to a solid-state as when the relaxation modulus (how much of an initial stress is stored) has a finite value at long times, he calls it an equilibrium modulus.<sup>79</sup>

$$G_e = \lim_{t \rightarrow \infty} G(t)$$

Where:  $G_e$  is the equilibrium modulus and  $G(t)$  is the relaxation modulus. If a strain,  $\epsilon$ , is applied to the bone cement once an equilibrium modulus is present and is not allowed to recover then it will result in residual stress:

$$\tau = G_e \gamma$$

Where:  $G_e$  is the equilibrium modulus,  $\gamma$  is the applied strain and  $\tau$  is the resulting stress. The literature is not clear on how the equilibrium modulus may be identified within a short time frame. It would be difficult to halt the polymerisation of PMMA bone cement and perform stress relaxation experiments. Winter states that an equilibrium modulus develops at the moment of gelation, also known as the LST.<sup>79, 88</sup> Identification of when this occurs would provide crucial information regarding when bone cement begins to store strains as residual stresses indefinitely, thus potentially creating weaknesses in the cement.

Rheological characterisation is used to measure the flow properties of viscoelastic materials.<sup>224</sup> The general principle is to measure the response of a material to an applied stress or strain. Previous studies investigating the rheological behaviour of bone cement have generally used dynamic mechanical analysis (DMA).<sup>225, 226</sup> This involves applying an oscillating stress or strain and measuring the response of a material. The response of a perfectly elastic material to an applied strain will be instantaneous and therefore have a phase angle of  $0^\circ$ . The response of a perfectly viscous material will have a lag and the phase angle will be  $90^\circ$ . A viscoelastic material will have a phase angle somewhere in between the two.<sup>77</sup>

So, if a material is subject to a sinusoidal strain,<sup>77</sup>

$$\gamma(t) = \gamma_0 \exp(i\omega t)$$

the stress response can be written as:

$$\tau(t) = \tau_0 \exp(i(\omega t + \delta))$$

Where:  $\gamma$  is the strain,  $\gamma_0$  is the strain amplitude,  $i = \sqrt{-1}$ ,  $\tau$  is the stress,  $\tau_0$  is the stress amplitude,  $\omega$  is frequency,  $t$  is time and  $\delta$  is the phase angle. The complex modulus,  $G^*$ , can be written as:

$$G^* = \frac{\tau(t)}{\gamma(t)}$$

Therefore,

$$G^* = \frac{\tau_0}{\gamma_0} \frac{\exp(i(\omega t + \delta))}{\exp(i\omega t)}$$

Using exponential algebra,

$$G^* = \frac{\tau_0}{\gamma_0} \frac{\exp(i\omega t) \exp(i\delta)}{\exp(i\omega t)}$$

$$G^* = \frac{\tau_0}{\gamma_0} \exp(i\delta)$$

$$G^* = \frac{\tau_0}{\gamma_0} (\cos(\delta) + i \sin(\delta))$$

And in the complex plane:

$$G^* = G' + iG''$$

Where:  $G'$  is the storage modulus and represents the elastic component of the response of the material and  $G''$  is the loss modulus and describes the viscous component of a materials response. And it follows that:

$$\tan(\delta) = \frac{G''}{G'}$$

Where  $\tan(\delta)$  is known as the loss tangent or the tangent of the phase angle.

It may be possible to determine when a material behaves more like a solid than a liquid by determining the moment that the storage modulus becomes larger than the loss modulus, this occurs when:  $\delta = 45^\circ$  and  $\tan(\delta) = 1$ . Winter investigates this property in cross-linking materials that are stoichiometrically balanced and far from their glass transition temperature. Many materials exhibit shear thinning (increasing frequency of deformation reduces the viscosity) and some experience shear thickening (increasing frequency of deformation increases the viscosity). Therefore, this may mean that altering the testing parameters, namely the frequency, would alter how liquid- or solid-like the material is and therefore may affect whether a material can store stresses indefinitely. There is no direct mathematical relationship between the development of the equilibrium modulus and  $\tan(\delta) = 1$ . Although there is much literature discussing when the rheological LST can be detected, most of the articles discuss very specific materials. Spiegelberg states that the LST can be detected when  $\tan(\delta)$  becomes independent of frequency.<sup>89</sup> The article referenced for this claim, by Scanlan and Winter, states that the rate of change of the dynamic mechanical modulus and viscosity scales as a power law function with frequency but is specific to a particular material.<sup>227</sup> The experiment performed by Spiegelberg is very narrow in scope so an investigation of how viscosity and  $\tan(\delta)$  change due to the frequency of deformation over a range of temperatures for multiple cements was performed.

This experiment was designed to measure the parameters that are used to define the rheological properties of PMMA bone cement and to establish a more data focussed understanding of the evolution of the handling properties.

Objectives:

1. To investigate how the brand of the PMMA bone cement affects the rheological properties during curing.
2. To investigate how the temperature during curing affects the rheological properties of PMMA bone cement.
3. To determine when the moment of gelation occurs during polymerisation of PMMA bone cement.
4. To identify a more data-focused methodology for the determination of curing parameters of PMMA bone cements.

## 2.2 Materials

This section describes the materials used in this experiment. The methodology is described in the following section.

This experiment was undertaken at Malvern Panalytical. A Kinexus DSR+ rheometer was used for measurements. As previously stated, rheological analysis involves the application of a force or displacement to a sample and measuring the response, the Kinexus DSR+ rheometer is a rotational rheometer. Analysis can be performed with many geometries (Figure 2.1). There are positives and negatives to each option.<sup>76</sup> The cup and bob geometry is suitable for low viscosity specimens as if the sample is placed into either of the other two geometries it may not stay in place. The cone and plate geometry is ideal for most samples and is preferable to the parallel plate geometry due to the rotational nature of the displacement the sample near the edge of the parallel plate configuration will be strained more. The cone and plate configuration allows a larger gap at the edge of the diameter meaning that the deformation is distributed to more material and therefore the material will deform a similar amount to the material near the centre thus creating a uniform strain rate. It was decided that the cone and plate geometry was not suitable for PMMA bone cement as it is advised that the gap between the plates should be at least 5x as large as the largest particles in the sample and this would create a very large gap for PMMA bone cement.<sup>77</sup> The cup and bob geometry is not suitable as cement is of a larger viscosity than what is recommended for this geometry. Therefore, the parallel plate geometry was selected for this experiment. Disposable parallel plates were also available so that experiments could run until full solidification of the cement. The largest PMMA particles in the powder are in the order of 150  $\mu\text{m}$ ,<sup>228</sup> therefore a gap of 1mm was selected. The plates used were 25 mm in diameter.

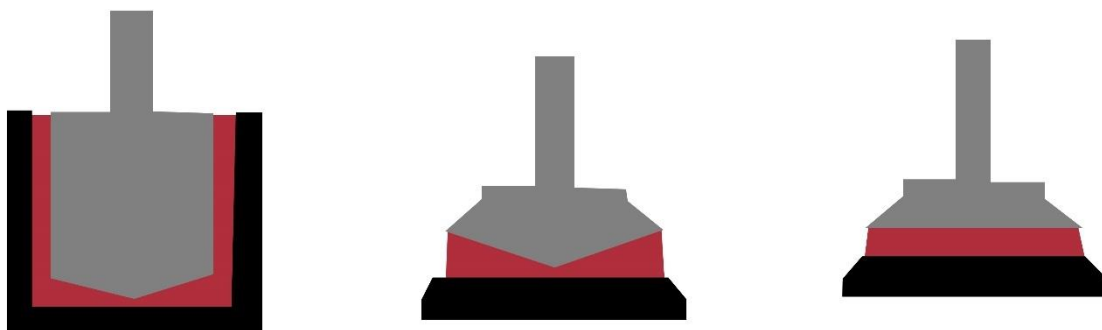


**Figure 2.1** Various geometries available for rheological characterisation: (left) cup and bob configuration, (middle) cone and plate configuration, and (right) parallel plate configuration.<sup>76</sup>

Three commercially available bone cements were tested: Simplex P, CMW 2, and Palacos R. These cements have a long clinical history, are commonly used in total hip replacement, and cover a range of viscosities: Simplex P is a low viscosity cement and Palacos R and CMW 2 are both high viscosity cements.

## 2.3 Methods

The temperature and humidity of the lab were within the ISO standards for testing acrylic bone cement ( $23^{\circ}\text{C} \pm 1^{\circ}\text{C}$ ).<sup>55</sup> The cements were stored in the lab for 24 hours prior to testing.

The rheometer was used in dynamic oscillation mode with a controlled strain of 0.01%. For each test, the rheometer performed frequency sweeps of 1Hz, 5Hz and 10Hz as this was similar to previous experiments performed.<sup>77, 79, 89, 228, 229</sup> The three bone cements were tested at three temperatures:  $23^{\circ}\text{C}$ ,  $33^{\circ}\text{C}$  and  $43^{\circ}\text{C}$  to resemble room temperature, near body temperature and a heightened temperature similar to what causes thermal necrosis. The viscosity and  $\tan(\delta)$  were measured. Three repeats were performed for each testing condition.

The cement was mixed with a metal spatula in a PTFE beaker to ensure it was homogenous. After 60s, a small amount was loaded into the rheometer and the plates were brought together and excess cement was removed from the edge (Figure 2.2). The thermal cover was placed over the sample and the measurements were started. The time between the start of mixing and the start of measurements being taken was always between 100 and 200 seconds. The experiment was stopped once the viscosity had reached a constant value. This was repeated three times for each cement at each temperature.

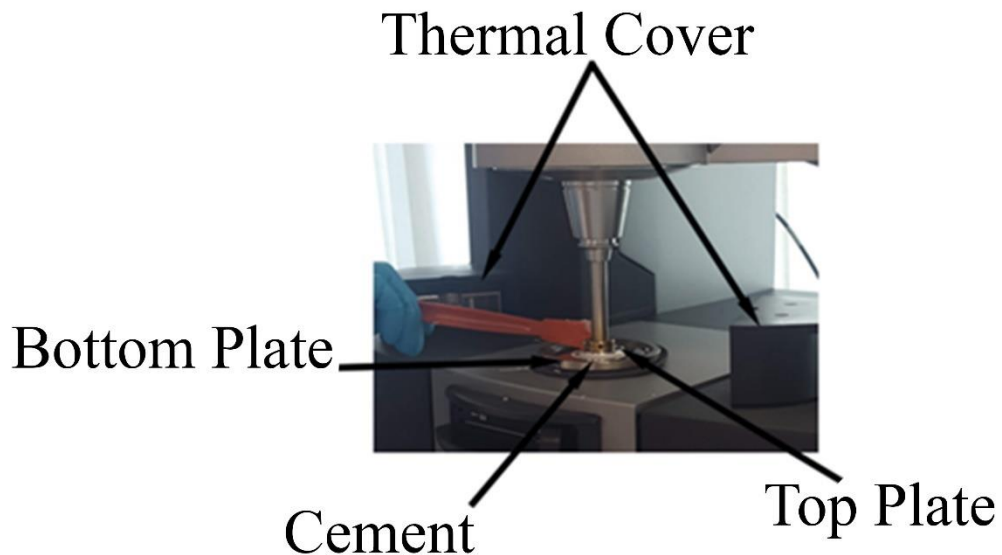


**Figure 2.2** Labelled image of the experimental set-up during one of the rheological tests.

The cure time was calculated as the moment that the viscosity reached a constant value.

For statistical analysis, Minitab (Minitab, US) was used. All measurements from each repeat within each minute were grouped together. If there were less than three measurements in a minute, no statistical analysis was performed. Each set of results were checked for normality using a Ryan-Joiner test, if the data were found to be normal then a Welch's ANOVA test was performed to determine whether the independent variable (temperature, frequency, and brand of cement) had a significant effect on the dependent variable (viscosity,  $\tan(\delta)$ ). If the results were non-normal a Kruskal-Wallis Test was performed as this statistical test allows for

comparison of three or more sets of non-normal data to determine whether there is a significant difference in the mean, this test assumed that the distributions were similar.

## 2.4 Results

Each one of the figures below is representative of nine other graphs for the testing conditions. All graphs are similar; therefore, a representative example is given within this chapter, full results can be seen in the appendix (Appendix B). For each measured variable, a typical plot through time has been provided as well as the statistical tests for each minute for every initial condition.

### 2.4.1 Viscosity – Brand

**Table 2.1** Statistical results for each minute and each initial condition. A Y signifies that the brand of cement caused a significant difference in the viscosity. A \* indicates that at least one of the data sets was not normal and therefore a Kruskal-Wallis test was used. Each statistical result used at least three measurements.

Sample Details		Minutes												
Temperature (°C)	Frequency (Hz)	3	4	5	6	7	8	9	10	11	12	13	14	15
23	1			Y	Y	Y	Y	Y*	Y	Y				
	5				Y	Y	Y	Y*	Y	Y	Y		Y	
	10		Y	Y	Y	Y	Y*	Y*	Y	Y				
33	1			Y	Y	Y	Y	N	N	N	N	N	N*	
	5	Y	Y	Y	Y	N	N	N	N	N	N	N	N	
	10	Y	Y	Y	Y	Y	N	N	N	N	N	N	N	
43	1	N	Y	Y	N*	N*								
	5	Y	Y	Y	N	N								
	10	N*	N*	N	N									

As can be seen from the statistical results (Table 2.1) there is a difference in viscosity due to brand for all frequencies at 23°C. There was a significant difference due to the brand near the end of the experiments performed at 33° and 43°C for all frequencies of deformation. There was never a significant difference due to brand for experiments performed at 43°C and deformed at a frequency of 10 Hz; this is also true for the 3<sup>rd</sup> minute of experiments performed at 43°C and deformed at 1Hz. It can be seen below (Figure 2.3) that each cement starts at a similar viscosity and then cures at different times and at different rates before once again reaching a similar value when the cement has solidified.

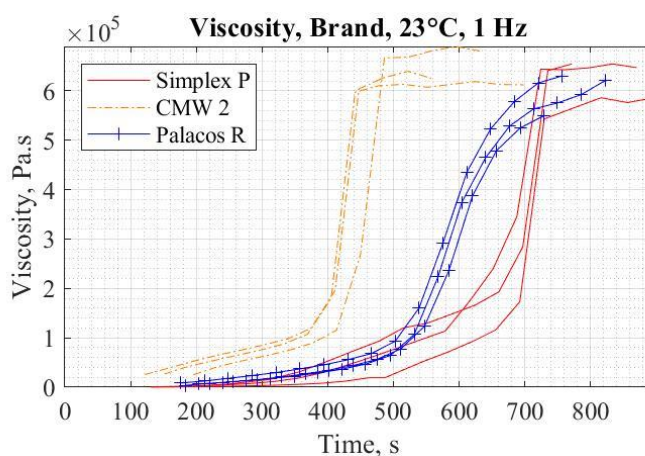


**Figure 2.3** Time-viscosity plot for each brand of cement at 23°C with a deformation rate of 1Hz. Three repeats were used for each testing condition.

#### 2.4.2 Viscosity – Temperature

**Table 2.2** Statistical results detailing whether there is a significant difference in the viscosity due to the temperature of the experiment for each minute and each initial condition. A Y signifies that the temperature of the experiment caused a significant difference in the viscosity. A \* indicates that at least one of the data sets was not normal and therefore a Kruskal-Wallis test was used. Each statistical result used at least three measurements.

Sample Details		Minutes												
Cement Brand	Frequency (Hz)	3	4	5	6	7	8	9	10	11	12	13	14	15
Simplex P	1		Y	Y	Y	Y	Y	Y*						
	5		Y	Y	Y	Y	Y							
	10		Y	Y	Y	Y	Y	Y	Y					
CMW 2	1				Y	Y	Y*	N*						
	5			N	Y	Y	Y	Y						
	10		N	Y	Y	Y								
Palacos R	1				Y	Y	Y	Y						
	5				Y	Y	Y	N*						
	10		Y*	Y*	N	N	N	Y						

There is always a significant difference in viscosity due to temperature for Simplex P (Table 2.2). The temperature almost always significantly affected the viscosity of CMW 2, the only times when it didn't was in the third minute when the cement was deformed at a frequency of 5 and 10 Hz and the 7<sup>th</sup> minute at 1 Hz. There are only three minutes where the temperature didn't make a significant difference for Palacos R; the 7<sup>th</sup> minute when the cement is deformed at 5Hz and the 5<sup>th</sup> and 6<sup>th</sup> minute when the cement was deformed at 10Hz. It can be seen from the figure that the time to cure decreases and the rate of curing increases with an increase in temperature (Figure 2.4).

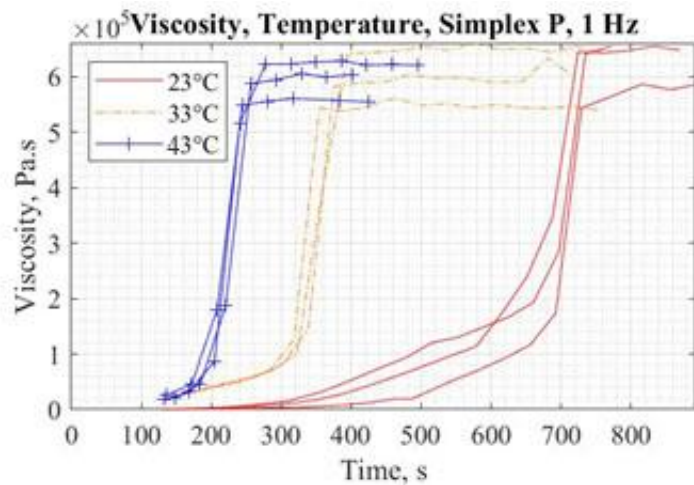


**Figure 2.4** Time-viscosity plot for each temperature using Simplex P with a deformation rate of 1Hz. Three repeats were used for each testing condition.

#### 2.4.3 Viscosity – Frequency

**Table 2.3** Statistical results for each minute and each initial condition. A Y signifies that the frequency of deformation caused a significant difference in the viscosity. A \* indicates that at least one of the data sets was not normal and therefore a Kruskal-Wallis test was used. Each statistical result used at least three measurements.

Cement Brand	Temperature (°C)	Minutes													
		3	4	5	6	7	8	9	10	11	12	13	14	15	
Simplex P	23	N	N	N	N	N	Y	Y	Y	Y	Y	Y*	Y*	Y*	
	33	Y	Y	Y	N	Y	Y	Y	Y	Y	Y	Y	Y	Y	
	43	Y	N	Y	Y	Y									
CMW 2	23	Y	Y	Y	Y	Y*	Y*	Y							
	33				Y	Y	Y	Y	Y	Y					
	43	N	Y	Y	Y*										
Palacos R	23			Y	Y	Y	Y	Y	Y	Y	Y	Y	Y	Y	
	33	Y	Y	Y	Y	Y	Y	Y	Y	Y	Y	Y	Y	Y	
	43	Y*	N*	N	Y	Y									

The bone cements tested exhibited shear thinning behaviour (Figure 2.5). The magnitude of the effect of shear thinning increases with time. For Simplex P there are several instances, particularly at the beginning of tests performed at 23°C and tests performed at 43°C where there was not a significant difference in viscosity due to frequency of deformation. There is only one instance in the third minute, for CMW 2 tested at 43°C, where frequency does not significantly

affect the viscosity. And for Palacos R there was no significant difference in the viscosity due to frequency of deformation in the 4<sup>th</sup> and 5<sup>th</sup> minute at 43°C (Table 2.3).

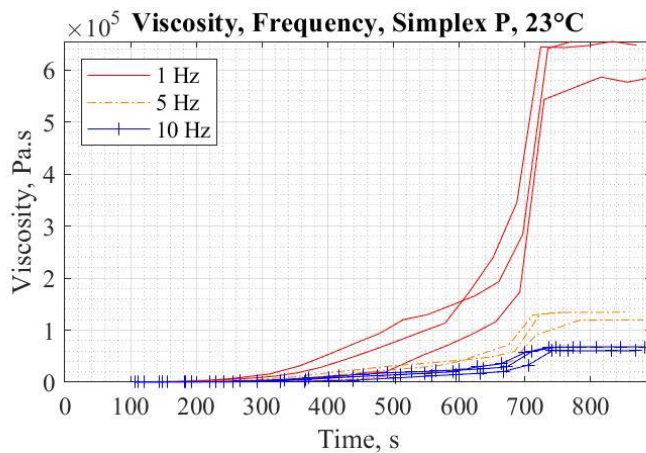


**Figure 2.5** Time-viscosity plot for each frequency of deformation using Simplex P at a temperature of 23°C. Three repeats were used for each testing condition.

#### 2.4.4 Phase Angle – Brand

**Table 2.4** Statistical results for each minute and each initial condition. A Y signifies that the brand of cement caused a significant difference in  $\tan(\delta)$ . A \* indicates that at least one of the data sets was not normal and therefore a Kruskal-Wallis test was used. Each statistical result used at least three measurements.

Sample Details		Minutes												
Temperature (°C)	Frequency (Hz)	3	4	5	6	7	8	9	10	11	12	13	14	15
23	1			Y	Y	Y	Y	Y*	Y	Y				
	5			Y*	Y*	Y	Y	Y*	Y	Y				
	10	Y	Y	Y	Y	Y*	N	Y						
33	1			Y	Y	Y*	Y	N	N	N				
	5	Y	Y	Y	Y	N*	N	N	N	N				
	10	N*	Y	Y*	Y	Y*	Y	N*	N					
43	1	Y	N*	Y	N	N								
	5	Y	N	Y*	N	N								
	10	Y	N	Y*	N									

There is only one instance when  $\tan(\delta)$  is not significantly affected by the brand of cement at 23°C and that is at the 8<sup>th</sup> minute when the cement is deformed at 10Hz. There are more instances where  $\tan(\delta)$  is not significantly affected by the brand of cement near the end of testing for both 33°C and 43°C (Table 2.4). There does not seem to be an obvious pattern as to when there is a significant difference in the value of  $\tan(\delta)$  due to brand, this can also be seen below (Figure 2.6).

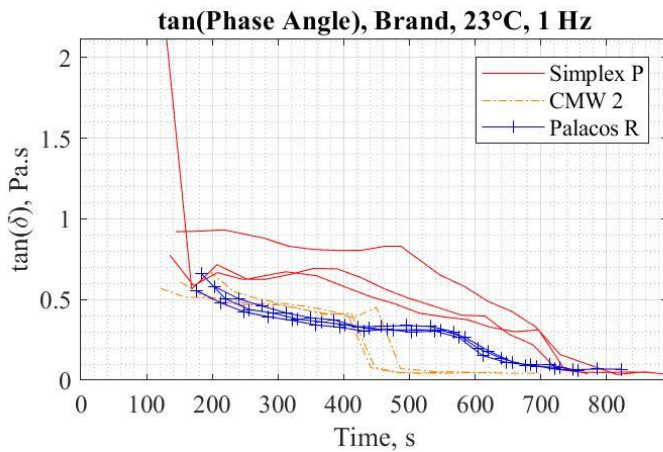


**Figure 2.6** Time-tan( $\delta$ ) plot for each brand of cement at 23°C with a deformation rate of 1Hz. Three repeats were used for each testing condition.

#### 2.4.5 Phase Angle – Temperature

**Table 2.5** Statistical results for each minute and each initial condition. A Y signifies that the temperature of the experiment caused a significant difference in tan( $\delta$ ). A \* indicates that at least one of the data sets was not normal and therefore a Kruskal-Wallis test was used. Each statistical result used at least three measurements.

Cement Brand	Frequency (Hz)	Minutes												
		3	4	5	6	7	8	9	10	11	12	13	14	15
Simplex P	1		Y*	Y	Y	Y*	Y	Y						
	5		Y	Y*	Y*	Y	Y*							
	10	Y*	Y	Y	Y	Y*	Y							
CMW 2	1			Y	Y	Y	Y							
	5			N*	Y*	Y*	Y	Y						
	10		N	Y	Y*	Y								
Palacos R	1				Y	Y	Y	Y						
	5				Y	Y	Y	Y	Y*					
	10		Y	Y	Y*	Y	Y							

The temperature that the testing was conducted at almost always caused a significant difference in the value of tan( $\delta$ ) for Simplex P and Palacos R. There were only two instances for CMW 2 where there was not a significant difference in tan( $\delta$ ) due to the temperature. They were both near the start of testing when the rate of deformation was 5Hz and 10Hz (Table 2.5, Figure 2.7).

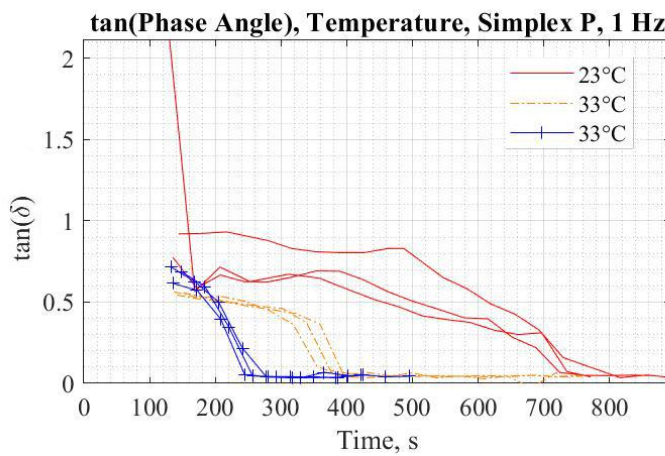


**Figure 2.7** Time-tan( $\delta$ ) plot for each temperature using Simplex P with a deformation rate of 1 Hz. Three repeats were used for each testing condition.

#### 2.4.6 Phase Angle – Frequency

**Table 2.6** Statistical results for each minute and each initial condition. A Y signifies that the frequency of deformation caused a significant difference in the tan( $\delta$ ). A \* indicates that at least one of the data sets was not normal and therefore a Kruskal-Wallis test was used. Each statistical result used at least three measurements.

Cement Brand	Temperature (°C)	Minutes														
		3	4	5	6	7	8	9	10	11	12	13	14	15		
Simplex P	23		N*	N*	N*	N	N	N	N	N	N	N	N	N		
	33		N*	Y	Y	N*	N*	N	N*	Y	N*	N	N*	N		
	43	N	N	Y*	N	N										
CMW 2	23		N*	Y*	Y	Y	Y*	N*	N							
	33				Y	N*	N	N	N							
	43	Y	N	Y*	N											
Palacos R	23				N	N	N	N	N	N	N	Y*	Y	Y		
	33		N	N	N	N	N*	N	N	N						
	43	Y	Y	N*	N	N										

For most of the testing, the frequency of deformation does not significantly affect tan( $\delta$ ) during testing (Table 2.6). There were only three instances for Simplex P, and these were in the 4<sup>th</sup> and 5<sup>th</sup> minute at 33°C, and the 5<sup>th</sup> minute for 43°C. The frequency of deformation significantly affected tan( $\delta$ ) from the 4<sup>th</sup> till the 7<sup>th</sup> minute at 23°C, the 4<sup>th</sup> minute at 33°C, and in the 3<sup>rd</sup> and 5<sup>th</sup> minute at 43°C for CMW 2. For Palacos R, the frequency that the cement was deformed at significantly affected tan( $\delta$ ) in the 11<sup>th</sup>, 12<sup>th</sup> and 13<sup>th</sup> minute at 23°C, and the 3<sup>rd</sup> and 4<sup>th</sup> minute when the cement was tested at 43°C. There is no clear pattern as to when the frequency makes a significant difference to the phase angle (Figure 2.8).

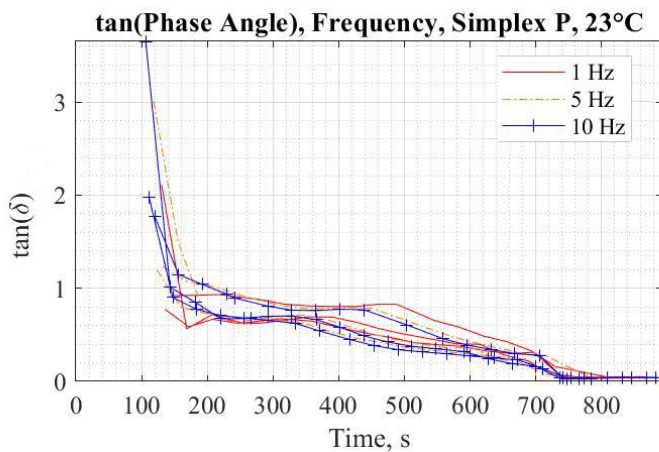


**Figure 2.8** Time-tan( $\delta$ ) for each frequency of deformation using Simplex P at a temperature of 23°C. Three repeats were used for each testing condition.

#### 2.4.7 Cement Curing Timings

**Table 2.7** The averages and means of the time till full cure for each temperature of experiment and each brand of cement. The frequency of deformation did not significantly affect the time till cure, this is due to the frequency sweep methodology. Each statistical result used at least three measurements.

Cement Brand	Cure time at 23°C/ seconds (mean $\pm$ SD)	Cure time at 33°C/ seconds (mean $\pm$ SD)	Cure time at 43°C/ seconds (mean $\pm$ SD)
Simplex P	730 $\pm$ 4.50	375 $\pm$ 16.5	260 $\pm$ 13.2
CMW 2	458 $\pm$ 19.9	306 $\pm$ 8.38	234 $\pm$ 12.0
Palacos R	770 $\pm$ 39.4	478 $\pm$ 8.65	324 $\pm$ 0.816

The time taken for all the cements to cure at each temperature can be seen above (Table 2.7). The difference between the cure times due to temperature was statistically significant with a p-value less than 0.05. An increase in temperature decreases the time taken for the cement to cure which was taken as the moment the viscosity reached a constant value. There is also a significant difference in the cure time due to the brand of cement.

#### 2.4.8 Elastic Component of the Complex Modulus

It can be seen below that the elastic modulus increases as the polymerization reaction progresses (Figure 2.9).

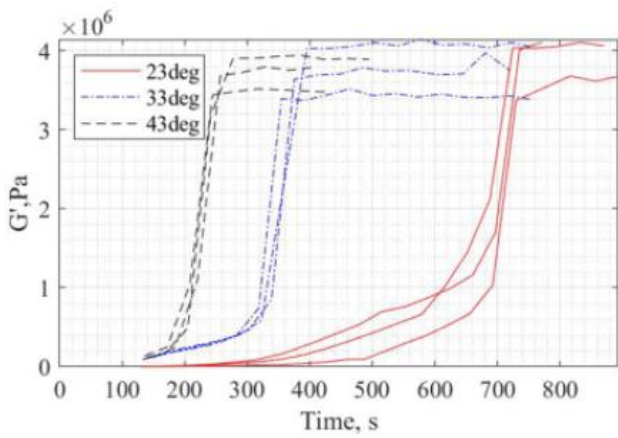


**Figure 2.9** A graph showing the evolution and dependence of the elastic component of the complex modulus on the experiment temperature through time for Simplex P bone cement, deformed at 1Hz. Three repeats were used for each testing condition.

## 2.5 Discussion

Current international standards regarding the curing properties of PMMA bone cement are insufficient for describing the complicated process that occurs during polymerisation.<sup>55</sup> The only two measurable moments are the “dough time” and the “setting time”. The first is measured when the cement no longer adheres to an unpowdered latex surgical glove. The second is measured when the temperature of the cement reaches halfway between the temperature of the cement at mixing and the maximum temperature reached during curing. There does not seem to be a reason within rheological theory for measuring these points. The dough time is helpful for the surgeon to determine when they can start to work with the cement. There is no comment within the standard as to why the setting time is calculated.

### 2.5.1 Viscosity

Viscosity is a measure of the resistance of a material to flow; cement needs to flow into the trabecular bone in order to secure fixation; therefore, the viscosity of PMMA bone cement is important for the success of the cemented implants. There are several factors that should be considered when regarding the viscosity of bone cement. The viscosity of cement needs to be small enough so that flow into bone is possible – several studies have shown that lower viscosity cement penetrates bone more,<sup>50, 84</sup> and it has also been shown that more penetration creates a stronger interface.<sup>187</sup> When considering this alone, one may think that inserting the cement into bone at as low a viscosity as possible would be advantageous, but there are several reasons why this is not desirable. Firstly, the surgeon needs to be able to control the cement. Secondly, lower viscosity cement is more damaging to bone as it is likely that there is more toxic MMA still unreacted within the mass which is known to cause chemical necrosis.<sup>230</sup> Finally, a runny cement may penetrate the bone too far and block vital blood vessels supplying the surrounding tissue.

### **2.5.1.1 Viscosity – Brand**

It can be seen in the results section (Table 2.1) that the viscosity is significantly affected by the brand of cement at most time points. This includes all time points for 23°C, at all frequencies, which is the most clinically relevant temperature as that is the temperature the operating room is held at. At higher temperatures, there are more times and frequencies where the brand does not make a significant difference. This may be due to the faster polymerisation rates, causing the cement to fully solidify sooner. For 33°C the brand of cement does not significantly affect the viscosity of the cement later in the experiment. This is also true for 43°C but happens earlier (for all time points at 10Hz). This effect can be seen in the plot (Figure 2.3). As the cement solidifies the viscosity reaches a similar value although the cements solidify at different speeds.

The differences in viscosity due to the brand of cement is intentional, different viscosities are required for different applications.<sup>39</sup> There are several causes for the difference in viscosity between brands of cement. Firstly, the initial rise in viscosity is governed by the dissolving of PMMA particles in the liquid MMA – this process is governed by diffusion of MMA liquid into the particles; therefore, the morphology of the particles is key. If the polymer beads are smaller there is a larger surface area:volume (SA:V) ratio – the MMA has more area to penetrate into the particle and less volume of PMMA to be dissolved.<sup>228</sup> Finally, differences in the ratios of each of the reactants will change the speed with which the polymerisation reaction progresses. More hydroquinone within the mixture is likely to slow the reaction as more of the radicals produced during polymerisation will be caught and will not go on to trigger even more radicals being produced.<sup>39</sup>

All these variables can be adjusted so that a cement of a specific viscosity can be created.

### **2.5.1.2 Viscosity – Temperature**

The viscosity of the cement is frequently significantly affected by the temperature of the experiment. The viscosity of Simplex P is significantly affected at all time points and frequencies. The viscosity of CMW 2 is mostly affected except for the 3<sup>rd</sup> minute when the cement is deformed at 5 Hz and 10 Hz, and in the 7<sup>th</sup> (last) minute when it is deformed at 1Hz. No trend in when the viscosity of Palacos R is affected by the temperature could be identified – there is no significant difference in viscosity due to temperature in the 5<sup>th</sup> and 6<sup>th</sup> minute when the cement is deformed at 10Hz and the 7<sup>th</sup> (last) when the cement is deformed at 5Hz. However, in general, it was found that – the hotter the experiment the faster the viscosity of the cement increases and the faster the cement fully hardens (Table 2.7).

This is expected for two different reasons. Firstly, the initial rise in viscosity is due to the dissolving of the PMMA polymer beads in the MMA liquid and is governed by the diffusion of the MMA liquid into the beads. This was originally described by Pascual,<sup>80</sup> and can be seen in these data. The second half of the viscosity rise is governed by the polymerisation of the MMA monomers into long PMMA polymer chains. This is a chemical reaction that progresses more rapidly when there is more energy available to activate each reaction. Discrepancies seen for CMW 2, and Palacos R do not conform to this understanding. More data points should be collected to determine whether there is a significant difference.

### 2.5.1.3 Viscosity – Frequency

There is variation in regard to how frequency affects the viscosity of cements. At 23°C, the frequency of deformation does not significantly affect the viscosity of Simplex P near the start of testing but as the extent of polymerisation increases, it does. At 33°C and 43°C, there are only two time points where the frequency of deformation does not significantly affect the viscosity of the cement. There is almost always a statistically significant difference in viscosity due to the frequency of deformation for CMW 2 and Palacos R except for the 3<sup>rd</sup> minute for CMW 2 at 43°C, and the 4<sup>th</sup> and 5<sup>th</sup> minute for Palacos R when tested at 43°C. Simplex P has several instances where the frequency of deformation does not significantly affect the viscosity, this is for the 3<sup>rd</sup> to the 7<sup>th</sup> minute when testing at 23°C, the 6<sup>th</sup> minute when testing at 33°C, and the 4<sup>th</sup> minute when testing at 43°C.

All cements were found to be pseudoplastics that experience shear thinning; this is widely reported in the literature.<sup>81, 82, 84, 200, 231</sup> As can be seen above (Figure 2.5) this is especially true the later in the polymerisation process the deformation occurs. This phenomenon could be exploited in THA. If during cement pressurisation the cement were forced to vibrate, using a vibrating pressuriser, the viscosity of the cement would decrease and interdigitation with the bone may be enhanced. The time that the cement is implanted is constrained. It is implanted late enough so that more of the toxic MMA particles have polymerised into inert PMMA particles and to ensure it is possible for the surgeon to adequately control the cement, yet it is implanted as early as possible so that the viscosity is low enough to ensure sufficient penetration and interdigitation with the bone. Utilising a vibrating pressuriser so that the cement can be implanted later may reduce the damage done by the toxic monomer, and the quality of interdigitation could be enhanced. A study by Thomas *et al.* studied the effect that low frequency vibration had on the quality of the cement bone interface using SEM and microfocal radiography (MFR). They found that the quality of the interface was improved.<sup>19</sup> In another study published in The Lancet, Thomas *et al.* showed that the flow of cement into the cancellous bone of a mock femur increased with increasing vibration.<sup>197</sup> Drew *et al.* found that less force was required to insert the femoral stem into a mock femur when a vibration of 19Hz was applied.<sup>196</sup>

## 2.6 Phase Angle

As discussed in the introduction, the phase angle is a measure of how elastic or viscous a material is. It is a ratio between the elastic modulus and the viscous modulus. The moment of gelation or the liquid-solid transition coincides with the development of an equilibrium modulus (when an imposed stress never fully relaxes).<sup>79</sup> There is no clear agreement regarding when this occurs for PMMA bone cement. Some authors suggest that it is when  $\tan(\delta)$  becomes independent of frequency,<sup>79, 88</sup> others suggest that the gel point of some plastics occurs when  $\tan(\delta)$  becomes smaller than one (indicating that the elastic modulus is larger than viscous modulus).<sup>77</sup>

Identification of when a PMMA bone cement can store strains applied during curing as residual stresses indefinitely is crucial for improving the mechanical properties of the PMMA bone cement mantle.

### 2.6.1.1 *Tan(Phase Angle) < 1*

There were only a handful of measurements, all at the start of testing when Simplex P was tested at 23°C when  $\tan(\delta)$  was greater than 1. There were no measurements made for the other two cements where  $\tan(\delta)$  was greater than 1. This indicates that, according to the definition where the equilibrium modulus develops when  $\tan(\delta) < 1$ , all cements tested could store residual stresses indefinitely except the very start of mixing for Simplex P

The second definition will be discussed in the *Phase Angle – Frequency* section.

### 2.6.1.2 *Phase Angle - Brand*

As can be seen, the results for the statistical tests regarding whether the brand of cement significantly affected  $\tan(\delta)$  do not follow a discernible pattern (Table 2.4). At 23°C there is only one point during the experiments that the brand did not have a significant impact on the value of  $\tan(\delta)$ , and this is in the 8<sup>th</sup> minute. This can be seen on the figure at 480s mark where one value of the CMW 2 cement increases before dropping to near 0. This likely gave the data enough spread so that the results for Simplex P were not discernibly different. At 33°C, it can be seen that it is only at the beginning of the experiment where there is a significant difference. This is likely due to the fact that the value for all three cements dropped to near 0 (fully elastic) sooner. The same can be said for the results at 43°C although the results become significantly different again in the 5<sup>th</sup> minute. The cause for this is unknown.

The results here primarily show that Simplex P (which is a low viscosity cement) stays more viscous than the other two cements for longer. This is expected as the polymerisation reaction which creates longer chains and thus creates a tangled macromolecule progresses slower as Simplex P is a low viscosity cement.

Farrar and Rose also found that Palacos R, deformed at 5Hz at 25°C, had a value for  $\tan(\delta) < 1$ , this value is consistent with the results found here. They also found that  $\tan(\delta) < 1$  at 350s for Simplex P at the same frequency and temperature.<sup>77</sup> This is later than is seen in these data. Spiegelberg found one measurement for Simplex P at 25°C at 5Hz where the moment of gelation occurred before measurements started; this is consistent with the findings reported here.<sup>89</sup>

### 2.6.1.3 *Phase Angle - Temperature*

There are only two instances where the temperature does not significantly affect the value of  $\tan(\delta)$  – these are in the 3<sup>rd</sup> minute for CMW 2 at 5 Hz and 10 Hz deformation rate. As this is so early it is likely that it is because the effect that temperature has on the rate of dissolution of the PMMA beads into the MMA liquid and the rate of the polymerisation reaction has not had the opportunity to become large enough.

It is expected that we see a significant difference in the value of  $\tan(\delta)$  due to temperature as the rate of dissolution of the PMMA particles and the rate of the polymerisation reaction are both increased by the temperature of the cement dough.<sup>80</sup> With a faster rate of reaction, we get longer chains developing faster and those longer chains will tangle with each other, creating a macromolecule. It is the bonds within the polymer and the forces between the chains that

determine the materials ability to store residual stresses indefinitely as they cannot move around easily and therefore cannot relax back into the maximum entropy state.<sup>79</sup>

#### **2.6.1.4 Phase Angle – Frequency**

Some of the literature regarding the identification of the moment of gelation states that for a stoichiometrically balanced reaction the critical gel point occurs when the dependence of  $\tan(\delta)$  on frequency becomes a power law.<sup>79, 88, 226, 232</sup>

Although there are several instances where the frequency of deformation does make a statistically significant difference to the value of  $\tan(\delta)$ , they are infrequent and do not have any distinct pattern. Due to the sporadic nature of the times and variables under which frequency does make a significant difference, it is difficult to say what the cause is. And whether there is a relationship between  $\tan(\delta)$  and frequency of deformation.

Once a bond has developed during polymerisation and the chains have become intertwined with each other it is difficult to say with the obtained data whether the frequency of deformation can break those bonds or untangle the chains. It is believed that for most common materials there is a frequency of deformation capable of breaking the material, as the frequency of deformation is a way of controlling the amount of energy being put into the material. It is believed that the frequencies used in this experiment were not large enough to properly test the hypothesis proposed. Prior to performing these experiments, it would have been prudent to perform an amplitude or frequency sweep to determine at what value the material started to be damaged. For this experiment, the values for the frequency of deformation used were determined using the literature<sup>77, 79, 89, 228, 229</sup>, which retrospectively, was an oversight. Therefore, it is not possible to conclude whether frequency independence of  $\tan(\delta)$  is indicative of the moment of gelation.

#### **2.6.2 Curing Times**

It can be seen above (Table 2.7) that different brands of cement result in different times to full cure and increasing the temperature of the experiment decreases the time till full cure. Other studies have also observed this sensitivity to temperature, most notably is a study performed by Nicholas *et al.*. They found that increasing the temperature from 25°C to 37°C reduced the time to cure by 372 s.<sup>229</sup> Nzihou *et al.* reports that the rapid conversion of MMA monomer to PMMA polymer stops around 491 s after mixing for Simplex P at 25°C, this value is earlier than the present study, which would predict 620 s for 25°C using interpolation.<sup>233</sup> No information on curing volume was reported and this will affect the speed of polymerisation. A conference proceeding published by Stephen H. Spiegelberg reported a curing time of 680 s which again is faster than the present study.<sup>89</sup> Nicholas *et al.* reported that Palacos R cured in 768 s at 25°C and 396 s at 37°C.<sup>229</sup> This roughly agrees with the interpolated figures found in this experiment, 700 s for 25°C and 400 s for 37°C.

The dough time is a frequently used measure for determining the curing parameters of PMMA bone cement. The dough time is defined within ISO 5833:2002 as the time when the cement no longer sticks to an unpowdered surgical glove in a room that is 23°C.<sup>55</sup> This is a useful metric for the surgeon as this can be identified during surgery, but it is subjective. In his book, Kuhn states dough times for all the cements used in this study.<sup>36</sup> CMW doughs in 85 s, Simplex P in

165 s and Palacos R doughs in 65 s. As the dough times stated here occur before measurements started, in the present study, no correlation between dough time and rheological properties could be found. As the temperature evolution of the PMMA bone cement is dependent on the size of the bolus studies cannot be directly compared.

### ***2.6.3 Clinical Relevance and Other Thoughts***

Although rheological characterisation is abstracted from a clinical setting the findings that are drawn from the data are clinically relevant.

Some conclusions were expected and have been widely known in the literature. Specifically, that the brand of cement and the temperature of the cements surroundings alter the rate of polymerisation and thus the development of the viscosity. The finding that the viscosity of PMMA bone cement is significantly reduced with an increased rate of deformation is also widely known; however, the literature regarding the application of vibration to PMMA bone cement whilst setting is not extensive, and the experiments are not thorough.<sup>19, 196-198</sup> This experiment does not achieve nor attempt this, but it may reopen the doors to that route of research as this project is taken forward.

Other conclusions are less widely known, mainly, the variables affecting the phase angle of PMMA bone cement during curing. The transition from a primarily viscous material to a primarily elastic material is a complex process involving many variables and material transformations. For example, CMW 2 cement transforms from a pliable dough into a rigid solid within 7 minutes when allowed to cure at 23°C. Within this time the phase angle reduces from 0.5 to approximately 0 and the viscosity decreases by a magnitude of 30. A difficulty in studying this transition is that the required experiments take time to take measurements. Ideally, stress relaxation tests would be performed to investigate the appearance of an equilibrium modulus, but it is difficult to pause the polymerisation reaction of PMMA bone cements. The primary interesting finding regarding the tangent of the phase angle was that for all measurements except for several at the very start of testing Simplex P at 23°C it was already below 1, meaning that the elastic modulus was larger than the viscous modulus. As previously mentioned, if the material is more elastic than viscous residual stresses may be able to form for most of the curing process of PMMA bone cement. However, as it is so difficult to determine this moment, a more direct method of determination of when this may happen is required.

Rheological characterisation is a more scientific, objective method for the determination of the timings of the curing process of PMMA bone cement. The current timings set out in ISO 5833:2002 are insufficient and are only extrapolations of the curing properties.<sup>55</sup> The dough and the setting time are convenient measurement techniques, especially for the surgeon, but neither are actual measurements of curing properties. The standards should include more rigorous, objective, and repeatable curing parameters.

### ***2.6.4 Future Work***

The work in this experiment was limited by the number of repeats, to improve the statistical strength of this study, more repeats should be performed. More work should also be done with

other brands of cement so that it can be determined whether the conclusions made here are applicable to a broader range of cements.

A frequency or amplitude sweep should have been performed prior to testing to determine the frequencies of deformation that should have been used. In the experiment reported here, the frequency did not significantly affect the value of  $\tan(\delta)$  for most conditions.

For most measurements, the value of  $\tan(\delta)$  was already below 1 meaning the elastic component of the modulus was larger than the viscous component. The cement could be cooled in an ice bath prior to experiments to attempt to delay reactions and thus it would be possible to further investigate the transition from a primarily viscous substance to a more elastic one.

More comparison with other rheological studies of PMMA bone cement is required. There is difficulty on this point due to the variety of testing variables. Studies could be specifically designed to directly compare with other papers on this topic although this would be limited to one study at a time.

Finally, other experiments may be performed to investigate the development of residual stresses. The strength of a control specimen should be compared to a specimen that has undergone deformation during curing to see whether these strains develop into residual stresses and thus weaken the cement.

## 2.7 Conclusions

This study is in good agreement with most of the literature regarding how bone cement behaves. This includes the increased rate of polymerisation (seen in both the value of  $\tan(\delta)$  and the value of viscosity) due to increased temperature. A difference can also be seen in these values due to the brand of cement. The results reported here also agree with the consensus in the literature that PMMA bone cement experiences shear thinning: an increased rate of deformation reduces the viscosity. Other findings are more significant. At the frequencies tested an increased rate of deformation does not reduce the value of  $\tan(\delta)$ . This implies that polymer bonds are not broken, nor polymer chains untangled at the frequencies tested. No correlation was found between any rheological properties and the curing parameters defined in the standards. It was found that for all conditions, except a few measurements at the start of testing for Simplex P at 23°C, the elastic component of the modulus was larger than the viscous component for all times. This is one of the possible indicators that a material can store applied strains as residual stresses.

## Chapter 3. Does Deformation During the Working Phase Significantly Weaken PMMA Bone Cement?

### 3.1 Disclaimer

Sections of this chapter have been taken and altered from a version that has been submitted for publication in the Proceedings of the Institution of Mechanical Engineers, Part H: Journal of Engineering in Medicine.

### 3.2 Introduction

Mechanical failure of PMMA bone cement is widely known to occur after implantation of a cemented THA. This is evidenced by reports of catastrophic fracture of the cement mantle as seen by a total fracture of the cement mantle<sup>91, 234-236</sup> and histological evidence of PMMA particulate in RLLs that are known to be indicative of later failure.<sup>138, 237-240</sup>

Many attempts have been made to maximise the strength of the cement mantle, either by introducing additives<sup>115</sup> or improving surgical techniques<sup>161</sup>; however, there were no studies in the literature investigating whether deformation during curing weakens PMMA bone cement. The previously reported rheological study (Chapter 2) showed that for all bone cements tested, the elastic component of the complex modulus is larger than the viscous component soon after mixing. It is generally agreed that stresses can be stored indefinitely in bone cement.<sup>73</sup> As seen in the literature review, some authors state that the elastic component becoming larger than the viscous component may indicate that the curing cement is now more “solid” than “liquid” and could store strains as residual stresses indefinitely (Chapter 1.5.4.4). It was hypothesised that if this crucial moment occurred before the start of the working phase, then all strains applied to the cement during the working phase would result in residual stresses and therefore weaken the cement.

Weakening of plastics due to deformation during curing has been observed in other plastics.<sup>97, 241</sup> It has been most frequently studied in injection moulded products. When injection moulded components are produced, the part is released from the mould after the plastic has set, making them unconstrained. The residual stresses caused by thermal shrinkage and deformation during curing effects cause warpage of thin-walled components. The cement mantle is a constrained component and therefore residual stresses created in the formation of the cement mantle, if present, will cause one of two outcomes: either the reaction forces constraining the cement between bone and implant will be overcome causing separation (perhaps seen as immediate RLLs). Alternatively, the cement mantle will remain constrained but will be weaker as the residual stresses will not be able to relax. If the loading forces are in the same direction as these residual stresses, then the loads required to cause failure will be smaller and the cement mantle will be weaker. Many of the methods for measuring residual stress directly are either inappropriate for bone cement or the required equipment was not accessible at the university.<sup>242</sup> Therefore, a simple experiment was devised which aimed to simulate deformation during surgery and to see whether it reduced the UTS of the cement. There is some work in the literature regarding whether vacuum mixing weakens or strengthens the cement,<sup>172, 177, 243</sup> but

work regarding the UTS is limited. Therefore, the effect of the method of mixing on the UTS and the porosity was measured.

### **3.2.1 Objectives**

1. To determine whether the deformation of bone cement during curing or whether the cement was mixed under vacuum or in atmospheric pressure had a significant effect on the magnitude or the characteristics of the porosity at the fracture surface.
2. To determine whether the deformation of bone cement during the working phase or the method of mixing had a significant effect on the UTS of dog bone samples.

## **3.3 Materials**

Two cements commonly used in arthroplasty were used in this experiment: Simplex P (Stryker, Michigan) and Refobacin R (Zimmer Biomet, Warsaw). The Refobacin R cement was supplied in a cement delivery system called Optipac (Figure 3.1). This system is designed to operate under vacuum and therefore this cement was always vacuum mixed. The Simplex P cement was supplied as a bag of powder (primarily containing PMMA granules) and an ampule of liquid (primarily consisting of MMA) (Figure 3.2). The Simplex P cement was mixed in a Hivac (Summit Medical) mixing bowl (Figure 3.3) connected to a vacuum pump when mixed under vacuum and if mixed at atmospheric pressure it was mixed in a glass bowl with a PTFE (polytetrafluoroethylene) spatula.



**Figure 3.1** Optipac Cement Delivery System (Zimmer Biomet, Warsaw)



**Figure 3.2** Simplex P Bone Cement packaging (Stryker, Michigan).



**Figure 3.3** Hivac bowl used for mixing the Simplex P bone cement (Summit Medical).

The moulds used to produce the dog bone samples were manufactured from PE (polyethylene) in line with the standards for the tensile testing of plastics (Figure 3.4)<sup>104</sup>. However, the dimensions of the dog bones were smaller than in the standards. This was done so that more repeats could be performed with less cement and so that the cross-sectional area (CSA) of the fracture site could fit within the frame of the SEM (Figure 3.5).

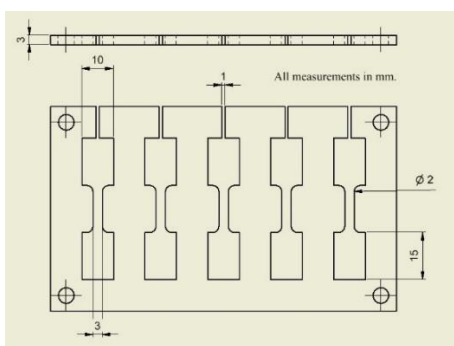


**Figure 3.4** Technical drawings of the PE moulds used to produce the dog bone samples.

The samples were tested in a Shimadzu AGS-X with a 1 kN load cell and were held in place using a pair of centralised metal grips, in line with the standards, to ensure that all force applied was tensile in nature (Figure 3.6)<sup>104</sup>.

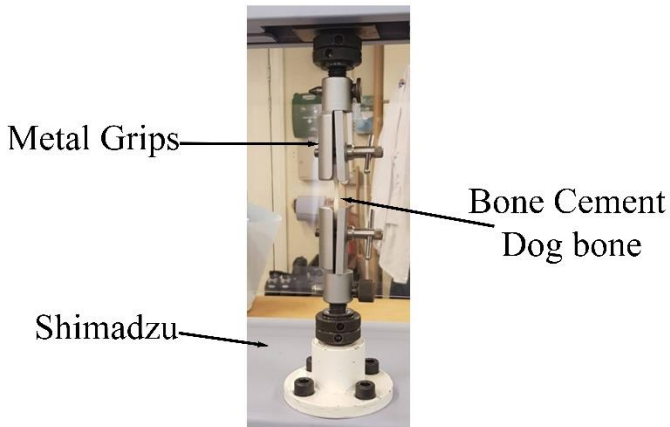


**Figure 3.5** Universal tester fitted with centralised metal grips used to hold the bone cement specimens.

After failure, the dog bones were sectioned about 5 mm away from the fracture site (Figure 3.7), cleaned and placed into a SEM (Hitachi TM3030).

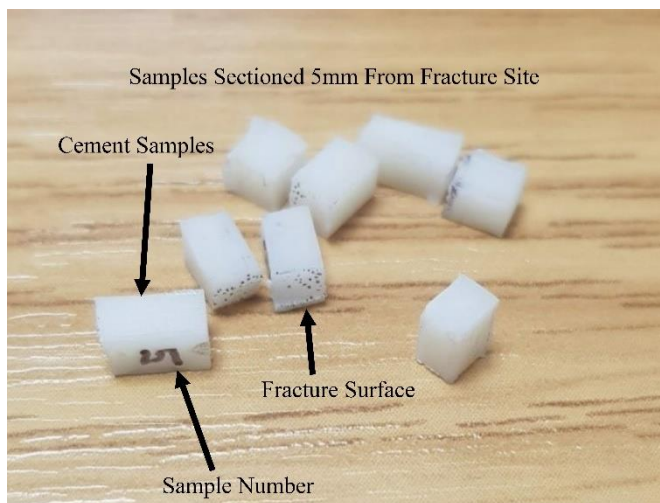


**Figure 3.6** Failed specimens sectioned a few millimetres away from the fracture site for SEM analysis.

### 3.4 Methods

All equipment was left in the laboratory where the experiments were to take place for around 48 hours to allow the equipment to equilibrate to the same temperature. All experiments were performed at a temperature of  $23\text{ }^{\circ}\text{C} \pm 1\text{ }^{\circ}\text{C}$  and a relative humidity of between 45 % and 50 % as measured using a digital thermo-hygrometer that was in the laboratory where the experiments took place. All figures were inside the parameters defined in the standards relevant to bone cement curing experiments.<sup>55</sup>

There were 6 sets of samples, each with different initial conditions, they are detailed below (Table 3.1).

**Table 3.1** Number of samples tested per testing condition.

<b>Bone Cement</b>	<b>Mixing Method</b>	<b>Deformation Phase</b>	<b>Number of Samples</b>
Refobacin R	Vacuum Mixed	Non-Deformed	10
		Deformed	7
Simplex P	Vacuum Mixed	Non-Deformed	8
		Deformed	8
	Non-Vacuum Mixed	Non-Deformed	10
		Deformed	10

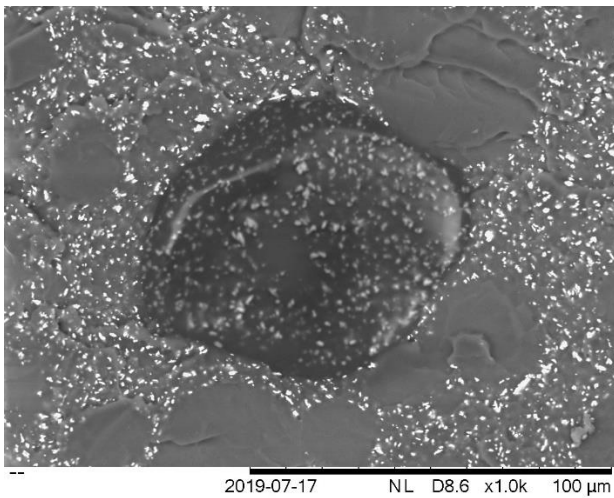
The first step for the vacuum mixed Refobacin R was to connect the vacuum pump to the Optipac mixing system. A pressure of around 0.4 bar (absolute) was then maintained which was within the manufacturers guidelines.<sup>175</sup> The powder and liquid were mixed, and the timer started. For the cement mixed at atmospheric pressure, the liquid and powder were combined in a glass bowl, the timer started and mixed with a PTFE spatula. For each of the initial conditions the cement was mixed at around 1 Hz and for as long as the curing curve indicated the cement was still in the mixing phase. After this, the pump was turned off, the cement mixing system opened, and the cement was touched with an unpowdered surgical latex glove to test whether the cement had entered the working phase. Once the cement had entered the working phase, the cement was either allowed to rest or was deformed via gentle kneading, attempting to avoid air entrapment, at around 1 Hz, for half of the working phase. Once this time had elapsed the cement was then forced, by hand, into the dog bone moulds. The top layer of the mould was then placed on top and then clamped to extrude any excess cement from the leakage holes seen above (Figure 3.4).

The samples were then left to cure, at the same temperature, for 48 hours. Once this time had elapsed the moulds were opened, and the samples were removed. Any samples with obvious external defects were rejected.

Each sample was placed into the universal tester and strained at 0.5 mm/min until failure. This is within the recommended crosshead speeds given in the tensile testing for plastics standards.<sup>104</sup> Although this standard is not specifically for PMMA bone cement, it was deemed appropriate as it is for plastics. The fractured samples were then removed from the tester. Once all experiments had been completed the specimens were sectioned 5 mm away from the fracture site, cleaned and placed into a SEM. Two images were taken, one at 40X (Figure 3.14) magnification, for calculation of total pore area and total fracture surface area, and one at 1000X magnification (Figure 3.7), which was used to check for micropores. The images taken at 40X magnification were then be loaded into Photoshop; each of the pores was modelled as an ellipse and the length and width were taken. This was done for both sides of the fracture surface and several values were calculated. Firstly, the total area of the fracture surface as a function of the external dimensions was calculated, this was taken as the theoretical maximum surface area. Secondly, the total area of the fracture surface occupied by pores was calculated; this would be used to calculate the true UTS. Thirdly, the number of pores was counted and then this was used to calculate the average pore area. Finally, the true UTS was calculated:

$$\text{Ultimate Tensile Strength (MPa)} = \frac{\text{Force at Failure (N)}}{\text{True fracture area (mm}^2\text{)}} \quad (1)$$

Where the true fracture area is the total area of the fracture surface using the external dimensions minus the total pore area.



Nexus Newcastle University

**Figure 3.7** A typical example of an SEM image taken at 1000X magnification of one of the pores present on the fracture surface of a failed dog bone sample.

An Anderson-Darling test was used to check for normality.<sup>244</sup> If the data set was normally distributed a student t-test was used.<sup>245</sup> If either or both sets were found to not have a normal distribution, and they were distributed in a similar way, a Mann-Whitney test was used.<sup>246</sup> For all tests, if  $p \leq 0.05$  it was concluded that there was a significant difference in the means.

## 3.5 Results

### 3.5.1 Force-Stroke Plots

In some of the tests, there was slipping of the specimens from the universal tester grips, a comparison between a test with no slip and a test with slip can be seen below (Figure 3.8, Figure 3.9). This was concluded due to the rapid loss of force at various points in some of the tests with no reduction in the stroke. This issue was resolved by tightening the grips. It is difficult to say from the experiments with slip whether there was a yield point; however, there were a sufficient number of experiments without slip to say that there was no clear yield point but rather a gradual transition from an elastic to a plastic region. This makes the usual method of calculating the yield point (a deviation of more than 5% in the gradient of the curve from the elastic region) not valid as there is no clearly defined elastic region. For all samples, no necking occurred before fracture and according to the relevant ISO, the bone cement is brittle.<sup>104</sup>

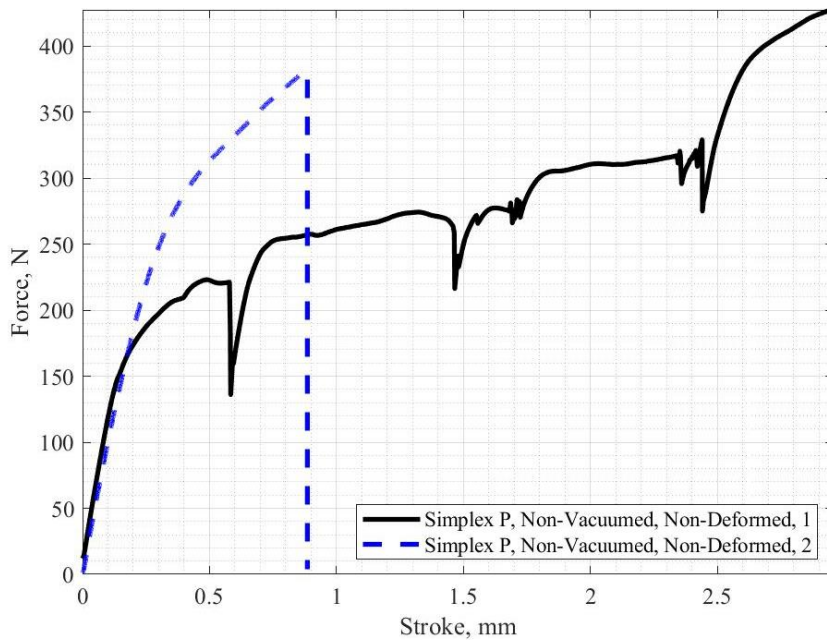


**Figure 3.8** Typical Force-Stroke plots for the test specimens. One sample showed slip in the centralised grips and the other did not.

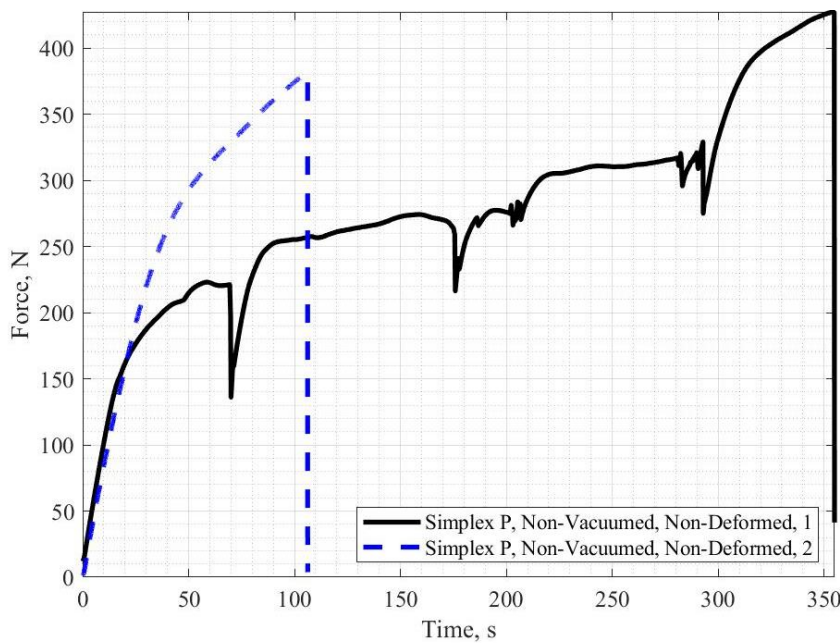


**Figure 3.9** Typical Force-Time plots for the test specimens. One sample showed slip in the centralised grips and the other did not.

### 3.5.2 Porosity

There were no significant differences in the overall area of porosity due to whether the cement was deformed during curing but there is variation in the spread of the data (Figure 3.10). There are also differences in the spread of data depending on how the cement was mixed (Figure 3.11).

The number of pores was significantly reduced due to vacuum mixing for both deformation conditions. This can be seen in the SEM images (Figure 3.12). There was significant variation in the porosity of the vacuum mixed cements as there were often large air pockets trapped in the samples. No pores were visible on the 1000X SEM images that were not visible on the 40X images.

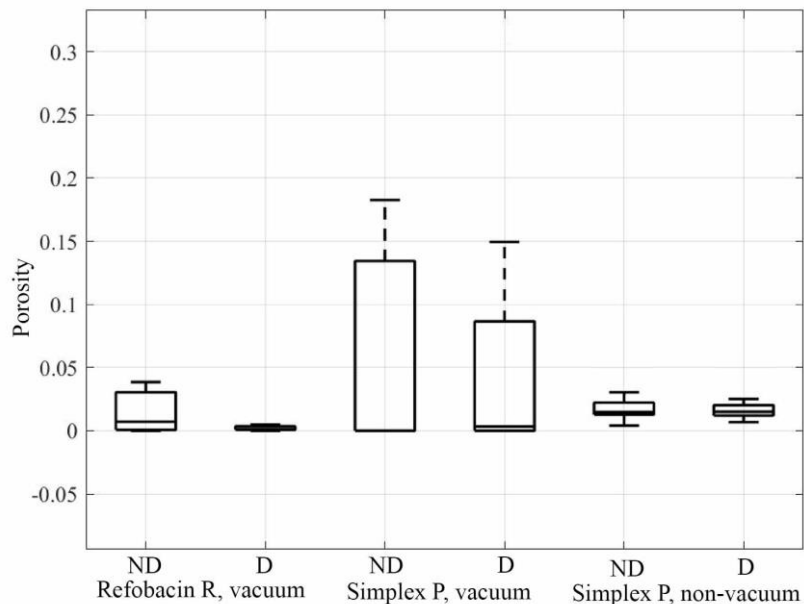


**Figure 3.10** Boxplots showing how deformation affects the porosity of each cement (D = deformed during curing, ND = no deformation during curing) The number of repeats for each test can be seen in Table 3.1. The bars indicate the maximum and minimum results, the box illustrates the interquartile range and the line within the box shows the mean.

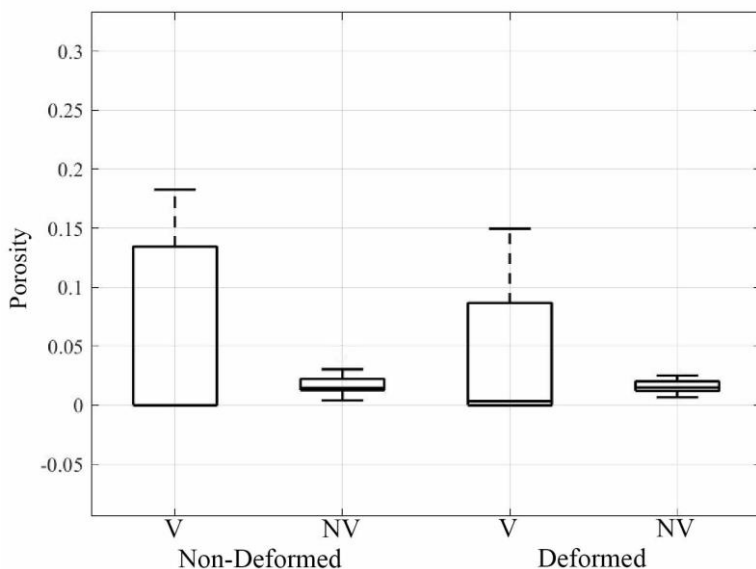


**Figure 3.11** Boxplots showing the porosity of Simplex P cements (V = vacuum mixed during curing, NV = not vacuum mixed during curing). The number of repeats for each test can be seen in Table 3.1. The bars indicate the maximum and minimum results, the box illustrates the interquartile range and the line within the box shows the mean.

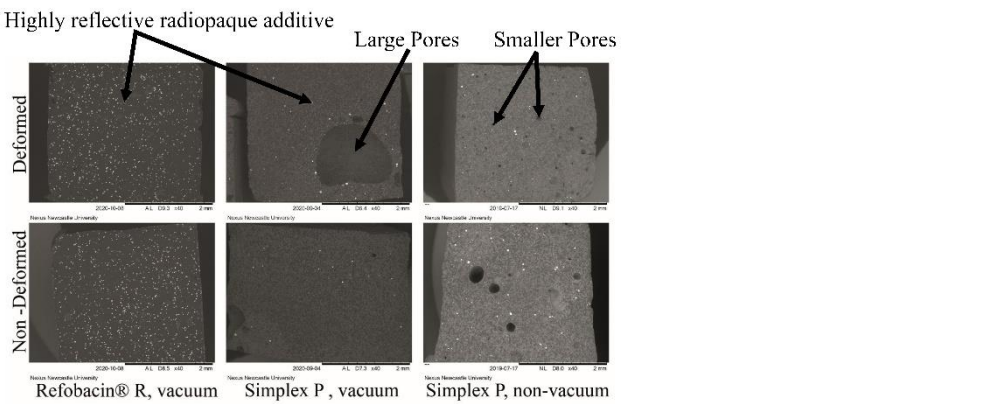


**Figure 3.12** Typical SEM images of the porosity at the fracture site for all cement samples. All images are given within the appendix (Appendix C).

### 3.5.3 Ultimate Tensile Strength

For both cements and mixing conditions, deformation during the working phase resulted in a significant decrease in the UTS. The mean number of pores, porosity, force at failure and UTS of the samples can be seen below (Table 3.2). For vacuum mixed Refobacin R, deformation during the working phase resulted in an 8.4% reduction in UTS. Deformation during the working phase for vacuum mixed and non-vacuum mixed Simplex P decreased the UTS by 18.4% and 6.7% respectively (Figure 3.13). The brand of cement also resulted in a significant difference in the UTS, Refobacin R was 7.3% stronger than Simplex P for non-deformed cement and 17.4 % stronger for deformed cement (Figure 3.14). The method of mixing did not significantly change the UTS.

**Table 3.2.** Pore number, porosity, force at failure and UTS of cement dog bone fracture samples. The number of repeats for each test can be seen in Table 3.1.

Bone Cement	Mixing Method	Deformation Phase	Pore Number	Porosity	Force at Failure (N)	UTS (MPa)
Refobacin R	Vacuum Mixed	Non-Deformed	7.67 ± 5.17	0.0155 ± 0.0154	385 ± 29.7	38.2 ± 1.95
		Deformed	2.86 ± 2.12	0.00193 ± 0.00182	352 ± 29.2	35.0 ± 3.07
Simplex P	Vacuum Mixed	Non-Deformed	0.625 ± 0.916	0.0564 ± 0.0823	372 ± 38.5	35.4 ± 1.97
		Deformed	1.88 ± 1.89	0.0612 ± 0.114	270 ± 42.7	28.9 ± 5.24
	Non-Vacuum Mixed	Non-Deformed	17.3 ± 8.04	0.0186 ± 0.0126	444 ± 50.6	34.4 ± 1.64
		Deformed	64.1 ± 34.2	0.0171 ± 0.00926	391 ± 42.7	32.1 ± 1.36

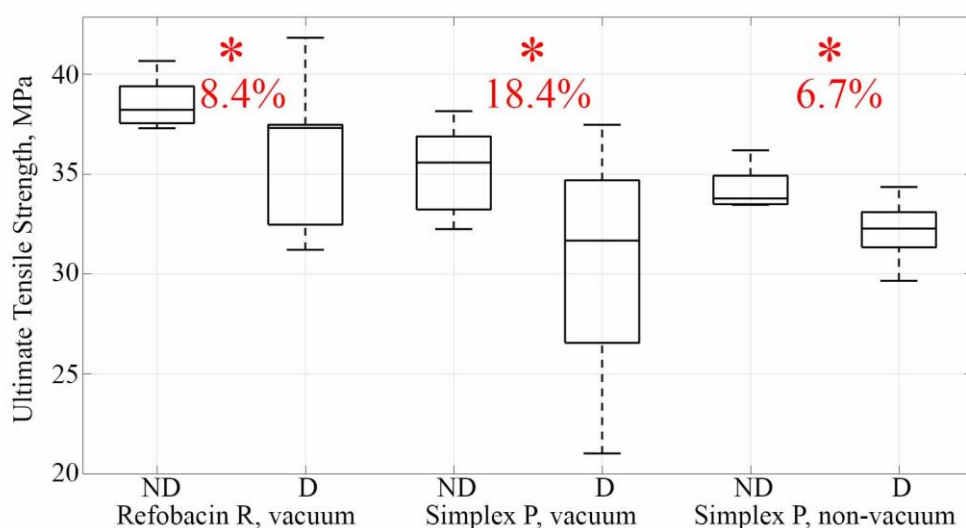


**Figure 3.13** Boxplots showing how deformation affects the UTS of each cement when they are vacuum mixed and non-vacuum mixed (D = deformed during curing, ND = no deformation during curing). The number of repeats for each test can be seen in Table 3.1. The bars indicate the maximum and minimum results, the box illustrates the interquartile range and the line within the box shows the mean.

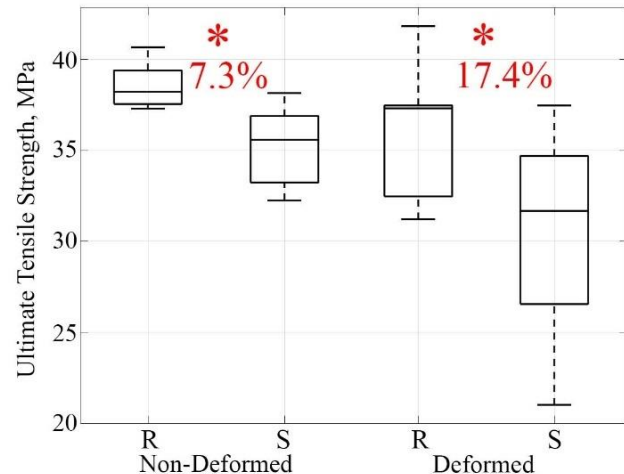


**Figure 3.14** Boxplots showing how the brand of cement affects the UTS of vacuum mixed cement (R = Refobacin R and S = Simplex P). The number of repeats for each test can be seen in Table 3.1. The bars indicate the maximum and minimum results, the box illustrates the interquartile range and the line within the box shows the mean.

### 3.6 Discussion

This study aimed to determine the effect that deformation during the working phase and the method of mixing (vacuum and non-vacuum) had on the UTS and porosity of PMMA bone cement. It was shown that irrespective of the mixing technique and brand of cement, deformation during curing weakens PMMA bone cement. The maximum reduction in strength due to deformation observed in this experiment was 18.4 % for vacuum mixed Simplex P. The brand of cement significantly affected the UTS with Refobacin R having a UTS 17.4 % larger than Simplex P for deformed, vacuum mixed cement. Whether the cement was mixed under a partial vacuum or not had no effect on the UTS of PMMA bone cement. Finally, there was no difference in the overall porosity of the fracture surface due to the method of mixing, but vacuum mixing significantly reduced the number of pores.

#### 3.6.1 Porosity

Vacuum mixing reduced the number of pores but not the porosity on the fracture surface. This suggests that PMMA bone cement shrinks by the same percentage volume irrespective of whether the cement is vacuum mixed. Cement shrinkage occurs due to two primary mechanisms: thermal shrinkage and polymerisation shrinkage.<sup>9, 39</sup> The first is a result of the increased temperature cement reaches during curing, reported to be between 41 °C<sup>66</sup> and 110 °C<sup>65</sup>; this causes expansion of the cement which subsequently shrinks as the cement cools – no studies could be found discussing how the increase in temperature affects the air trapped in the

pores nor the evaporation rate of the MMA monomer which is volatile. The second mechanism of shrinkage occurs due to an increase in the density of the MMA monomer to the PMMA polymer.<sup>39</sup> Neither of these mechanisms have been shown to be affected by the method of mixing. Therefore, it is not surprising that although vacuum mixing eliminates some of the pores, the overall magnitude of shrinkage is the same as seen by an equivalent porosity and constrained external dimensions. From the results presented here, it seems probable that the shrinkage will be split between whatever pores are present. Experiments should be performed which aim to determine how the nature of shrinkage of PMMA bone cement changes dependent on the number of pores trapped in the cement.

Whether or not the cement was deformed did not significantly affect the porosity, nor the number of pores present at the fracture surface. This shows that the methodology used to deform the cement did not introduce pores into the samples.

Tensile specimens fail at the location with the smallest cross-sectional area therefore the fracture area is not representative of the entire sample and the porosity results should not be taken as an indication of the average porosity of the cements.

### **3.6.2 Ultimate Tensile Strength**

Bone cement relies on a close mechanical interlocking with bone for fixation, to achieve this some deformation of cement must occur.<sup>184</sup> “Flow induced residual stresses” are studied in the field of injection moulding.<sup>241</sup> These residual stresses can weaken and warp the solidified polymer. Flow induced residual stresses occur when the polymer is deformed during curing after the moment of gelation, this deformation aligns the polymer chains, if the applied deformation is not removed and the chains cannot fully relax to their equilibrium state before solidification a residual stress will be present in the resulting cement mantle.<sup>98</sup> The equilibrium modulus describes how much of an applied, unrecovered strain will result in a stress after the material has fully relaxed. As reported by Winter *et al.* the equilibrium modulus appears at the moment of gelation and continues to increase as time progresses.<sup>79</sup> The study presented here is novel in investigating the effects that deformation during curing has on the mechanical properties of bone cement. It was found that deformation during the first half of the working phase significantly reduced the UTS of both brands of cement and both mixing conditions. Deformation reduced the UTS by 8.38 % for vacuum mixed Refobacin, 18.4 % for vacuum mixed Simplex P and 6.69 % for non-vacuum mixed Simplex P. This indicates that it is likely that the cement dough has passed the moment of gelation before the working phase for both cements tested and thus deformation results in residual stresses. With the data presented here, it is not possible to determine what fraction of residual stresses measured in other studies are created due to the flow of PMMA bone cement, but existing computational studies do not account for this phenomenon.<sup>92, 95, 247</sup>

The UTS of the samples can be found above (Table 3.2). The values of the UTS of Simplex P are within other reports in the literature. Friis *et al.* reported that for vacuum mixed Simplex P the UTS was 36.7 MPa. They also report that for cement mixed at atmospheric pressure the strength was 31.4 MPa.<sup>243</sup> Lewis cites Saha and Kamar who report a strength of 36.7 MPa<sup>11</sup> and Davis *et al.*, 36.2 MPa.<sup>248</sup> Kraus and Hofman report that Simplex P soaked in saline for 1, 7 and 35 days had a UTS of 27.1 MPa, 30 MPa and 30.2 MPa respectively, they do not report

the UTS with no soaking. No studies regarding the UTS of Refobacin R could be found. This may be due to the relatively short clinical history compared with Simplex P. No studies that investigate the effect of deformation on the UTS of cement could be found in the literature. It is already well documented that the brand of cement has a significant effect on the UTS.<sup>39</sup> It was found that Refobacin R was 2.8 MPa, or 17.4 % stronger than Simplex P when the cement was vacuum mixed and non-deformed.

Statistical tests showed no significant difference in the ultimate tensile strength for Simplex P due to the method of mixing. This can also be seen in the boxplots in Figure 3.13. Wixson *et al.* measured a significant difference in the tensile strength of PMMA bone cement samples that were mixed under vacuum and at atmospheric pressure. However, they determine that this is due to a significantly lower porosity.<sup>174</sup> In this study, the porosity was not significantly reduced and therefore these results concur with the findings of Wixson *et al.*. This is also consistent with a publication by Lidgren *et al.* who determined that a reduction in porosity improved the mechanical performance of PMMA bone cement. They measured the porosity of the bone cement using radiographs; however, it is uncertain how this was done as bone cement is radiopaque.<sup>172</sup>

### ***3.6.3 Clinical Relevance and Other Thoughts.***

Current surgical techniques and equipment are designed without the knowledge gained in this study regarding cement weakening when deformed during curing. Further investigations characterising the nature of the residual stresses in arthroplasty-specific geometries should be performed and further investigation into the parameters that control the magnitude and nature of the residual stresses is needed. Simple redesigns in surgical equipment may alleviate cement-weakening residual stresses.

The polyethylene moulds are in line with the standards for the tensile testing of plastics and for the testing of PMMA bone cement and therefore it is felt that this is appropriate. The metal clamp grips used created some slippage of the specimens during testing and there is a risk that this invalidates the results of this experiment. More experiments should be done using a fixation methodology which avoids any slippage. This would increase the validity of the conclusions drawn from this experiment.

### ***3.6.4 Future Work***

There are two main categories of future work that should be undertaken as a result of this study.

Firstly, more data should be gathered to strengthen the findings of this study. This will involve performing more experiments to ensure that the results are reproducible. Testing on a wider selection of cement could also be performed to ensure this phenomenon is not specific to the two cements tested. To ensure the findings reported here are not a result of the testing methodology alternative testing methodologies should be used. The method of deformation, the material used to shape the specimens, the dimensions of the specimens, the technique used to grip the samples and the testing speed are all examples of parameters that may affect the result. Experiments should also be performed to test whether the residual stress has a significant effect on the other mechanical properties of bone cement, specifically the fatigue strength as this is a

known common failure mechanism of cement mantles. Unlike the UTS, there are international standards established for fatigue, bending and compression tests for acrylic based bone cement.

Secondly, these results should be used to consider all designs of surgical equipment and all steps of surgical techniques, especially where deformation of the PMMA bone cement during the working phase occurs.

### **3.7 Summary**

The findings of this experiment highlight the importance of the design of surgical equipment and techniques. There is an interesting conflict between the necessity to deform the cement during the working phase to ensure sufficient fixation and the phenomenon of flow induced residual stresses. It would mean that when designing equipment or surgical techniques it is vital to reduce the *unnecessary* deformation of bone cement. This includes deformation of cement done by the surgeon prior to implantation and to ensure that equipment previously designed to maximise ingress of cement into bone should do so whilst minimising any extra deformation. The rheological theory also suggests that the equilibrium modulus increases through time, therefore all *necessary* deformation should be done *as early as possible*. This means the pre-existing balance between requiring a low viscosity to maximise cement penetration and needing to wait so there isn't excessive cement leakage, and the monomer toxicity is changed as flow induced residual stresses should be considered.

## Chapter 4. Does Vacuum Mixing Affect Diameter Shrinkage of a PMMA Cement Mantle During *In Vitro* Cemented Acetabular Cup Implantation?

### 4.1 Disclaimer

Sections of this chapter have been taken and altered from a version that has been published in the Proceedings of the Institution of Mechanical Engineers, Part H: Journal of Engineering in Medicine.<sup>249</sup>

### 4.2 Introduction

#### 4.2.1 Background and Motivation

Cementation is the gold standard method of fixation for THA according to NJR statistics, with the lowest rate of revision at all time points after surgery.<sup>2</sup> However, some acetabular cups still fail, aseptic loosening is the most common cause. In cases where the implant fails after a long time period, the cup becomes loose due to osteolysis causing resorption of bone around the implant; this is a slow process that occurs over many years.<sup>140</sup> Wear debris from the articulating surfaces of the implant bearing migrates into the interface between bone and cement, this results in an adverse reaction that triggers resorption of bone. This, in turn, creates a layer of soft tissue that can be seen on radiographs as a RLL.<sup>140</sup> However, this long-term bone resorption process does not explain reports of RLLs on immediate post-operative radiographs around the cement mantle of acetabular cups.<sup>127, 129, 161, 250-252</sup> Authors have suggested these may develop due to thermal necrosis,<sup>4-12</sup> chemical necrosis,<sup>10, 11, 13, 14</sup> fluid imposition<sup>15-19</sup> and cement shrinkage.<sup>6, 9-11, 20, 21</sup>

When the bone cement powder and liquid are mixed, a polymerisation reaction starts which continues until full cure and rigidification.<sup>50</sup> Polymerisation results in an increase in molecular density and therefore volume shrinkage will occur.<sup>39</sup> The reaction is exothermic so the cement mantle will generate and expel heat; this will cause thermal expansion of the cement mantle followed by shrinkage as the temperature falls to that of the surroundings.

Vacuum mixing was introduced into the standard cement preparation methodology to reduce the porosity of the cement mantle as it was believed that pores act as crack propagation sites and therefore weakens the cement.<sup>177</sup> Vacuum mixing of bone cement reduces the porosity of the cement mantle created and therefore increases the amount of shrinkage from 2-5% for hand mixed cement<sup>9</sup> to 3-6% for vacuum mixed cement.<sup>253</sup> Haas *et al.* reported that preventing the creation and expansion of pores within the cement through vacuum mixing may contribute to this increased extent of shrinkage.<sup>9</sup> Bone cement does not form adhesive bonds but rather relies on mechanical interlock with bone trabeculae for fixation. Any shrinkage of bone cement after the mantle has been formed may result in a reduction in the quality of the fixation between the bone and the bone cement. A secondary concern regarding shrinkage of bone cement is that any interstices created between cement and bone provides migration paths for wear debris from the articulating bearing to penetrate the interface and cause particulate-mediated osteolysis and

subsequent aseptic loosening.<sup>254</sup> There is limited literature investigating the clinical implications of vacuum mixing. One study that used data from the Swedish national hip arthroplasty registry reports that the risk of failure is initially increased due to vacuum mixing. However, the risk of failure gradually reduced and the risk of revision, when compared to open bowl hand mixing, is lower after eight years.<sup>168</sup>

This chapter focuses on cement shrinkage between the acetabulum and the cement mantle as this is where many primary hip replacements fail.<sup>126, 160, 162, 194</sup>

No studies were found in the literature that tried to quantify the interstice created between the cement mantle and acetabulum during cemented acetabular implantation during *in vivo* or *in vitro* experiments. This is surprising considering that cement mantle shrinkage is commonly stated as one of the most likely contenders for early failure of the acetabular component.<sup>6, 9-11, 20, 21</sup>

#### **4.2.2 Objectives**

1. To determine whether there is significant diametric shrinkage of the bone cement mantle after mock cemented acetabular cup implantation when the PMMA bone cement is mixed by hand at atmospheric pressure.
2. To determine whether there is significant diametric shrinkage of the bone cement mantle after mock cemented acetabular cup implantation when the PMMA bone cement is mixed under vacuum.
3. To determine whether the diametric shrinkage is uniform across the whole acetabulum cement mantle.

#### **4.3 Materials**

This section describes the materials used in this experiment. The methodology is described in the following section.

The model acetabulum was manufactured from stainless steel 304 to have a 52mm diameter hemispherical bore, a typical diameter to which the acetabulum is reamed (Figure 4.1).<sup>45</sup> A coordinate measuring machine (CMM) was used to measure the diameter of the cavity and confirmed that the bore diameter was within 0.01 mm of the expected value. The blanking bolts seen below filled holes for pressure sensors in a separate experiment which is not reported here (Figure 4.1).

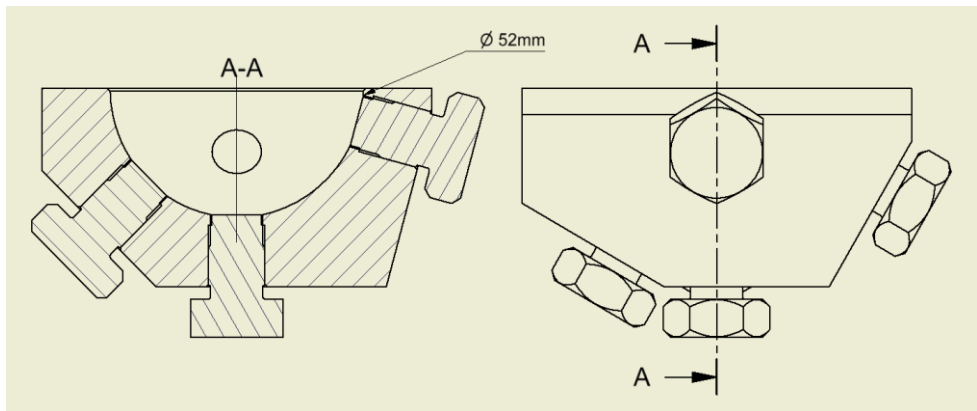


**Figure 4.1** Technical drawing of the model acetabulum used for cement pressurisation experiments (blanking bolts cover holes for a different experiment).

A Depuy Smartseal acetabular pressuriser (DePuy, UK) was used for the pressurisation of the cement. The pressuriser consists of a silicone spherical segment. When force is applied, the pressuriser seals the acetabulum cavity with the cement still inside, thus pressurising the cement (Figure 4.2).

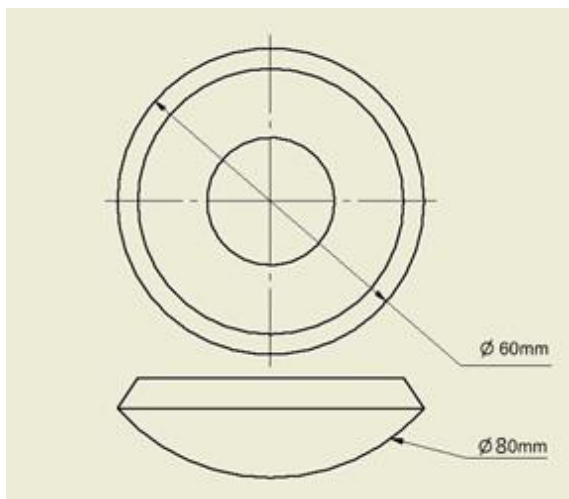


**Figure 4.2** Technical drawing of the Depuy Smartseal Pressuriser used for cement pressurisation for all experiments.

To represent a real acetabular cup, a flanged cup design was chosen and manufactured from HXLPE, which had an external diameter of 50mm which is representable of what is implanted *in vivo* (Figure 4.3).

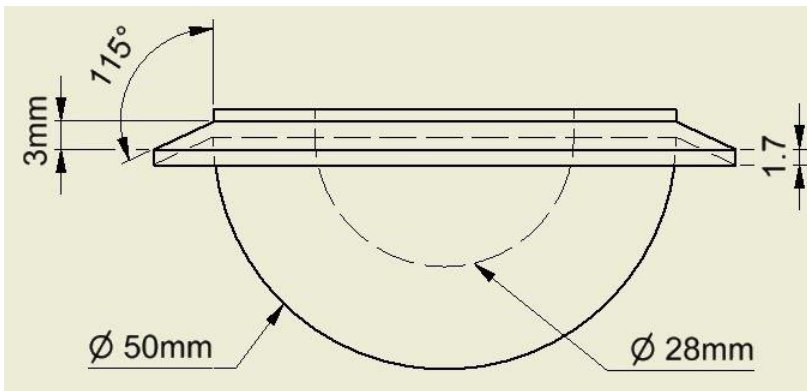


**Figure 4.3** Technical drawing of the flanged acetabular cup used for the experiments.

CMW 2 fast set bone cement (DePuy, UK) was used to secure the acetabular cup. CMW 2 was used as it is frequently used by surgeons to fix the acetabular cup.

The assembled rig, consisting of mock acetabulum and pressuriser (Figure 4.4) was mounted into a Shimadzu AGS-X, which was used to apply the load to the cup and pressuriser. The Shimadzu was fitted with a 1 kN load cell and was force controlled with a maximum stroke rate of 40 mm/min.

All equipment manufactured had a tolerance of  $+\text{-} 0.05$  mm. Due to the design of the rig, this means that the force would be applied within 0.25mm of the centre of the acetabulum cavity.

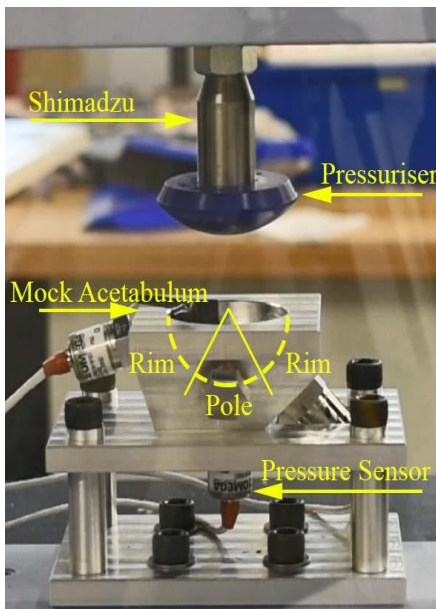


**Figure 4.4** Mock acetabulum and Depuy pressuriser experimental set-up in the Shimadzu universal tester.

#### 4.4 Methods

All equipment used in the experiments were kept at room temperature. Experiments were performed between  $20.5^{\circ}\text{C}$  and  $23^{\circ}\text{C}$  which is outside the range defined in ISO 5833 ( $22^{\circ}\text{C}$  to  $24^{\circ}\text{C}$ ) and the relative humidity was between 45% and 50% which is within ISO 5833

recommendations.<sup>55</sup> Mould release spray (Silicone Mould Release Agent, Ambersil) was used to ensure that the cement mantle could be removed from the model acetabulum.

The bone cement was mixed by hand in an open bowl in five experiments and mixed under vacuum in five other experiments. A sample size analysis was not performed but the number of repeats performed was limited due to the amount of bone cement available. For the open bowl, non-vacuum mixed conditions the cement was mixed in an inert glass bowl with an inert PTFE spatula by hand at around 1 Hz until homogeneous and then left to rest until the cement was no longer tacky. For vacuum mixing, the cement was mixed using a Hivac Bowl (Summit Medical, UK) under a 0.4 bar (absolute) vacuum. The cement was mixed for 1 minute under vacuum then removed to test whether the cement was still tacky, defined as the dough point in ISO 5833.<sup>55</sup>

For both mixing conditions, the cement was inserted into the model acetabulum when it was no longer tacky and pressurised with a Depuy Smartseal pressuriser for 100 s at 100 N as this is typical of the forces used in the literature and was within the range of forces generated in an *in vivo* experiment (Figure 4.5)<sup>195</sup>.

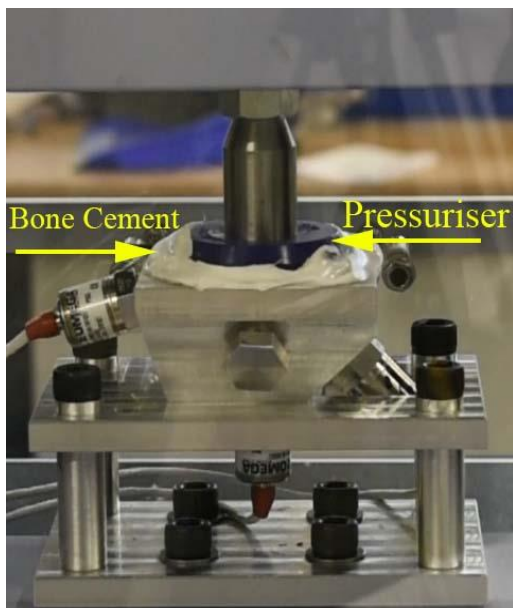


**Figure 4.5** A 100 N force was applied to the Depuy Pressuriser with the bone cement sealed within the acetabulum model in the Shimadzu universal tester.

After the pressuriser was removed, the acetabular cup was inserted into the cement mantle and a force of 50 N was applied. The force was removed after the cement had fully cured (Figure 4.6).

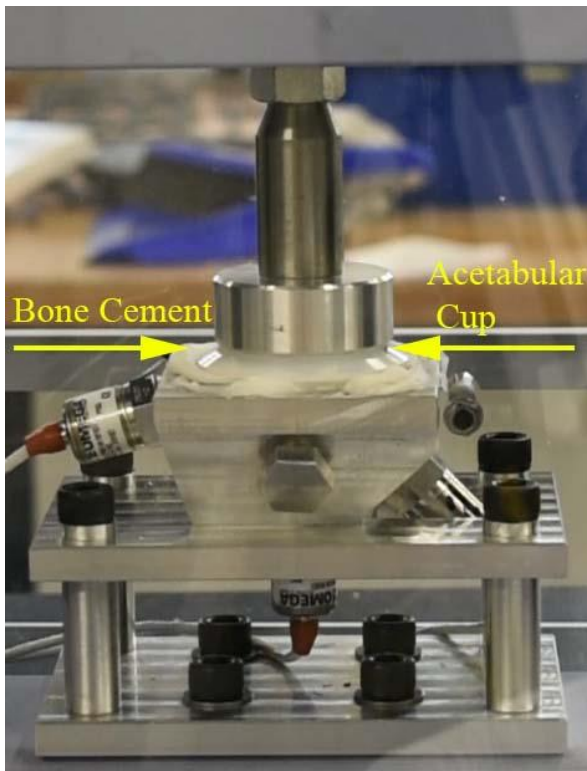


**Figure 4.6** A 50 N force applied to the flanged acetabular cup in the Shimadzu universal tester.

The magnitude and duration of the applied load were within the range of typical values found in the literature.<sup>190, 192, 193</sup> Measurements detailed in a later chapter indicate that the pressures produced at the surface of the acetabulum were comparable to other studies in the literature.<sup>190, 192, 195, 255</sup>

At the conclusion of the experiment, once the cement mantle had returned to room temperature, the cement mantle was removed from the acetabulum. The diameter of the resulting cement mantle was measured using a Mitutoyo Quickscope. The mantle was secured in the microscope and eight to fifteen coordinates were taken around the circumference. A script was used to calculate the diameter of the mantle using the circumferential coordinates (Appendix D). This was repeated five times for each mantle. The precision of the coordinates taken were 0.0025 mm. This technique was then performed separately for the rim and the pole of the cement mantle to investigate whether the shrinkage was uniform. The rim was defined as the top 22.5° from the opening of the cavity (zone I and III) and the pole was all the mantle below this (zones II) as this criterion was used by Delee and Charnley to describe the three zones of the acetabulum (Figure 4.7).

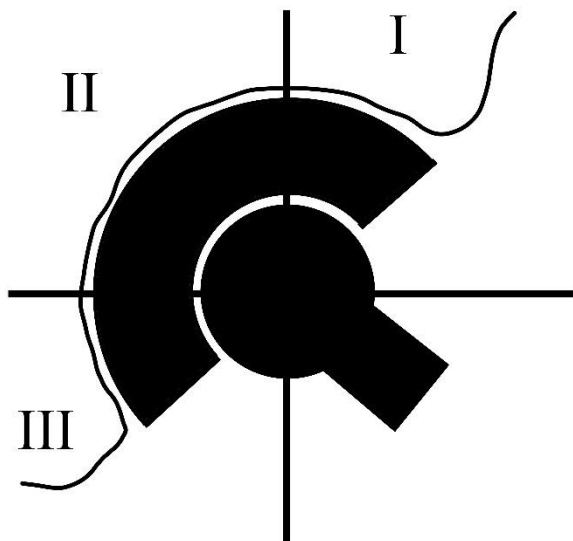


**Figure 4.7** Acetabular Zones as described by Delee and Charnley.<sup>127, 129</sup>

The measurement technique described above was validated as follows: A spherical test piece of known diameter was measured, and the result was found to be within 0.05 mm of the true value. In addition, a CMM was used to check the Quickscope measurements, and this also found the result to be within 0.05 mm.

Two cement mantles from each mixing condition were sectioned so that the porosity and the mantle thickness could be measured. As the bone cement-bone interface was the focus of this study the internal diameter was not measured. The thickness was determined using a Vernier calliper; 10 measurements for the rim and the pole were taken and the results averaged. The porosity, reported as a ratio of pore area to the total area, was determined using images taken on a Hitachi TM3030 SEM (Hitachi, Japan). Eight images were taken in total for each mantle – one in each quadrant of the sectioned area – and loaded into Photoshop (Adobe, San Jose) so that the area of the pores could be measured. This was repeated for the other half of the sectioned mantle.

A simplified model of the bone cement mantle was created to determine the impact of porosity on the overall volume of the mantles. The measured external diameter and the diameter of the implanted cup were used. The measured thickness of the mantles at the pole was used as the offset between these two diameters. The hollow hemisphere created with these two diameters was cut off at the top of the model acetabulum. These values and the measured porosity of the cement mixed under non-vacuum conditions were used to determine what the external diameter would be if all pores were eliminated, and the other variables were constant.

A Ryan-Joiner test was used to see whether data were normally distributed; if so, a standard student t-test<sup>245</sup> was used to determine whether there was a significant difference between compared variables shown in the table below (Table 4.1). If the data were not distributed normally, a Mann-Whitney test was used.<sup>246</sup> A one-sample t-test was used to determine whether the diameter was significantly different from the diameter of the model acetabulum. The results were considered significant if  $p \leq 0.05$ .

## 4.5 Results

Independent of whether the cement was mixed under vacuum or under non-vacuum conditions a significant interstice between the PMMA cement and the mock acetabulum was created when CMW 2 fast set bone cement was used to implant a 50 mm diameter HXLPE cup into a 52 mm diameter mock acetabulum. Including the standard deviation and the precision of the manufactured acetabulum, the average size of the interstice is dependent on the method of mixing:  $0.60 \text{ mm} \pm 0.0921 \text{ mm}$  for vacuum mixed CMW 2 bone cement and  $0.38 \text{ mm} \pm 0.1455 \text{ mm}$  for non-vacuum mixed CMW 2 bone cement. There was a significant difference in the external diameters of the cement mantles due to the method of mixing (Figure 4.8). There was no significant difference between the magnitude of shrinkage at the rim and at the pole of the acetabulum for either mixing technique (Table 4.1).

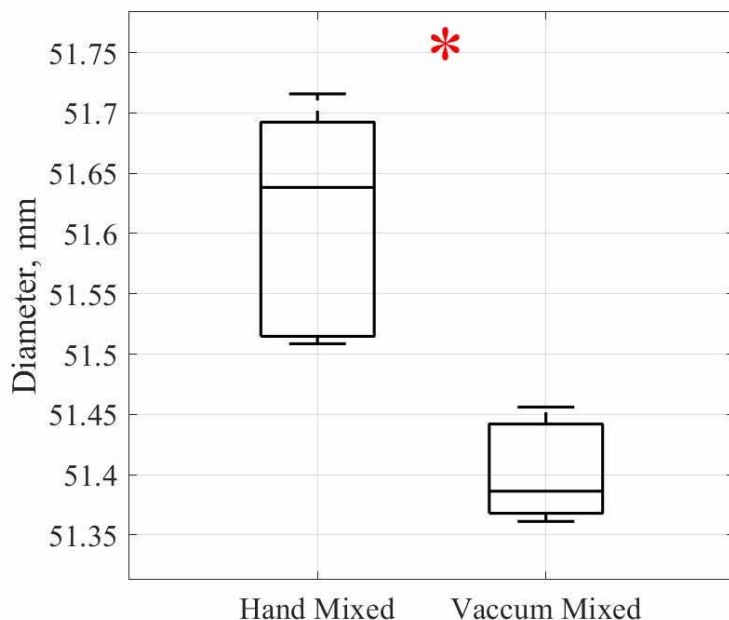


**Figure 4.8** Boxplot displaying the significant difference in the external diameter due to the method of mixing. Five repeats were performed for each experiment. The bars indicate the maximum and minimum results, the box illustrates the interquartile range and the line within the box shows the mean.

The thickness at the pole of the cement mantles was larger than at the rim for every cement mantle (Table 4.1). Vacuum mixing resulted in a thicker mantle at the rim compared to non-vacuum mixing but there was no difference in the thickness at the pole due to the method of mixing (Table 4.1).

Vacuum mixing significantly reduced the porosity of the cement mantle when compared to cement mixed by hand at atmospheric pressure (Table 4.1, Figure 4.9).

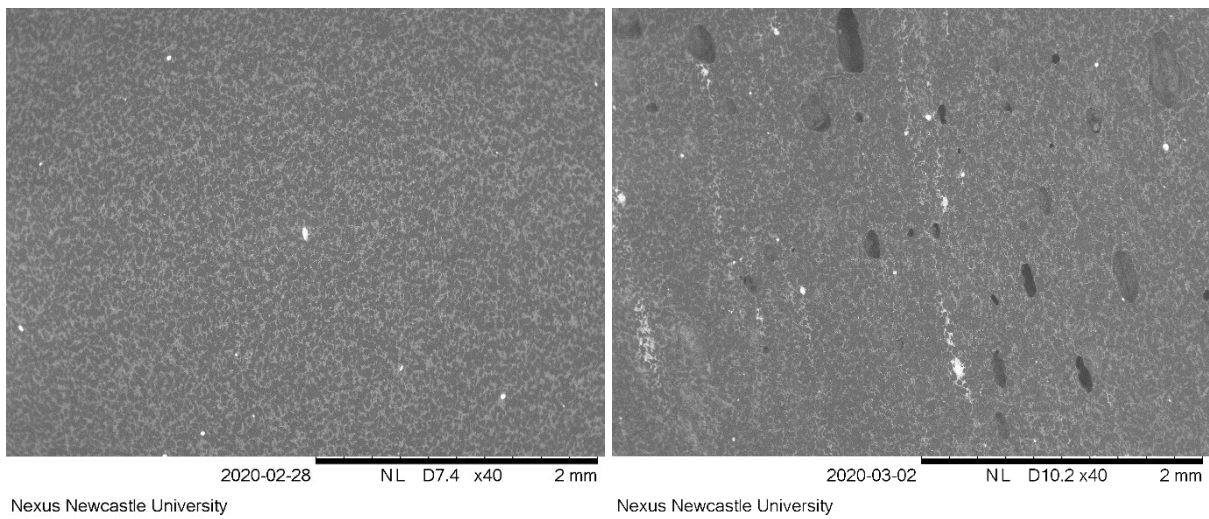


**Figure 4.9** Typical examples of SEM images taken to measure the bone cement porosity. The image on the left shows the vacuum mixed cement with minimal pores and the image on the right shows cement mixed by hand at atmospheric pressure with a significant number of pores.

The simplified model of the cement mantle volume showed that there was a decrease in the volume for the mantles created using vacuum mixed cement compared to non-vacuum mixed cement. This model was also used to calculate the theoretical volume of the non-vacuum mixed mantles if all pores were eliminated. If the difference in shrinkage was due to pores, a mantle created using cement mixed in non-vacuum conditions with all pores eliminated should have the same volume as the vacuum mixed mantles. The volume of the zero-pore hand mixed cement was within 0.26 % of the vacuum mixed component showing that the cement shrinkage could be accounted for by pore elimination (Table 4.1).

**Table 4.1** Results of bone cement mantle dimensions measured for vacuum mixed and hand mixed cements for a 52 mm mock acetabulum and 50 mm HXLPE cup. All mean values with +/- standard deviations where appropriate, five repeats were performed for each experimental condition (student t-test as standard, \*for Mann-Whitney statistical tests)

	Vacuum Mixed	Non-Vacuum Mixed	Statistical Difference?
Overall Diameter (mm)	51.40 +/- 0.0421	51.61 +/- 0.0955	Y
Diameter at Rim (mm)	51.31 +/- 0.169	51.61 +/- 0.104	Y
Diameter at Pole (mm)	51.37 +/- 0.109	51.56 +/- 0.08205	Y
Thickness at Rim (mm)	4.935 +/- 0.8706	4.120 +/- 1.065	Y*
Thickness at Pole (mm)	10.09 +/- 0.7029	9.628 +/- 0.3412	N*
Porosity	0.002253 +/- 0.006377	0.02368 +/- 0.02279	Y*
Calculated Volume (mm <sup>3</sup> )	275800	283300	
Theoretical Pore Free Volume (mm <sup>3</sup> )		276500	
Statistical Difference? Rim : Overall Diameter	N	N	
Statistical Difference? Pole : Overall Diameter	N*	N	
Statistical Difference? Rim : Pole Thickness	Y*	Y*	

## 4.6 Discussion

This study investigated whether there was significant diametric shrinkage of the bone cement mantle after cemented cup implantation when mixed under vacuum or in non-vacuum conditions and whether shrinkage was uniform across the acetabulum. There was significant shrinkage of the bone cement mantle after acetabular cup implantation. Vacuum mixing significantly increased the magnitude of this shrinkage,  $0.60 \text{ mm} \pm 0.0921 \text{ mm}$  when compared to  $0.39 \text{ mm} \pm 0.1455 \text{ mm}$  for cement mixed in non-vacuum conditions. This shrinkage is uniform across the whole acetabulum. The statistical results presented in Table 4.1 are significant as they indicate that there is a statistical difference in the mean for all measured variables except the thickness of the cement mantle at the pole due to the mixing methodology.

The results presented in this study found that the outer diameter cement mantles shrinks by an average of 0.39 mm when the cement is mixed under non-vacuum conditions, and by 0.60 mm when the cement is mixed under vacuum. This is when CMW 2 fast set bone cement is used to implant a 50 mm acetabular cup into a 52 mm reamed acetabulum. This result may explain the presence of RLLs on immediate post-operative radiographs and the increased risk of failure soon after implantation as reported by Malchau *et al.*<sup>168</sup> A study by Green *et al.* showed that particles  $0.3\mu\text{m}$ - $10\mu\text{m}$  in diameter are the most biologically damaging; this is at least 39x smaller than the potential interstice created due to cement mass shrinkage.<sup>254</sup> It is hypothesised that the larger the interstice between the bone cement and the bone, the faster resorption of the bone will occur as it will allow more wear debris from the articulating surface to penetrate deeper into the interface and this wear debris is known to cause resorption of the bone. As the only difference between the cement mantles created in the Malchau *et al.* is whether the cement was vacuum mixed or not, the cause of the increase in rapid failure of cement mantles is due to a result of vacuum mixing. Although more studies are required to determine the effect of mixing technique on other factors known to cause radiolucent lines such as chemical and thermal necrosis, the findings in this study indicate that the increased shrinkage is a likely contender for the primary cause of early failure.

As a percentage diametric shrinkage: hand mixed cement shrank by 0.75% and vacuum mixed cement shrank by 1.15%. The literature states that vacuum mixed cement is expected to shrink by 3-6% and hand mixed cement should shrink by 2-5%.<sup>39</sup> The difference between the literature and the figures found in this study may be due to the shrinkage not being homogenous. Only diametric shrinkage was measured but there may have been more shrinkage circumferentially, although that was not measured.

The cement mantle at the pole for all experiments was thicker than the rim, this difference was found to be statistically significant. The thickness of the cement mantle at the rim was 4.935 mm and at the pole was 10.09 mm for vacuum mixed cement ( $p < 0.05$ ) and the thickness at the rim was 4.120 mm and 9.628 mm at the pole for cement mixed at atmospheric pressure ( $p < 0.05$ ). This was due to the insertion of the cup being forced controlled rather than position controlled. Despite the discrepancy of the cement mantle thickness, the shrinkage of the cement was uniform across the entire mantle.

This study agrees with the hypothesis put forward by Davies and Harris that if the porosity is reduced, the reduction in the external dimensions would have to account for the shrinkage.<sup>183</sup> However, their findings conflicted with both their hypothesis and the findings reported here.

#### **4.6.1 Clinical relevance**

Although there are differences between this study and the clinical setting the results are still relevant.

In the previous chapter (Chapter 3), there was no significant difference in porosity due to the mixing method. However, it is hypothesised that this was due to where the porosity measurements were taken. The fracture surface in the UTS experiments will likely be in the location with the smallest cross-sectional area as this is where the stresses due to the applied load will be highest; therefore, the porosity measurements would not be representative of the overall porosity of the sample. The porosity results presented in this chapter are more likely to be representative of the overall porosity as the location of the measurements was controlled.

The findings reported here that vacuum mixing increases the size of the interstice created between the trabecula bone and the cement, aligns with the findings of Malchau *et al.* that there is an increased risk of loosening in the first few years post-operation which will then decrease through time as the body adapts to the gap. This implies that the later loosening that occurs at the cement-bone interface is not connected to the size of the interstice created at surgery. It also provides an explanation for RLLs found on immediate post-operative radiographs.

#### **4.6.2 Study Limitations**

There are differences between this study and the clinical setting. The mock acetabulum was machined smooth whereas *in vivo* the cement will be pressurised into the porous bone with holes drilled into it aid interdigitation. If the cement is sufficiently interlocked with the bone a complete separation of cement and bone may be avoided. However, this means the cement shrinkage will lead to straining of interdigitated bone trabeculae and cement fingers which may also cause damage. Although the findings presented here are important for observing the extent to which the cement would shrink in a simplified setting, it is a limitation of this study that there was no resistance to contraction. In a clinical setting, the cement will cool to 37°C, however, in this experiment it cooled to room temperature (20.5 – 23 °C). It is expected that this would result in less shrinkage in a clinical setting. The conductivity of the steel acetabulum was also not representative of bone. Sean *et al.* found that bovine cortical bone had a thermal conductivity of  $0.58 \pm 0.018$  W/mK in the longitudinal direction,  $0.53 \pm 0.030$  W/mK in the circumferential direction, and  $0.54 \pm 0.020$  W/mK in the radial direction.<sup>256</sup> The thermal conductivity of stainless steel 304 according to the manufacture is between 14 W/mK and 17 W/mK.<sup>257</sup> This means less heat will be conducted away from the cement in a clinical setting and therefore the maximum temperature, the resulting thermal expansion and the consequential shrinkage upon cooling that the cement will experience *in vivo* will be larger than in this experiment. The geometry of this experiment was simplified from the clinical setting so the results would be reproducible, anatomically the rim of the acetabulum has many irregularities. The reaming and the cup insertion both occurred at 0° inclination for this experiment whereas

in a clinical setting there would be an inclination of 40°, it was assumed that this would have a small effect on the geometry of the cement mantle.

For this study the acetabulum model was dry, N'Diaye *et al.* found that PMMA bone cement experiences swelling due to water absorption, this swelling may negate some of the shrinkage effects observed in this study in a dry environment.<sup>258</sup> Ideally, during implantation the acetabulum should be dry to maximise interface strength and therefore the effects of swelling on the volume of the cement mantle will occur sometime after implantation.

The final placement of the cup was not controlled. This does not reflect a true implantation, during surgery a surgeon will vary the magnitude and direction of the force to ensure that the acetabular cup is fixed in an anatomically accurate location. For future work, either a methodology should be developed which ensures that the cup is seated in the mock acetabulum in an anatomically accurate position, or the cup could be inserted by a trained surgeon to closer mimic a true implantation.

The diameter of the acetabular cup used was 2mm larger than that which is generally recommended by surgeons and manufacturers. This should not detract from the findings of this study since if a smaller cup were used it, is expected that the size of this interstice would increase. The effect of cup size on the size of the interstice created between the cement mantle and bone, and the pressure at the model acetabulum surface should receive further attention.

#### **4.6.3 Future Work**

More cements should be tested to determine whether the results presented here are representative of other brands of PMMA bone cement. Also, a more clinically representative set-up should be used, this would increase the clinical relevance of these findings. Finally, the effect of the cup size on the interstice created between the acetabulum and the cement mantle could be investigated.

#### **4.7 Summary**

This study found that the average size of the bone cement-bone interstice created when a 50mm diameter cup is implanted into a 52mm model acetabulum is  $0.39 \text{ mm} \pm 0.1455 \text{ mm}$  when the cement is mixed in non-vacuum conditions and  $0.60 \text{ mm} \pm 0.0921 \text{ mm}$  when the cement is mixed under vacuum. This interstice is uniform across the cement mantle for each mixing methodology.

These findings may explain the increased risk of failure in the first 4-5 years after THA. It has been shown that immediate postoperative RLLs are a good indicator for early failure of THA. The cause of these lines has been thoroughly debated in the literature; the evidence presented here suggests that shrinkage of the bone cement is a contributing factor to immediate RLLs and therefore early failure of cemented acetabular cups.

Caution should be taken not to presume that the optimal cementing technique has been established. The best clinical evidence for the determination of the efficacy of operative techniques is arthroplasty registries. Unfortunately, many registries do not contain enough detail to make any conclusions regarding cement preparation techniques.

## Chapter 5. Does the Addition of a Flange to the Acetabular Cup Improve the Pressures Generated at the Acetabulum Surface During Mock Cemented Acetabular Cup Implantation?

### 5.1 Disclaimer

Sections of this chapter have been taken and altered from a version that has been accepted for publication in Journal of Biomedical Materials Research: Part B - Applied Biomaterials.

### 5.2 Introduction

#### 5.2.1 *Background and Motivation*

THA involves the implantation of an artificial acetabular cup in the acetabulum and a new femoral head onto the femur. Cemented THR's require cement pressurisation, the low viscosity cement is pressurised so that it flows into the trabecula bone voids and forms small fingers (digits) of cement which resist shear forces encountered in daily function. Therefore, pressurisation of bone cement is crucial for both immediate post-operative, and long-term acetabular cup stability.

The operative procedure consists of the surgeon removing the cartilage and the dense cortical bone that are present on the outer layers of the bone. This exposes the porous cancellous bone underneath. After cleaning away loose debris and fat present in the trabecular pores using some form of lavage, the surgeon reduces the blood flow using a swab soaked in adrenaline. The bone cement is then mixed, left to cure until it reached the dough point, then placed into the cavity and pushed into the bone using a device called an acetabular pressuriser. Once the cement has been pressurised, the acetabular cup is inserted into the cement where the surgeon applies a force that pushed the cup into the cement, further pressurising the cement until the cup is correctly positioned. The prevalence of early loosening of the acetabular cup shows that innovations in cementation techniques are still necessary.<sup>2</sup>

The opaque white lines visible are wire markers on the acetabular cup used for observation of the positioning of the cup on radiographs.

Of all failed THRs, many fail due to aseptic loosening of the cup.<sup>2,3</sup> The reamed acetabulum is a shallow cavity with a large, irregular opening; this makes it difficult to maintain a high pressure at the bone surface during pressurisation and cup insertion. The addition of a flange to the acetabular cup was claimed to improve pressurisation, prevent the acetabular cup from bottoming out (where the cup makes contact with the bone at the pole of the acetabulum cavity, thus stopping further pressurisation), and minimise cup movement during implantation.<sup>130</sup> A flange was proposed to provide uniform pressurisation and thereby optimise cement intrusion into the subchondral bone which has been shown to improve the interface strength.<sup>184</sup>

The literature on this topic contains limited data regarding the pressures generated at the acetabulum surface and there is contradictory experimental evidence regarding the efficacy of flanged acetabular components.<sup>47, 194, 209-211, 213, 259</sup> Therefore, the aim of this experiment was to

investigate whether the addition of a flange to the acetabular component improves the cement pressure distribution at the surface of a model acetabulum during cup implantation using a simplified model. It also aimed to provide a detailed pressure profile at the acetabulum surface which all other similar studies have yet failed to provide.

### **5.2.2 Objectives**

1. To determine the nature of the cement pressure at the acetabulum surface during the pressurisation stage of THA.
2. To measure the effect of the addition of a flange to the acetabular component on the magnitude of the pressures generated at the cement-bone interface.
3. To determine whether the addition of a flange to the acetabular component affects the pressure distribution at the cement-bone interface.
4. To determine whether the pressure is maintained throughout pressurisation and cup implantation and whether the addition of a flange significantly affects this.

## **5.3 Materials**

This section describes the materials used in this experiment. The methodology is described in the following section.

An acetabulum model was manufactured from stainless steel 304 with a 52 mm hemispherical bore, a diameter to which the acetabulum is often reamed in a clinical setting. Steel was selected as it would provide an accurate surface for the pressure transducers to lay flush on, a porous model would closer represent the surface texture of the acetabulum; however, the cement should only contact the surface of the transducer flush with the acetabulum, this would be impossible using a porous model; previous studies use a rubber glove to separate the pressure transducer from the cement but this would alter the pressures recorded.<sup>255</sup> The diameter was confirmed to be within 0.01 mm of the expected value using a CMM. The model included tapped holes for pressure transducers at 0° (pole), 45°, and 75° (rim) from the direction of forcing (Figure 5.1a).

A Hivac™ bowl (Summit Medical LTD, Gloucestershire) or an inert glass bowl and an inert PTFE spatula were used to mix the cement.

A Depuy Smartseal acetabular pressuriser (DePuy, UK) was used for the pressurisation of the cement. It consists of a silicone hemispherical segment, 80 mm in diameter and is designed to seal off the acetabulum cavity with the cement still inside (Figure 5.1b).

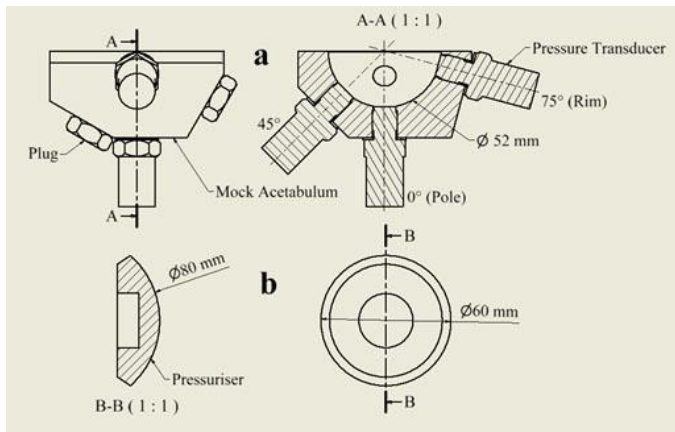


**Figure 5.1** Technical drawings with all relevant dimensions of the mock acetabulum (a) and the Depuy Smartseal pressuriser (b).

The acetabular cups were manufactured from HXLPE. A flanged and unflanged cup were designed so that the only difference between them was the flange. Both had an external diameter of 50mm and an internal diameter of 28mm, this would leave a cement mantle of around 1mm thick if the centres of the cup and the acetabulum cavity were aligned. The flange had a thickness of 1.7mm and a diameter of 63mm (Figure 5.2). The design of the cup was loosely based on an Exeter X3 Rimfit cup (Stryker).

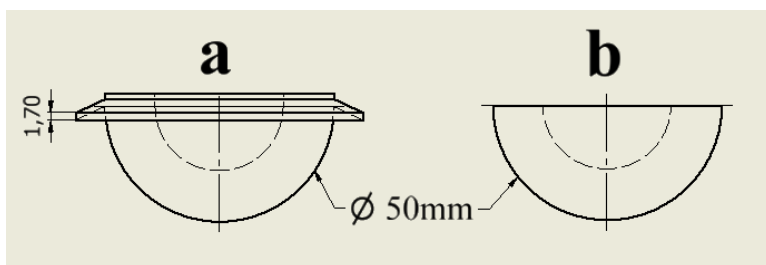


**Figure 5.2.** Technical drawings of a flanged (a) and unflanged (b) acetabular cup.

Omega PX61V0 pressure transducers were used with an Omega TXDIN1600S bridge for amplification and data acquisition (Appendix F). The pressure transducers were received from Omega fully calibrated with calibration certificates. Upon reception of the sensors, a set of control data were generated using a loading program and a doughy substance similar to the consistency of bone cement; this loading program was repeated prior to each experiment to re-calibrate the sensors (Appendix E). The transducers were made flush to the acetabulum hemispherical surface using shim washers. The data was filtered using a first order, low pass Butterworth filter with a cut off frequency of 160 Hz which is half the sampling rate of the Omega TXDIN1600S bridge, selected using the Nyquist criterion which allows for the filtering of electrical noise (Appendix H).

A Type K thermocouple was used to monitor the temperature, as the temperature is often used to monitor the progress of polymerisation (Appendix G). The thermocouple was inserted into the acetabulum cavity between the acetabular rim and the pressuriser. The location of the tip of the thermocouple was not controlled; therefore, the magnitude of the temperatures measured

cannot be directly compared between tests but the data can still be used to calculate the cure-time which is defined in the standards as the time at which the temperature of the cement was halfway between the ambient and the maximum temperature.<sup>260</sup>

The bone cement used was CMW 2 (Depuy Synthes); a high-viscosity cement, frequently used for fixation of the acetabular component.

The assembled rig was mounted into a Shimadzu ADS-X which was used to apply load. It was fitted with a 1 kN load cell (Figure 5.3). Note that during surgery, the cup is implanted 40° to the transverse plane; however, the force applied by the surgeon is orthogonal to the plane of the cup face, therefore the experimental set-up here is equivalent.

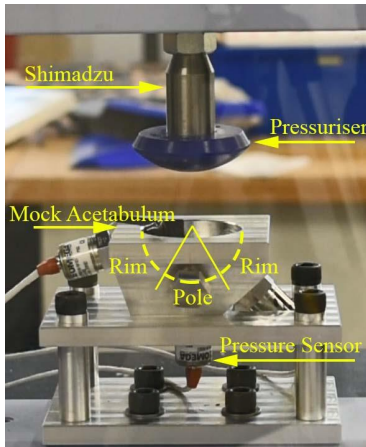


**Figure 5.3** Mock acetabulum and Depuy pressuriser experimental set-up in the Shimadzu universal tester showing the sensor positions in relation to the rim and pole.

All equipment used was manufactured with a tolerance of +/- 0.05 mm, with consideration of the design of the rig, the loading was always applied within 0.25 mm from the centre of the acetabulum cavity.

#### 5.4 Methods

The methodology employed here is similar to that of the previous chapter (Chapter 4) yet will be repeated here for completeness.

The temperature of the laboratory was between 20.5°C and 23°C for all experiments which is outside the range of temperatures specified in the standards (22°C – 24°C). The humidity of the lab was between 45% and 50%. All equipment was left in the lab to ensure that the temperature of the equipment was static.<sup>260</sup> Mould release spray (Silicone Mould Release Agent, Ambersil) was used to ensure that the cement mantle could be removed from the model acetabulum. The Shimadzu was force controlled with a maximum stroke rate of 40 mm/min.

The PMMA powder and the MMA liquid were either mixed by hand in an open glass bowl with a PTFE spatula at around 1 Hz until homogenous or in a Hivac™ bowl under a 0.4 bar (absolute) vacuum at a similar frequency until homogenous. For both conditions, the cement was then left to rest until the cement no longer adhered to surgical gloves (clinically defined as the dough

point).<sup>260</sup> The cement was then inserted into the acetabular cavity and the loading program for pressurisation was started. The cement was pressurised for 100 s at 100 N (Figure 5.4).

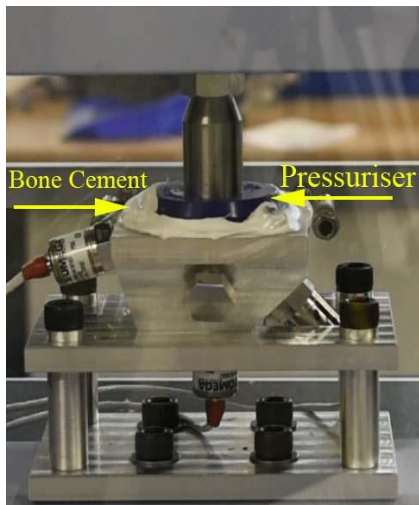


**Figure 5.4** A 100 N force was applied to the Depuy Pressuriser with the bone cement sealed within the acetabulum model in the Shimadzu universal tester.

The universal tester was raised, and the pressuriser twisted as it was then removed from the cement to minimise adhesion and an acetabular cup was lightly pressed into the centre of the cement. A metal disk was placed on top of the cup and the ram of the universal tester was brought down until the two made contact, ensuring that the cup was inserted with the correct orientation. The cup implantation program was started, and a load of 50 N was applied until the cement was fully cured (Figure 5.5). After the cement had fully cured, the cement mantle was removed. This was repeated five times for each of the four testing conditions: two cup designs and two mixing methodologies. The experiment was repeated five times to ensure that enough data was acquired for each test to compare the testing conditions, but it was limited due to a limited supply of cement.

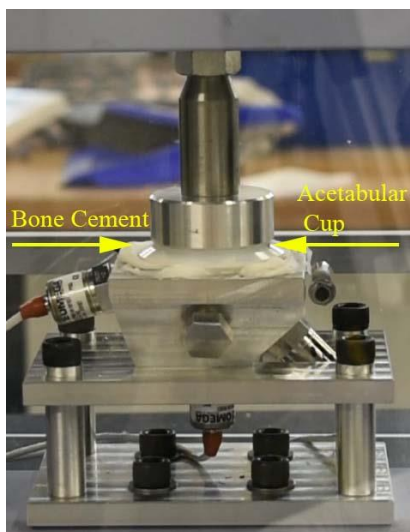


**Figure 5.5** A 50 N force applied to the flanged acetabular cup in the Shimadzu universal tester.

For this experiment, pressurisation and cup insertion were performed within the working time advised by the cement manufacturer. The cup load was decided upon after preliminary tests showed that the cup would be correctly positioned after full cure of the cement.

The end of cup implantation was taken to be when there was a deviation from the average pressure. To allow a more detailed analysis of the continuous pressure curves they were divided into fifths and the pressure at each of these five time points was taken and used for statistical comparisons. (Figure 5.6). This technique also allowed for analysis of how the pressure evolves, previous studies often only state the average or maximum pressure achieved during surgery, but this is insufficient for a full analysis.

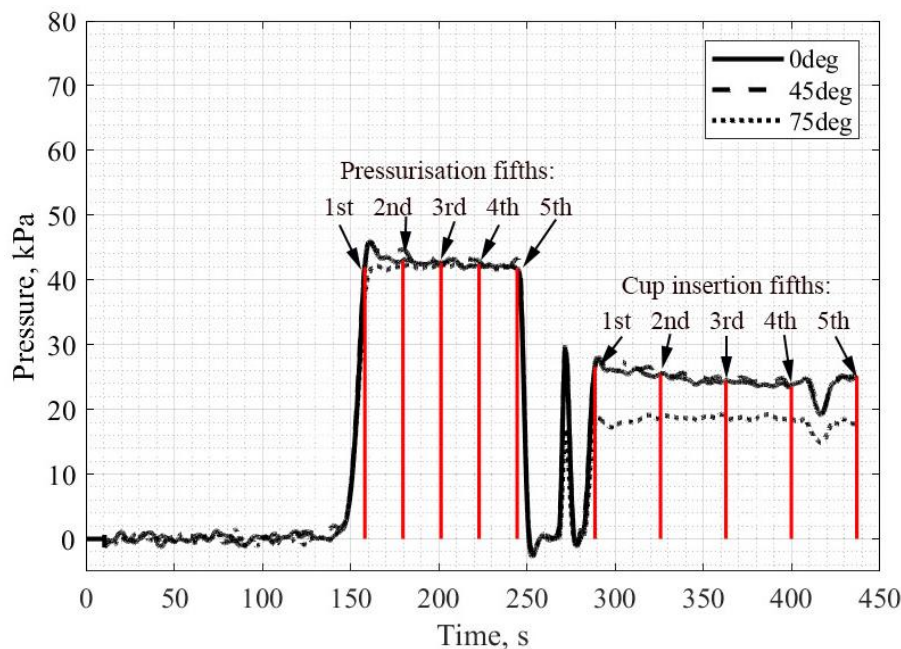


**Figure 5.6** A typical plot with an indication of how data is split up into fifths (pentiles) for further analysis.

A Ryan-Joiner test was used to determine whether data were normally distributed; if so, a standard student t-test<sup>245</sup> was used to determine whether there was a significant difference between compared variables. If the data were not distributed normally, a Mann-Whitney test was used.<sup>246</sup> The results were considered significant if  $p \leq 0.05$ .

## 5.5 Results

Typical annotated plots showing cement pressure and temperature over time for both vacuum mixed and non-vacuum mixed flanged and unflanged acetabular cup implantation can be seen below (Figure 5.7). A full collection of the plots can be seen in the appendix (Appendix I). Three sets of pressure measurements were recorded at positions 0° (rim), 45° and 75° (pole). There were two key stages of the experiment: pressurisation and cup insertion. The end of cup insertion always occurred near the cure time. An animated, annotated video can be found by following the link or using the QR code below (Figure 5.8).

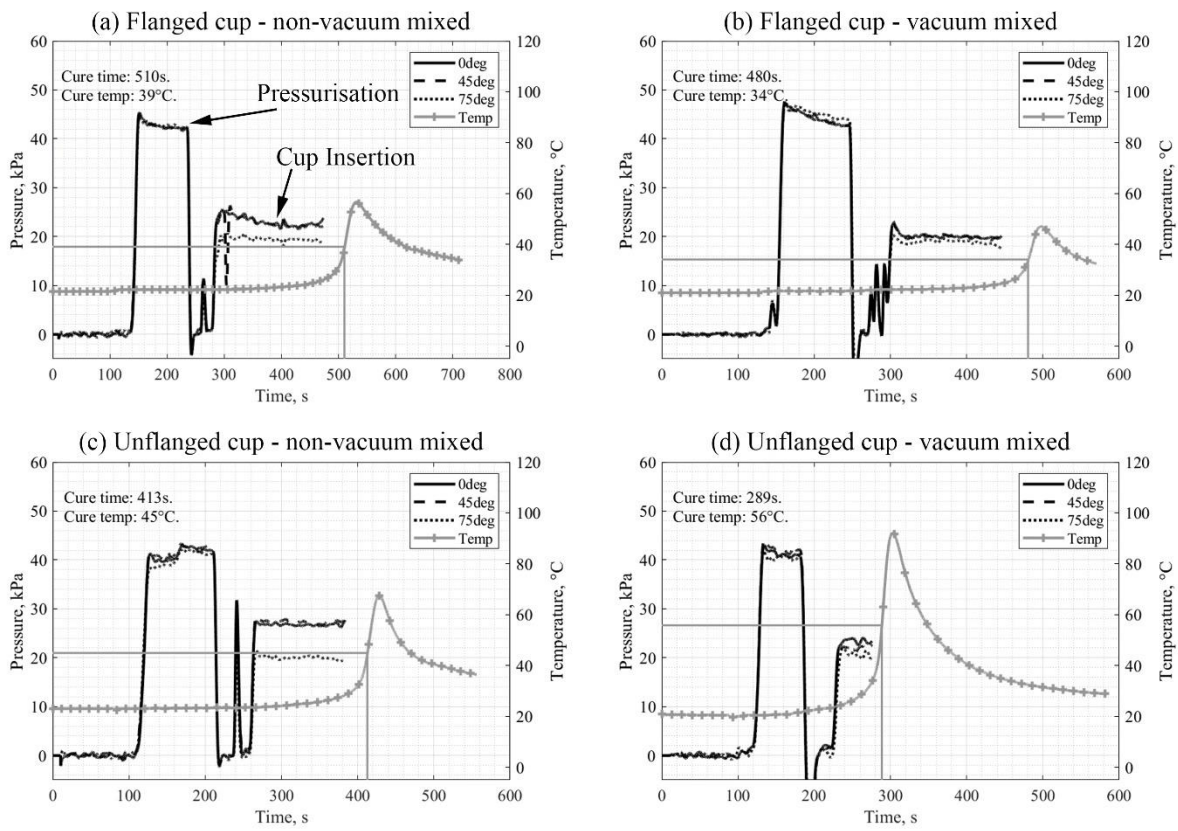


**Figure 5.7.** Four graphs showing examples of the pressure, temperature – time plot from each of the testing conditions. The pressure at various angles from the direction of forcing and the temperature through time are plotted. Pressurisation and cup insertion are indicated in (a) and are in similar positions in (b-d). The time and temperature of the cure point are also indicated.



**Figure 5.8** QR code that contains a link ([youtu.be/dzs6CdNYWr0](https://youtu.be/dzs6CdNYWr0)) to a YouTube video of an animated, annotated video of one of the experiments. Either scan QR code or enter URL to watch.

### 5.5.1 Pressurisation

A table containing the averages and standard deviations of the pressures achieved during the pressurisation stage for each pentile (fifth) of cup insertion, at each angle, for each condition can be seen below (Table 5.1).

**Table 5.1** A table containing the average pressure and standard deviations in brackets for each testing condition, at each angle from the direction of loading, at each pentile during the pressurisation stage of the experiment. A \* indicates that the data set was non-normal. Five repeats were performed for each testing condition.

Sample	Angle (°)	1st (kPa)	2nd (kPa)	3rd (kPa)	4th (kPa)	5th (kPa)
Flanged Cup, Non-Vacuum Mixed	0	40.42 (2.27)	41.75 (1.63)	41.54 (1.52)	41.16 (1.74)	40.83 (1.70)
	45	40.94 (2.04)	42.47 (1.96)	*41.89 (11.67)	*41.61 (1.85)	41.24 (2.14)
	75	37.92 (2.77)	40.93 (1.66)	41.23 (1.61)	41.02 (1.96)	40.50 (1.96)
Flanged Cup, Vacuum Mixed	0	40 (7.35)	43.11 (9.22)	42.29 (9.15)	41.45 (9.04)	40.09 (9.31)
	45	39.64 (7.11)	42.55 (9.03)	41.36 (9.20)	40.61 (9.23)	40.51 (8.77)
	75	39.68 (7.22)	43.95 (8.94)	42.41 (9.33)	42.12 (9.19)	41.67 (8.95)
Unflanged Cup, Non-Vacuum Mixed	0	41.11 (4.39)	41.70 (1.39)	42.08 (0.56)	41.81 (0.81)	41.14 (1.29)
	45	40.29 (4.41)	41.67 (0.97)	41.67 (1.05)	41.05 (1.32)	40.54 (1.45)
	75	37.02 (5.31)	39.63 (0.82)	40.75 (1.36)	40.36 (1.65)	39.93 (1.71)
Unflanged Cup, Vacuum Mixed	0	40.69 (2.32)	42.28 (0.26)	41.74 (0.65)	41.22 (0.59)	41.41 (0.66)
	45	*39.69 (1.44)	41.76 (0.62)	41.17 (0.73)	40.43 (0.58)	40.77 (1.06)
	75	38.75 (1.55)	40.64 (0.61)	40.96 (0.50)	40.22 (0.33)	40.00 (0.87)

#### 5.5.1.1 Pressure Magnitude

There were no instances when there was a significant difference in the magnitude of the pressures generated during pressurisation due to the cup implanted after pressurisation.

#### 5.5.1.2 Pressure Change

There were no instances where the pressure significantly reduced from the start to the end of pressurisation (Table 5.2).

**Table 5.2** A table containing statistical results comparing the pressures generated at the beginning of pressurisation to the pressures generate at the end. A \* indicates one or both sets of data being compared are non-normal. Five repeats were performed for each testing condition.

Sample	Angle (°)	1st vs 5th	2nd vs 5th
Flanged Cup, Non-Vacuum Mixed	0	N	N
	45	N	N
	75	N	N
Flanged Cup, Vacuum Mixed	0	N	N
	45	N	N
	75	N	N
Unflanged Cup, Non-Vacuum Mixed	0	N	N
	45	N	N
	75	N	N
Unflanged Cup, Vacuum Mixed	0	N	N
	45	*N	N
	75	N	N

### 5.5.1.3 Pressure Differential

Results of statistical tests indicate two instances where there was a significant pressure differential between the pole and the rim of the acetabulum (Table 5.3, Figure 5.7). These occurred at the second pentile for both mixing conditions of the unflanged acetabular cup. As can be seen from the table above (Table 5.1) the maximum difference was 2.07 kPa which represented a 5.22 % increase in pressure from the rim to the pole for the non-vacuum mixed cement and unflanged cup in the second pentile.

**Table 5.3** A table containing the statistical results comparing the pressure at the pole of the acetabulum to the pressure at the rim during the pressurisation stage of cemented THA. Five repeats were performed for each testing condition.

Sample	1st	2nd	3rd	4th	5th
Flanged Cup, Non-Vacuum Mixed	N	N	N	N	N
Flanged Cup, Vacuum Mixed	N	N	N	N	N
Unflanged Cup, Non-Vacuum Mixed	N	Y	N	N	N
Unflanged Cup, Vacuum Mixed	N	Y	N	N	N

### 5.5.2 Cup Insertion

The averages and the standard deviations of the cement pressures generated during each pentile (fifth) of cup insertion, at each angle, for each condition can be seen below (Table 5.4).

**Table 5.4** A table containing the average pressures and standard deviations in brackets for each testing condition, at each angle from the direction of loading at each pentile during the cup insertion phase of the experiment. Statistical differences between flanged and unflanged cups are indicated using [a]. A \* indicates that one or both data sets were non-normal. Five repeats were performed for each testing condition.

Sample	Angle (°)	1st (kPa)	2nd (kPa)	3rd (kPa)	4th (kPa)	5th (kPa)
Flanged Cup, Non-Vacuum Mixed	0	24.16 (3.47)	25.74 (1.07)	24.78 (1.55)	[a] 24.28 (1.65)	25.93 (1.55)
	45	24.16 (3.30)	25.79 (1.40)	25.13 (1.78)	24.32 (1.98)	24.99 (2.30)
	75	18.75 (4.07)	20.70 (1.97)	20.46 (1.77)	20.02 (1.50)	19.44 (1.52)
Flanged Cup, Vacuum Mixed	0	20.23 (4.2)	21.21 (1.97)	20.8 (1.94)	20.39 (2.39)	20.65 (2.97)
	45	19.81 (4.64)	20.7 (2.2)	20.54 (2.13)	20.11 (1.84)	* 19.61 (2.34)
	75	18.4 (4.12)	19.86 (2.17)	19.34 (1.46)	19.25 (1.79)	18.64 (1.92)
Unflanged Cup, Non-Vacuum Mixed	0	25.70 (2.14)	26.61 (1.64)	26.80 (1.45)	[a] 27.01 (1.79)	27.85 (2.36)
	45	24.96 (2.41)	25.88 (1.59)	25.81 (2.08)	25.43 (2.05)	25.69 (2.90)
	75	19.67 (1.73)	21.08 (2.59)	21.41 (2.69)	21.73 (3.11)	21.76 (3.92)
Unflanged Cup, Vacuum Mixed	0	22.64 (0.80)	22.37 (1.37)	*21.98 (1.58)	22.71 (1.26)	22.74 (0.71)
	45	22.20 (1.09)	22.02 (1.20)	21.58 (1.53)	22.45 (0.79)	22.85 (0.43)
	75	20.78 (1.97)	20.41 (1.84)	19.79 (1.35)	20.00 (1.50)	19.29 (1.91)

### 5.5.2.1 Pressure Magnitude

The addition of a flange had a significant effect on the pressure in one pentile, at one angle for one mixing condition. The unflanged cup produced a larger pressure than the flanged cup in the 4<sup>th</sup> pentile at 0° from the direction of loading for non-vacuum mixed cement. The difference was 2.73 kPa, or an 11.24% increase in pressure.

### 5.5.2.2 Pressure Change

There was no statistically significant drop in pressure for any set of data (Table 5.5).

**Table 5.5** A table containing the statistical results comparing the pressure at the beginning of cup insertion to the end of cup insertion. A \* indicates that one or both sets of data being compared are non-normal. Five repeats were performed for each testing condition.

Sample	Angle (°)	1st vs 5th	2nd vs 5th
Flanged Cup, Non-Vacuum Mixed	0	N	N
	45	N	N
	75	N	N
Flanged Cup, Vacuum Mixed	0	N	N
	45	*N	*N
	75	N	N
Unflanged Cup, Non-Vacuum Mixed	0	N	N
	45	N	N
	75	N	N
Unflanged Cup, Vacuum Mixed	0	N	N
	45	N	N
	75	N	N

### 5.5.2.3 Pressure Differential

There were instances when there was a differential between the pressures generated at the pole and at the rim of the acetabulum (Table 5.6). It appears that overall, there is not a significant difference in the pressure differential due to the cup used but the non-vacuum mixed cement had a pressure differential more regularly than the vacuum mixed cements (Figure 5.9). The only instance where there was no pressure differential at any time during cup insertion was when a flanged cup was implanted into vacuum mixed cement. The cause for this was unknown.

**Table 5.6** A table containing the statistical results comparing the pressure at the pole of the mock acetabulum to the rim of the acetabulum at each pentile of cup insertion. A \* indicates that one or both sets of data being compared are non-normal. Five repeats were performed for each testing condition.

Sample	1st	2nd	3rd	4th	5th
Flanged Cup, Non-Vacuum Mixed	N	Y	Y	Y	Y
Flanged Cup, Vacuum Mixed	N	N	N	N	N
Unflanged Cup, Non-Vacuum Mixed	Y	Y	Y	Y	Y
Unflanged Cup, Vacuum Mixed	N	N	*N	Y	Y

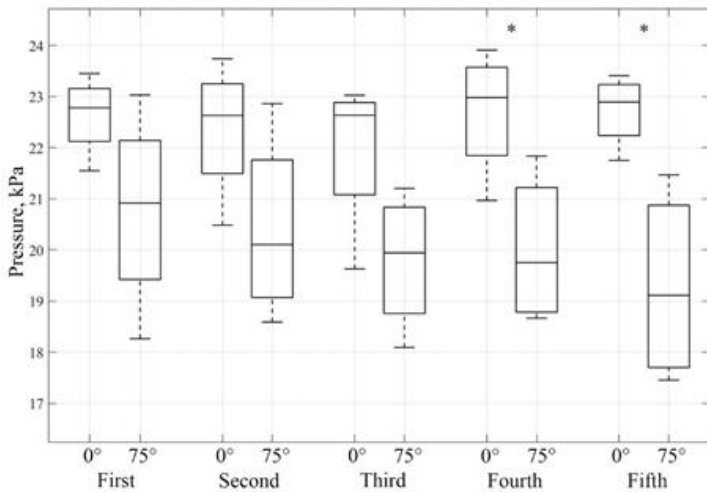


**Figure 5.9** Boxplots of the average pressure for the unflanged, vacuum mixed condition. Each pair of boxplots represents the pressure at  $0^\circ$  and  $75^\circ$  for each pentile of cup insertion. Five repeats were performed for each testing condition. The bars indicate the maximum and minimum results, the box illustrates the interquartile range and the line within the box shows the mean.

Upon inspection of the removed cement mantles, it was found that none of the cups bottomed out and the cement mantle was thicker than 2mm for all repeats at all angles from the direction of loading.

## 5.6 Discussion

The aim of this study was to address four concerns regarding the behaviour of PMMA bone cement in the acetabulum during pressurisation and implantation of unflanged and flanged acetabular cups.

Firstly, it was found that there was no decrease in pressure during pressurisation. There were two instances, both for the unflanged acetabular cup, where there was a significant pressure differential between the rim and the pole of the acetabulum.

Secondly, it was found that the addition of a flange to the acetabular cup did not increase the pressure generated in the cement at the acetabulum bone surface during cup implantation. There was one pentile where the unflanged cup generated a larger pressure in the 4<sup>th</sup> pentile, at  $0^\circ$  from the direction of loading for non-vacuum mixed cements than flanged cups.

Thirdly, it was found that there was no decrease in pressure over time for any of the testing conditions at the cup implantation stage.

Finally, there were many instances where the pressure generated at the pole of the acetabulum was larger than the pressures generated at the rim. There were more significant differences for non-vacuum mixed cement and there were none when a flanged cup was inserted into vacuum mixed cement. The cause for this is unknown.

As seen throughout this thesis, a good bond between the bone cement and bone is key for the longevity of THA implants as close contact between the bone and the cement is the only form of fixation. More interdigitation increases the contact area between cement and bone and thus decreases contact stresses placed on the bone trabecular.<sup>184</sup> As seen in chapter 4, there is also the risk of a gap developing between the cement and the bone due to PMMA bone cement shrinkage. Suboptimal bonding can be observed on postoperative radiographs as a RLL between the cement and the bone. These lines may develop soon after implantation or after a period has passed, it has still not been determined what causes these lines. They are most frequently observed near the rim of the acetabulum.<sup>129</sup> It has been shown that the penetration depth of bone cement into the bone is dependent on the pressure generated during implantation, the larger the pressure the deeper the cement penetrated.<sup>192</sup> The strength of the cement-bone interface is dependent on the depth of penetration;<sup>184, 261</sup> therefore, it is key that the cement pressure generated during pressurisation and cup insertion should be uniform across the acetabulum and sufficiently large to achieve optimal penetration. No investigation has determined whether the magnitude of pressure applied during the pressurisation phase of implantation affects the rate of RLL development, but there are sufficient studies and data to suspect that there may be a link.

## **5.6.1 Pressurisation**

### **5.6.1.1 Pressure Magnitude**

In 1999, New *et al.* measured pressures generated *in vivo* during pressurisation and found values of  $49 +/- 17$  kPa and  $47 +/- 17$  kPa for two surgeons.<sup>195</sup> The results reported in our study are within that range.

### **5.6.1.2 Pressure Change**

There was no significant decrease in the pressures achieved at the acetabulum surface over time. This suggests that the Depuy pressuriser effectively sealed the model acetabulum during the pressurisation phase of acetabular cup implantation. No other study reports on this.

### **5.6.1.3 Pressure Differential**

Pressures were measured at the rim and the pole in a study by Bernowski *et al.* however, they do not report figures for the “sustained pressure” but only provide the peak pressure at the rim. It is possible to estimate the value from the chart, it appears that the sustained pressure at the rim was between 80 kPa and 90 kPa and between 60 kPa and 80 kPa at the pole. This is for an applied load of 201 N. This finding is not reflected in our results where for most of the testing conditions there was no significant pressure differential between the pole and the rim of the acetabulum. In a chapter on “optimal cementing technique”, Parsch *et al.* published a graph that reported the pressures generated across the acetabular surface using a standard acetabular pressuriser. Although the pressures generated were larger than in our study, they found no significant pressure differential during pressurisation which agrees with this study.<sup>18</sup> The

pressuriser effectively seals the acetabulum cavity and the viscosity of the cement is still sufficiently small so that the pressure is equalised.

The occasions where there was a significant difference between the pressure at the pole and the pressure at the rim of the acetabulum occurred in the 2<sup>nd</sup> pentile. No explanation is offered for this.

As cup insertion occurs after pressurisation, and there is no decrease in pressure throughout pressurisation all values for the pressure at 0° can be compared to the pressures at 75° for each mixing condition. It was found that there was a significant pressure differential for non-vacuum mixed cement but no significant difference for vacuum mixed cement. The reason that there is a significant difference for non-vacuum mixed cement and not for vacuum mixed cement is unclear. No studies in the literature comparing the viscosity of vacuum mixed cement to non-vacuum mixed cement could be found; this should receive further attention.

## 5.6.2 Cup Insertion

### 5.6.2.1 Pressure Magnitude

There was only one pentile where the design of the cup resulted in a significant difference in the pressures generated. In the 4<sup>th</sup> pentile at 0° from the direction of loading with non-vacuum mixed cement, an unflanged cup created a larger pressure than the flanged cup. The difference was 2.73 kPa, or an 11.24% increase in pressure. The cause for this difference is unknown.

In an *in vitro* experiment Oh *et al.* found that a flanged cup produced pressures of 1440 kPa at the pole and 1050 kPa at the rim for flanged acetabular cups, and just 113 kPa at the pole and 73 kPa at the rim for unflanged components. This significant difference is accounted for by the insertion load for the cups. A force of 2167 N was used for the flanged component and just 113 N was used for the unflanged cup. There was no justification for this difference in the methodology section, presumably, it was due to the instrument being used in position-control mode rather than load-control. Those results are therefore not comparable with ours nor are they clinically relevant as no surgeon could maintain a 2 kN force.<sup>209</sup> A study by Beverland *et al.* used a similar methodology to our study. A 98.1 N load was applied to the cup using a 10 kg mass. Flanged and unflanged cups were implanted into an irregular mock acetabulum but only the pressure at the pole of the acetabulum was reported. They found an average pressure of 28.4 kPa for flanged components and 41.5 kPa for the unflanged component. The larger pressure for an unflanged cup at the pole of the acetabulum can also be seen in our data but the magnitude of the difference was less significant. Lankester *et al.* used position controlled load application and report pressure profiles which reflect the methodology with the force increasing rapidly until peaking at 30 s then quickly decaying to 0 MPa, this is not advisable *in vivo* as a consistent pressure is required to resist back bleeding.<sup>192</sup> The addition of a flange increased pressure by a factor of 10 at the rim but by a factor of 2 – 4 at the pole.<sup>259</sup> This was not seen in the present study. Parsch *et al.* performed cadaver experiments with an applied force of 60 – 100 N. They found that the addition of a flange increased the peak pressure but not the average pressure, the average pressure is a more important measure in cementation to prevent back bleeding.<sup>16</sup> There were only minor differences found between the average pressures generated due to the cup design in the present study.

### 5.6.2.2 Pressure Change

No significant pressure drop during cup insertion was found for any of the testing conditions.

In an *in vitro* study, Beverland *et al.* found that the pressure decayed significantly for both unflanged and flanged acetabular cups.<sup>211</sup> This was not found in these results; this may be because Beverland *et al.* used a model acetabulum with an irregular rim.

### 5.6.2.3 Pressure Differential

As previously discussed, there is frequently a significant pressure differential at the cup implantation stage. There seems to be more pentiles with a significant pressure differential when non-vacuum mixed cement is used and there are no pentiles with a statistically significant pressure differential when a flanged cup was implanted into vacuum mixed cement.

It is thought that there are several possible causes for the pressure differential created between the pole and the rim of the acetabulum when inserting a cup into the cement.

Firstly, it is thought that when the acetabular cup first contacts the cement there is a small area of contact between them due to the mismatch in the radii between the cement indentation and the acetabular cup (Figure 5.10). This would mean that the load applied to the cup could only be effectively transferred to the acetabulum surface at the pole and very weakly near the rim. However, this will only apply in the very early stages of cup insertion and should level out as the cup is further inserted into the cement.

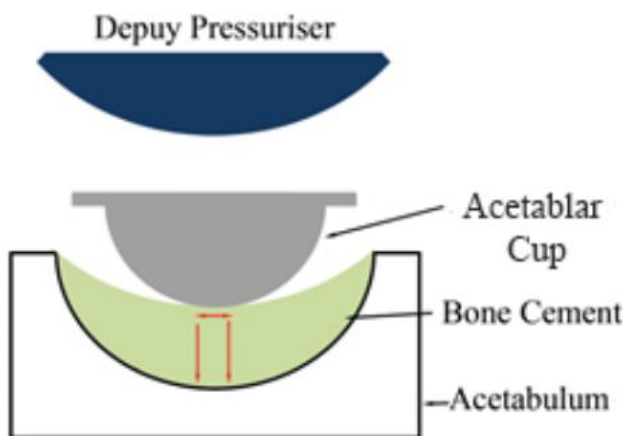


**Figure 5.10** A diagram showing that immediately upon insertion of the cup into the pressurised cement there will be a small contact area between them. This may result in a larger pressure generated at the pole of the acetabulum than at the rim.

Secondly, the necessary flow of cement out of the acetabulum creates a pressure differential. As the pressure of the cement outside of the acetabulum cavity is effectively zero, any pressure applied to the cement will create a flow of cement out of the cavity. This flow of cement will create a lower pressure near the rim of the acetabulum and therefore would explain the pressure differential measured in this experiment.

Finally, when the cement is solidified, it will begin to abide by Newton's third law whereby every action has an equal and opposite reaction. As the pole of the acetabulum is normal to the direction of loading the pressure transducers, which are designed to measure normal forces, will fully register that force. However, the pressure transducers near the rim of the acetabulum are at a steep angle from the direction of loading and will therefore only measure a small component of the applied force (Figure 5.11).

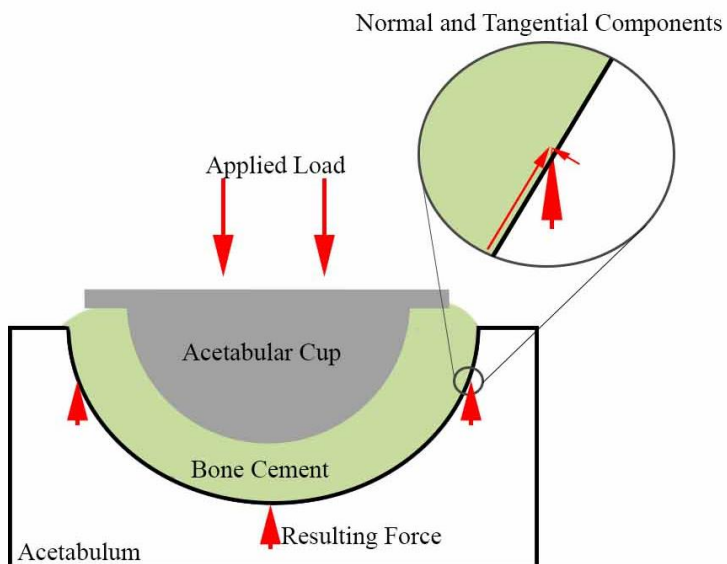


**Figure 5.11** Reaction forces for a solid acetabular cement mantle according to Newton's third law. The normal (and measured) forces near the rim will be smaller than at the pole of the acetabulum if the cement behaves more like a solid.

It is unclear which of these mechanisms is the cause of the pressure differential measured. It may be a combination of all three.

### 5.6.3 Broader Context

The study reported here is novel as the methodology included pressurisation of the cement prior to cup insertion, thus more closely simulating an *in vivo* implantation. It is also novel as the whole pressure profile through time was recorded and is reported here, allowing future researchers to refer to this study when a methodology is being designed. Preliminary testing was performed to ensure that the forcing program wouldn't cause "bottoming out" or "flanging out" where some part of the cup comes into direct contact with the acetabulum, preventing further pressurisation. Although contact between the acetabulum and the flange was not observed, the cement that separates the cup and the mock acetabulum would have increased the contact surface area between cup and cement, and therefore the pressure generated due to the applied load is reduced. This may account for the unflanged acetabular cup producing larger pressures.

The function of the flange should not simply be thought of as a way to increase the pressures generated in the acetabulum. With the same applied load and a larger projected area (due to the flange) a smaller pressure should be generated, as found here. Instead, the flange should be seen as a feature to slow the insertion of the cup into the cement, in this way the surgeon must apply

a larger load in order to correctly position the acetabular cup and therefore produce larger pressures. This may explain the discrepancy often seen between the lower pressures generated by flanged components seen in this study and the improved longevity of flanged acetabular cups observed *in vivo*.<sup>130</sup> The final placement of the cup was not measured in this study but no significant difference in the final positioning of the cup was found in the previous chapter. An experiment should be designed so that this hypothesis can be tested in isolation.

One of the hypotheses explaining why there is often a pressure differential between the pole and the rim of the acetabulum relates to an excess amount of cement within the acetabulum. This, taken with the conclusion that deformation of the cement during curing reduces the UTS (Chapter 3), and the conclusion that the elastic component of the complex modulus increases as polymerisation continues (Chapter 2); may suggest that the Depuy pressuriser is not optimally designed. It is desirable that at the pressurisation stage more cement is excavated from the acetabulum before cup insertion. A new design of pressuriser would attempt to mitigate the effects of two key findings: it would ensure that necessary deformation of bone cement would occur earlier in the polymerisation process, and it would reduce the amount of cement that must be excavated during cup insertion and thus may reduce the pressure differential found during this experiment. An additional benefit may be a closer match between the pressurised cement radii and the cup to be inserted.

The results suggest that flanged cups provide no advantage in terms of improving the pressure differential between rim and pole. Nor does the addition of a flange increase the pressure magnitude compared to unflanged acetabular cups. The data reported here suggest that unflanged cups may produce larger cement pressures than flanged cups during acetabular cup insertion for the same insertion load.

#### **5.6.4 Clinical relevance**

There are differences between this experimental *in vitro* study and the clinical *in vivo* setting, however, this study was designed to reduce confounding factors so that the results were reproducible.

#### **5.6.5 Study Limitations**

Only one cement was used in this study, more cements should be tested to determine whether the conclusions drawn apply more generally. The outer diameter of the cup used was 50 mm. This is 2 mm larger than should be used for an acetabulum 52 mm in diameter. It is not known what effect this would have on the pressure generated but this should be subject to further study. The rim of an anatomically accurate acetabulum is irregular, this would lead to larger gaps between the pressuriser and the acetabulum as well as between the cup and the acetabulum. Although the cement penetration was not directly measured it has been shown that penetration is improved with increased pressure.<sup>184</sup> If the surface of the acetabulum was porous the experiment would be more clinically accurate; however, it would also reduce the accuracy of the pressure transducers as cement may contact other non-measuring surfaces of the transducers or a barrier would have to be placed between the cement and the transducers thus altering the pressure data.

### **5.6.6 Future Work**

For future experiments, more work should be done to make the model acetabulum more representative of a clinical environment. It would be more difficult to maintain pressure during both pressurisation and cup insertion.

Also, vacuum mixed, and non-vacuum mixed cement should be rheologically characterised to determine whether the method of mixing results in a statistically significant difference in the viscosity.

Finally, the effect of the design of the external surface of the acetabular cup on the pressures generated during cemented acetabular cup insertion should be investigated.

### **5.7 Summary**

Firstly, it is clear from the data that pressure is sustained through time for both the pressurisation and cup insertion phase. It was found that the Depuy pressuriser works well but leaves a large amount of cement that must be displaced during cup insertion in order for the acetabular cup to be correctly positioned. It was found that upon cup insertion, there was a significant pressure differential in the cement between the pole and the rim of the acetabulum for both flanged and unflanged acetabular cups. The detailed pressure data gathered and presented here demonstrates that the addition of a flange to the acetabular component does not improve the pressures generated for the same applied load.

## Chapter 6. Designing a Novel Pressuriser to Improve Cement Fixation

### 6.1 Introduction

Results from the experiments detailed in the chapters preceding this, as well as the existing literature, indicate a need for an improved acetabular pressuriser. This chapter will discuss the specific motivations, the resulting design features, the materials used, the manufacturing process, and the issues that arose from preliminary testing and the solutions found for those issues. The following chapter (Chapter 7) will contain details of the experiment performed to test the efficacy of the novel pressuriser.

### 6.2 Motivation

The experiments previously described have highlighted two key motivations for an improved pressuriser. The first relates to the minimisation of residual stresses in the cement mantle. The second motivation relates to improving the pressure profile at the acetabulum during acetabular cup insertion.

The rheology experiment (Chapter 2) demonstrated that the elastic component of the complex modulus of PMMA bone cement was larger than the viscous component for almost all measurements, the only exception was the first measurement for Simplex P at 23°C (Figure 6.1). Several authors suggest it is past this moment that the elastic component of the complex modulus becomes larger than the viscous modulus that a curing material can store applied strains as residual stresses.<sup>77, 79, 88, 262</sup> The UTS experiments showed that strains applied to the cement during curing significantly reduced the UTS of the bone cement (Figure 6.2). There is agreement in the literature and the findings reported in a previous chapter (Chapter 2) that the elastic component of the complex modulus (the storage modulus) of a curing material increases through time (Figure 2.9) and thus a strain of equal magnitude applied later in the curing process will result in a larger residual stress.<sup>77, 82, 225</sup> This was the first motivation for the design of an improved pressuriser. PMMA bone cement relies on interdigitation and close mechanical contact for fixation, therefore some deformation is unavoidable and necessary. What can be controlled is when that deformation is performed. The majority of the deformation should be performed as early as possible in the curing process, the later a deformation is applied, the larger the residual stress will be as the cement can relax less.<sup>73-75</sup> Currently, the sole aim of an acetabular pressuriser is to pressurise the cement.<sup>190</sup> *It is argued that it should have another purpose, to excavate more cement earlier so that minimal deformation of cement occurs during acetabular cup insertion and therefore the residual stresses will be minimised – this additional surface is named the excavating surface.*

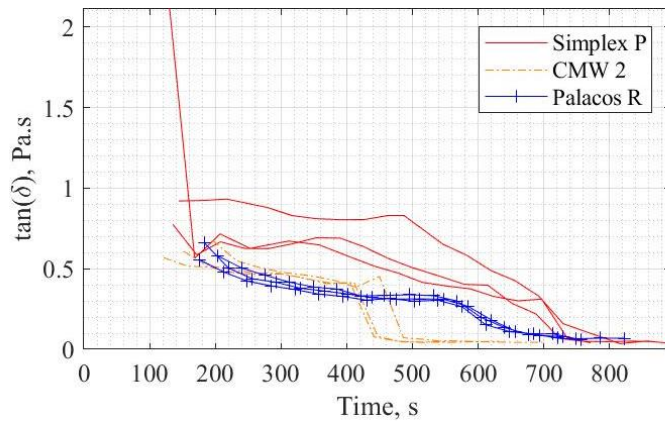


**Figure 6.1** Graph showing how the brand of PMMA bone cement affects the value of  $\tan(\delta)$  through time at 23°C with a frequency of deformation of 1 Hz.

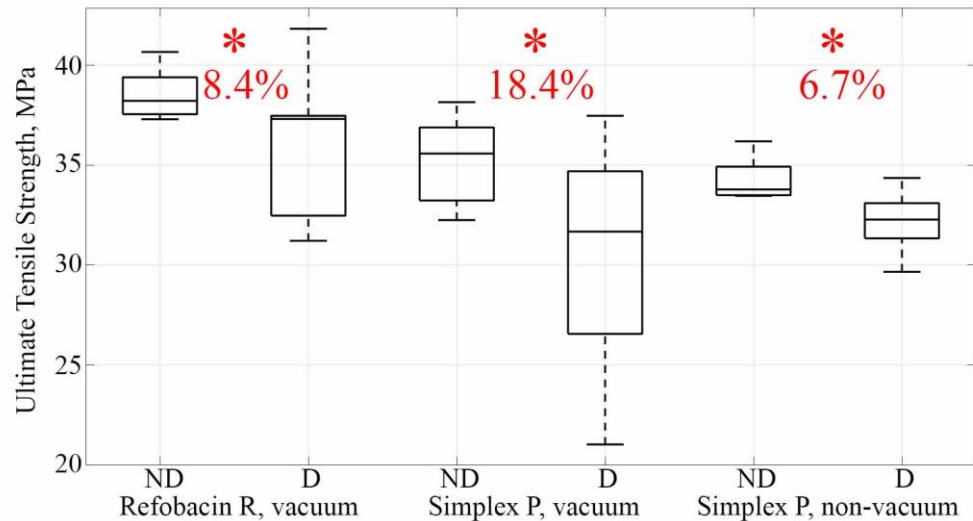


**Figure 6.2** Boxplots showing how deformation weakens PMMA bone cement for vacuum mixed Refobacin R and Simplex P and non-vacuum mixed Simplex P (ND = non-deformed, D = deformed). The number of repeats for each test can be seen in Table 3.1. The bars indicate the maximum and minimum results, the box illustrates the interquartile range and the line within the box shows the mean.

The second motivation for an improved pressuriser was the presence of a pressure differential from the pole to the rim of the acetabulum during the insertion of the acetabular cup. Findings from previous experiments showed that the Depuy pressuriser sufficiently seals the acetabulum, creating an equal pressure across the acetabulum surface which does not diminish through time during pressurisation (Figure 6.3). However, upon cup insertion it was shown that there is often a pressure differential; the pressure at the pole of the acetabulum was significantly larger than the rim (Figure 6.3). It is argued that this may be due to the excessive amount of cement left in the acetabulum after pressurisation. Several possible causes of this pressure differential are discussed in the previous chapter (Chapter 4). An improved pressuriser design should ensure that the acetabular cup will contact more of the cement on initial insertion and therefore create

less flow of cement out of the acetabulum in order for correct positioning to be achieved (Figure 6.4) and thus lower residual stress that has been shown to weaken cement (Figure 6.2).

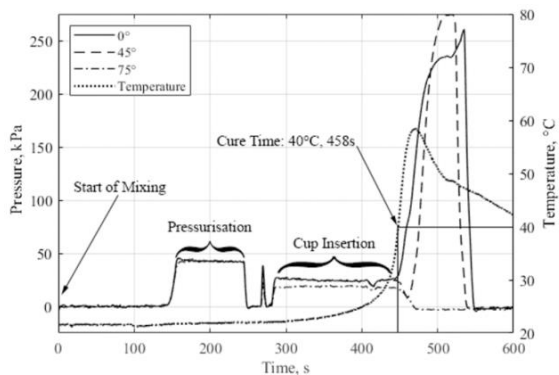


**Figure 6.3** Typical example of a pressure-time plot when using a Depuy pressuriser and Simplex P bone cement to implant a flanged acetabular cup into a mock steel acetabulum.

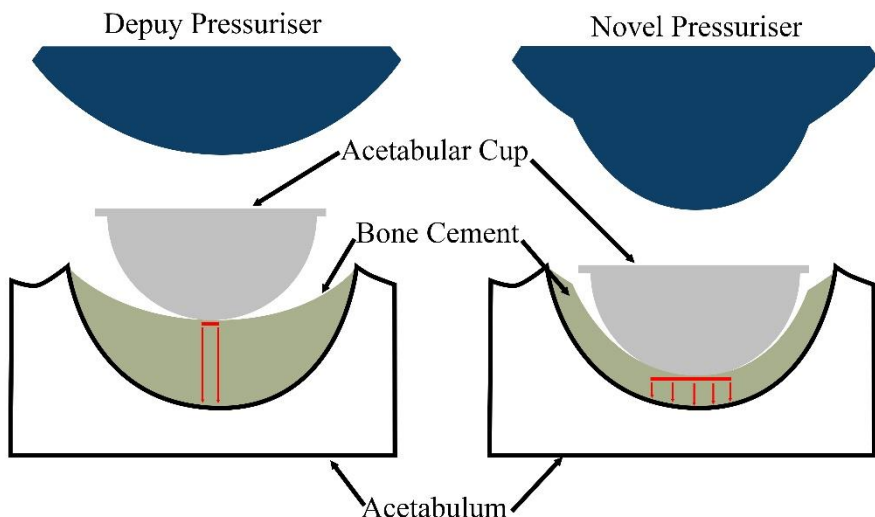


**Figure 6.4** The amount of pressure generated at the surface of the acetabulum is dependent upon how much of the cement and acetabular cup are in contact with each other. The indentation made in the cement after pressurisation with an improved novel pressuriser may result in a more uniform pressure across the acetabulum surface.

It was thought that a suitable pressuriser design that would address both of the aforementioned motivations is one that would excavate more cement during the pressurisation stage. Firstly, more of the cement deformation occurs earlier in the curing process and thus should result in less residual stresses creating a stronger cement mantle.<sup>92</sup> Secondly, more of the acetabular cup will contact the cement upon insertion, resulting in a smaller pressure differential which may result in fewer RLLs near the rim of the acetabulum and thus improve the longevity of the bone cement-bone interface.

A surplus of cement should still be present in the acetabulum after pressurisation so that it can be moulded to the acetabular cup. It has been shown in the literature that the majority of the cement interdigitation occurs during pressurisation; therefore, only just enough cement needs

to be present in the acetabulum so that pressure can be maintained to prevent cement expulsion from the pores within the trabecular matrix due to back bleeding.<sup>24</sup>

### 6.3 Novel Pressuriser #1

The Depuy pressuriser consists of a Silicone spherical cap. The spherical cap is 80 mm in diameter and is cut off so that the radius of the top-down view is 60 mm as can be seen below (Figure 6.5). When the pressuriser is applied to the cement and is forced against the acetabular rim, due to the pliable silicone, it conforms to the irregularities of the rim and creates a space in which the cement is contained. Upon further loading, the pressuriser deforms further which reduces the space in which the cement is contained. Boyle's law states that if the space in which a controlled amount of fluid is contained decreases, the temperature and pressure will increase.<sup>263</sup> In this case, it is the increase in pressure that is desirable. The increase in pressure will force the cement into the bone, creating an interdigitated cement-bone interface which is desirable for a well-fixed component. It was shown that the existing Depuy pressuriser sufficiently seals the acetabulum and increases the pressure of the cement inside the cavity, forcing it into the exposed trabecular. This is evidenced by the sustained pressures measured at the acetabulum model surface.

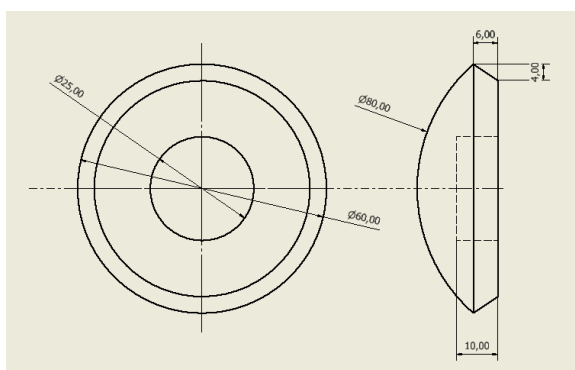


**Figure 6.5** Technical drawing of a Depuy acetabular pressuriser showing the single domed sealing surface. All values in mm.

To excavate a larger volume of cement at an earlier stage of curing, a novel pressuriser was designed and tested which features an excavating radius that protrudes from a sealing surface (Figure 6.6). The dimensions of the sealing surface were kept similar to those of the Depuy pressuriser as the data showed that this design effectively seals and pressurises the cement. The two key dimensions that needed to be determined were the radius of the excavating surface and the offset from the centroid of the sealing surface.

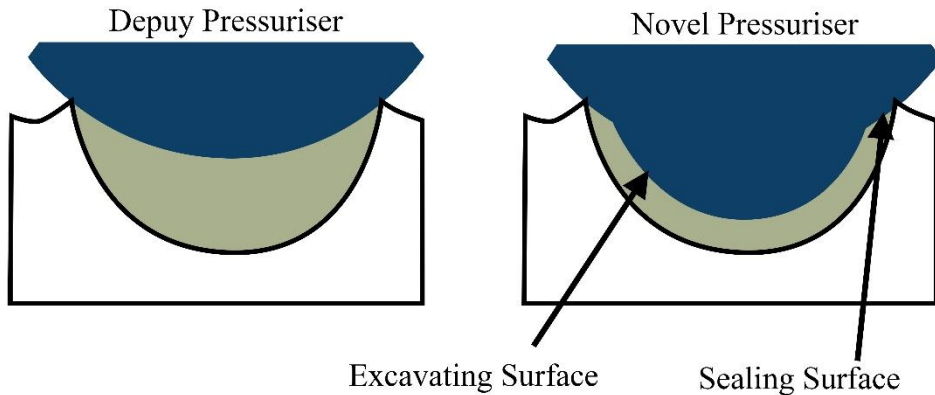


**Figure 6.6** A side by side comparison of a cross-section of the Depuy pressuriser and the novel pressuriser. A larger volume of cement is excavated at the pressurisation stage when using the novel pressuriser due to the excavating surface labelled in the diagram.

### 6.3.1 Material

The Depuy pressuriser is manufactured from silicone. The novel pressuriser will be made of a similar material as this is the industry standard and therefore has a long clinical history. Silicone is also cheap, easy to mould, and deforms under pressure allowing for pressurisation.

Silicone is primarily categorised by its hardness value; therefore, the hardness of the Depuy acetabular pressuriser was measured so that a similar grade of silicone could be found. The average Shore A hardness of the Depuy acetabular pressuriser is  $40.65 \pm 0.53$ .

There are several types of silicone rubber available, each with its own properties.<sup>264</sup> RTV silicone is one of the hardest silicones available and there were several products available which matched the hardness value required. RTV silicone is an air curing silicone meaning that nothing had to be mixed. This has the advantage that the amount of air trapped through mixing would be minimised. However, preliminary tests showed that even after leaving the silicone to cure for a long time, the centre would not set as there was not enough air available for the silicone to cure.

The other type of silicone considered was addition cure silicone. The advantage of addition cure silicone is that air is not required for curing, this means that even the centre of the pressuriser would cure. AS40 addition cure silicone was available from Easy Composites and had a Shore A hardness of 40, sufficiently close to the value of the hardness of the Depuy pressuriser. However, when mixed, the high viscosity silicone trapped a large number of air bubbles. It was possible to remove some of these by placing the mixture in a vacuum chamber and also by stretch pouring the mixture into the mould. In this instance, both techniques were used and worked quite well although a larger vacuum chamber that can reach a more perfect vacuum would be able to remove even more of the trapped air (Figure 6.7).



**Figure 6.7** A number of bubbles can be seen on the backside of the novel pressuriser. As this is a non-functional surface it is not critical that it is free from imperfections.

Another important consideration when determining which material should be used is the magnitude of shrinkage. The components will be created using a mould, so it was important that the silicone has minimal shrinkage so that the dimensions are not changed. AS40 addition cure silicone has a sufficiently low volumetric shrinkage.

### 6.3.2 Dimensions

A technical drawing of the first design can be seen below (Figure 6.8)

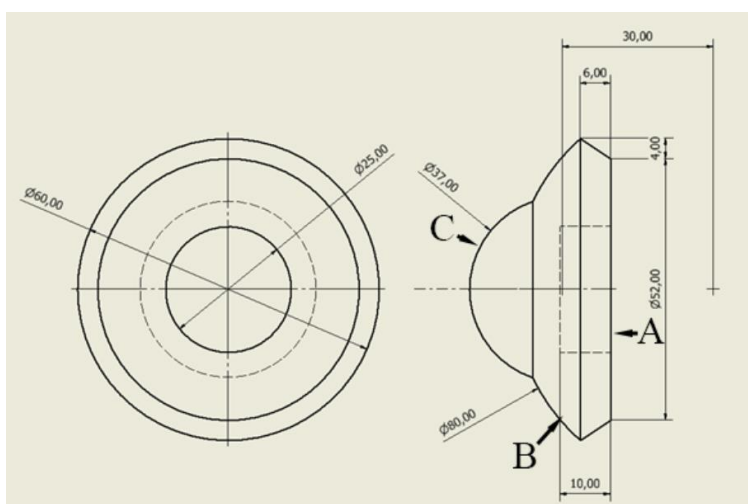


**Figure 6.8** Technical drawing of the novel pressuriser, all values are in mm. Significant surfaces are labelled and discussed further below.

#### 6.3.2.1 Connector

On the rear surface, labelled A in the figure above, is a bore 25 mm in diameter and 10 mm deep which is designed to connect to a handle (Figure 6.8).

### 6.3.2.2 Sealing Surface

The sealing surface is noted as point B in the figure above (Figure 6.8). It consists of a spherical cap, 80mm in diameter, cut off so that the circle made from the top down is 60 mm in diameter (similar to the Depuy pressuriser). It is this surface that is designed to contact the acetabular rim and seal the cement inside the acetabulum.

The mould splits at the edge in between the sealing surface and the face where the connector is located. The chamfered surface that leads to the surface where the connector is located is non-functional.

### 6.3.2.3 Excavating Surface

The excavating surface is labelled as C in the figure (Figure 6.8).

The two key dimensions of the excavating surface are the radius and the offset from the sealing surface centroid.

For the radius of the excavating surface, it is important to consider the size of the acetabular cup to be implanted. There are three options for the size of the excavating radius relative to the cup: it could be smaller, larger or the same radius as the cup to be implanted. For the first design, it was felt that a smaller radius than the cup to be inserted would be most suitable so that there is some cement left in the acetabulum cavity to form to the acetabular cup. A diameter for the excavating surface of 37 mm was arbitrarily chosen for an acetabular cup radius of 50 mm.

The offset between the centroids of the excavating and the sealing surface must be within two extremes. The first is the minor extreme which is defined as when the offset is so small the excavating surface does not protrude from the sealing surface. The major extreme is defined as when the offset is so large that there is some of the excavating surface is more than a  $90^\circ$  angle from the direction of the acetabulum or when some of the excavating surface would contact the acetabulum (Figure 6.9).

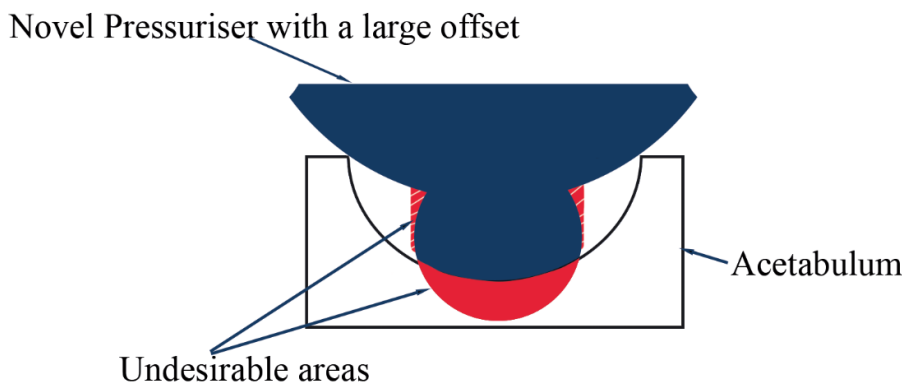


**Figure 6.9** A diagram demonstrating two issues that arise when the offset between the sealing centroid and the excavating centroid is too large. The red hatched area indicates some of the

excavating surface that is facing away from the acetabulum and the red solid area shows where some of the excavating surface overlaps with the acetabulum.

For the first iteration, an offset of 30 mm was arbitrarily chosen. This value was within the extremes outlined previously and would be adjusted after experience in the preliminary tests.

### 6.3.3 Manufacturing

#### 6.3.3.1 Mould

A split mould was manufactured from aluminium with the inner surface polished to a mirror finish allowing easy extraction of the pressuriser. The two halves of the mould came together at a non-functional edge (Figure 6.10).

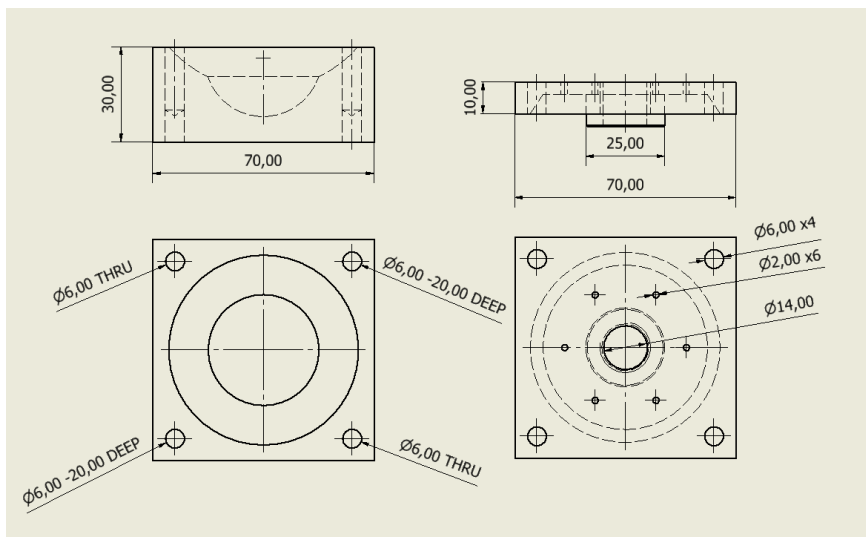


**Figure 6.10** Technical drawing of the aluminium mould used to create the novel pressuriser, all values in mm. No dimensions for the internal cavity are given as it is simply the negative of the novel pressuriser. The bottom plate is on the left and the top plate on the right.

Two of the four larger holes in the corners were machined 20 mm deep with a diameter of 6 mm to a high precision to ensure correct alignment using dowel pins. The other two holes were through holes, 6 mm in diameter, so that the two halves of the mould could be fixed together using bolts.

The central hole on the top plate was used for pouring the curing silicone mixture in. The circle of smaller holes surrounding it were for the escape of air. The mould design ensured that the cavity would fill from the bottom first and no air pockets would be trapped at the bottom and therefore the functional sealing and excavating surfaces would be free of bubbles.

#### 6.3.3.2 Moulding Methodology

The appropriate amount of silicone and catalyst were measured out and mixed in a large plastic container. The mixture was then stretch poured into an identical plastic container – this technique involved pouring the mixture from a large height slowly so that entrapped bubbles of

air burst as they pass through the thin stream of silicone. The silicone mixture was then placed into a chamber with a vacuum in the order of  $10^{-3}$  mbar (absolute). Once the mixture had expanded and collapsed, marking the successful destruction of any remaining entrapped bubbles, the mixture was removed from the chamber and stretch poured into the mould until it was completely full.

The silicone was then allowed to set over the course of a week to ensure that it had fully set.

The solidified novel pressuriser was then removed and was ready for testing (Figure 6.11).



**Figure 6.11** The first design of novel pressuriser with a smaller excavating surface of radius 25mm.

#### 6.3.4 Preliminary Testing

The novel pressuriser was subject to preliminary testing. This involved repeating tests described in a previous chapter with the novel pressuriser and inspecting the mantle after pressurisation and after acetabular cup insertion (Chapter 5).

There were imperfections in the set cement mantle (Figure 6.12). The impression made by the novel pressuriser in the cement prior to cup insertion looked adequate. However, upon insertion of the acetabular cup, there was an amount of air that becomes trapped due to the impression made by the excavating surface having a smaller radius than the acetabular cup. This meant that as the cup is forced into the dough, the edge where the cup and the cement make contact collapses and wrinkles are made in the dough. A radius equal to, or larger than that of the acetabular cup to be inserted would be more suitable (Figure 6.13).

The offset selected seemed to be satisfactory and there were no issues due to the material selected.

It was deemed that the radius of the excavating surface should be larger than the radius of the cup to be implanted (Figure 6.13). This would ensure that all the air in between the cup and the cement has a way to escape and it also ensured that the cement can uniformly envelop the cup as it is displaced from the cavity rather than crumple it inwards.



**Figure 6.12** Wrinkles can be seen on the solidified acetabulum when the radius of the acetabular cup is larger than that of the excavating surface of the pressuriser.

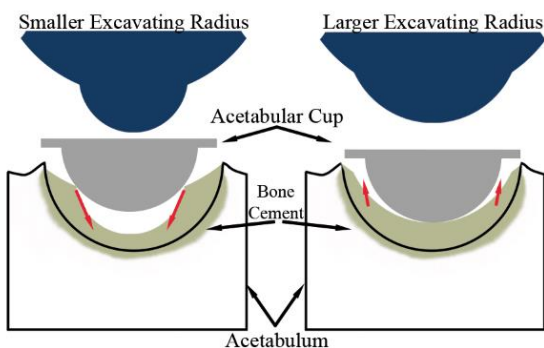


**Figure 6.13** A side-by-side comparison of the pressurisers with a radius smaller and larger than that of the acetabular cup to be inserted. The red arrows indicate the expected movement of cement upon implantation of the acetabular cup. With the smaller excavating radius, it is expected that the cement will crumple down towards the centre, this is evidenced by wrinkles seen on the cement mantle in figure 6.12. With a larger radius we expect the cement to move up and envelope the cup which is desirable.

#### 6.4 Novel Pressuriser #2

Due to the findings of preliminary testing with the first iteration of the novel pressuriser, a new mould was manufactured with a radius of 26 mm; 1 mm larger than the radius of the acetabular cup to be inserted. The offset was adjusted to 21.5 mm, this ensured that a similar amount of sealing surface is retained as the first iteration as it appeared the cement was properly sealed.

##### 6.4.1 Dimensions

The dimensions of the second novel pressuriser can be seen below (Figure 6.14).

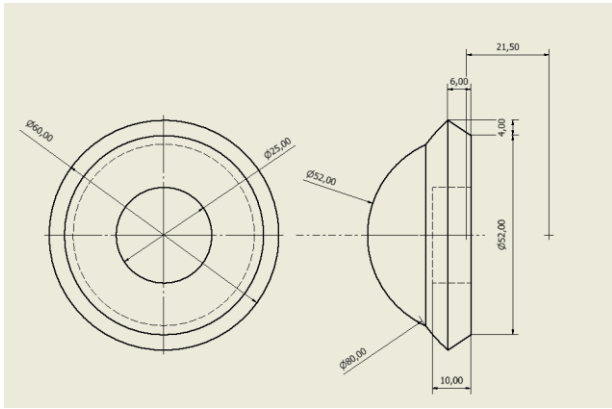


**Figure 6.14** Technical drawing of the second iteration of novel pressuriser design, all values in mm.

#### 6.4.2 Preliminary Testing

Once again, the methodology of the experiment previously described (Chapter 5) was used to determine whether the novel pressuriser design created any immediate problems.

The cement mantles appeared uniform and continuous and no issues in the procedure could be identified. Therefore, full testing commenced so that the novel pressuriser could be fully analysed.

#### 6.5 Discussion

From preliminary testing of the second iteration of the pressuriser design, it was seen that the novel pressuriser creates a uniform cement mantle with no apparent defects.

Further testing is required to determine how well the novel pressuriser pressurised the cement within the mock acetabulum. The novel pressuriser already provides the advantage of excavating excess cement earlier in the curing process. This will be discussed further after full testing in the following chapter.

So far, the dimensions for the pressuriser have been determined to be within a certain range, further testing is required to optimise the value of these dimensions. The sealing surface is the most constrained design feature as it is based on an already functional design. The excavating surface has two key parameters which can be adjusted to maximise the effectiveness of the pressuriser – the radius and the offset from the sealing centroid.

## **Chapter 7. Does use of the Novel Acetabular Pressuriser Significantly Improve the Nature of the Pressures Generated at the Surface of a Mock Acetabulum During Pressurisation and the Acetabular Cup Implantation?**

### **7.1 Disclaimer**

Sections of the Materials and Methods are taken from Chapter 5 as the experimental design was almost identical, it is included here for completeness.

### **7.2 Introduction**

#### ***7.2.1 Background and Motivation***

As seen in the previous chapter, the novel pressuriser was designed to excavate more cement from the acetabulum during the pressurisation stage of the implantation process. It does this through an excavating surface that protrudes from the sealing surface. Upon application of force to the novel pressuriser, the excavating surface will expel excess cement from the acetabulum, the remaining cement will be sealed by the sealing surface and the cement will be pressurised upon further loading of the pressuriser.

Due to the design, it is already known that the necessary deformation of cement will occur earlier in the cement curing process which should reduce the magnitude of the stresses generated within the cement mantle.<sup>14, 73</sup> The magnitude of this reduction will be dependent upon many factors including the geometry of the acetabulum, the brand of the cement, the timing of pressurisation, and by the design of the pressuriser. However, the pressures achieved during both pressurisation and during cup insertion are important. The link between the pressures generated, the penetration of cement and the strength of the bone cement-bone interface has already been discussed (Chapter 5.6.1).

The key motivation of this experiment was to compare the efficacy of the novel pressuriser to the Depuy pressuriser (DePuy, UK). There are several key characteristics of the cement pressure plot that will be analysed to compare the novel pressuriser to the Depuy pressuriser.

As was seen in the flanged acetabular cup vs unflanged acetabular cup experiment (Chapter 5), there are two key phases during cemented acetabular cup implantation. First, the pressurisation of the cement within the acetabulum and second is the cup insertion stage. Most other *in vitro* experiments that focus on the pressurisation stage of cemented acetabular arthroplasty neglect the phase of implantation that the experiment is not focused on, thereby disregarding half of the potential variables involved in the implantation process.<sup>189, 190, 192, 193, 195</sup> The pressurisation stage is key to the cup implantation stage as it dictates the cement indentation that the cup will be initially placed into.

The key pressure characteristics that will be investigated are the magnitude of the pressure, the pressure change through time, and the pressure differential between the pole and the rim of the acetabulum. The magnitude of the pressure is arguably the most important measurement as

previous experiments have linked this to the strength of the cement bone interface.<sup>184, 192, 261</sup> The pressure change refers to whether the pressure is maintained through time, this will be the best indication of how well the sealing surface of the pressuriser performs. This is important for the novel pressuriser as it must be shown that it can seal and pressurise the cement within the acetabulum during the pressurisation stage. The pressure differential will also be investigated. Differences between the pressure differential created by the novel pressuriser and the Depuy pressuriser could be demonstrative of the differences between the pressuriser designs.

### 7.2.2 Objectives

1. To determine whether the novel pressuriser improves the magnitude of the pressures generated at the acetabulum surface during pressurisation and during cup insertion when compared to the Depuy pressuriser.
2. To determine whether the Depuy pressuriser and the novel pressuriser seal the acetabulum during pressurisation effectively and to determine whether the pressuriser used makes a significant difference to the pressure changes during cup implantation.
3. To determine whether the design of acetabular pressuriser affects the differential between the pressures generated at the pole and at the rim of the mock acetabulum during pressurisation and cup insertion.
4. To determine whether the novel pressuriser is functional and to use the findings to suggest further improvements.

## 7.3 Materials

This section describes the materials used in this experiment. The methodology is described in the following section.

An acetabulum model was manufactured from stainless steel 304 with a 52 mm hemispherical bore, a diameter to which the acetabulum is often reamed *in vivo*. Steel was selected as it would provide accurate surface for the pressure transducers to lay flush on, a porous model would closer represent the surface texture of the acetabulum; however, the cement should only contact the surface of the transducer flush with the acetabulum, this would be impossible using a porous model. Previous studies use a rubber glove to separate the pressure transducer from the cement but this would invalidate the pressures recorded.<sup>255</sup> The diameter was confirmed to be within 0.01 mm of the expected value using a CMM. The model included tapped holes for pressure transducers at 0° (pole), 45°, and 75° (rim) from the direction of forcing (Figure 7.1).

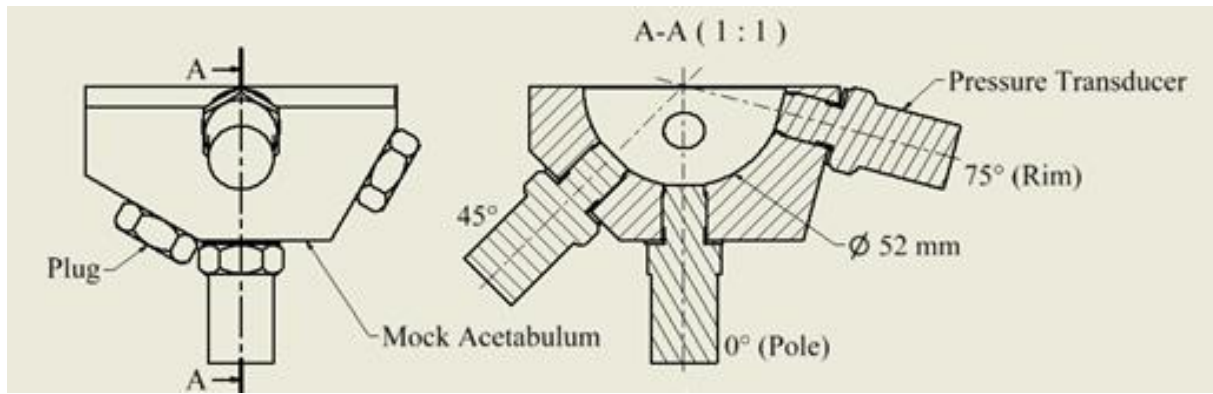


**Figure 7.1** Technical drawings with all relevant dimensions of the mock acetabulum. All dimensions are in mm.

The bone cements used were CMW 2 (Depuy Synthes); a high-viscosity cement, frequently used for fixation of the acetabular component.; and Refobacin R (Zimmer Biomet) which is a high viscosity bone cement.

The CMW 2 bone cement was mixed in a Hivac™ bowl (Summit Medical LTD, Gloucestershire) and the Refobacin R bone cement was pre-packaged and mixed in the Optipac 60 cement delivery system.

Pressurisation was performed with either a Depuy Smartseal acetabular pressuriser or a novel acetabular pressuriser (Figure 7.2).

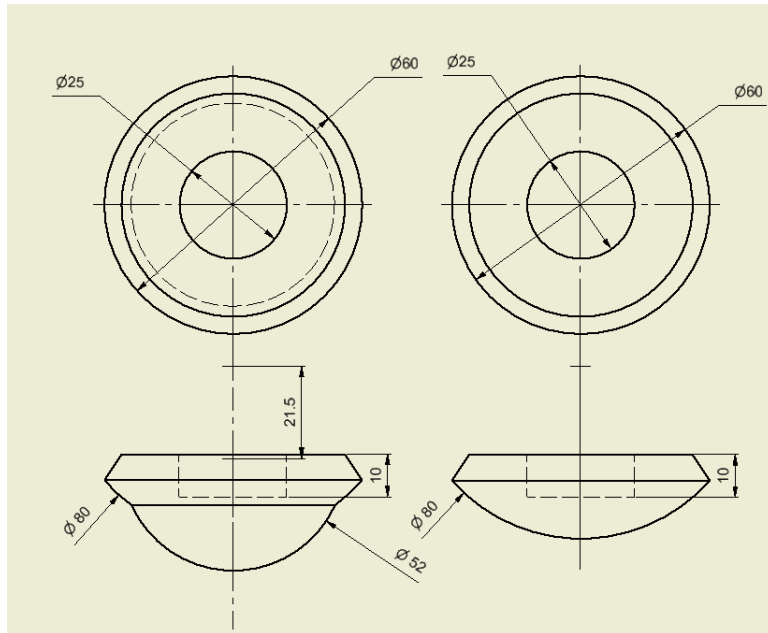


**Figure 7.2** Technical drawings of the Depuy pressuriser (right) and the novel pressuriser (left) with all relevant dimensions. All dimensions are in mm.

A flanged acetabular cup was manufactured from HXLPE. The external diameter was 50mm and an internal diameter of 28mm, this would leave a cement mantle of around 1mm thick if the centres of the cup and the acetabulum cavity were aligned. The flange had a thickness of 1.7mm and diameter 63mm (Figure 7.3).

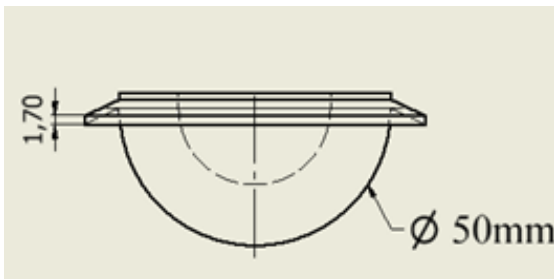


**Figure 7.3.** Technical drawing of the flanged HXLPE acetabular cup. All measurements in mm.

Omega PX61V0 pressure transducers were used with an Omega TXDIN1600S bridge for amplification and data acquisition (Appendix F). The pressure sensors were received from Omega fully calibrated with calibration certificates. Upon receiving the sensors, a set of control data was generated using a loading program and a doughy substance similar to the consistency of bone cement; this loading program was repeated prior to each experiment to re-calibrate the sensors (Appendix E). The transducers were made flush to the acetabulum hemispherical surface using shim washers. The data was filtered using a first order, low pass Butterworth filter with a cut off frequency of 160 Hz which is half the sampling rate of the Omega TXDIN1600S bridge, selected using the Nyquist criterion which allows for the filtering of electrical noise (Appendix H).

A Type K thermocouple was used to monitor the temperature, as the temperature is often used to monitor the progress of polymerisation (Appendix G). The thermocouple was inserted into the acetabulum cavity between the acetabular rim and the pressuriser.

The assembled rig was mounted into a Shimadzu ADS-X which was used to apply load. It was fitted with a 1 kN load cell (Figure 7.4). Note that during surgery, the cup is implanted at 40° to the transverse plane; however, the force applied by the surgeon is orthogonal to the plane of the cup face, therefore the experimental set-up here is equivalent.

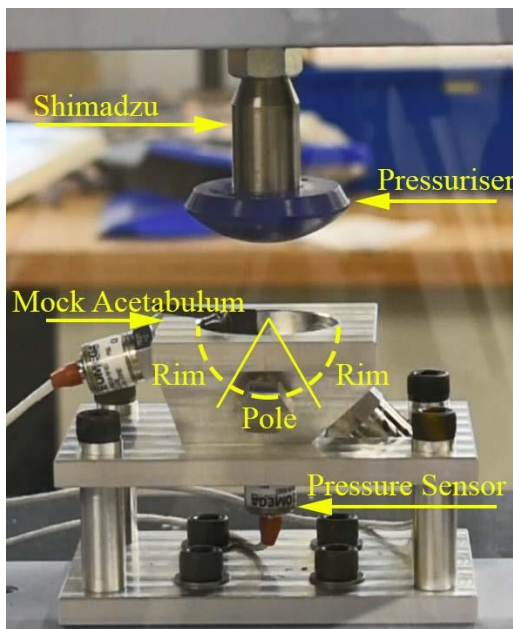


**Figure 7.4** Mock acetabulum and Depuy pressuriser experimental set-up in the Shimadzu universal tester showing the sensor positions in relation to the rim and pole.

All equipment used was manufactured with a tolerance of +/- 0.05 mm, with consideration of the design of the rig, the loading was always applied within 0.25 mm from the centre of the acetabulum cavity.

#### 7.4 Methods<sup>249</sup>

The temperature of the laboratory was between 20.5°C and 23°C for all experiments which is outside of the range of temperatures defined in the standards.<sup>260</sup> The humidity of the lab was between 45% and 50%. All equipment was left in the lab to ensure that the temperature of the equipment was static.<sup>260</sup> Mould release spray (Silicone Mould Release Agent, Ambersil) was used to ensure that the cement mantle could be removed from the model acetabulum. The Shimadzu was force controlled with a maximum stroke rate of 40 mm/min.

The PMMA powder and the MMA liquid were mixed under vacuum in their respective vacuum mixing containers in a partial vacuum of around 0.4 bar (absolute) vacuum at a frequency of around 1 Hz until homogenous. For both conditions, the cement was then left to rest until the cement no longer adhered to surgical gloves (clinically defined as the dough point.<sup>260</sup>). The cement was then inserted into the acetabular cavity and the loading program for pressurisation was started. The cement was pressurised for 100 s at 100 N (Figure 7.5).

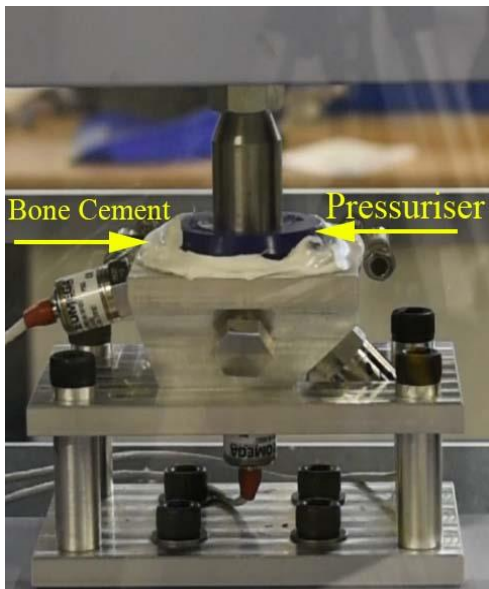


**Figure 7.5** A 100 N force was applied to the Depuy Pressuriser with the bone cement sealed within the acetabulum model in the Shimadzu universal tester.

The pressuriser was then removed from the universal tester and the flanged acetabular cup was placed into the cement. The cup implantation program was started, a load of 50 N was applied until the cement was fully cured (Figure 7.6). After the cement had fully cured, the cement mantle was removed, and another test was performed. This was repeated four times for each of the four testing conditions: two pressuriser designs and two cements.

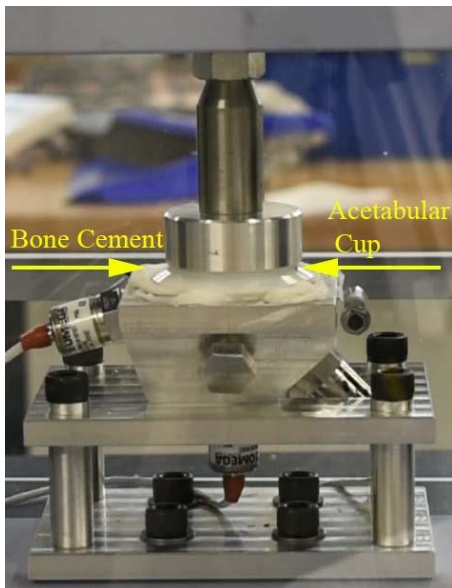


**Figure 7.6** A force of 50 N is applied to the acetabular cup to force it into the bone cement in the Shimadzu universal tester.

For this experiment, pressurisation and cup insertion were performed within the working time advised by the cement manufacturer. The cup load was decided upon after preliminary tests showed that the cup would be correctly positioned after full cure of the cement.

The end of cup implantation was taken to be when there was a deviation from the average pressure. To allow a more detailed analysis of the continuous pressure curves they were divided into fifths and the pressure at each of these five points in time was taken and used for statistical comparisons (Figure 7.7). This technique also allowed for analysis of how the pressure evolved, previous studies often only state the average or maximum pressure achieved during surgery, but this is insufficient for proper analysis.

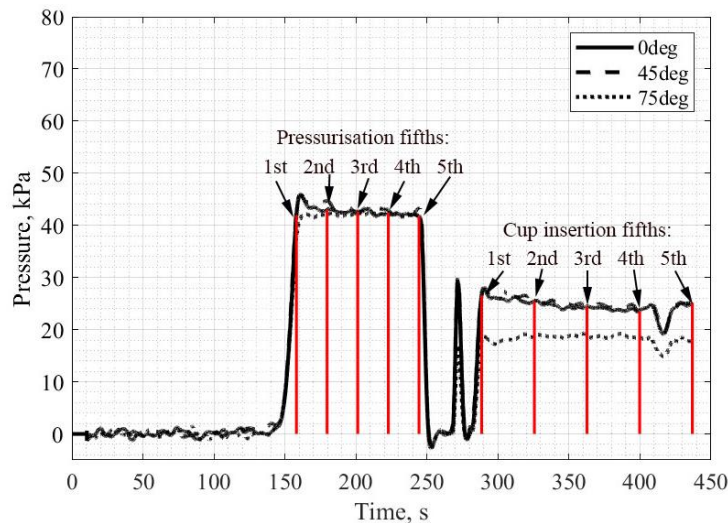


**Figure 7.7** A typical plot with an indication of how data is split up into fifths (pentiles) for further analysis.

A Ryan-Joiner test was used to see whether data were normally distributed; if so, a standard student t-test<sup>245</sup> was used to determine whether there was a significant difference between compared variables. If the data were not distributed normally, a Mann-Whitney test was used.<sup>246</sup> The results were considered significant if  $p \leq 0.05$ .

## 7.5 Results

Typical annotated plots showing cement pressure and temperature over time when flanged acetabular cups are implanted using CMW 2 bone cement or Refobacin R bone cement which had been pressurised using a Depuy acetabular pressuriser or the novel acetabular pressuriser can be seen below (Figure 7.8). A full set of graphs is provided within the appendix (Appendix I). Pressure measurements were recorded at positions 0° (rim), 45° and 75° (pole).

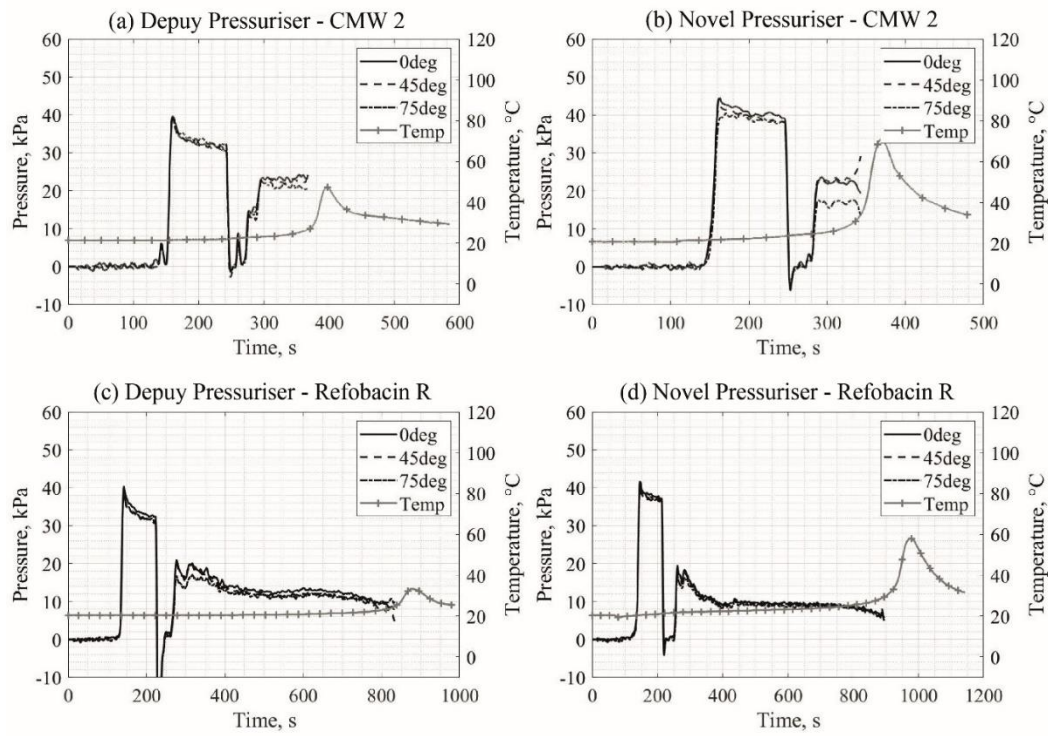


**Figure 7.8.** Four graphs showing a typical example of the pressure, temperature – time plot from each of the testing conditions. The pressure at various angles from the direction of forcing and the temperature through time are plotted.

### 7.5.1 Pressurisation

The table containing the averages and standard deviations of the pressures generated during the pressurisation stage for each pentile (fifth) of cup implantation, at each angle, for each condition can be seen below (Table 7.1).

**Table 7.1** A table containing the average pressure and standard deviations in brackets for each testing condition, at each angle from the direction of loading, at each pentile during the pressurisation stage of the experiment. Statistical differences between the pressures generated due to which pressuriser was used are highlighted using [a]-[j] to indicate the relevant pair. A \* indicates that the data set was non-normal. Four repeats of each testing condition were performed.

Sample	Angle (°)	1st (kPa)	2nd (kPa)	3rd (kPa)	4th (kPa)	5th (kPa)
CMW 2 Cement, Depuy Pressuriser	0	40 (7.35)	43.11 (9.22)	42.29 (9.15)	41.45 (9.04)	40.09 (9.31)
	45	39.64 (7.11)	42.55 (9.03)	41.36 (9.20)	40.61 (9.23)	40.51 (8.77)
	75	39.68 (7.22)	43.95 (8.94)	42.41 (9.33)	42.12 (9.19)	41.67 (8.95)
CMW 2 Cement, Novel Pressuriser	0	41.3 (2.42)	42.39 (0.83)	40.91 (0.84)	40.69 (0.95)	40.01 (1.01)
	45	*39.67 (2.22)	41.03 (0.11)	40.06 (0.75)	39.38 (1.08)	39.13 (0.92)
	75	35.19 (1.99)	*39.55 (0.59)	39.33 (0.89)	38.65 (1.47)	38.07 (0.38)
Refobacin R Cement, Depuy Pressuriser	0	37.53 (1.35)	36.47 (2.19)	[a] 35.17 (2.26)	[b] 34.05 (2.83)	[c] 33.49 (2.75)
	45	36.29 (1.48)	[d] 34.81 (2.26)	33.67 (2.49)	[e] 32.92 (2.47)	[f] 32.18 (2.76)
	75	35.47 (1.17)	[g] 35.05 (2.13)	[h] 33.87 (2.27)	[i] 33.21 (2.86)	[j] 32.39 (2.87)
Refobacin R Cement, Novel Pressuriser	0	*38.25 (4.33)	40.66 (1.31)	[a] 39.97 (1.16)	[b] 39.64 (1.3)	[c] 39.47 (1.49)
	45	*37.42 (4.21)	[d] 39.4 (1.33)	38.86 (1.23)	[e] 38.46 (1.14)	[f] 38.29 (1.06)
	75	37.99 (3.76)	[g] 40.45 (1.44)	[h] 39.65 (1.67)	[i] 39.07 (1.39)	[j] 38.4 (1.25)

### 7.5.1.1 Pressure Magnitude

There were no significant differences between the pressures generated due to the pressuriser when CMW 2 was used but the novel pressuriser frequently produced larger pressures than the Depuy pressuriser when Refobacin R cement was used (Table 7.1). These were generally later in the pressurisation stage and occurred at all angles from the direction of loading.

### 7.5.1.2 Pressure Change

There was only one statistically significant difference in the pressures generated at the beginning and the end of the pressurisation stage which occurred at 75° from the direction of loading for the novel pressuriser using CMW 2 bone cement (Table 7.2). The value for the pressure increased from the first pentile to the last; however, this is because the start of each stage was determined as when the pressuriser contacted the cement and not when the pressure reached its maximum value. If the second pentile is compared to the last pentile, it can be seen that when the novel pressuriser is used to pressurise CMW 2 bone cement the pressure significantly drops for all angles. There is no significant pressure drop for either pressuriser when Refobacin R bone cement is used.

**Table 7.2** A table containing the statistical results comparing the pressure at the beginning of pressurisation to the end of pressurisation. A \* indicates that one or both sets of data being compared are non-normal. Four repeats of each testing condition were performed.

Sample	Angle (°)	1st vs 5th	2nd vs 5th
CMW 2 Cement, Depuy Pressuriser	0	N	N
	45	N	N
	75	N	N
CMW 2 Cement, Novel Pressuriser	0	N	Y
	45	*N	Y
	75	Y	*Y
Refobacin R Cement, Depuy Pressuriser	0	N	N
	45	N	N
	75	N	N
Refobacin R Cement, Novel Pressuriser	0	*N	N
	45	*N	N
	75	N	N

### 7.5.1.3 Pressure Differential

Results of statistical tests indicated that there were several instances when there was a significant differential between pressures generated at the pole and at the rim of the acetabulum during the pressurisation stage when CMW 2 bone cement was implanted using the novel pressuriser but none for the Depuy pressuriser and none for either pressuriser when Refobacin R was used (Table 7.3).

**Table 7.3** A table containing the statistical results comparing the pressure at the pole of the mock acetabulum to the rim of the acetabulum at each pentile of pressurisation. A \* indicates

that one or both sets of data being compared are non-normal. Four repeats of each testing condition were performed.

Sample	1st (kPa)	2nd (kPa)	3rd (kPa)	4th (kPa)	5th (kPa)
CMW 2 Cement, Depuy Pressuriser	N	N	N	N	N
CMW 2 Cement, Novel Pressuriser	Y	*Y	Y	N	Y
Refobacin R Cement, Depuy Pressuriser	N	N	N	N	N
Refobacin R Cement, Novel Pressuriser	*N	N	N	N	N

### 7.5.2 Cup Insertion

The averages and the standard deviations of the cement pressure for each pentile (fifth) of cup insertion, at each angle, for each condition can be seen below (Table 7.4).

**Table 7.4** A table containing the average pressure and standard deviations in brackets for each testing condition, at each angle from the direction of loading, at each pentile during the cup insertion stage of the experiment. Statistical differences due to which pressuriser was used are highlighted using [a]-[c], indicating the relevant pair. A \* indicates that one or both data sets were non-normal. Four repeats of each testing condition were performed.

Sample	Angle (°)	1st (kPa)	2nd (kPa)	3rd (kPa)	4th (kPa)	5th (kPa)
CMW 2 Cement, Depuy Pressuriser	0	20.23 (4.2)	21.21 (1.97)	20.8 (1.94)	20.39 (2.39)	20.65 (2.97)
	45	19.81 (4.64)	20.7 (2.2)	20.54 (2.13)	[a] 20.11 (1.84)	*[b] 19.61 (2.34)
	75	18.4 (4.12)	19.86 (2.17)	19.34 (1.46)	19.25 (1.79)	18.64 (1.92)
CMW 2 Cement, Novel Pressuriser	0	22.04 (2.56)	23.25 (1.15)	23.74 (1.12)	23.57 (1.33)	23.94 (1.26)
	45	23.1 (3.15)	23.56 (0.99)	24.73 (1.47)	[a] 24.58 (1.86)	[b] 25.62 (2.28)
	75	16.78 (3.15)	17.74 (1.11)	17.74 (1.14)	17.26 (0.66)	17.06 (1.17)
Refobacin R Cement, Depuy Pressuriser	0	[c] 20.68 (1.2)	16.78 (2.16)	14.46 (1.82)	14.27 (1.62)	11.89 (2.51)
	45	19.29 (0.76)	15.86 (2)	14.08 (2.04)	13.08 (1.33)	10.17 (1.98)
	75	15.57 (0.42)	14.32 (1.85)	13.01 (1.7)	12.46 (1.07)	11.57 (1.2)
Refobacin R Cement, Novel Pressuriser	0	[c] 17.93 (2.06)	14.48 (3.58)	13.81 (3.29)	13.22 (3.09)	10.47 (3.15)
	45	17.74 (2.15)	14.18 (3.95)	13.7 (3.46)	12.96 (3.26)	10.69 (3.35)
	75	14.8 (1.92)	13.34 (3.04)	12.68 (2.83)	12.18 (2.38)	11.2 (2.97)

#### 7.5.2.1 Pressure Magnitude

There were several instances where there was a significant difference in the pressures generated in the mock acetabulum during cup insertion due to the which pressuriser was used beforehand. There were two instances for CMW 2 cement where the novel pressuriser generated significantly larger pressures, both of these in the final two fifths of cup insertion at 45° from the direction of loading. There was only one instance when there was a difference in the magnitude of the pressure generated when Refobacin R cement was used: a larger pressure was produced in the first pentile at the pole of the acetabulum when a cup was inserted into Refobacin R bone cement after it was pressurised using the Depuy pressuriser (Table 7.4).

#### 7.5.2.2 Pressure Change

When comparing the first pentile to the last there was almost always a significant drop in the pressures generated at the surface of the acetabulum when a flanged acetabular cup was inserted into Refobacin R bone cement, except at 75° for the novel pressuriser. There was never a significant drop in the pressure during cup insertion when CMW 2 bone cement was used (Table 7.5).

This pattern is similar when comparing the second pentile to the fifth pentile. However, there was less significant differences when a cup was inserted into Refobacin R which had been

pressurised using the novel pressuriser. It is felt that for cup insertion the first pentile compared to the last pentile is a better measure of the pressure change as the initial peak created when the cup is inserted is so large and occurs instantaneously at the pole. Therefore, the discussion will only consider the results for the first pentile compared to the last.

**Table 7.5** A table containing the statistical results comparing the pressure at the beginning of cup insertion to the end of cup insertion. A \* indicates that one or both sets of data being compared are non-normal. Four repeats of each testing condition were performed.

Sample	Angle (°)	1st vs 5th	2nd vs 5th
CMW 2 Cement, Depuy Pressuriser	0	N	N
	45	*N	*N
	75	N	N
CMW 2 Cement, Novel Pressuriser	0	N	N
	45	N	N
	75	N	N
Refobacin R Cement, Depuy Pressuriser	0	Y	Y
	45	Y	Y
	75	Y	N
Refobacin R Cement, Novel Pressuriser	0	Y	N
	45	Y	N
	75	N	N

### 7.5.2.3 Pressure Differential

There was always a differential in the pressure between the pole and the rim of the acetabulum upon insertion of the acetabular cup after CMW 2 bone cement was pressurised using the novel pressuriser. There was always a statistically significant pressure differential in the first pentile of cup insertion when Refobacin R was used, irrespective of which pressuriser was used (Table 7.6).

Larger pressures were always generated at the pole when there was a significant difference.

**Table 7.6** A table containing the statistical results comparing the pressure at the pole of the mock acetabulum to the rim of the acetabulum at each pentile of cup insertion. A \* indicates that one or both sets of data being compared are non-normal. Four repeats of each testing condition were performed.

Sample	1st (kPa)	2nd (kPa)	3rd (kPa)	4th (kPa)	5th (kPa)
CMW 2 Cement, Depuy Pressuriser	N	N	N	N	N
CMW 2 Cement, Novel Pressuriser	Y	Y	Y	Y	Y
Refobacin R Cement, Depuy Pressuriser	Y	N	N	N	N
Refobacin R Cement, Novel Pressuriser	Y	N	N	N	N

## 7.6 Discussion

The overall aim of this study was to determine the efficacy of the novel pressuriser. Several key measurables were analysed: the magnitude of the pressure, the pressure changes over time for each stage and the pressure differential between the rim and the pole. This study found that overall, the performance of the novel pressuriser was equivalent to that of the Depuy pressuriser.

### 7.6.1 Pressure Magnitude

The magnitude of the pressures generated during pressurisation and cup insertion phases were mostly independent of which pressuriser was used, although the novel pressuriser often generated larger pressures than the Depuy pressuriser when Refobacin R cement was used. The novel pressuriser also produced larger pressures at 45° from the direction of loading during cup insertion for CMW 2 cement.

There was one instance where the Depuy pressuriser created a larger pressure than the novel pressuriser; this occurred at the pole at the very start of the cup insertion phase for Refobacin R. This may be explained by the indentation left by the Depuy pressuriser, there will be little contact between the cup and the cement at the start of implantation and therefore larger pressures will be generated initially at the pole (Figure 7.9).

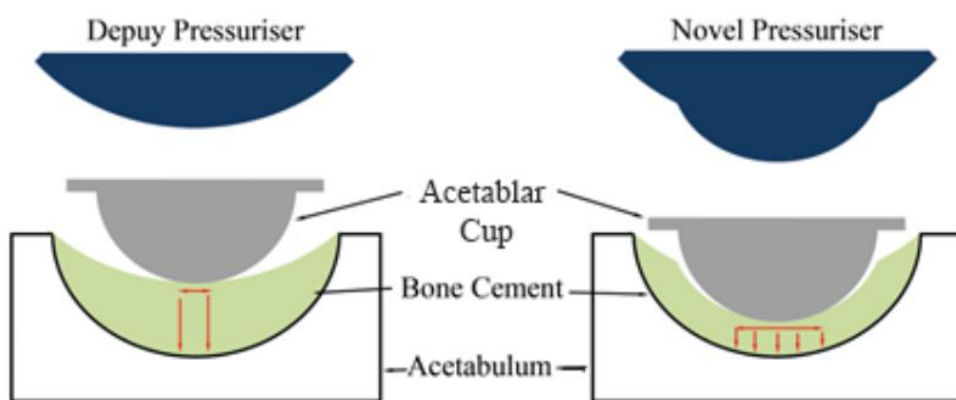


**Figure 7.9** The amount of pressure generated at the surface of the acetabulum is dependent upon how much of the cement and acetabular cup are in contact with each other. The impression made in the cement after pressurisation with the novel pressuriser may result in a larger, more uniform pressure across the acetabulum surface.

The magnitude of pressures generated for both pressurisers were equivalent to other studies that used equivalent implantation forces.<sup>189, 190, 192, 193, 195</sup>

Generally, there was no difference in the magnitude of the pressures generated due to the design of the pressuriser used. This was anticipated as the magnitude of the force used to pressurise the cement and to insert the cup are the same and therefore the changes in pressures generated are expected to be small.

### 7.6.2 Pressure Change

Statistical tests were performed to determine whether the acetabulum was effectively sealed during pressurisation for each pressuriser. It was found that there was only one instance where there was a significant difference in the pressure generated in the first and the fifth pentile and this occurred at 75° from the direction of loading when the novel pressuriser pressurised CMW 2 bone cement. However, upon inspection of the pressures it was found that the pressure increased. It is thought that the cause for this is that the first pentile was determined to occur when the pressuriser contacted the cement and therefore was not at the peak of the pressures

generated; therefore, the second pentile was used to determine how the pressure changed through time during pressurisation and it was found that when CMW 2 bone cement was pressurised using the novel pressuriser there was always a significant decrease in the pressure. The cause for this is unknown. However, despite this slow decay of pressure, the pressures were not significantly smaller than those of the Depuy pressuriser and therefore the novel pressuriser is still functional. Experiments should be performed on an acetabulum model with an irregular rim to properly determine the sealing efficacy of both pressurisers.

It was determined that it was valid to use the first pentile for the pressure change tests for cup insertion as there was such a large and instantaneous peak at the start of cup insertion that it accurately represented the diminishment of pressure through time (Figure 7.8). During cup insertion into Refobacin R, except at 75° when the novel pressuriser was used, there was always a significant drop in the pressures generated at the acetabulum. The cause for this is unknown. There was never a significant drop in the pressure during cup insertion when CMW 2 bone cement was used. These observations may relate to the polymerisation of the cement, as the cement becomes more polymerised the density of the cement mass increases and thus the volume taken up by the cement decreases and the deformation of the measuring diaphragm of the pressure transducers will decrease resulting in a reduction of the recorded pressure. Once the cement starts to warm, the cement mass will expand and as expected, this results in an increase in the pressures recorded as can be seen from the full pressure curve (Figure 7.10). The raise in temperature may also affect the functioning of the pressure transducers. It is unknown why the pressure significantly reduced for Refobacin R but not for CMW 2. It may relate to the large spread of data recorded for the pressures generated for CMW 2 cement.

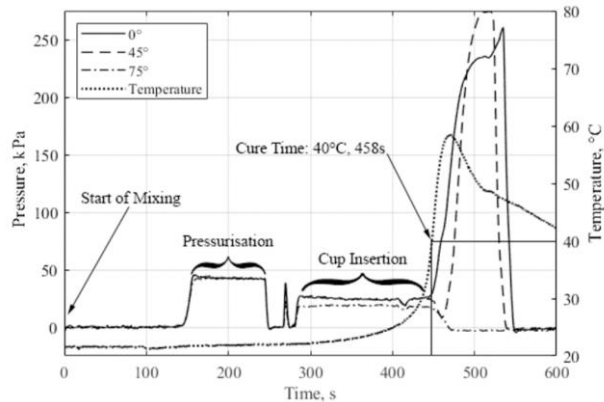


**Figure 7.10** A plot showing the full pressure and temperature - time plots even after the cure time. This shows how the solidification, and the subsequent heating and expansion of the mantle created unexpected pressure readings.

These results are once again positive for the novel pressuriser, the only difference between the pressures generated by the Depuy pressuriser and the novel pressuriser was that the novel pressuriser created a larger pressure at the end of pressurisation, 75° from the direction of loading for Refobacin R than at the start. The novel pressuriser was also responsible for the only instance where there was not a significant pressure drop during cup insertion for Refobacin R.

### **7.6.3 Pressure Differential**

The design of the novel pressuriser was intended to excavate as much cement as possible during the pressurisation stage so that there was less cement to be excavated during the cup insertion phase. This would minimise deformation of the cement later in the curing process and also it was hoped that it would reduce the pressure differential between the pole and the rim of the acetabulum during cup insertion due to reasons discussed in the previous chapter. The novel pressuriser achieved the former, but not the latter.

Except the 4<sup>th</sup> pentile, there is always a significant pressure differential between rim and pole when the novel pressuriser is used to pressurise CMW 2 cements, there is never a significant difference when the Depuy pressuriser is used. There is no significant difference in the pressures generated at the rim and the pole for either pressuriser when Refobacin R cement is used. The cause for the significant differences is not known but it may relate to the large spread of data obtained for the experiments performed with the Depuy pressuriser.

The results for CMW 2 are not consistent with the idea that the requirement for the flow of cement creates the pressure differential. The only difference between the two experimental conditions during the cup implantation stage is the indentation left after pressurisation. The cause for the significant differential between the pressures produced at the pole and the rim when the novel pressuriser is used but not when the Depuy pressuriser is used is not known. Further experiment must be performed to further investigate this.

### **7.6.4 Summary**

Overall, the performance of the novel pressuriser was adequate in terms of the pressure generated. There were several measurements where the novel pressuriser produced a larger pressure than the Depuy pressuriser and only one measurement where the Depuy pressuriser produced a larger pressure than the novel pressuriser and this was in the first pentile of cup insertion at 0° from the direction of loading for Refobacin R cement.

There are two areas of concern. First is the pressure drop during pressurisation when CMW 2 bone cement was pressurised using the novel pressuriser; however, as the pressures were still as large as the pressures generated when the Depuy pressuriser was used this drop does not appear to be a concern. More tests need to be performed to determine whether design changes are needed to ensure the novel pressuriser sufficiently seals the acetabulum during pressurisation. Secondly, when the acetabular cup was inserted into CMW 2 cement that had been pressurised by the novel pressuriser there was always a larger pressure at the pole than at the rim. It was hypothesised that the pressure differential was created by incomplete contact between cement and cup, but this cannot be true as with the novel pressuriser there is more complete contact than with the Depuy pressuriser. It was also hypothesised that this pressure differential was the result of the flow of cement but there is less flow of cement when the cup is inserted into cement that had been pressurised with the novel pressuriser so this also cannot be the case. Further experiments with the aid of mathematical models, would be beneficial to further the understanding of the fluid dynamics that occur inside the acetabulum during THA.

Despite the concerns regarding the pressure differential and the pressure drop during pressurisation, the novel pressuriser still tends to perform better than the Depuy pressuriser in terms of the magnitude of the pressures generated.

### **7.6.5 Study Limitations**

The number of repeats it was possible to perform was limited. To further strengthen the power of the statistical results, more repeats should be performed. Additionally, the number of variables was controlled. More combinations of designs, brands and sizes of components should be tested to check how universal the conclusions drawn here are.

### **7.6.6 Clinical Relevance and Future Work**

As with previous experiments, a more anatomically accurate acetabulum model would provide valuable data that could be used to further test the efficacy of the novel pressuriser. One of the key differences between the model used in this experiment and a natural acetabulum is the irregular acetabulum rim. It is important to understand whether the novel acetabulum could effectively seal the cotyloid notch found on the inferior edge of the acetabulum rim.

It would be advantageous to perform experiments where the force used for pressurisation and cup insertion were applied by a surgeon. This would give valuable data regarding the forces and timings that are used in a more clinically accurate situation. It would also be an opportunity to gather feedback from clinical practitioners on the novel pressuriser.

Repeating this methodology with the Exeter pressuriser would give more data allowing for further analysis of each pressuriser.

Finally, it is felt that it would be advantageous to build a mathematical model which simulates the generation of residual stress within the acetabulum due to all causes of residual stress including deformation of cement and comparing this to the residual stresses measured *in vitro*. This would give a qualitative measure of whether the novel pressuriser successfully reduced the magnitude of residual stress generated in the acetabular mantle. The residual stresses within the cement mantle could also be measured to determine whether there is a difference due to the pressuriser used.

## **7.7 Summary**

In summary, with a single exception in the first pentile of cup insertion into CMW 2 cement, use of the novel pressuriser produced equivalent, and occasionally superior, pressures at the acetabulum surface during both pressurisation and cup insertion than when a Depuy pressuriser was used. There are some concerns regarding how effectively the novel pressuriser seals the acetabulum during pressurisation and the pressure differential created between the pole and the rim of the acetabulum. Although these concerns should be further investigated, the generally equivalent or larger pressures generated by the novel pressuriser is encouraging.

The results reported here indicate that the novel pressuriser is functional. There is no data presented that suggests the device should not be used *in vivo*. Further testing is planned where

the pressures generated within the acetabulum will be measured when a surgeon implants an acetabular cup into a more anatomically accurate acetabulum model and into cadaveric models to further investigate the efficacy of the novel pressuriser.

## Chapter 8. General Discussion and Conclusion

The aim of this thesis was to investigate the factors of cemented THR that cause RLLs on postoperative radiographs. Several possible causation pathways were examined, these included the curing parameters of PMMA bone cement, the volumetric shrinkage of the PMMA cement mantle, and the pressures generated at the acetabulum bone surface upon pressurisation and cup insertion during cemented acetabular arthroplasty. Through the experiments, the focus of the thesis shifted, and it became an examination of the curing and pressurisation behaviours of PMMA bone cement within the acetabulum during cemented acetabular cup implantation.

### 8.1 Overview of Experiments

The rheology experiment aimed to determine whether frequency sweeps could be used to identify the moment that curing PMMA bone cement would start to store strains as residual stresses and to determine whether a more data focused approach to the determination of curing variables than is currently offered by the international standards could be found (Chapter 2). Ultimate tensile tests were performed on PMMA cement samples that were deformed during curing and samples that were allowed to rest during curing to determine whether the strain history of PMMA bone cement during curing affected the tensile strength of PMMA bone cement (Chapter 3). An acetabulum model was designed and manufactured from steel so that mock cemented acetabular implantation could be performed. Using this model, it was possible to closer examine both the shrinkage of the PMMA cement mantle after implantation and the pressures of the bone cement at the acetabulum surface generated during implantation. The diametric shrinkage of the cement mantle when it is vacuum mixed and when it is mixed at atmospheric pressure was investigated and the results were tested to determine whether there were any significant differences (Chapter 4). The pressures generated during both the pressurisation phase and the cup implantation phase of cemented acetabular implantation were examined using the acetabular model, which was fitted with pressure transducers, the quality and detail of this data surpass that of any data currently available in the literature (Chapter 5).

The findings of the rheology experiment, the deformation experiment, and the pressure data gathered in the mock acetabulum experiment provided the impetus for a new design of acetabular pressuriser (Chapter 6). The acetabulum model and the methodology used for previous experiments was used to determine the efficacy of the novel pressuriser (Chapter 7). A patent has been filed for the resulting novel pressuriser and further experiments are planned to further test and improve the pressuriser.

### 8.2 Summary

Total joint replacements have improved the quality of life for millions of patients. Sir John Charnley successfully designed, manufactured, and implanted the first low friction hip arthroplasty in the early 60s.<sup>1</sup> After this initial success, the expected longevity of total hip arthroplasties (THA) has increased thanks to improvements in materials, surgical techniques, and designs.<sup>2</sup>

In 2013, Abdulkarim *et al.* reported that cemented metal on polymer was still the gold standard choice of implant.<sup>40</sup> According to the NJR, it has the best Kaplan-Meier estimates of cumulative revision rate at 5.46% at 15 years, second best is hybrid fixation, which has an estimated cumulative revision rate of 5.65% at 15 years.<sup>2</sup> Using cement to fix both femoral and acetabular components has also been reported to be the cheapest method of fixation.<sup>265</sup> Despite this, cemented THA has decreasing popularity in the UK. Cemented THA's are often performed on older patients who are less likely to require revision; 64.4 years  $\pm$  11.3 years for uncemented THRs and 73.0 years  $\pm$  9.1 years for cemented hip replacements.<sup>2</sup> Often, cemented fixation is required for older patients<sup>2</sup> as they do not have the required bone stock to support uncemented components.

The most common cause of failure for cemented metal and polymer hips is aseptic loosening.<sup>2</sup> Aseptic loosening often occurs on the acetabular side of the joint at the bone cement-bone interface which is created during the operation.<sup>160, 162, 194</sup> A key factor in the surgical technique is the bone cement.

PMMA bone cement is a complex material. There are several difficulties when attempting to study it. Firstly, is its sensitivity to environmental conditions. As can be seen in the curing tables (Chapter 1.5.4.1)<sup>36</sup>, a small change in the environmental temperature can result in a large difference in the curing rates. Even the variation in temperature allowed in the standards makes a significant difference to the curing parameters. Secondly, once mixed, the characteristics of the cement change rapidly. Within 6-8 minutes CMW 2 bone cement goes from relatively low viscosity dough to a completely solidified cement.<sup>266</sup> This makes taking measurements difficult both due to the restricted time available to take multiple results for the same cement but also because taking measurements takes time and the variable being measured has likely changed over the course of the measurement. Finally, the high sensitivity to temperature, and the fact that the polymerisation reaction is exothermic means that the shape and size of the cement sample will affect its rate of curing.<sup>12, 56, 57</sup> A large mass of cement will release more thermal energy and heat will be transferred to the environment less efficiently than when a mass of cement has a smaller surface area to volume ratio. This means that the results that are collected will be specific to the size of the sample making comparison between results gathered from different testing methodologies difficult and comparison to the literature also difficult, especially considering the lack of detail in many of the key papers on this topic. With consideration to these difficulties, an ethos of simplification was determined to be advantageous to the quality of research into PMMA bone cement.

The first experiment to be performed was rheological characterisation of PMMA bone cement. The methodology employed was designed to incorporate frequency sweeps for each test. This was done as the viscosity of PMMA bone cement is dependent upon the rate of deformation and because the literature states that the tangent of the phase angle, which is used as a measure of how elastic or viscous a material is, is dependent upon the frequency.<sup>79, 89, 227</sup> The literature available regarding this is limited and is often undetailed.<sup>89</sup> This experiment provided a solid foundation from which further experiments could be designed. Some of the findings of the experiment confirmed what was already known within the literature; namely that the rate of polymerisation decreased with an increase in temperature,<sup>77</sup> the brand of cement significantly affected the time to full cure,<sup>12, 77</sup> and an increased rate of deformation reduced the viscosity.<sup>82-84</sup> However, there were also some more interesting findings that resulted from the rheological

experiments. The frequency of deformation did not significantly alter the phase angle, although this may be a result of the frequencies used. Apart from the very first measurement for Simplex P at 23°C, the elastic component of the complex modulus was always larger than the viscous component. The methodology used in this experiment could be employed again, using larger frequencies, to further probe whether the phase angle is altered by larger rates of deformation.

The elastic component of the complex modulus being larger than the viscous component, and the literature stating that the stress relaxation behaviour of hardened PMMA bone cement is well modelled by a viscoelastic model which includes an atemporal elastic component<sup>73</sup> served as motivation to investigate the generation of residual stresses in PMMA bone cement and how they affect the strength of hardened cement. Although there are several techniques that are suitable for measuring residual stress within PMMA bone cement<sup>242</sup> they were not employed; instead, an experiment was designed to simulate the operative techniques for the preparation of PMMA bone cement and to directly measure the strength. The cement was either mixed under vacuum or at atmospheric pressure during the mixing phase, it was then either allowed to rest or was deformed. The cement was then forced into PE dog bone shaped moulds and allowed to cure. After 48 hours, they were removed from the moulds and the UTS was measured. The results showed a significant decrease in the strength of the cement specimens that were deformed during the working phase. The act of deformation significantly decreased the UTS of the samples. It was determined that it was likely that this reduction in strength was due to the generation of residual stress. Further experiments that measure the residual stresses directly are required to confirm this finding.

Another important finding from the UTS experiment was that the reduction in the number of pores at the fracture surface of the dog bone samples. It is known in the literature that, generally, vacuum mixing decreases the porosity of PMMA bone cement. It does this by decreasing the amount of air trapped within the cement during the mixing phase.<sup>39, 173</sup> Some of the literature states that vacuum mixing increases the shrinkage of PMMA bone cement,<sup>39</sup> but it should be considered that vacuum mixing does not have a specific mechanism for increasing the shrinkage, only that it redirects the shrinkage that must happen due to density changes and thermal contraction from the pores within the cement to the external dimensions. Implantation of an acetabular cup into a steel acetabulum model was performed replicating surgical technique. In half of the experiments, the cement was mixed under a partial vacuum and in the other half, the cement was mixed at atmospheric pressure. It was found that there was a significantly larger reduction in the external diameter of the cement mantles when the cement was vacuum mixed. The porosity of the vacuum mixed cement was approximately an order of magnitude smaller than when the cement was mixed at atmospheric pressure.

The steel acetabulum model was also used to measure the pressures generated at the acetabulum surface during cemented acetabular cup implantation. Three pressure transducers were mounted into the mock acetabulum at three angles from the direction that force would be applied during pressurisation and cup insertion, 0°, 45°, and 75°. One of the key points of discussion regarding RLLs and their correlation with early loosening of the acetabular components is the location.<sup>127, 132</sup> Many authors have drawn a link between the development of progressive RLLs near the rim of the cement-bone interface and later loosening<sup>129, 133, 134</sup> and Schmalzried detailed a series of events that may explain why this is the case (Chapter 1.6.1.2).<sup>140</sup> Therefore, the experiment aimed to determine whether current surgical techniques adequately pressurised the cement

across the whole acetabulum surface. The experiment also investigated whether the addition of a flange to the acetabular cup would significantly affect the pressures generated. Although there were only minor differences between the pressures generated at the acetabulum surface due to the design of the cup, there was frequently a significant pressure differential between the pole and the rim of the acetabulum for both cups tested (Chapter 5).

Although the cause of this pressure differential was not determined, three possible causes were hypothesised (Chapter 6.2). Firstly, incomplete contact between the cup and the cement meant that initially the pressure was concentrated at the pole of the acetabulum. Increasing the contact area between the acetabular cup and the cement may spread this pressure more evenly and reduce the pressure differential. Secondly, as there is an excess of cement in the acetabulum upon cup insertion, the cement will flow out of the acetabulum as the pressure is lower outside of the acetabulum. This will in turn reduce the pressure generated adjacent to the rim and thus create a pressure differential. If the amount of excess cement in the acetabulum is reduced, there will be a smaller gap between the flange of the acetabular cup and the rim of the acetabulum, this will reduce the cement flow to a minimum and thus reduce the pressure differential. Finally, as polymerisation continues the cement will become more solid, the surface next to the rim of the acetabulum is at a steeper angle from the direction of forcing. As pressure is measured normal to the surface, the component of the load being applied will be smaller near the rim of the acetabulum due to the increased angle.

Considering the hypotheses which resulted from the mock implantation experiment, and the findings from the rheology and deformation experiments, a novel pressuriser was designed to address these issues. The design and motivation for the novel pressuriser have been discussed previously (Chapter 6). The use of the novel pressuriser results in the necessary deformation of the cement being performed earlier in the polymerisation process. It also occasionally resulted in a larger pressure than the Depuy pressuriser, a larger pressure has been linked to more cement penetration into the trabecular bone which has been linked to a stronger interface.<sup>184, 192, 261</sup> However, the novel pressuriser did not reduce the pressure differential and also did not maintain the pressure throughout pressurisation or cup insertion.

The novel pressuriser tested was one of the first iterations of the design and it performed well. It is believed that through alteration of the values of the sealing radius, the excavation radius, and the offset between them, the issues described in the previous chapter (Chapter 7) can be resolved and the novel pressuriser could be an improvement on currently available acetabular pressurisers.

The experiments presented here were logical investigations regarding the cause of immediate RLLs that appear between the PMMA bone cement and the acetabulum bone. Further investigation is required.

### **8.3 Key Results and Limitations**

The key results of the experimental chapters are detailed below.

### **8.3.1 Chapter 2 – Rheological Characterisation of PMMA Bone Cements**

- The rate of PMMA bone cement polymerisation is increased with an increase in temperature as seen in Figure 2.4 and Figure 2.7 and statistical results seen in Table 2.2 and Table 2.5. This is expected as polymerisation is a chemical reaction and an increase in temperature speeds up chemical reactions.
- The parameters of curing PMMA bone cement are significantly affected by the brand of cement as seen in Figure 2.3 and Figure 2.6 and statistical results seen in Table 2.1 and Table 2.4. This is expected as the composition and morphology of PMMA bone cements are tailored to specific applications that may need faster or slower curing times.
- An increase in the rate of deformation reduces the viscosity of curing PMMA bone cement but does not affect the value of  $\tan(\delta)$  at the frequencies tested as seen in Figure 2.5 and Figure 2.8 and statistical results seen in Table 2.3 and Table 2.6. PMMA bone cement is widely known to be a pseudoplastic.
- There is no correlation between the rheological parameters measured and the curing parameters of PMMA bone cement defined in the ISO standards. This was determined by investigating whether there were any significant changes in the viscosity or  $\tan(\delta)$  at the dough time. This finding should be investigated further investigated.
- Excluding the first measurement for Simplex P at 23°C, the elastic component of the complex modulus was larger than the viscous component for all bone cements tested, at all temperatures tested, at all frequencies tested as seen in Figure 2.6, Figure 2.7, and Figure 2.8. This finding is in agreements with some but not all of the literature. More work should be done investigating this behaviour.
- It was assumed that the frequency of deformation used was adequate to investigate the rheological behaviour of PMMA bone cement. After further conversations with experts in the field, it is now believed that faster deformation would have revealed more properties about the cement.
- Halting the polymerisation reaction and measuring the properties of the cement in further detail would have provided the opportunity for investigating the stress relaxation behaviour of PMMA bone cement. With the methodology used it was impossible to investigate this behaviour.

### **8.3.2 Chapter 3 – Does Deformation During the Working Phase Significantly Weaken PMMA Bone Cement?**

- Within the variables tested, irrespective of the mixing technique, and brand of bone cement, deformation during curing results in a statistically significant reduction in the UTS of PMMA bone cement as seen in Figure 3.10. This finding is novel and may be due to the residual stresses generated due to the deformation during curing.
- The UTS of PMMA bone cement is dependent on the brand of cement as seen in Figure 3.10. This is widely known in the literature and is likely due to the different composition of the bone cements.
- Whether the cement was mixed under vacuum or at atmospheric pressure did not significantly affect the UTS as seen in Figure 3.11. This implies that the reduction seen in the UTS due to curing is not related to the mixing pressure.

- Vacuum mixing did not significantly reduce the porosity of the fracture surface although it did reduce the number of pores when compared to the bone cement mixed at atmospheric pressure as seen in Figure 3.10. It is theorised that this is due to the bone cement undergoing a fixed amount of shrinkage through curing. As the external dimensions of the cement were fixed, and there were less pores in the vacuum mixed cement, all the shrinkage occurred at a more concentrated number of sites.
- It was assumed at the time of testing that the porosity at the fracture surface was representative of the whole specimen, but it is now believed that this is not true.
- It was assumed that the UTS of the bone cement was a good characteristic to investigate but measurements of the bending strength and the compression would have provided valuable insights into how deformation affected the mechanical strength of PMMA bone cement.

### ***8.3.3 Chapter 4 – Does Vacuum Mixing Affect Diameter Shrinkage of a PMMA Cement Mantle During In Vitro Cemented Acetabular Cup Implantation?***

- The mean size of the interstice created between the PMMA bone cement and the acetabulum model when a 50 mm acetabular cup is inserted into a 52 mm bore is  $0.39 \text{ mm} \pm 0.1455 \text{ mm}$  when the cement is mixed in non-vacuum conditions and  $0.60 \text{ mm} \pm 0.0921 \text{ mm}$  when the cement is mixed under vacuum as seen in Figure 4.8. It is believed that this is due to the shrinkage occurring at the external dimensions for vacuum mixed cement due to the reduced number of pores in the mantle.
- The magnitude of diametric shrinkage of PMMA bone cement appears to be uniform across the acetabular mantle for both vacuum mixed cement and cement mixed at atmospheric pressure as seen by measuring the external diameter at the rim of the cement mantle and at the pole.
- The measured porosity of cement mantles created using vacuum mixing was smaller than when the cement is mixed at atmospheric pressure. The volume of the vacuum mixed cement and the hypothetical pore-free volume of the cement mixed at atmospheric pressure are equivalent. This implies that the extent of shrinkage of cement is the same irrespective of the mixing pressure and the shrinkage simply occurs in a different location: the external dimension for vacuum mixed cement and the pores for cement mixed at atmospheric pressure.
- It was assumed that measuring the external radius of the implant was sufficient for this investigation; however, this only provides insights into the bone cement – bone interface. Although that was the focus of this thesis, valuable insights could have been made if the internal radius was also measured.
- It was assumed that as the surface where the porosity was measured was controlled that it would be representative of the whole specimen. This may not be true and a more comprehensive measurement techniques would have been valuable for this experiment.

### ***8.3.4 Chapter 5 – Does the Addition of a Flange to the Acetabular Cup Improve the Pressures Generated at the Acetabulum Surface During Mock Cemented Acetabular Cup Implantation?***

- There were no differences in the magnitude of the pressure generated within the mock acetabulum during pressurisation due to the acetabular cup that was to be implanted as seen in Figure 5.9 and Table 5.3. This is expected as up to this point in the experiment the methodology was the same.
- There is no decrease in the pressure during pressurisation of PMMA bone cement in the acetabulum at any angle from the direction of forcing as seen in Table 5.2. This means that the Depuy pressuriser sufficiently seals the cement within the acetabulum.
- There were two instances where the pressures generated at the pole of the mock acetabulum was larger than the pressures generated at the rim of the acetabulum during pressurisation of PMMA bone cement as seen in Table 5.3. It is unknown why this occurs.
- There was only one instance when the unflanged cup generated larger pressures in the acetabulum than the flanged cup: the fourth pentile of cup insertion at 0° for non-vacuum mixed PMMA bone cement as seen in Table 5.4.
- There was no decrease in pressure during cup implantation for either design of acetabular cup and for whether the PMMA bone cement was mixed under vacuum or at atmospheric pressure as seen in Table 5.5.
- The pressure generated in the PMMA bone cement at the pole of the acetabulum was frequently larger than the pressures generated at the rim of the acetabulum during acetabular cup implantation as seen in Table 5.6. There are several potential causes for this discussed in the chapter: the contact area between the cup and the cement is directly over the pole at the start of pressurisation, the flow of cement out of the acetabulum, and the increased angle of the rim from the direction of loading compared to the pole will result in a smaller normal force.
- Due to the existing literature, it was assumed that the magnitude of the pressures generated were proportional to the quality of the bone cement – bone interface created. Data regarding the depth of penetration of bone cement would have been valuable.
- It was also assumed that the material used for the mock acetabulum would not significantly affect the result measured. However, the difference in the thermal conductivity of steel and bone are very different and this may have affected the results.

### ***8.3.5 Chapter 7 – Does use of the Novel Acetabular Pressuriser Significantly Improve the Nature of the Pressures Generated at the Surface of a Mock Acetabulum During Pressurisation and the Acetabular Cup Implantation?***

- There were several instances where the use of the novel design of acetabular pressuriser generated larger pressures in the PMMA bone cement at the acetabulum surface than when the Depuy Smartseal pressuriser was used as seen in Table 7.1.
- There was a drop in the pressure generated at the acetabulum surface during pressurisation when the novel pressuriser was used to pressurise CMW 2 bone cement within the mock acetabulum as seen in Table 7.2. The cause for this is unknown.

- The pressures generated within the PMMA bone cement at the pole of the mock acetabulum were always larger than the pressure generated at the rim of the acetabulum when the acetabular cup was inserted into cement that had been pressurised with the novel pressuriser as seen in Table 7.3. The cause for this is the same as for the same conclusion in chapter 5.
- The assumptions made for this experiment are the same as those for the previous chapter.

#### 8.4 Conclusion

To conclude, the overall aim of this project was to investigate the potential biomechanical causes of immediate RLLs at the cement-bone interface on post-operative radiographs. It was decided at an early stage that the best way to do this was through investigation of the curing and the pressurisation behaviour of PMMA bone cement and through investigation of the operative steps involved during implantation of a cemented acetabular cup. This investigation was successful and a novel contribution to the understanding of the curing and pressurisation behaviour of bone cement during acetabular cup implantation in cemented hip replacements has been made.

There is a lot of further work required that could not be completed due to the large scope of this project. However, many of the key objectives stated at the beginning of this thesis have been achieved.

Through rheological characterisation, the curing parameters of three commonly used PMMA bone cements were measured. The methodology used was only briefly detailed in a conference abstract and thus most of the methodology was developed during this project. The data gathered confirmed several known behaviours of PMMA bone cement. An increase in the rate of deformation reduces the viscosity and an increase in temperature reduces the time to cure. Several key findings were completely novel and have been detailed in the previous section. A concluding thought on this experiment relates to the moment of gelation. There are several rheological theories that attempt to define the moment of gelation that have been discussed previously (Chapter 1.5.4.6). Knowing when the moment of gelation occurs for PMMA bone cement is crucial as this is the moment past which residual stresses cannot fully relax.<sup>79</sup> The moment of gelation was not conclusively found; however, the findings were suggestive that the moment had already passed before measurements commenced. This should be investigated fully as all reviewed mathematical models and computer simulations are incomplete as they do not account for when the moment of gelation occurs.<sup>82, 96, 200, 267</sup> A material scientist should investigate this subject further to fully describe the rheological mechanisms that are occurring within curing PMMA bone cement.

An experiment was devised that would determine whether deformation during the curing phase of the PMMA bone cement would significantly affect the strength of the solidified cement mantle. This experiment was also necessary as there is no mention in all of the accessed literature that mentioned the minimisation of deformation of the curing PMMA bone cement. It was felt that this may be an oversight in regard to the operative technique. It was indeed found that deformation during the waiting phase significantly weakened the solidified bone cement.

A mock acetabulum was designed and manufactured from steel with the ability to fit pressure transducers. However, it was not only the pressures generated in the bone cement during implantation that was to be the subject of investigation but also the shrinkage behaviour of bone cement. This experiment partially resulted from the previously described deformation experiment. It was seen that although the number of pores at the fracture surface of the cement specimens were significantly reduced by vacuum mixing the overall porosity was not. Some of the literature suggests that the overall shrinkage of bone cement is increased by vacuum mixing,<sup>39</sup> but it was felt that this was inaccurate. Vacuum mixing increases the shrinkage of the *external dimensions* of the bone cement due to the elimination of the pores within the cement where the shrinkage that occurs through density changes and thermal contraction would usually occur. The experiment described here investigated the diametric shrinkage and the porosity of mantles created when a flanged acetabular cup was implanted into the mock steel acetabulum using both vacuum mixed and non-vacuum mixed cements. It was found that vacuum mixing significantly reduced the porosity of the cement and increased the shrinkage of the external radius of the cement mantle left after flanged acetabular cup implantation. When the hypothetical volume of the hand mixed cement mantle when the pores were eliminated was calculated, the volume was equivalent to that of the vacuum mixed mantle. This is evidence that the magnitude of volumetric shrinkage is not increased when PMMA bone cement is mixed under vacuum, but that the shrinkage takes place on the external dimensions instead of the internal pores. This experiment was novel in the fact that it attempted to tie the porosity and the measured shrinkage together, it is also the only study that attempted to quantify the magnitude of the shrinkage that occurs within the specific geometry of the acetabulum.

The mock steel acetabulum was also used to investigate the pressures generated at the cement-bone interface during acetabular cup implantation. Several studies in the literature that focus on this topic have been discussed previously but all are inadequate (Chapter 1.6.5) Firstly, many of them did not attempt to replicate all of the implantation process and this means that vital information is lost as important steps are not replicated such as pressurisation or cup insertion. Secondly, the data presented in the studies were often undetailed which makes using the data to make informed judgments about the operative procedure impossible. This may have been due to attempts by the authors to closely replicate the clinical situation which creates severe limits on the quality of the data it is possible to collect. This study specifically focused on comparing differences in the pressures generated in the acetabulum due to whether the acetabular cup to be implanted had a flange or not. It was found that with the testing methodology used, the addition of a flange to the acetabular cup did not provide any improvement in the pressures generated and there was frequently a differential in the pressures generated at the pole of the acetabulum and the rim. The question has been frequently debated, but the results presented within this thesis are the most detailed available. A hypothesis regarding the function of the flange resulting from this experiment may be significant and requires further work: the flange increases the resistance to insertion, slowing its implantation into the cement and therefore, the surgeon must apply a larger load in order for the cup to be correctly positioned.

It was felt that current acetabular pressurisers were underdeveloped, currently only designed to seal cement within the acetabulum cavity and pressurise it through the application of force. With the addition of an extra excavating surface, use of the novel pressuriser would result in an imprint closer to that of the cup to be implanted and therefore reduce the initial pressure

differential, necessary deformation of bone cement would occur earlier in the curing process and therefore a stronger cement mantle would be created and potentially less flow generated pressure differential from the pole to the rim of the acetabulum. Initial experiments showed that the pressures generated within the acetabulum using the novel pressuriser were equivalent to those of the Depuy pressuriser. However, a larger pressure differential from the pole to the rim of the acetabulum and a pressure drop during each stage of the surgical procedure was observed. These issues may be mitigated by altering the dimensions of the pressuriser, more designs should be manufactured and tested as the improvements in the nature of the cement deformation are still likely true.

Finally, it is important to comment on the levels of evidence available for many of the aspects of the surgical procedure for the implantation of a cemented acetabular cup and the curing parameters of PMMA bone cement. The current international standards are inadequate for proper understanding of PMMA bone cement. They are sufficient for the surgeon as they are easy to measure. The variability of the curing PMMA bone cement means that no tests are universal, an experiment that uses a thin slice of curing cement is not comparable to one that uses a large mantle. Proper study and understanding of this material are difficult and it is a mistake to think that no more research is required on it. National registries are an excellent tool for determining which innovations are successful and which are not. Unfortunately, not enough data is gathered regarding the tools used in the operation. It is also a limiting factor that there are no studies regarding which implant is revised with what. Although the proportion of total hip arthroplasties that used bone cement to fix the acetabular component is reducing, there is little evidence to suggest that cement is an inadequate methodology of fixation. A frequently raised is that it is difficult to revise a cemented cup. A study investigating the complication rate at revision surgery of cement implants, and the subsequent longevity of the revised component, when compared to uncemented components, would be useful for determining whether fixation of implants using cement is inferior to uncemented fixation.

The experiments presented here are broad in scope and therefore many routes of further investigation have become apparent. These routes will be explored, and the novel pressuriser will be tested to further define its efficacy and hopefully, to realise the potential improvements to the longevity of cemented acetabular components; therefore, improving the quality of life for many patients.

## 8.5 Further Work

- More rheological tests should be performed, with larger rates of deformation, with temperature curves that simulate the curing temperatures seen *in vivo*, with more cements. This would allow further investigation into the moment of gelation of bone cements and the correlation between rheological parameters and ISO defined curing timings. It could also be used to acquire more detail regarding the curing parameters and help to build an accurate mathematical model of curing PMMA bone cement.
- Further investigations should be performed to determine whether the vibration of PMMA bone cement could be used to increase cement penetration into the cancellous bone, taking advantage of the shear thinning properties of bone cement. Some research

has already been performed on this, but it is insufficient, especially regarding the application of this technology in cemented acetabular cup implantation.

- The effect of the cup size on the interstice created between the acetabulum and the cement mantle should be investigated and the nature and location of bone cement shrinkage could be more closely measured after cemented acetabular cup implantation.
- The residual stress in deformed and non-deformed PMMA bone cement should be measured. Further tests should be done to determine whether other mechanical measures of strength are affected by deformation during curing including fatigue and toughness. Experiments should be designed that aim to determine whether deformation later in the curing process affects the strength of bone cement more than deformation applied earlier.
- For all the mock acetabulum experiments more repeats should be performed, with a higher degree of control on the temperature and humidity. More cements should also be tested.
- A more clinically accurate acetabulum model should be manufactured and used for testing. An individual trained in implanting cemented acetabular components should perform the experiments and apply the force to the pressuriser and acetabulum as they would in an *in vivo* setting.
- The effect of the design of the external surface of the acetabular cup on the pressures generated during cemented acetabular cup insertion should be investigated.
- The effect of the addition of a flange to the cemented acetabular cup on the load required to achieve correct positioning within the PMMA bone cement should be investigated.
- The sensitivity of the pressuriser transducers and the acute attention to the pressures achieved in these experiments should be employed in other scenarios such as total knee replacement and vertebroplasty. This could be performed in conjunction with the development of mathematical models that predict the pressures achieved at the bone surface.
- Further investigation into the efficacy of the novel pressuriser should be performed. This should include more repeats with a larger range of design parameters with a more clinically accurate acetabular model. The use of the pressuriser by a surgeon would provide valuable feedback that could be used to improve the pressuriser. Eventually, it is hoped that the pressuriser will be used in a clinical setting; therefore, cadaveric experiments should be performed.
- There is a lot of potential for examination of data collected in the NJR. Firstly, it would be interesting to compare the longevity of the revised components of cemented primary and uncemented primary implants. It would also be positive to campaign for a more detailed registry which would include which cement was used, which surgical instruments are used, and the operative technique employed.

## Chapter 9. References

1. Charnley J. Arthroplasty of the hip: a new operation. *Clinical Orthopaedics and Related Research®* 1961; 95: 4-8.
2. NJR. *National Joint Registry 17th Annual Report 2020*. 2020.
3. Callaghan JJ, Albright JC, Goetz DD, et al. Charnley total hip arthroplasty with cement: minimum twenty-five-year follow-up. *Jbjs* 2000; 82: 487.
4. Gergely RC, Toohey KS, Jones ME, et al. Towards the optimization of the preparation procedures of PMMA bone cement. *Journal of Orthopaedic Research* 2016; 34: 915-923.
5. Whitehouse MR, Atwal NS, Pabbruwe M, et al. Osteonecrosis with the use of polymethylmethacrylate cement for hip replacement: thermal-induced damage evidenced in vivo by decreased osteocyte viability. *European Cells and Materials* 2014; 27: 50-63. DOI: 10.22203/eCM.v027a05.
6. Ormsby R, McNally T, Mitchell C, et al. Effect of MWCNT addition on the thermal and rheological properties of polymethyl methacrylate bone cement. *Carbon* 2011; 49: 2893-2904.
7. Bishop N, Ferguson S and Tepic S. Porosity reduction in bone cement at the cement-stem interface. *The Journal of Bone and Joint Surgery British Volume* 1996; 78: 349-356.
8. Revie I, Wallace M and Orr J. The effect of PMMA thickness on thermal bone necrosis around acetabular sockets. *Proceedings of the Institution of Mechanical Engineers, Part H: Journal of Engineering in Medicine* 1994; 208: 45-51.
9. Haas S, Brauer G and Dickson G. A characterization of polymethylmethacrylate bone cement. *The Journal of Bone and Joint Surgery American Volume* 1975; 57: 380-391.
10. Park JB. Acrylic bone cement: In vitro and in vivo property-structure relationship—A selective review. *Annals of Biomedical Engineering* 1983; 11: 297-312.
11. Lewis G. Properties of acrylic bone cement: state of the art review. *Journal of Biomedical Materials Research* 1997; 38: 155-182.
12. Dunne N and Orr J. Thermal characteristics of curing acrylic bone cement. *ITBM-RBM* 2001; 22: 88-97.
13. Stańczyk M and Van Rietbergen B. Thermal analysis of bone cement polymerisation at the cement–bone interface. *Journal of Biomechanics* 2004; 37: 1803-1810.
14. Yetkinler DN and Litsky AS. Viscoelastic behaviour of acrylic bone cements. *Biomaterials* 1998; 19: 1551-1559.
15. Ranawat CS, Peters LE and Umlas ME. Fixation of the acetabular component. The case for cement. *Clinical Orthopaedics and Related Research* 1997: 207-215.
16. Majkowski R, Bannister G and Miles AW. The effect of bleeding on the cement-bone interface. An experimental study. *Clinical Orthopaedics and Related Research* 1994: 293-297.
17. Benjamin J, Gie G, Lee A, et al. Cementing technique and the effects of bleeding. *The Journal of Bone and Joint Surgery British Volume* 1987; 69: 620-624.
18. Parsch D, New A and Breusch S. *The Well-Cemented Total Hip Arthroplasty Theory and Practice*. 1 ed.: Springer-Verlag Berlin Heidelberg, 2005, p.377.
19. Thomas A, McMinn D, Haddaway M, et al. The effect of polymethylmethacrylate bone cement vibration on the bone-cement interface. *Cells and Materials* 1992; 2: 7.
20. Ahmed A, Pak W, Burke D, et al. Transient and residual stresses and displacements in self-curing bone cement—Part I: Characterization of relevant volumetric behavior of bone cement. *Journal of Biomechanical Engineering* 1982; 104: 21-27.
21. Roques A, Browne M, Taylor A, et al. Quantitative measurement of the stresses induced during polymerisation of bone cement. *Biomaterials* 2004; 25: 4415-4424.

22. Bengochea K. Hip and Thigh Anatomy, <https://www.kenhub.com/en/library/anatomy/hip-and-thigh-anatomy> (2020, accessed 02/02/2021 2021).

23. Paul J. Paper 8: forces transmitted by joints in the human body. In: *Proceedings of the Institution of Mechanical Engineers, Conference Proceedings* 1966, pp.8-15. SAGE Publications Sage UK: London, England.

24. Abdulghani S, Wang JS, McCarthy I, et al. The influence of initial pressurization and cup introduction time on the depth of cement penetration in an acetabular model. *Acta Orthopaedica* 2007; 78: 333-339. 2007/07/06. DOI: 10.1080/17453670710013889.

25. Bergmann G, Deuretzbacher G, Heller M, et al. Hip contact forces and gait patterns from routine activities. *Journal of Biomechanics* 2001; 34: 859-871.

26. Learmonth ID, Young C and Rorabeck C. The operation of the century: total hip replacement. *The Lancet* 2007; 370: 1508-1519.

27. Convery FR. Hip arthroplasty. Edited By HC Amstutz. New York: Churchill Livingstone, 1991. 1,001 pp, \$195. Wiley Online Library, 1992.

28. Smith-Petersen M. Evolution of Mould Arthroplasty of the Hip Joint. *Clinical Orthopaedics and Related Research (1976-2007)* 1948; 453: 17-21.

29. Eynon-Lewis N, Ferry D and Pearse M. Themistocles Gluck: an unrecognised genius. *BMJ: British Medical Journal* 1992; 305: 1534.

30. Brand RA, Mont MA and Manring M. Biographical Sketch: Themistocles Gluck (1853-1942). *Clinical Orthopaedics and Related Research®* 2011; 469: 1525-1527.

31. Wiles P. The surgery of the osteo-arthritic hip. *British Journal of Surgery* 1958; 45: 488-497.

32. Knight SR, Aujla R and Biswas SP. Total Hip Arthroplasty-over 100 years of operative history. *Orthopedic Reviews* 2011; 3.

33. Charnley J. The Bonding of Prostheses to Bone by Cement. *Clinical Orthopaedics and Related Research®* 1964; 468: 3149-3159.

34. Pramanik S, Agarwal AK and Rai K. Chronology of total hip joint replacement and materials development. *Trends in Biomaterials & Artificial Organs* 2005; 19: 15-26.

35. Kurtz SM, Gawel HA and Patel JD. History and systematic review of wear and osteolysis outcomes for first-generation highly crosslinked polyethylene. *Clinical Orthopaedics and Related Research®* 2011; 469: 2262-2277.

36. Kühn K-D. *Bone Cements*

*Up-to-Date Comparison of Physical and Chemical Properties of Commercial Materials.* 2000.

37. Smith DC. The genesis and evolution of acrylic bone cement. *The Orthopedic Clinics of North America* 2005; 36: 1-10.

38. Charnley J. Anchorage of the femoral head prosthesis to the shaft of the femur. *The Journal of bone and joint surgery British volume* 1960; 42: 28-30.

39. Kühn K-D. *PMMA Cements.* 1 ed. Berlin: Springer-Verlag Berlin Heidelberg, 2013, p.291.

40. Abdulkarim A, Ellanti P, Motterlini N, et al. Cemented versus uncemented fixation in total hip replacement: a systematic review and meta-analysis of randomized controlled trials. *Orthopedic Reviews* 2013; 5.

41. Yamada H, Yoshihara Y, Henmi O, et al. Cementless total hip replacement: past, present, and future. *Journal of Orthopaedic Science* 2009; 14: 228-241.

42. Grigoris P, Roberts P, Panousis K, et al. The evolution of hip resurfacing arthroplasty. *Orthopedic Clinics* 2005; 36: 125-134.

43. Stryker. Exeter V40 Stem Cement in Cement Surgical Technique. 2014.

44. Stryker. Exeter Contemporary Flanged Cup Operative Technique. 2007.

45. Stryker. Exeter X3 RimFit Acetabular Cup Surgical Technique. 2015.

46. Stryker. Options Matter Contemporary Hooded Cup. 2006.

47. Breusch S and Malchau H. *The well-cemented total hip arthroplasty.* Springer, 2005.

48. Zimmer. CPT 12/14 Hip System Primary Hip Arthroplasty Surgical Technique. 2015.

49. Zimmer. ZCA All-Poly Acetabular Cup. 2001.

50. Vaishya R, Chauhan M and Vaish A. Bone cement. *Journal of Clinical Crthopaedics and Trauma* 2013; 4: 157-163.

51. Ayre WN, Denyer SP and Evans SL. Ageing and moisture uptake in polymethyl methacrylate (PMMA) bone cements. *Journal of the Mechanical Behavior of Biomedical Materials* 2014; 32: 76-88.

52. Chang Y, Tai C, Hsu H, et al. Liquid antibiotics in bone cement: an effective way to improve the efficiency of antibiotic release in antibiotic loaded bone cement. *Bone & Joint Research* 2014; 3: 246-251.

53. Davey JR and Gandhi R. What Is the Role of Antibiotic Cement in Total Joint Replacement? *Evidence-Based Orthopaedics*. Elsevier, 2009, pp.556-560.

54. Wooley P and Schwarz E. Aseptic loosening. *Gene Therapy* 2004; 11: 402-407.

55. Standardization IOf. *ISO 5833:2002 Implants for surgery — Acrylic resin cements*. Acrylic resin cements2002, p. 22.

56. Eriksson A and Albrektsson T. Temperature threshold levels for heat-induced bone tissue injury: a vital-microscopic study in the rabbit. *Journal of Prosthetic Dentistry* 1983; 50: 101-107.

57. Lundskog J. Heat and bone tissue. An experimental investigation of the thermal properties of bone and threshold levels for thermal injury. *Scand J Plast Reconstr Surg* 1972; 9: 72-74.

58. DiPisa JA, Sih GS and Berman AT. The temperature problem at the bone-acrylic cement interface of the total hip replacement. *Clinical Orthopaedics and Related Research* 1976: 95-98.

59. Bayne S, Lautenschlager E, Compere C, et al. Degree of polymerization of acrylic bone cement. *Journal of Biomedical Materials Research* 1975; 9: 27-34.

60. Brauer G, Steinberger D and Stansbury J. Dependence of curing time, peak temperature, and mechanical properties on the composition of bone cement. *Journal of Biomedical Materials Research* 1986; 20: 839-852.

61. Berman AT, Reid JS, Yanicko Jr DR, et al. Thermally induced bone necrosis in rabbits. Relation to implant failure in humans. *Clinical Orthopaedics and Related Research* 1984: 284-292.

62. Li C, Mason J and Yakimicki D. Thermal characterization of PMMA-based bone cement curing. *Journal of Materials Science: Materials in Medicine* 2004; 15: 85-89.

63. Jefferiss C, Lee A and Ling R. Thermal aspects of self-curing polymethylmethacrylate. *The Journal of Bone and Joint Surgery British Volume* 1975; 57: 511-518.

64. Meyer Jr P, Lautenschlager E and Moore B. On the setting properties of acrylic bone cement. *Journal of Bone and Joint Surgery* 1973; 55: 149-156.

65. Huiskes R. Thermal injury of cancellous bone, following pressurized penetration of acrylic cement. *Trans Orthop Res Soc* 1981; 6: 134.

66. Sih G, Connelly G and Berman A. The effect of thickness and pressure on the curing of PMMA bone cement for the total hip joint replacement. *Journal of Biomechanics* 1980; 13: 347-352.

67. Freire E. Differential Scanning Calorimetry. In: Shirley BA (ed) *Protein Stability and Folding: Theory and Practice*. Totowa, NJ: Humana Press, 1995, pp.191-218.

68. Charnley J. Acrylic cement in orthopaedic surgery. *Acrylic cement in orthopaedic surgery*. 1970, pp.vi, 131-vi, 131.

69. Stürup J, Nimb L, Kramhøft M, et al. Effects of polymerization heat and monomers from acrylic cement on canine bone. *Acta Orthopaedica Scandinavica* 1994; 65: 20-23.

70. Scheuermann H. Bestimmung des monomergehaltes von knochenzenmenten und bestimmung der monomerfreisetzung an wässrigen. Ingenierarbeit Fachhochschule Fresenius, Wiesbaden, Germany, 1976.

71. Rudigier J, Scheuermann H, Kotterbach B, et al. Restmonomerabnahme und-freisetzung aus Knochenzementen. *Unfallchirurgie* 1981; 7: 132-137.

72. Mathiesen D, Vogtmann D and Dupaix RB. Characterization and constitutive modeling of stress-relaxation behavior of poly (methyl methacrylate)(PMMA) across the glass transition temperature. *Mechanics of Materials* 2014; 71: 74-84.

73. Eden O, Lee A and Hooper R. Stress relaxation modelling of polymethylmethacrylate bone cement. *Proceedings of the Institution of Mechanical Engineers, Part H: Journal of Engineering in Medicine* 2002; 216: 195-199.

74. Lee A, Ling R, Gheduzzi S, et al. Factors affecting the mechanical and viscoelastic properties of acrylic bone cement. *Journal of Materials Science: Materials in Medicine* 2002; 13: 723-733.

75. Lee C. The mechanical properties of PMMA bone cement. *The Well-Cemented Total Hip Arthroplasty*. Springer, 2005, pp.60-66.

76. Wang L and Li C. A Brief Review of Pulp and Froth Rheology in Mineral Flotation. *Journal of Chemistry* 2020; 2020.

77. Farrar D and Rose J. Rheological properties of PMMA bone cements during curing. *Biomaterials* 2001; 22: 3005-3013.

78. Newton I. *Principia mathematica*. London, England: Mothe-Cajori 1934.

79. Winter HH and Mours M. Rheology of polymers near liquid-solid transitions. *Neutron Spin Echo Spectroscopy Viscoelasticity Rheology*. Springer, 1997, pp.165-234.

80. Pascual B, Vázquez B, Gurrachaga M, et al. New aspects of the effect of size and size distribution on the setting parameters and mechanical properties of acrylic bone cements. *Biomaterials* 1996; 17: 509-516.

81. Ferracane J and Greener E. Rheology of acrylic bone cements. *Biomaterials, Medical Devices, and Artificial Organs* 1981; 9: 213-224.

82. Kolmeder S and Lion A. Characterisation and modelling rheological properties of acrylic bone cement during application. *Mechanics Research Communications* 2013; 48: 93-99.

83. Soyka RPW, López A, Persson C, et al. Numerical description and experimental validation of a rheology model for non-Newtonian fluid flow in cancellous bone. *Journal of the Mechanical Behavior of Biomedical Materials* 2013; 27: 43-53.

84. Dunne N and Orr J. Flow characteristics of curing polymethyl methacrylate bone cement. *Proceedings of the Institution of Mechanical Engineers, Part H: Journal of Engineering in Medicine* 1998; 212: 199-207.

85. Castellani L and Lomellini P. Phase volume and size effects on the terminal relaxation of ABS melts. *Rheologica Acta* 1994; 33: 446-453.

86. Masuda T, Nakajima A, Kitamura M, et al. Viscoelastic properties of rubber-modified polymeric materials at elevated temperatures. *Pure and Applied Chemistry* 1984; 56: 1457-1475.

87. Mours M and Winter H. Mechanical spectroscopy of polymers. *Experimental Methods in Polymer Science*. Elsevier, 2000, pp.495-546.

88. Winter H. Can the gel point of a cross-linking polymer be detected by the G'-G "crossover? *Polymer Engineering & Science* 1987; 27: 1698-1702.

89. Spiegelberg S. Characterization of the curing process of bone cement with multi-harmonic shear rheometry. In: *ANNUAL MEETING-SOCIETY FOR BIOMATERIALS IN CONJUNCTION WITH THE INTERNATIONAL BIOMATERIALS SYMPOSIUM* 1998, pp.283-283. SOCIETY FOR BIOMATERIALS.

90. Withers P. Residual stress and its role in failure. *Reports on Progress in Physics* 2007; 70: 2211.

91. Lewis G. Fatigue testing and performance of acrylic bone-cement materials: state-of-the-art review. *Journal of Biomedical Materials Research: An Official Journal of The Society*

for Biomaterials, The Japanese Society for Biomaterials, and The Australian Society for Biomaterials and the Korean Society for Biomaterials 2003; 66: 457-486.

92. Lennon A and Prendergast P. Residual stress due to curing can initiate damage in porous bone cement: experimental and theoretical evidence. *Journal of Biomechanics* 2002; 35: 311-321.
93. Jasty M, Malone W, Bragdon C, et al. The initiation of failure in cemented femoral components of hip arthroplasties. *The Journal of Bone and Joint Surgery British Volume* 1991; 73: 551-558.
94. Orr J, Dunne N and Quinn J. Shrinkage stresses in bone cement. *Biomaterials* 2003; 24: 2933-2940.
95. Hingston J, Dunne N, Looney L, et al. Effect of curing characteristics on residual stress generation in polymethyl methacrylate bone cements. *Proceedings of the Institution of Mechanical Engineers, Part H: Journal of Engineering in Medicine* 2008; 222: 933-945.
96. Briscoe A and New A. Polymerisation stress modelling in acrylic bone cement. *Journal of Biomechanics* 2010; 43: 978-983.
97. Baaijens FP and Douven LF. Calculation of flow-induced residual stresses in injection moulded products. *Applied Scientific Research* 1994; 48: 141-157.
98. O'Connor TC, Alvarez NJ and Robbins MO. Relating chain conformations to extensional stress in entangled polymer melts. *Physical Review Letters* 2018; 121: 047801.
99. Guevara-Morales A and Figueroa-López U. Residual stresses in injection molded products. *Journal of Materials Science* 2014; 49: 4399-4415.
100. Bergmann G, Graichen F, Rohlmann A, et al. Realistic loads for testing hip implants. *Bio-medical Materials and Engineering* 2010; 20: 65-75.
101. Saha S and Pal S. Mechanical properties of bone cement: a review. *Journal of Biomedical Materials Research* 1984; 18: 435-462.
102. Lee A, Ling R and Vangala S. Some clinically relevant variables affecting the mechanical behaviour of bone cement. *Archives of Orthopaedic and Traumatic Surgery* 1978; 92: 1-18.
103. Weber SC and Bargar WL. A comparison of the mechanical properties of Simplex, Zimmer, and Zimmer low viscosity bone cements. *Biomaterials, Medical Devices, and Artificial Organs* 1983; 11: 3-12.
104. Standardization IOf. *ISO 527-1:2019. Plastics — Determination of tensile properties*. 2002, p. 22.
105. Dunne N, Buchanan F, Hill J, et al. In vitro testing of chitosan in gentamicin-loaded bone cement No antimicrobial effect and reduced mechanical performance. *Acta Orthopaedica* 2008; 79: 851-860.
106. Spierings PT. Testing and performance of bone cements. *The Well-Cemented Total Hip Arthroplasty*. Springer, 2005, pp.67-78.
107. Soltész U, Schäfer R, Jaeger R, et al. Fatigue Testing of Bone Cements—Comparison of Testing Arrangements. *Journal of ASTM International* 2005; 2: 1-11.
108. ASTM D2990-17.
109. Thomas P, Schuh A, Summer B, et al. Allergy towards bone cement. *Der Orthopade* 2006; 35: 956, 958-960.
110. Thomas P, Schuh A, Eben R, et al. Allergy to bone cement components. *Der Orthopade* 2008; 37: 117-120.
111. Fregert S. Occupational hazards of acrylate bone cement in orthopaedic surgery. Taylor & Francis, 1983.
112. Carlsson A and Möller H. Implantation of orthopaedic devices in patients with metal allergy. *Acta Dermato-Venereologica* 1989; 69: 62-66.
113. Goodman S. Does the immune system play a role in loosening and osteolysis of total joint replacements? *Journal of Long-term Effects of Medical Implants* 1996; 6: 91-101.

114. Haddad F, Cobb A, Bentley G, et al. Hypersensitivity in aseptic loosening of total hip replacements: the role of constituents of bone cement. *The Journal of Bone and Joint Surgery British Volume* 1996; 78: 546-549.

115. Arora M, Chan EK, Gupta S, et al. Polymethylmethacrylate bone cements and additives: A review of the literature. *World Journal of Orthopedics* 2013; 4: 67.

116. Ormsby R, McNally T, Mitchell C, et al. Influence of multiwall carbon nanotube functionality and loading on mechanical properties of PMMA/MWCNT bone cements. *Journal of Materials Science: Materials in Medicine* 2010; 21: 2287-2292.

117. Ormsby R, McNally T, O'Hare P, et al. Fatigue and biocompatibility properties of a poly (methyl methacrylate) bone cement with multi-walled carbon nanotubes. *Acta Biomaterialia* 2012; 8: 1201-1212.

118. Wang C, Yu B, Fan Y, et al. Incorporation of multi-walled carbon nanotubes to PMMA bone cement improves cytocompatibility and osseointegration. *Materials Science and Engineering: C* 2019; 103: 109823.

119. Tunney M, Brady A, Buchanan F, et al. Incorporation of chitosan in acrylic bone cement: effect on antibiotic release, bacterial biofilm formation and mechanical properties. *Journal of Materials Science: Materials in Medicine* 2008; 19: 1609-1615.

120. Khandaker M, Vaughan MB, Morris TL, et al. Effect of additive particles on mechanical, thermal, and cell functioning properties of poly (methyl methacrylate) cement. *International Journal of Nanomedicine* 2014; 9: 2699.

121. Endogan T, Kiziltay A, Kose GT, et al. Acrylic bone cements: Effects of the poly (methyl methacrylate) powder size and chitosan addition on their properties. *Journal of Applied Polymer Science* 2014; 131.

122. Méndez J, Aguilar MR, Abraham GA, et al. New acrylic bone cements conjugated to vitamin E: curing parameters, properties, and biocompatibility. *Journal of Biomedical Materials Research: An Official Journal of The Society for Biomaterials, The Japanese Society for Biomaterials, and The Australian Society for Biomaterials and the Korean Society for Biomaterials* 2002; 62: 299-307.

123. Morones J, Elechiguerra J, Camacho A, et al. Kouri, JT Ramirez and MJ Yacaman 2005. *Nanotechnology*; 16: 2346-2353.

124. Oei JD, Zhao WW, Chu L, et al. Antimicrobial acrylic materials with in situ generated silver nanoparticles. *Journal of Biomedical Materials Research Part B: Applied Biomaterials* 2012; 100: 409-415.

125. Alt V, Bechert T, Steinrücke P, et al. An in vitro assessment of the antibacterial properties and cytotoxicity of nanoparticulate silver bone cement. *Biomaterials* 2004; 25: 4383-4391.

126. Barrack RL, Mulroy R and Harris WH. Improved cementing techniques and femoral component loosening in young patients with hip arthroplasty. A 12-year radiographic review. *Bone & Joint Journal* 1992; 74: 385-389.

127. Delee JG and Charnley J. Radiological demarcation of cemented sockets in total hip replacement. *Clinical Orthopaedics and Related Research* 1976; 121: 20-32.

128. Mulroy R and Harris W. The effect of improved cementing techniques on component loosening in total hip replacement. An 11-year radiographic review. *Journal of Bone and Joint Surgery* 1990; 72: 757-760.

129. Kneif D, Downing MR, Ashcroft GP, et al. The correlation between immediate radiolucent lines and early implant migration in cemented acetabular components. *The Journal of Arthroplasty* 2006; 21: 215-220.

130. Hodgkinson JP, Maskell AP, Paul A, et al. Flanged acetabular components in cemented Charnley hip arthroplasty. Ten-year follow-up of 350 patients. *Bone & Joint Journal* 1993; 75: 464-467.

131. Garcia-Cimbrelo E, Diez-Vazquez V, Madero R, et al. Progression of radiolucent lines adjacent to the acetabular component and factors influencing migration after Charnley low-friction total hip arthroplasty. *JBJS* 1997; 79: 1373-1380.

132. Ritter M, Zhou H, Keating C, et al. Radiological factors influencing femoral and acetabular failure in cemented Charnley total hip arthroplasties. *Journal of Bone and Joint Surgery* 1999; 81: 982-986.

133. Iwaki H, Scott G and Freeman M. The natural history and significance of radiolucent lines at a cemented femoral interface. *Bone & Joint Journal* 2002; 84: 550-555.

134. Strömberg CN, Herberts P, Palmertz B, et al. Radiographic risk signs for loosening after cemented THA: 61 loose stems and 23 loose sockets compared with 42 controls. *Acta Orthopaedica Scandinavica* 2009; 67: 43-48. DOI: 10.3109/17453679608995607.

135. Lieberman JR, Leger RR, Tao JC, et al. Total hip arthroplasty surveillance: when do we see our patients postoperatively? *The Journal of Arthroplasty* 2011; 26: 1161-1164.

136. Reading A, McCaskie A and Gregg P. The inadequacy of standard radiographs in detecting flaws in the cement mantle. *Journal of Bone and Joint Surgery* 1999; 81: 167-170.

137. Claus AM, Engh CA, Sychterz CJ, et al. Radiographic definition of pelvic osteolysis following total hip arthroplasty. *Journal of Bone and Joint Surgery* 2003; 85: 1519-1526.

138. Goldring SR, Jasty M, Roelke MS, et al. Formation of a synovial-like membrane at the bone-cement interface: Its role in bone resorption and implant loosening after total hip replacement. *Arthritis & Rheumatism* 1986; 29: 836-842. DOI: 10.1002/art.1780290704.

139. Han C-D, Choe W-S and Yoo J-H. Effect of polyethylene wear on osteolysis in cementless primary total hip arthroplasty: minimal 5-year follow-up study. *The Journal of Arthroplasty* 1999; 14: 714-723.

140. Schmalzried TP, Kwong LM, Jasty M, et al. The Mechanism of Loosening of Cemented Acetabular Components in Total Hip Arthroplasty: Analysis of Specimens Retrieved at Autopsy. *Clinical Orthopaedics and Related Research* 1992; 274: 60-78.

141. Liu A, Richards L, Bladen CL, et al. The biological response to nanometre-sized polymer particles. *Acta Biomaterialia* 2015; 23: 38-51.

142. Jiang Y, Jia T, Wooley PH, et al. Current research in the pathogenesis of aseptic implant loosening associated with particulate wear debris. *Acta Orthop Belg* 2013; 79: 1-9.

143. Steffen J, Breusch HM, John Older. Operative steps - Acetabulum. 2005.

144. Mulroy WF, Estok DM and Harris WH. Total hip arthroplasty with use of so-called second-generation cementing techniques: a fifteen-year-average follow-up study. *Journal of Bone and Joint Surgery* 1995; 77: 1845-1852.

145. Klapach AS, Callaghan JJ, Goetz DD, et al. Charnley total hip arthroplasty with use of improved cementing techniques: a minimum twenty-year follow-up study. *Journal of Bone and Joint Surgery* 2001; 83: 1840-1848.

146. Rodop O, Kiral A, Arpacioglu O, et al. Effects of stem design and pre-cooling prostheses on the heat generated by bone cement in an in vitro model. *Journal of International Medical Research* 2002; 30: 265-270.

147. Wykman AG. Acetabular cement temperature in arthroplasty: effect of water cooling in 19 cases. *Acta Orthopaedica Scandinavica* 1992; 63: 543-544.

148. Breusch S, Malchau H and Older J. *The well-cemented total hip arthroplasty*. Springer, 2005.

149. Koh BT, Tan J, Ramruttun AK, et al. Effect of storage temperature and equilibration time on polymethyl methacrylate (PMMA) bone cement polymerization in joint replacement surgery. *Journal of Orthopaedic Surgery and Research* 2015; 10: 1-6.

150. Pelletier MH, Lau AC, Smitham PJ, et al. Pore distribution and material properties of bone cement cured at different temperatures. *Acta Biomaterialia* 2010; 6: 886-891.

151. Iesaka K, Jaffe WL and Kummer FJ. Effects of preheating of hip prostheses on the stem-cement interface. *Journal of Bone and Joint Surgery* 2003; 85: 421-427.

152. Li C, Schmid S and Mason J. Effects of pre-cooling and pre-heating procedures on cement polymerization and thermal osteonecrosis in cemented hip replacements. *Medical Engineering & Physics* 2003; 25: 559-564.

153. Aggarwal VK, Elbuluk A, Dundon J, et al. Surgical approach significantly affects the complication rates associated with total hip arthroplasty. *The Bone & Joint Journal* 2019; 101: 646-651.

154. Graves SC, Dropkin BM, Keeney BJ, et al. Does surgical approach affect patient-reported function after primary THA? *Clinical Orthopaedics and Related Research®* 2016; 474: 971-981.

155. Madsen MS, Ritter MA, Morris HH, et al. The effect of total hip arthroplasty surgical approach on gait. *Journal of Orthopaedic Research* 2004; 22: 44-50.

156. Cornell CN and Ranawat CS. The impact of modern cement techniques on acetabular fixation in cemented total hip replacement. *The Journal of Arthroplasty* 1986; 1: 197-202.

157. Vasu R, Carter D and Harris W. Stress distributions in the acetabular region—I. Before and after total joint replacement. *Journal of Biomechanics* 1982; 15: 155-164.

158. Mjöberg B. The theory of early loosening of hip prostheses. *Orthopedics* 1997; 20: 1169-1175.

159. Flivik G, Kristiansson I, Kesteris U, et al. Is Removal of Subchondral Bone Plate Advantageous in Cemented Cup Fixation?: A Randomized RSA Study. *Clinical Orthopaedics and Related Research* 2006; 448: 164-172.

160. Conroy JL, Chawda M, Kaushal R, et al. Does use of a “rim cutter” improve quality of cementation of the acetabular component of cemented exeter total hip arthroplasty? *The Journal of Arthroplasty* 2009; 24: 71-76.

161. Darmanis SN, Hubble MJ, Howell JR, et al. Benefits of using modern cementing techniques in the acetabulum: the Rim Cutter. *Journal of Orthopaedic Surgery* 2012; 20: 316-321.

162. Smith B, Lee A, Timperley AJ, et al. The effect of the Rim Cutter™ on cement pressurization and penetration on cemented acetabular fixation in total hip arthroplasty: An in vitro study. *Proceedings of the Institution of Mechanical Engineers, Part H: Journal of Engineering in Medicine* 2010; 224: 1133-1140.

163. Baker P, Rankin K, Naisby S, et al. Progressive radiolucent lines following the implantation of the cemented Rimfit acetabular component in total hip arthroplasty using the rincutter technique: cause for concern? *The Bone & Joint Journal* 2016; 98-B: 313-319. DOI: 10.1302/0301-620x.98b3.36613.

164. Dorr LD, Lindberg JP, Claude-Faugere M, et al. Factors influencing the intrusion of methylmethacrylate into human tibiae. *Clinical Orthopaedics and Related Research* 1984; 147-152.

165. Halawa M, Lee A, Ling R, et al. The shear strength of trabecular bone from the femur, and some factors affecting the shear strength of the cement-bone interface. *Archives of Orthopaedic and Traumatic Surgery* 1978; 92: 19-30.

166. Krause WR, Krug W and Miller J. Strength of the cement-bone interface. *Clinical Orthopaedics and Related Research* 1982; 290-299.

167. Majkowski R, Miles AW, Bannister G, et al. Bone surface preparation in cemented joint replacement. *The Journal of Bone and Joint Surgery British Volume* 1993; 75: 459-463.

168. Malchau H. Prognosis of total hip replacement: update and validation of results from the Swedish National Hip Arthroplasty Registry 1979-1998. In: *67th Annual Meeting AAOS, 2000* 2000.

169. Juliusson R, Flivik G, Nilsson J, et al. Circulating blood diminishes cement penetration into cancellous bone: In vivo studies of 21 arthrotic femoral heads. *Acta Orthopaedica Scandinavica* 1995; 66: 234-238.

170. Parsch D, New A, Breusch S, et al. *The Well-Cemented Total Hip Arthroplasty*. Springer, 2005.

171. Lewis G. Relative roles of cement molecular weight and mixing method on the fatigue performance of acrylic bone cement: Simplex® P versus Osteopal®. *Journal of Biomedical Materials Research: An Official Journal of The Society for Biomaterials, The Japanese Society for Biomaterials, and The Australian Society for Biomaterials and the Korean Society for Biomaterials* 2000; 53: 119-130.

172. Lidgren L, Bodelind B and Möller J. Bone cement improved by vacuum mixing and chilling. *Acta Orthopaedica Scandinavica* 1987; 58: 27-32.

173. Wang J-S, Franzén H, Jonsson E, et al. Porosity of bone cement reduced by mixing and collecting under vacuum. *Acta Orthopaedica Scandinavica* 1993; 64: 143-146.

174. Wixson RL, Lautenschlager EP and Novak MA. Vacuum mixing of acrylic bone cement. *The Journal of Arthroplasty* 1987; 2: 141-149.

175. Mau H, Schelling K, Heisel C, et al. Comparison of various vacuum mixing systems and bone cements as regards reliability, porosity and bending strength. *Acta Orthopaedica Scandinavica* 2004; 75: 160-172.

176. Coultrup OJ, Hunt C, Wroblewski BM, et al. Computational assessment of the effect of polyethylene wear rate, mantle thickness, and porosity on the mechanical failure of the acetabular cement mantle. *Journal of Orthopaedic Research* 2010; 28: 565-570.

177. Hansen D and Jensen JS. Mixing does not improve mechanical properties of all bone cements: manual and centrifugation-vacuum mixing compared for 10 cement brands. *Acta Orthopaedica Scandinavica* 1992; 63: 13-18.

178. Macaulay W, DiGiovanni CW, Restrepo A, et al. Differences in bone-cement porosity by vacuum mixing, centrifugation, and hand mixing. *The Journal of Arthroplasty* 2002; 17: 569-575.

179. Geiger MH, Keating EM, Ritter MA, et al. The clinical significance of vacuum mixing bone cement. *Clinical Orthopaedics and Related Research (1976-2007)* 2001; 382: 258-266.

180. Wang J-S. The Benefit of Vacuum Mixing. *The Well-Cemented Total Hip Arthroplasty*. Springer, 2005, pp.107-112.

181. Davies J, Jasty M, O'Connor D, et al. The effect of centrifuging bone cement. *The Journal of Bone and Joint Surgery British Volume* 1989; 71: 39-42.

182. Burke DW, Gates E and Harris W. Centrifugation as a method of improving tensile and fatigue properties of acrylic bone cement. *The Journal of Bone and Joint Surgery American Volume* 1984; 66: 1265-1273.

183. Davies JP and Harris WH. Comparison of diametral shrinkage of centrifuged and uncentrifuge simplex P® bone cement. *Journal of Applied Biomaterials* 1995; 6: 209-211.

184. Askew MJ, Steege JW, Lewis JL, et al. Effect of cement pressure and bone strength on polymethylmethacrylate fixation. *Journal of Orthopaedic Research* 1983; 1: 412-420.

185. Markolf KL, Kabo JM, Stoller DW, et al. Flow characteristics of acrylic bone cements. *Clinical Orthopaedics and Related Research* 1984: 246-254.

186. Walker P, Soudry M, Ewald F, et al. Control of cement penetration in total knee arthroplasty. *Clinical Orthopaedics and Related Research* 1984: 155-164.

187. MacDonald W, Swarts E and Beaver R. Penetration and shear strength of cement-bone interfaces in vivo. *Clinical Orthopaedics and Related Research* 1993: 283-288.

188. Krause W, Krug W and Miller J. The effect of cement types and pressurization on the mechanical properties of acrylic bone cement. *Proceedings of the 26th Annual ORS Atlanta, GA, USA* 1980; 253.

189. Oh I, Merckx DB and Harris WH. Acetabular Cement Compactor An Experimental Study of Pressurization of Cement in the Acetabulum in Total Hip Arthroplasty. *Clinical Orthopaedics and Related Research* 1983; 177: 289-293.

190. Wadia F, Malik MA, Leonard D, et al. Cement pressurisation in the acetabulum. *International Orthopaedics* 2006; 30: 237-242.

191. Lee A and Ling R. A device to improve the extrusion of bone cement into the bone of the acetabulum in the replacement of the hip joint. *Biomedical Engineering* 1974; 9: 522-524.

192. Flivik G, Wulff K, Sanfridsson J, et al. Improved acetabular pressurization gives better cement penetration: in vivo measurements during total hip arthroplasty. *The Journal of Arthroplasty* 2004; 19: 911-918.

193. Bernoski FP, New AM, Scott RA, et al. An in vitro study of a new design of acetabular cement pressurizer. *The Journal of Arthroplasty* 1998; 13: 200-206.

194. Parsch D, Diehm C, Schneider S, et al. Acetabular cementing technique in THA—flanged versus unflanged cups, cadaver experiments. *Acta Orthopaedica Scandinavica* 2004; 75: 269-275.

195. New A, Northmore-Ball M, Tanner K, et al. In vivo measurement of acetabular cement pressurization using a simple new design of cement pressurizer. *The Journal of Arthroplasty* 1999; 14: 854-859.

196. Drew T, Talih S, Thaker E, et al. Mechanical Vibration As A Means Of Optimising Cement Micro Interlock In Cemented Hip Arthroplasty. In: *Orthopaedic Proceedings* 2009, pp.294-294. The British Editorial Society of Bone & Joint Surgery.

197. Thomas A, Dunn J and Luo D. Low-frequency vibration in application of bone cement. *The Lancet* 1988; 331: 116-117.

198. Wang Y, Han P, Gu W, et al. Cement oscillation increases interlock strength at the cement–bone interface. *Orthopedics* 2009; 32.

199. Boger A, Wheeler K, Schenk B, et al. Clinical investigations of polymethylmethacrylate cement viscosity during vertebroplasty and related in vitro measurements. *European Spine Journal* 2009; 18: 1272-1278.

200. Baroud G and Yahia F. A finite element rheological model for polymethylmethacrylate flow: analysis of the cement delivery in vertebroplasty. *Proceedings of the Institution of Mechanical Engineers, Part H: Journal of Engineering in Medicine* 2004; 218: 331-338.

201. Charnley J. *Low friction arthroplasty of the hip: theory and practice*. Springer Science & Business Media, 2012.

202. Kurtz SM. *UHMWPE biomaterials handbook: ultra high molecular weight polyethylene in total joint replacement and medical devices*. Academic Press, 2009.

203. McKellop H, Shen Fw, Lu B, et al. Development of an extremely wear-resistant ultra high molecular weight polyethylene for total hip replacements. *Journal of Orthopaedic Research* 1999; 17: 157-167.

204. Muratoglu O, Bragdon CR, O'Connor D, et al. A novel method of crosslinking UHMWPE to improve wear with little or no sacrifice of mechanical properties. In: *ANNUAL Meeting-Society for Biomaterials in Conjunction with the International Biomaterials Symposium* 1999, pp.496-496.

205. Oral E and Muratoglu OK. Radiation cross-linking in ultra-high molecular weight polyethylene for orthopaedic applications. *Nuclear Instruments and Methods in Physics Research Section B: Beam Interactions with Materials and Atoms* 2007; 265: 18-22.

206. Mall NA, Nunley RM, Zhu JJ, et al. The incidence of acetabular osteolysis in young patients with conventional versus highly crosslinked polyethylene. *Clinical Orthopaedic Related Research* 2011; 469: 372-381. 2010/09/09. DOI: 10.1007/s11999-010-1518-y.

207. Baxter RM, MacDonald DW, Kurtz SM, et al. Characteristics of highly cross-linked polyethylene wear debris in vivo. *Journal of Biomedical Materials Research Part B: Applied Biomaterials* 2013; 101: 467-475.

208. Oral E, Christensen SD, Malhi AS, et al. Wear resistance and mechanical properties of highly cross-linked, ultrahigh-molecular weight polyethylene doped with vitamin E. *The Journal of arthroplasty* 2006; 21: 580-591.

209. Oh I, Sander TW and Treharne RW. Total hip acetabular cup flange design and its effect on cement fixation. *Clinical Orthopaedics and Related Research* 1985; 195: 304-310.

210. Shelley P and Wroblewski B. Socket design and cement pressurisation in the Charnley low-friction arthroplasty. *Journal of Bone and Joint Surgery* 1988; 70: 358-363.

211. Beverland D, Kernohan W, Nixon J, et al. Pressurization of bone cement under standard, flanged and custom acetabular components for total hip replacement. *Proceedings of the Institution of Mechanical Engineers, Part H: Journal of Engineering in Medicine* 1993; 207: 19-23.

212. Ørskov M, Abdulghani S, McCarthy I, et al. Comparison of flanged and unflanged acetabular cup design: An experimental study using ceramic and cadaveric acetabuli. *Acta Orthopaedica* 2010; 81: 556-562.

213. Bhattacharya R, Attar FG, Green S, et al. Comparison of cement pressurisation in flanged and unflanged acetabular cups. *Journal of Orthopaedic Surgery and Research* 2012; 7: 5.

214. Lynch MC. The assessment of Charnley acetabular cup malposition. *The Journal of Bone and Joint Surgery British Volume* 1990; 72: 521-521.

215. Lewinnek GE, Lewis J, Tarr R, et al. Dislocations after total hip-replacement arthroplasties. *Journal of Bone and Joint Surgery* 1978; 60: 217-220.

216. Derbyshire B and Raut VV. The efficacy of a “double-D-shaped” wire marker for radiographic measurement of acetabular cup orientation and wear. *Hip International* 2013; 23: 546-551.

217. Wroblewski B, Lynch M, Atkinson J, et al. External wear of the polyethylene socket in cemented total hip arthroplasty. *The Journal of Bone and Joint Surgery British Volume* 1987; 69: 61-63.

218. Kobayashi S, Eftekhar NS, Terayama K, et al. Risk factors affecting radiological failure of the socket in primary Charnley low friction arthroplasty. A 10-to 20-year followup study. *Clinical Orthopaedics and Related Research* 1994: 84-96.

219. Faris PM, Ritter MA, Keating EM, et al. The cemented all-polyethylene acetabular cup: factors affecting survival with emphasis on the integrated polyethylene spacer: an analysis of the effect of cement spacers, cement mantle thickness, and acetabular angle on the survival of total hip arthroplasty. *The Journal of Arthroplasty* 2006; 21: 191-198.

220. Lichtinger T and Müller R. Improvement of the cement mantle of the acetabular component with bone cement spacers. *Archives of Orthopaedic and Trauma Surgery* 1998; 118: 75-77.

221. Goodman S and Carter D. Acetabular lucent lines and mechanical stress in total hip arthroplasty. *The Journal of Arthroplasty* 1987; 2: 219-224.

222. Chen FS, Di Cesare PE, Kale AA, et al. Results of cemented metal-backed acetabular components: a 10-year-average follow-up study. *The Journal of arthroplasty* 1998; 13: 867-873.

223. Andrade EdC. The viscosity of liquids. *Nature* 1930; 125: 309-310.

224. Phan-Thien N and Mai-Duy N. *Understanding viscoelasticity: an introduction to rheology*. Springer, 2013.

225. De Santis R, Mollica F, Ambrosio L, et al. Dynamic mechanical behavior of PMMA based bone cements in wet environment. *Journal of Materials Science: Materials in Medicine* 2003; 14: 583-594.

226. Hodgson DF and Amis EJ. Dynamic viscoelastic characterization of sol-gel reactions. *Macromolecules* 1990; 23: 2512-2519.

227. Scanlan JC and Winter HH. The evolution of viscoelasticity near the gel point of end-linking poly (dimethylsiloxane) s. In: *Makromolekulare Chemie Macromolecular Symposia* 1991, pp.11-21. Wiley Online Library.

228. Lewis G and Carroll M. Rheological properties of acrylic bone cement during curing and the role of the size of the powder particles. *Journal of Biomedical Materials Research Part A* 2002; 63: 191-199.

229. Nicholas M, Waters M, Holford KM, et al. Analysis of rheological properties of bone cements. *Journal of Materials Science: Materials in Medicine* 2007; 18: 1407-1412.

230. Lu J, Huang Z, Tropiano P, et al. Human biological reactions at the interface between bone tissue and polymethylmethacrylate cement. *Journal of Materials Science: Materials in Medicine* 2002; 13: 803-809.

231. Krause WR, Miller J and Ng P. The viscosity of acrylic bone cements. *Journal of Biomedical Materials Research* 1982; 16: 219-243.

232. Muller R, Gerard E, Dugand P, et al. Rheological characterization of the gel point: a new interpretation. *Macromolecules* 1991; 24: 1321-1326.

233. Nzihou A, Attias L, Sharrock P, et al. A rheological, thermal and mechanical study of bone cement—from a suspension to a solid biomaterial. *Powder Technology* 1998; 99: 60-69.

234. Heaton-Adebile P, Zant NP and Tong J. In vitro fatigue behaviour of a cemented acetabular reconstruction. *Journal of Biomechanics* 2006; 39: 2882-2886.

235. Tong J, Zant N, Wang J-Y, et al. Fatigue in cemented acetabular replacements. *International Journal of Fatigue* 2008; 30: 1366-1375.

236. Zant NP, Wong CK and Tong J. Fatigue failure in the cement mantle of a simplified acetabular replacement model. *International Journal of Fatigue* 2007; 29: 1245-1252.

237. Ingham E and Fisher J. Biological reactions to wear debris in total joint replacement. *Proceedings of the Institution of Mechanical Engineers, Part H: Journal of Engineering in Medicine* 2000; 214: 21-37.

238. Jones L, Frondoza C and Hungerford D. Effect of PMMA particles and movement on an implant interface in a canine model. *The Journal of Bone and Joint Surgery British Volume* 2001; 83: 448-458.

239. Margevicius KJ, Bauer TW, McMahon JT, et al. Isolation and characterization of debris in membranes around total joint prostheses. *Journal of Bone and Joint Surgery* 1994; 76: 1664-1675.

240. Bitar D and Parvizi J. Biological response to prosthetic debris. *World Journal of Orthopedics* 2015; 6: 172.

241. Baaijens F. Calculation of residual stresses in injection molded products. *Rheologica Acta* 1991; 30: 284-299.

242. Withers PJ and Bhadeshia H. Residual stress. Part 1—measurement techniques. *Materials Science and Technology* 2001; 17: 355-365.

243. Friis E, Stromberg L, Cooke F, et al. Fracture toughness of vacuum mixed PMMA bone cement. In: *Transactions of the 19th Annual Meeting of the Society for Biomaterials, April 28-May 2, 1993, Birmingham, AL, USA* 1993, p.301.

244. Scholz FW and Stephens MA. K-sample Anderson–Darling tests. *Journal of the American Statistical Association* 1987; 82: 918-924.

245. Livingston EH. Who was student and why do we care so much about his t-test? 1. *Journal of Surgical Research* 2004; 118: 58-65.

246. McKnight PE and Najab J. Mann-Whitney U Test. *The Corsini Encyclopedia of Psychology* 2010: 1-1.

247. Zor M, Küçük M and Aksoy S. Residual stress effects on fracture energies of cement–bone and cement–implant interfaces. *Biomaterials* 2002; 23: 1595-1601.

248. Davies JP, O'Connor DO, Greer JA, et al. Comparison of the mechanical properties of Simplex P, Zimmer Regular, and LVC bone cements. *Journal of Biomedical Materials Research* 1987; 21: 719-730.

249. Boote AT, Bigsby RJ, Deehan DJ, et al. Does vacuum mixing affect diameter shrinkage of a PMMA cement mantle during in vitro cemented acetabulum implantation? *Proceedings of the Institution of Mechanical Engineers, Part H: Journal of Engineering in Medicine* 2020: 0954411920964023.

250. Ranawat CS, Deshmukh RG, Peters LE, et al. Prediction of the long-term durability of all-polyethylene cemented sockets. *Clinical Orthopaedics and Related Research* 1995; 317: 89-105.

251. Acharya A, Petheram T, Hubble M, et al. Sealing the acetabular notch in cemented total hip arthroplasty. A radiological review of 380 cases. *Acta Orthopædica Belgica* 2010; 76: 199.

252. Flivik G, Sanfridsson J, Önnerfält R, et al. Migration of the acetabular component: effect of cement pressurization and significance of early radiolucency: a randomized 5-year study using radiostereometry. *Acta Orthopaedica* 2005; 76: 159-168.

253. Gilbert JL, Hasenwinkel JM, Wixson RL, et al. A theoretical and experimental analysis of polymerization shrinkage of bone cement: a potential major source of porosity. *Journal of Biomedical Materials Research* 2000; 52: 210-218.

254. Green T, Fisher J, Stone M, et al. Polyethylene particles of a 'critical size' are necessary for the induction of cytokines by macrophages in vitro. *Biomaterials* 1998; 19: 2297-2302.

255. Parsch D, Diehm C, New AMR, et al. A new bleeding model of the human acetabulum and a pilot comparison of 2 different cement pressurizers. *The Journal of Arthroplasty* 2004; 19: 381-386. DOI: 10.1016/j.arth.2003.09.014.

256. Davidson SR and James DF. Measurement of thermal conductivity of bovine cortical bone. *Medical Engineering & Physics* 2000; 22: 741-747.

257. AZoM. Stainless Steel - Grade 304 (UNS S30400), <https://www.azom.com/properties.aspx?ArticleID=965> (2001, accessed 04/08 2020).

258. N'Diaye M, Pascaletti-Grizon F, Massin P, et al. Water absorption of poly (methyl methacrylate) measured by vertical interference microscopy. *Langmuir* 2012; 28: 11609-11614.

259. Lankester BJ, Sabri O, Gheduzzi S, et al. In vitro pressurization of the acetabular cement mantle: the effect of a flange. *The Journal of Arthroplasty* 2007; 22: 738-744.

260. ASTM AF. Standard Specification for Acrylic Bone Cement. In: 1999, ASTM West Conshohocken, PA.

261. Panjabi MM, Cimino WR and Drinker H. Effect of pressure on bone cement stiffness: an in vitro study. *Acta Orthopaedica Scandinavica* 1986; 57: 106-110.

262. Winter HH and Chambon F. Analysis of linear viscoelasticity of a crosslinking polymer at the gel point. *Journal of Rheology* 1986; 30: 367-382.

263. Bonnar W. Boyle's Law and gravitational instability. *Monthly Notices of the Royal Astronomical Society* 1956; 116: 351-359.

264. Composites E. RTV Silicone Rubbers, <https://www.easycomposites.co.uk/rtv-silicone-rubbers> (2021, accessed 23/08 2021).

265. Pennington M, Grieve R, Sekhon JS, et al. Cemented, cementless, and hybrid prostheses for total hip replacement: cost effectiveness analysis. *BMJ* 2013; 346: f1026.

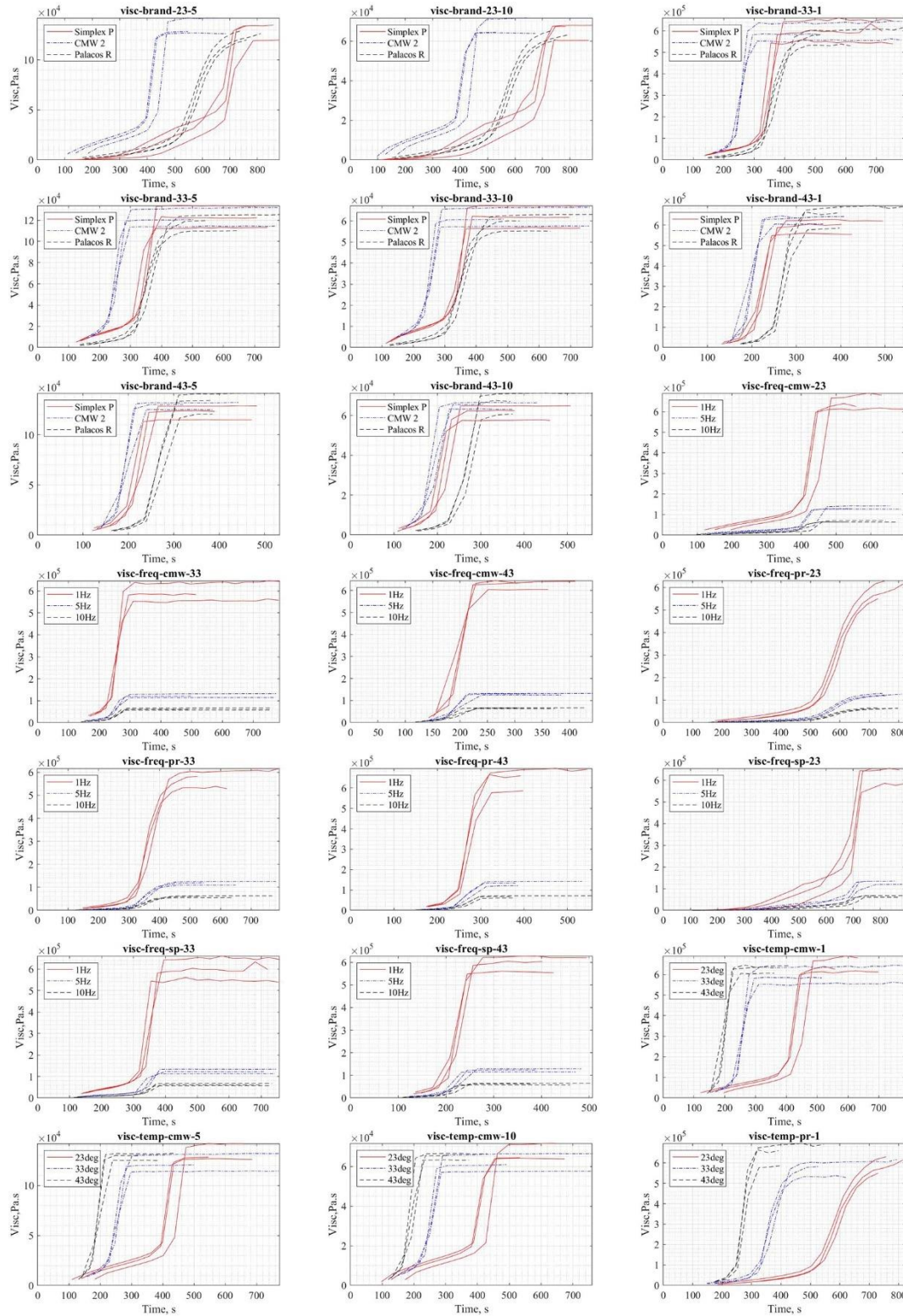
266. De Wijn J, Slooff T and Driessens F. Characterization of bone cements. *Acta Orthopaedica Scandinavica* 1975; 46: 38-51.

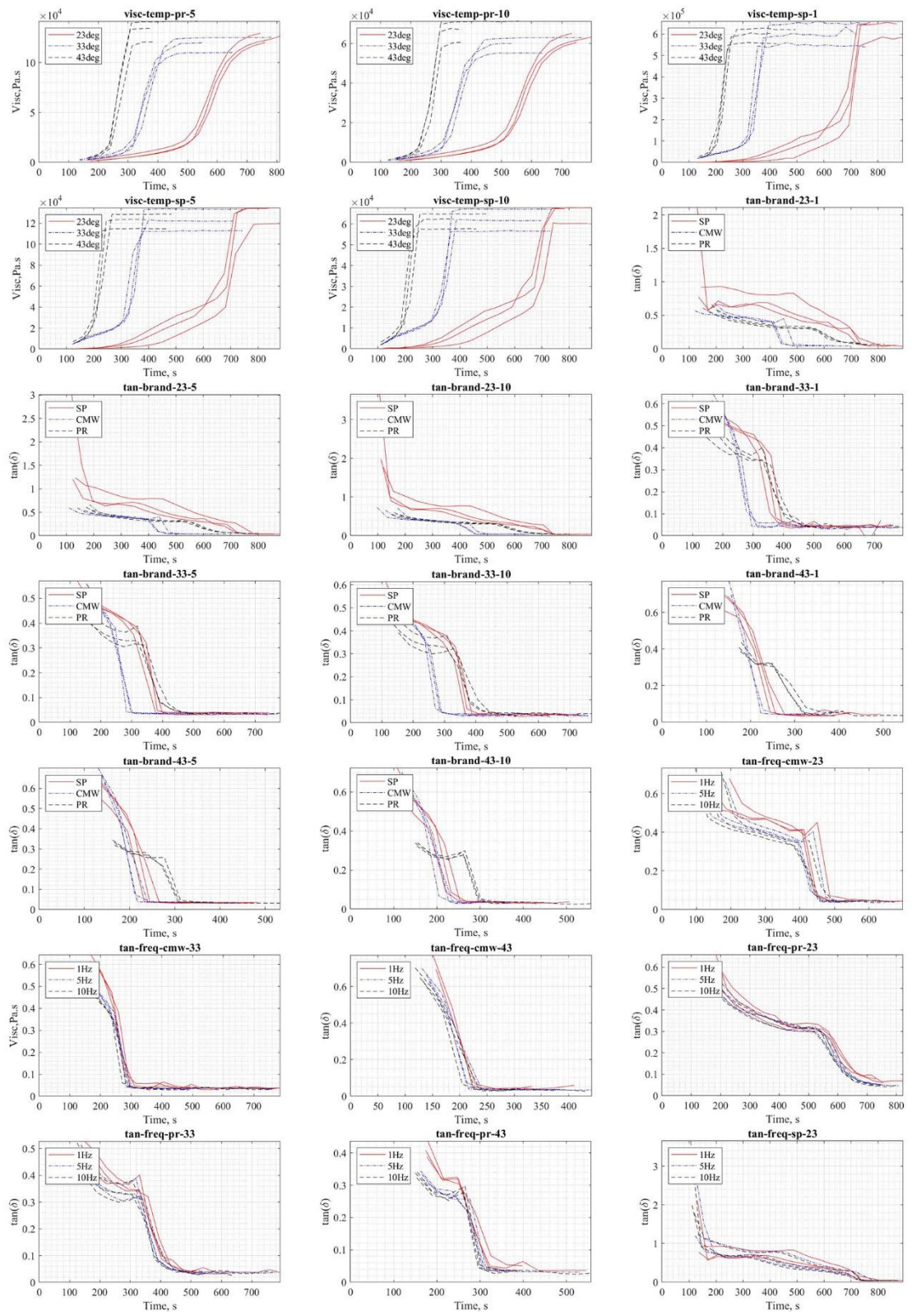
267. Stańczyk M. Study on modelling of PMMA bone cement polymerisation. *Journal of Biomechanics* 2005; 38: 1397-1403.

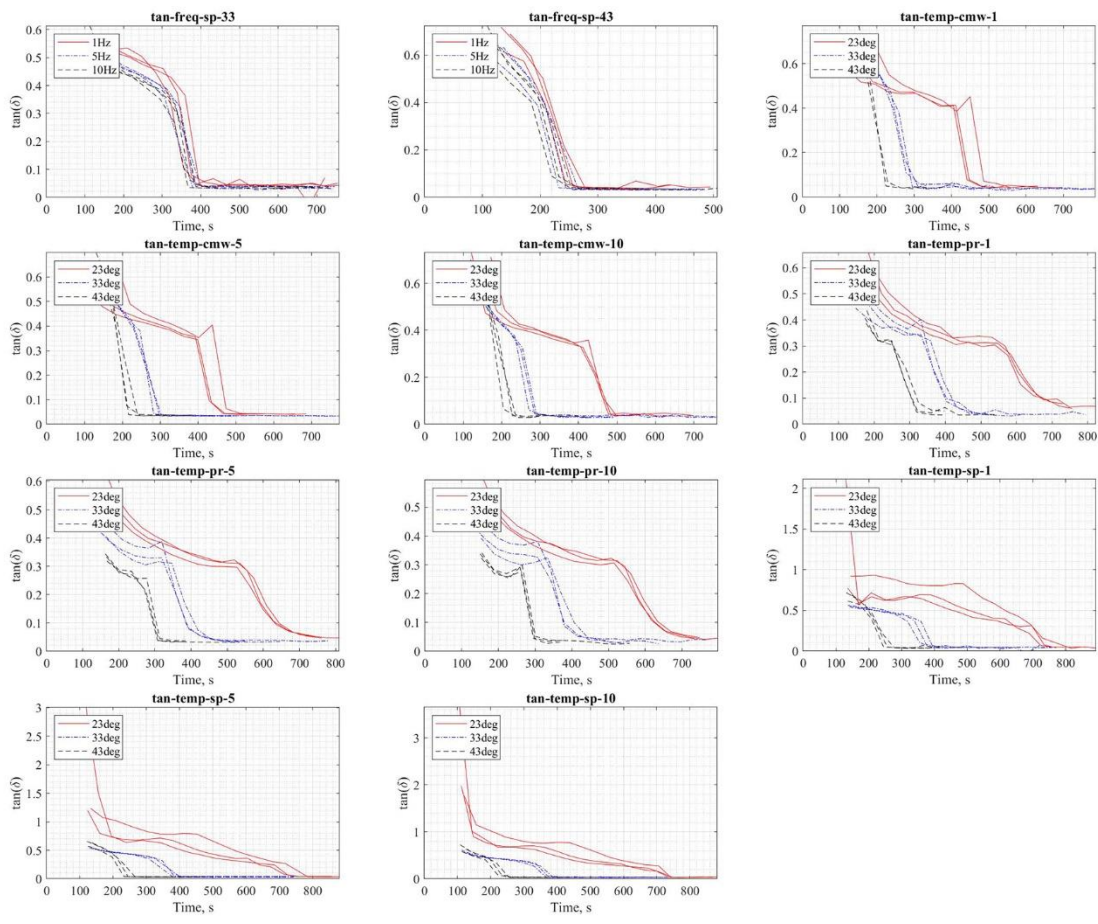
## **Appendix A. The UK National Joint Registry Data Collection Form for a Primary Hip Procedure.**

## Appendix B. Graphs for all Rheological Experiments, Testing Conditions, and Variables.

Code: Visc = Viscosity, tan =  $\tan(\delta)$  23deg, 33deg and 43deg refer to the temperature of the experiment in degrees Celsius and 1 Hz, 5 Hz, 10 Hz refer to the frequency of the deformation when the measurement was taken.

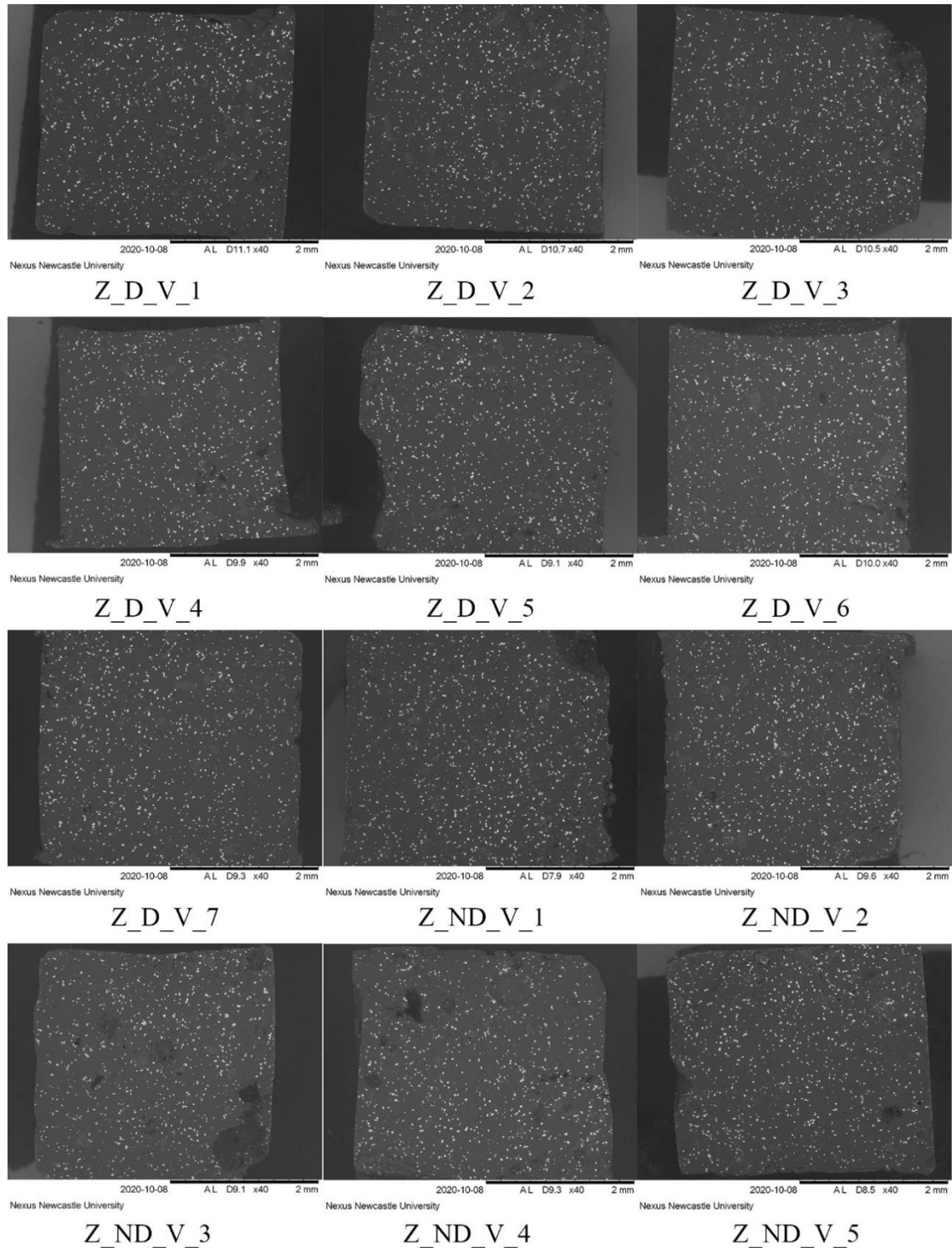


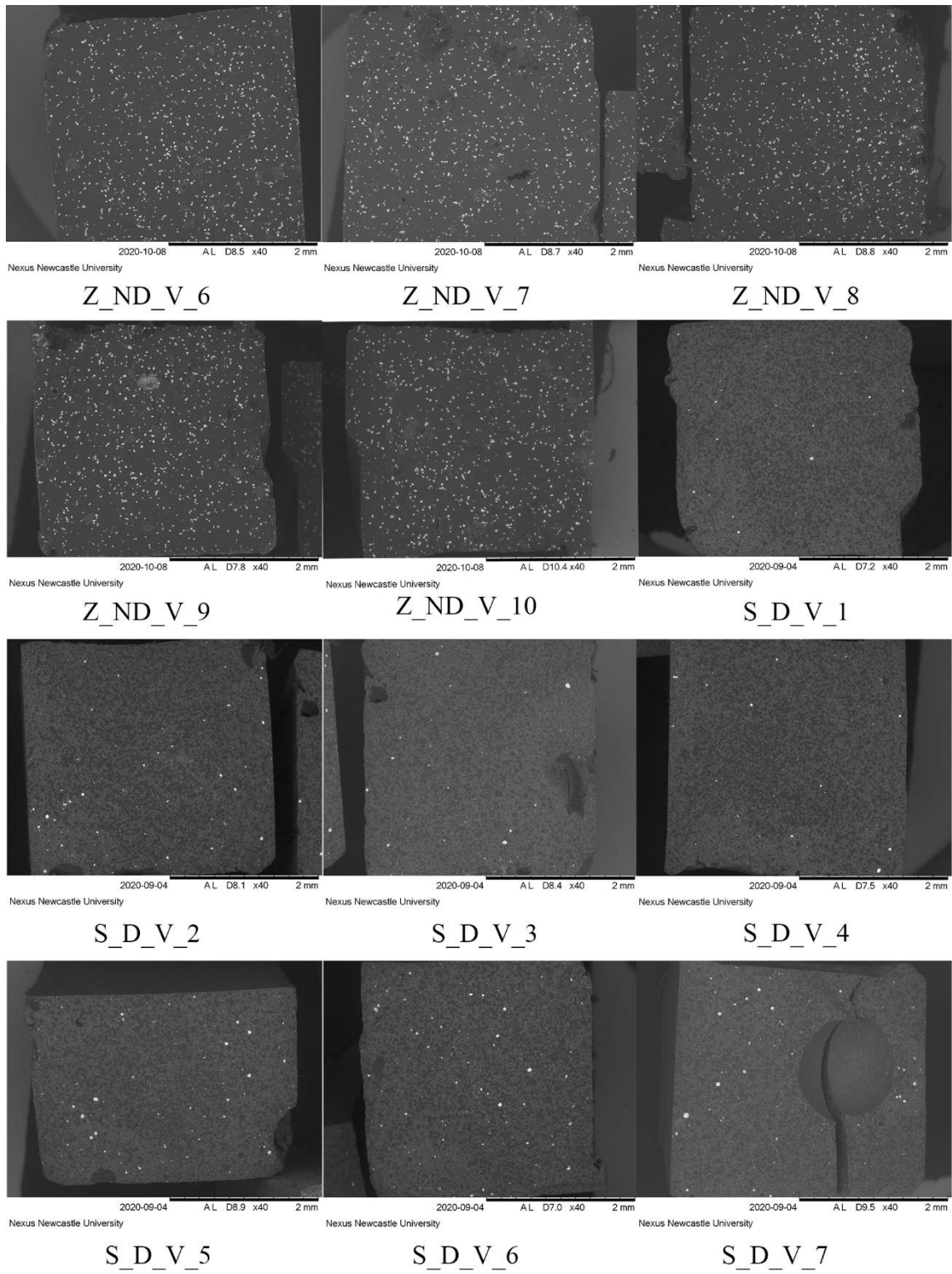


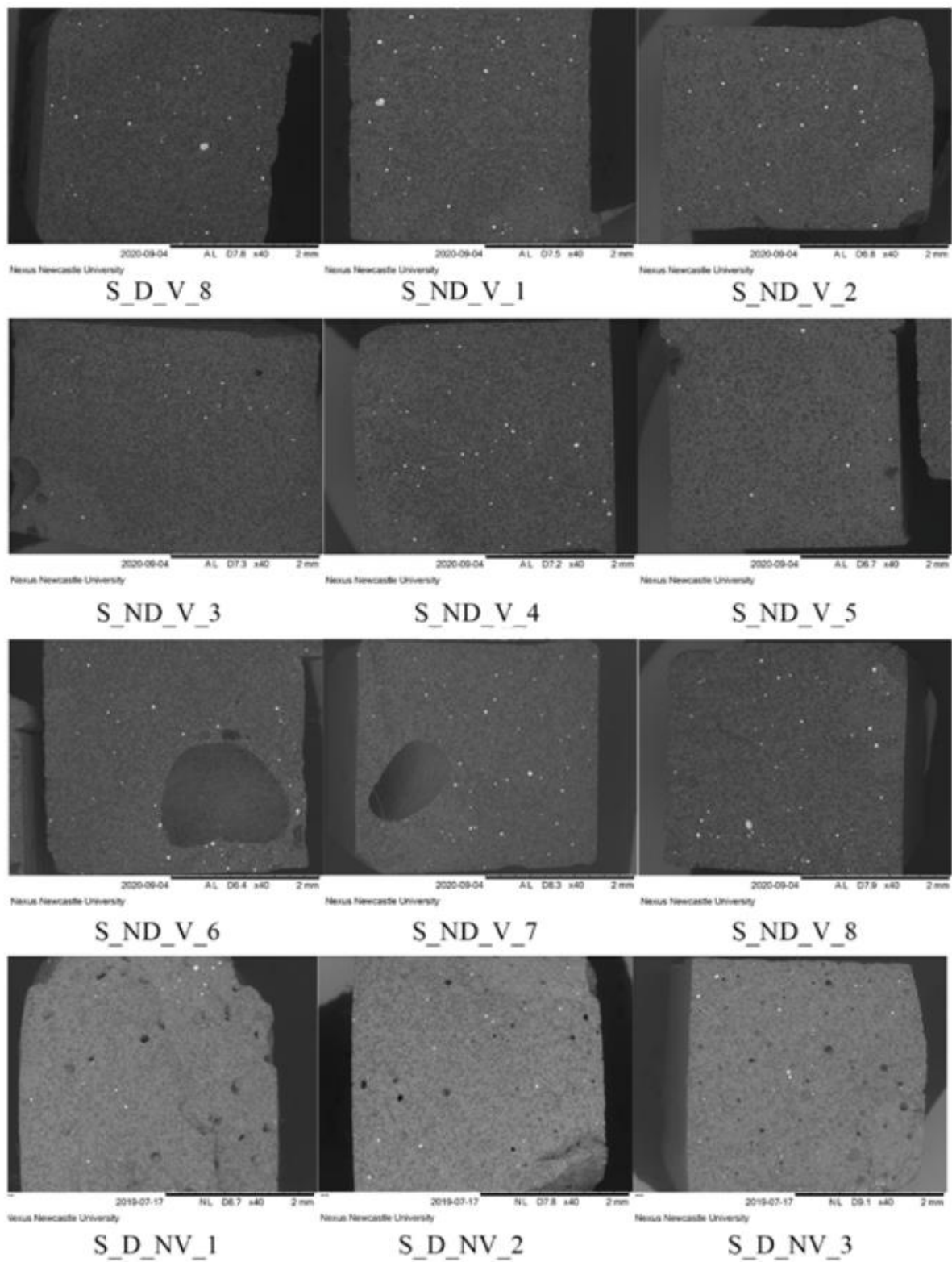


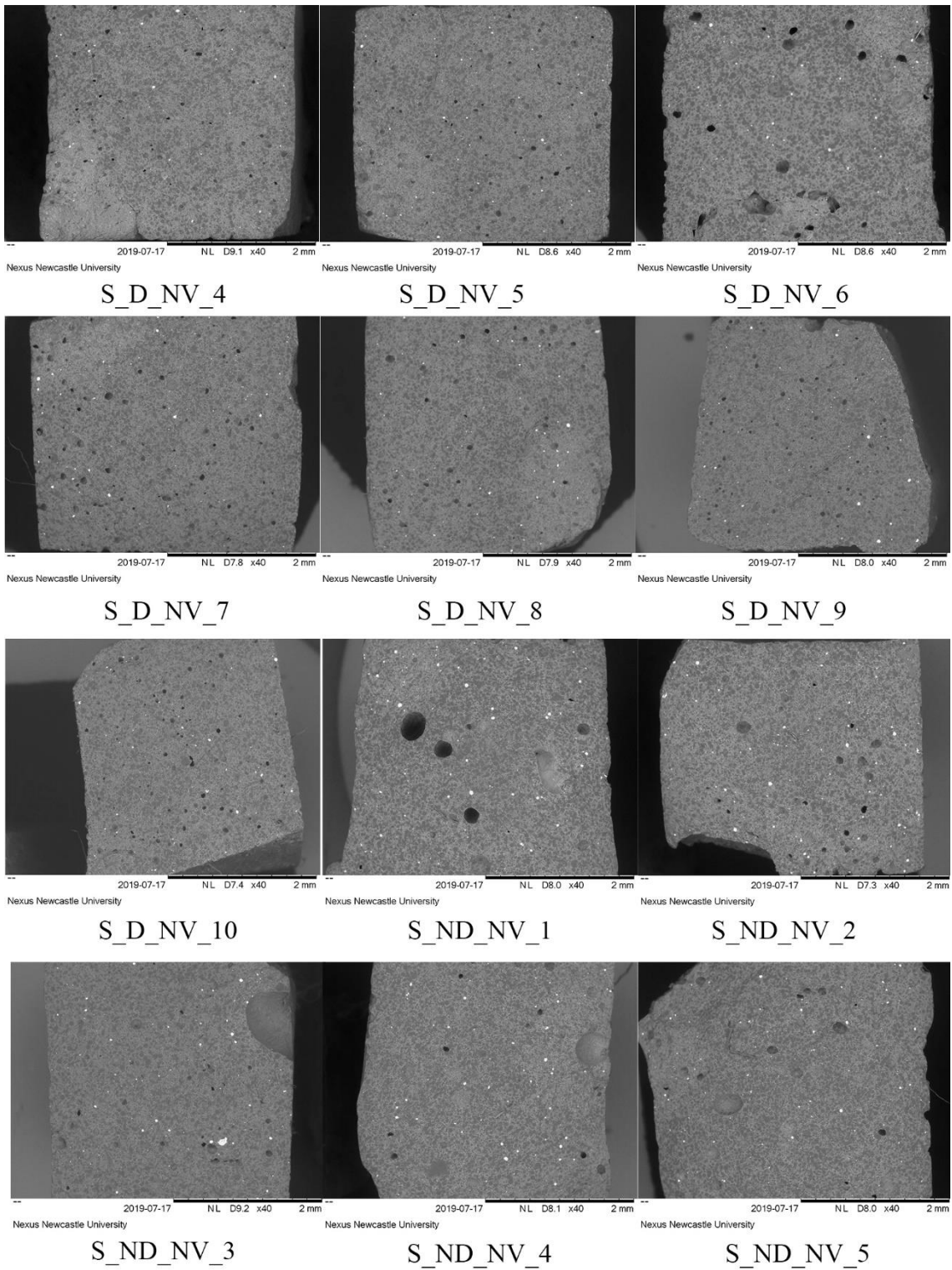
## Appendix C. SEM Images of the Fracture Surfaces from the PMMA Bone Cement Tensile Test Specimens.

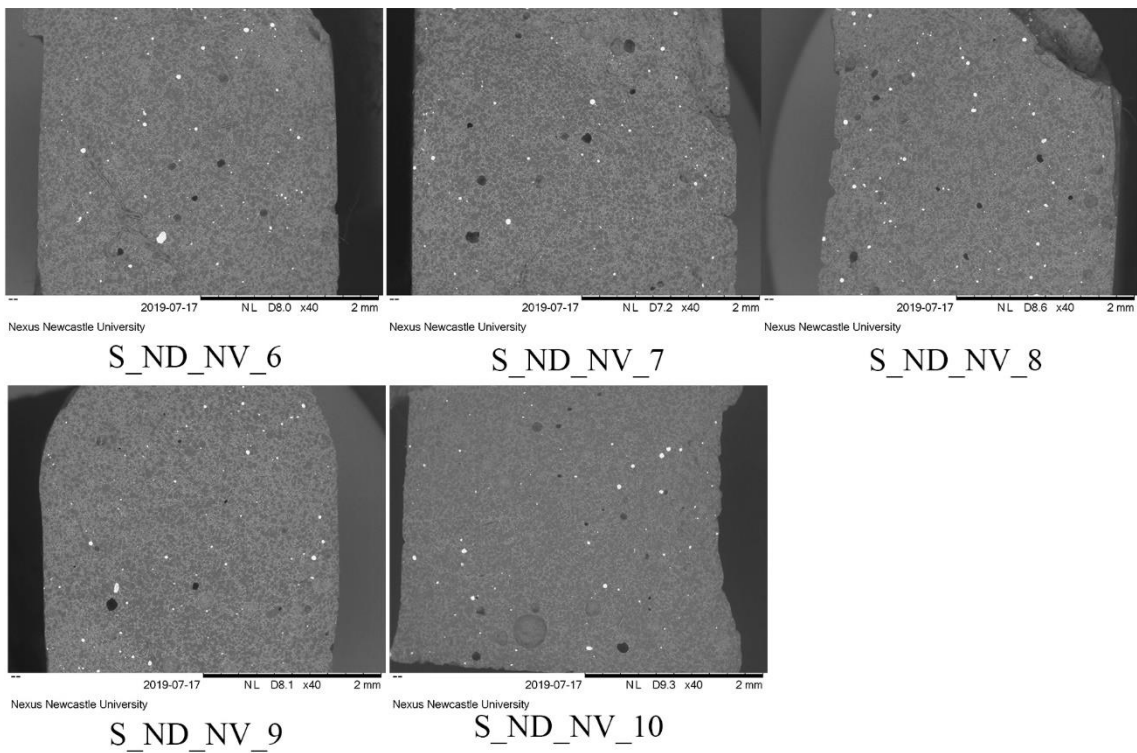
Code: Zimmer = Z, Simplex P = S, D = Deformed, ND = Non-Deformed, V = Vacuum Mixed, NV = Non-Vacuum Mixed and the number refers to the number of the sample.











## Appendix D. MATLAB Code for the Calculation of the Radius of the External Surface of the Cement Mantles Using 2-Dimensional Coordinates.

Credit given to Danylo Malyuta for the code for the code that was used for calculation of the radius. *Danylo Malyuta (2021). Fit circle through 3 points (<https://www.mathworks.com/matlabcentral/fileexchange/57668-fit-circle-through-3-points>), MATLAB Central File Exchange. Retrieved September 15, 2021.*

```

function [R,xcyc] = fit_circle_through_3_points(ABC)
% FIT_CIRCLE_THROUGH_3_POINTS
% Mathematical background is provided in http://www.regentsprep.org/regents/math/geometry/gcg6/RCir.htm
%
% Input:
%
% ABC is a [3 x 2n] array. Each two columns represent a set of three points which lie on
% a circle. Example: [-1 2;2 5;1 1] represents the set of points (-1,2), (2,5) and (1,1) in Cartesian
% (x,y) coordinates.
%
% Outputs:
%
% R is a [1 x n] array of circle radii corresponding to each set of three points.
% xcyc is an [2 x n] array of the centers of the circles, where each column is [xc_i;yc_i] where i
% corresponds to the {A,B,C} set of points in the block [3 x 2i-1:2i] of ABC
%
% Author: Danylo Malyuta,
% Version: v1.0 (June 2016)
% -----
%
% Each set of points {A,B,C} lies on a circle. Question: what is the circles radius and center?
% A: point with coordinates (x1,y1)
% B: point with coordinates (x2,y2)
% C: point with coordinates (x3,y3)
% ===== Find the slopes of the chord A-->B (mr) and of the chord B-->C (mt)
% mt = (y3-y2)/(x3-x2)
% mr = (y2-y1)/(x2-x1)
% // Begin by generalizing xi and yi to arrays of individual xi and yi for each {A,B,C} set of points provided in ABC array
x1 = ABC(1,1:2:end);
x2 = ABC(2,1:2:end);
x3 = ABC(3,1:2:end);
y1 = ABC(1,2:2:end);
y2 = ABC(2,2:2:end);
y3 = ABC(3,2:2:end);
% // Now carry out operations as usual, using array operations
mr = (y2-y1)./(x2-x1);
mt = (y3-y2)./(x3-x2);
% A couple of failure modes exist:
% (1) First chord is vertical ==> mr==Inf
% (2) Second chord is vertical ==> mt==Inf
% (3) Points are collinear ==> mt==mr (NB: NaN==NaN here)
% (4) Two or more points coincident ==> mr==NaN || mt==NaN
% Resolve these failure modes case-by-case.
idf1 = isnan(mr); % Where failure mode (1) occurs
idf2 = isnan(mt); % Where failure mode (2) occurs
idf34 = isequaln(mr,mt) | isnan(mr) | isnan(mt); % Where failure modes (3) and (4) occur
% ===== Compute xc, the circle center x-coordinate
xcyc = (mr.*mt.*((y3-y1)-mr.*((x2+x3)-mt.*((x1+x2))./(2*(mr-mt)))); % Failure mode (1) ==> use limit case of mr==Inf
xcyc(idf1) = ((mt(idf1)).*(y3(idf1)-y1(idf1))+((x2(idf1)-x3(idf1))).)/2; % Failure mode (2) ==> use limit case of mt==Inf
xcyc(idf2) = ((x1(idf2)-x2(idf2))-mr*(idf2)).*(y3(idf2)-y1(idf2)))./2; % Failure mode (3) or (4) ==> cannot determine center point, return NaN
% ===== Compute yc, the circle center y-coordinate
xcyc(2,:)= -1./mr.*((xcyc-(x1+x2)/2)+(y1+y2)/2);
idmr0 = mr==0;
xcyc(2,idmr0) = -1./mt(idmr0).*((xcyc(idmr0)-(x2(idmr0)+x3(idmr0))/2)+(y2(idmr0)+y3(idmr0))/2);
xcyc(2,idf34) = NaN; % Failure mode (3) or (4) ==> cannot determine center point, return NaN
% ===== Compute the circle radius
R = sqrt((xcyc(1,:)-x1).^2+(xcyc(2,:)-y1).^2);
R(idf34) = Inf; % Failure mode (3) or (4) ==> assume circle radius infinite for this case
end

```

Below is code that calculates the mean radius and the standard deviation using three coordinates.

```

% Example x and y coordinates.
XX = [0;12.1155;18.3140;22.0160;25.2600;25.2180;22.8455;20.7730;16.1770];
YY = [0;2.9410;7.3555;12.2045;19.1320;32.7465;38.5810;41.5450;45.8680];

% x and y coordinates combined so each line is a point in 2D space.
AXY = [XX,YY];

% Number of coordinates.
Length = length(XX);

% Vector which lists the index of each coordinate.
Index = 1:Length;

% Arbitrarily large number of iterations to be performed
Z = 100000;

% Results matrix
Radius = zeros(Z,1);

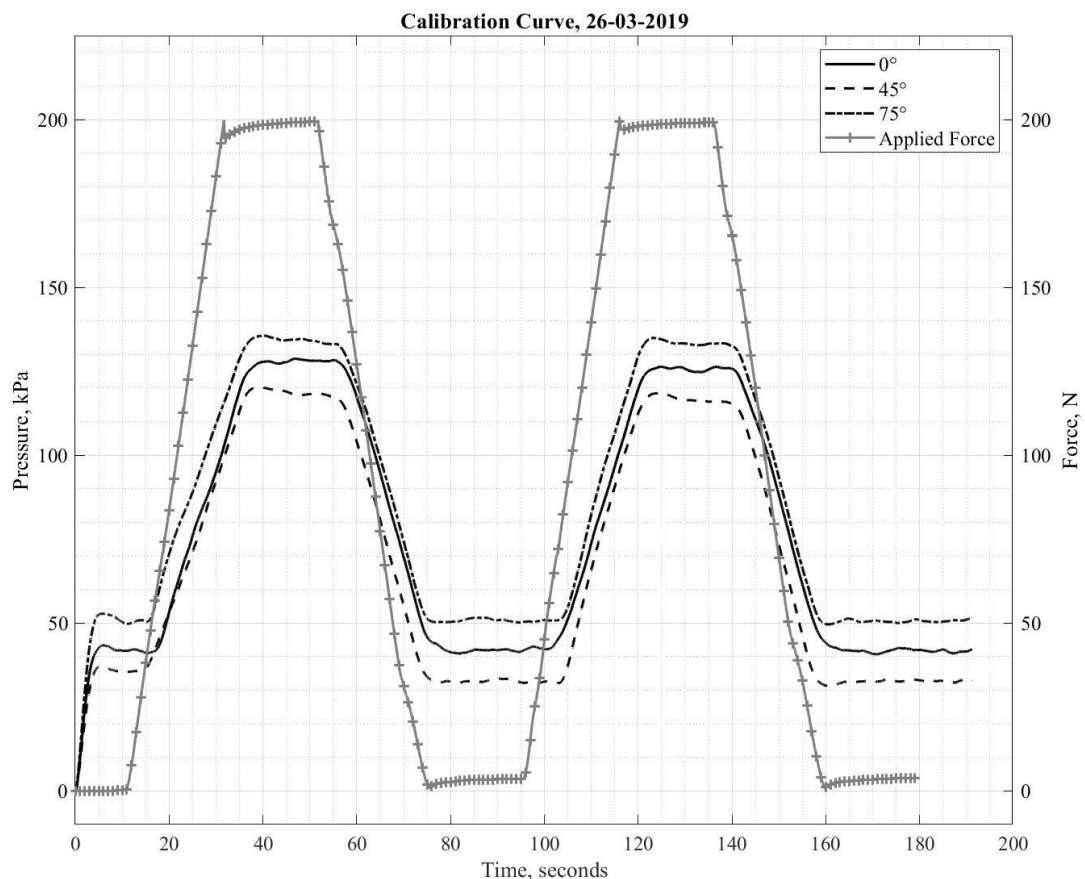
% for loop created to use 3 random coordinates to perform the calculation
% and store in results matrix.
for p = 1 : Z
    IND = randperm(numel(Index),3);
    ABC = [AXY(IND(1),1),AXY(IND(1),2);AXY(IND(2),1),AXY(IND(2),2);AXY(IND(3),1),AXY(IND(3),2)];
    [R,xcyc] = fit_circle_through_3_points(ABC);
    Radius(p) = R;
end

% Taking the mean and the standard deviation
Radius_Mean = mean(Radius);
Radius_STDV = std(Radius);

```

## Appendix E. An Example of the Graph Used for the Calibration of the Pressure Transducers.

When the pressure sensors arrived, they were fully calibrated. A simple experiment was done which involved the application of a 200N force at 10 N per second, then a 60s hold and then a release of the force at 10 N/s until no load was applied to the cement. This was regularly repeated and any adjustments to the zero error were made accordingly so that the readings from the pressure sensor were equivalent to when the sensors first arrived.



## Appendix F. Arduino Code used for the Acquisition of the Pressures of the Curing PMMA Cement Mantle.

```
float time;
int sensor1plus;
int sensor1minus;
int sensor2plus;
int sensor2minus;
int sensor3plus;
int sensor3minus;
const float voltCovert = 5.0 / 1023.0;

void setup() {
  Serial.begin(9600);
  Serial.print('\n');
  Serial.print("Time");
  Serial.print("\t");
  Serial.print("P(1)");
  Serial.print("\t");
  Serial.print("P(2)");
  Serial.print("\t");
  Serial.println("P(3)");
}

void loop() {

  // set time and print from serial opening
  time = millis();
  float timesecs = time/1000;
  Serial.print(timesecs); //prints time since program started

  // sensor 1
  delay(5);
  sensor1plus = analogRead(A0);
  sensor1minus = analogRead(A1);
  float voltage1 = (sensor1plus-sensor1minus) * voltCovert;
  float pressure1 = voltage1 * 137.9;
  Serial.print("\t");
  Serial.print(pressure1, 2);

  // sensor 2
  sensor2plus = analogRead(A2);
  sensor2minus = analogRead(A3);
  float voltage2 = (sensor2plus-sensor2minus) * voltCovert;
  float pressure2 = voltage2 * 137.9;
  Serial.print("\t");
  Serial.print(pressure2, 2);

  // sensor 3
  sensor3plus = analogRead(A4);
  sensor3minus = analogRead(A5);
  float voltage3 = (sensor3plus-sensor3minus) * voltCovert;
  float pressure3 = voltage3 * 137.9;
  Serial.print("\t");
  Serial.println(pressure3, 2);
}
```

## Appendix G. Arduino Code used for the Acquisition of the Temperature of the Curing PMMA Cement Mantle.

```
// load library
#include <SPI.h>
#include "Adafruit_MAX31855.h"

// digital IO pins.
#define MAXDO 3
#define MAXCS 4
#define MAXCLK 5

// initialize the Thermocouple
Adafruit_MAX31855 thermocouple(MAXCLK, MAXCS, MAXDO);

float time;

void setup() {
  Serial.begin(9600);
  Serial.print('\n');
  Serial.print("Time");
  Serial.print("\t");
  Serial.print("Temperature");
  Serial.print("\t");
  Serial.print("Room Temperature");
  Serial.println();
}

void loop() {
  // put your main code here, to run repeatedly:
  // check thermocouple works
  double c = thermocouple.readCelsius();
  if (isnan(c)) {
    Serial.println("Something wrong with thermocouple!");
  } else {

    // set time and print from serial opening
    time = millis();
    float timesecs = time/1000;
    Serial.print(timesecs);      //prints time since program started

    // Thermocouple
    // basic readout test, just print the current temp
    Serial.print("\t");
    float RT = thermocouple.readInternal();
    float CT = thermocouple.readCelsius()+2.75 ;
    Serial.print(CT);
    Serial.print("\t");
    Serial.print("\t");
    Serial.println(RT);
  }
}
```

## Appendix H. Filtering, Preliminary Plotting, and Storage of the Pressure and Temperature Data Acquired for each Acetabular Implantation Experiment.

```
1 % Piston Data Processing
2 %
3 % Names of Variables to be Imported
4
5 %Time
6 %P1
7 %P2
8 %P3
9 %Timel
10 %Temperature
11
12 %
13 %%%%%%%% %%%%%%%% %%%%%%%% %%%%%%
14 % MAKE SURE SENSORS ARE IN CORRECT POSITIONS %
15 %%%%%%%% %%%%%%%% %%%%%%
16
17 %%%%%%%% Filter data
18 % Using a second order butterworth filter and filtering at half the
19 % sampling frequency
20 - [B,A] = butter(2,0.00625);
21 - PF1 = filter(B,A,P1);
22 - PF2 = filter(B,A,P2);
23 - PF3 = filter(B,A,P3);
24
25 %
26 %%%%%%%% Adjust for 0 error calculated from calibration curve.
27 - PPPF1 = PF1;
28 - PPPF2 = PF2;
29 - PPPF3 = PF3;
30
31 %
32 %%%%%%%% Assign data to correct angle
33
34 - Deg_0_Press = PPPF3;
35 - Deg_45_Press = PPPF1;
36 - Deg_75_Press = PPPF2;
37
38 %
39 %%%%%%%% Convert temperature to be on the same time series
40
41 % Remember to remove NAN values from temp and time temp
42 - Timel = rmmissing(Timel);
43 - Temperaturea = rmmissing(Temperature)
```

```

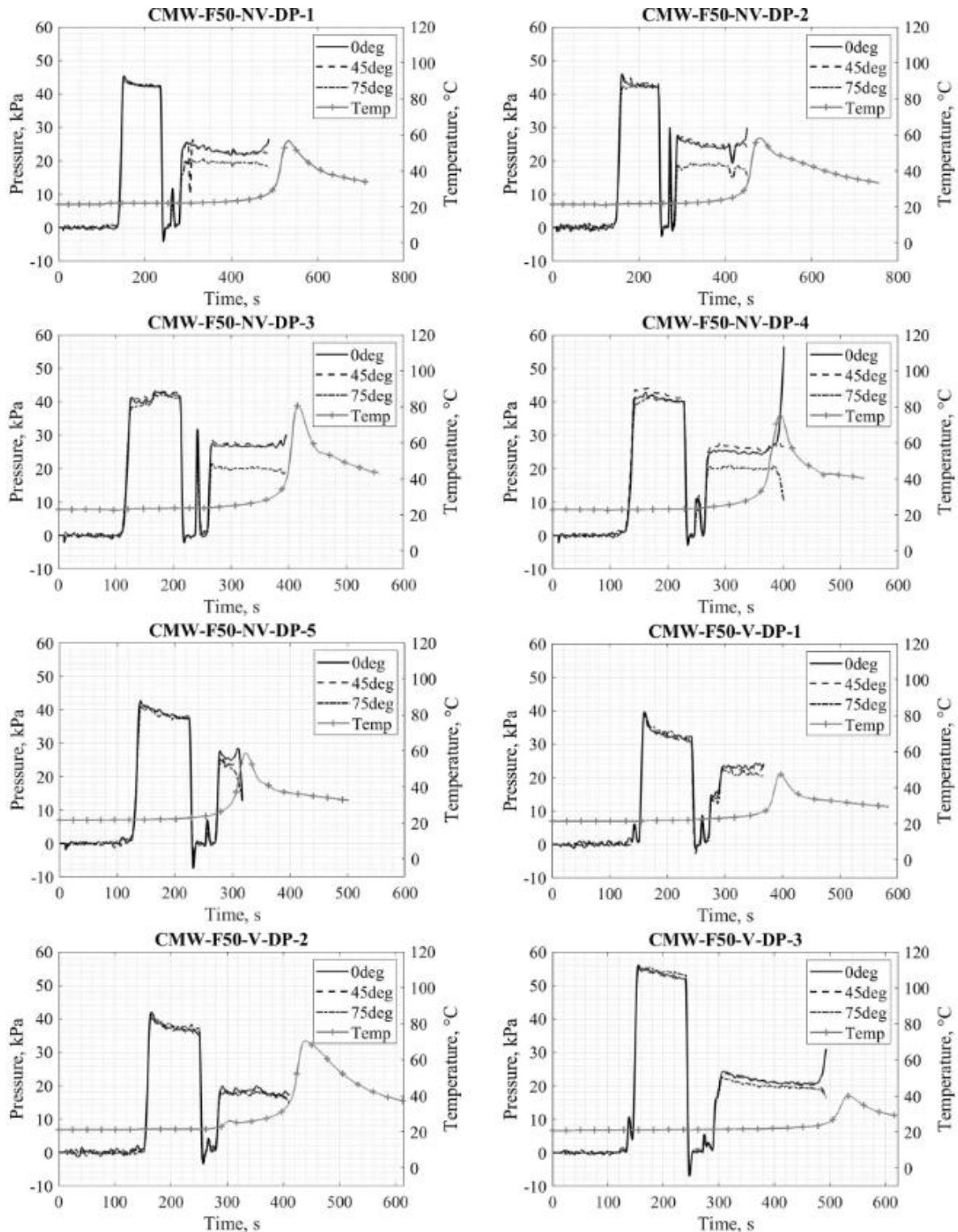
43 -     Temperaturea = rmmissing(Temperature)
44 -
45 -     Timel = categorical(Timel);
46 -     Temperatureb = categorical(Temperaturea);
47 -
48 -     for i = 1:numel(Temperatureb);
49 -         if Temperatureb(i) == "nan";
50 -             Temperatureb(i)=[];
51 -             Timel(i)=[];
52 -         end;
53 -     end;
54 -
55 -     % Rescaling the temperature
56 -     Timel = double(Timel)
57 -     Temperaturec = double(Temperatureb)
58 -
59 -     TimeLength = length(Time);
60 -     Temp=imresize(Temperaturec, [TimeLength,1]);
61 -
62 -     % Cure Temp
63 -     [Tmax,Tmax_L] = max(Temp);
64 -     Tmin = mean(Temp(1:50));
65 -     Tcure_temp = round(((Tmax-Tmin)/2) + Tmin)
66 -
67 -
68 -     % Cure Time
69 -     Temperatureround = round(Temperature);
70 -     TemperatureCure_ind = find(Temperatureround==Tcure_temp, 1, 'first');
71 -     TCure_time = Timel(TemperatureCure_ind)
72 -
73 -
74 -     %%
75 -     %%%%%%%%%%%%%% Plot data
76 -     fig = figure('Name','Pressure and Temperature at the Bone Cement - Bone Interface');
77 -     left_color = [0 0 0];
78 -     right_color = [0 0 0];
79 -     set(fig,'defaultAxesColorOrder',[left_color; right_color]);
80 -     plot(Time,Deg_0_Press,'r');
81 -     hold on
82 -     plot(Time,Deg_45_Press,'b--');
83 -     plot(Time,Deg_75_Press,'k-.');
84 -     ylabel("Pressure, kPa");
85 -     xlabel("Time, seconds");

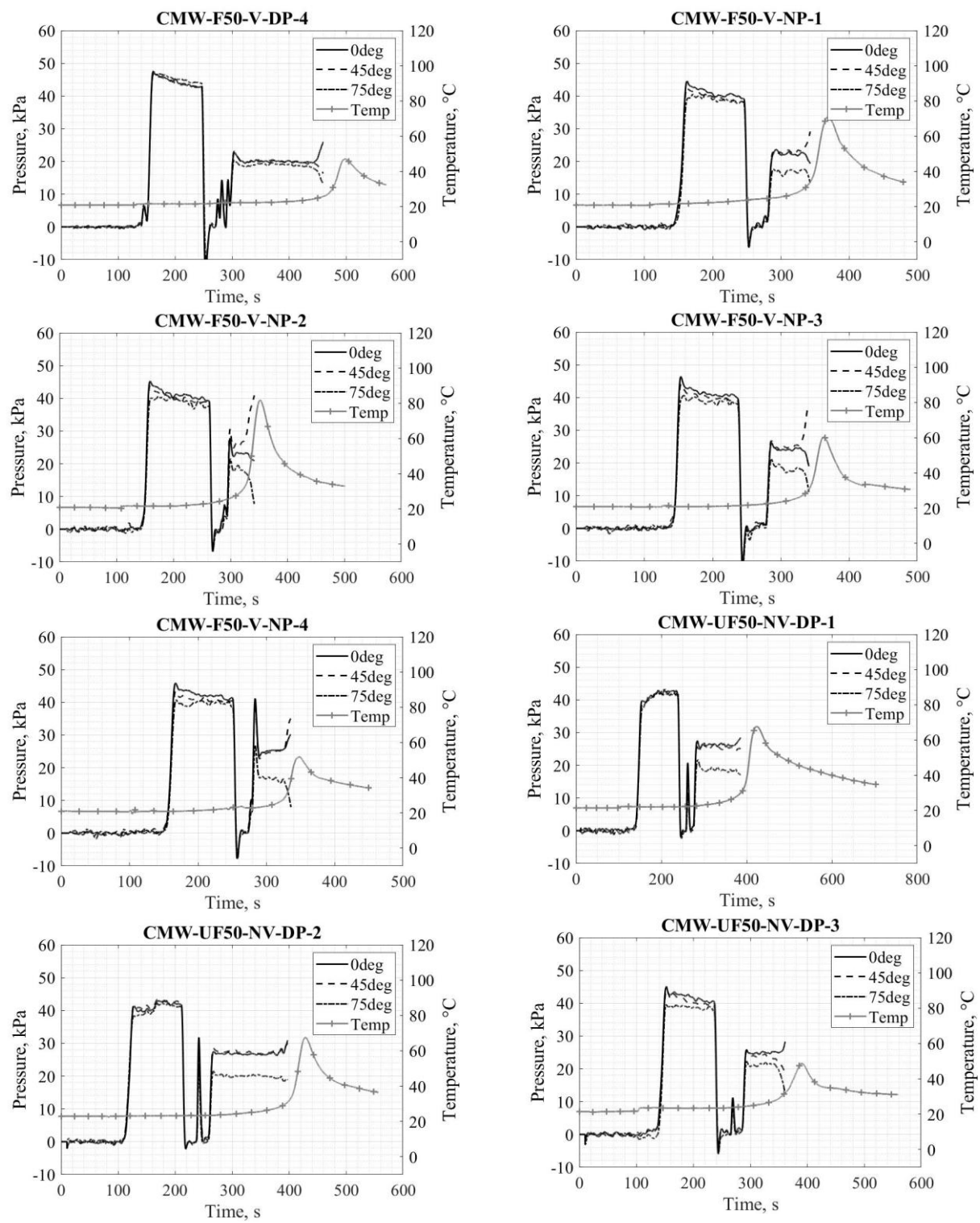
86 -     axis([0 1000 -25 500]);
87 -     yyaxis right
88 -     plot(Time,Temp,'Color',[1 0.5 0.05],'linestyle',':','LineWidth',2);
89 -     axis([0 1000 15 70]);
90 -     ylabel("Temperature, °C");
91 -     grid on
92 -     grid minor
93 -     legend('0°', '45°', '75°', 'Temperature')
94 -
95 -     %%
96 -
97 -
98 -     %%%%%%%%%%%%%%
99 -     % THE CORRECT DATA TO EXPORT TO EXCEL %
100 -     %%%%%%%%%%%%%%
101 -     Max_Temp = Fl_Tmax = Tmax
102 -     Cure_time = Fl_tCure = TCure_time
103 -     Cure_Temp = Fl_Tcure = Tcure_temp

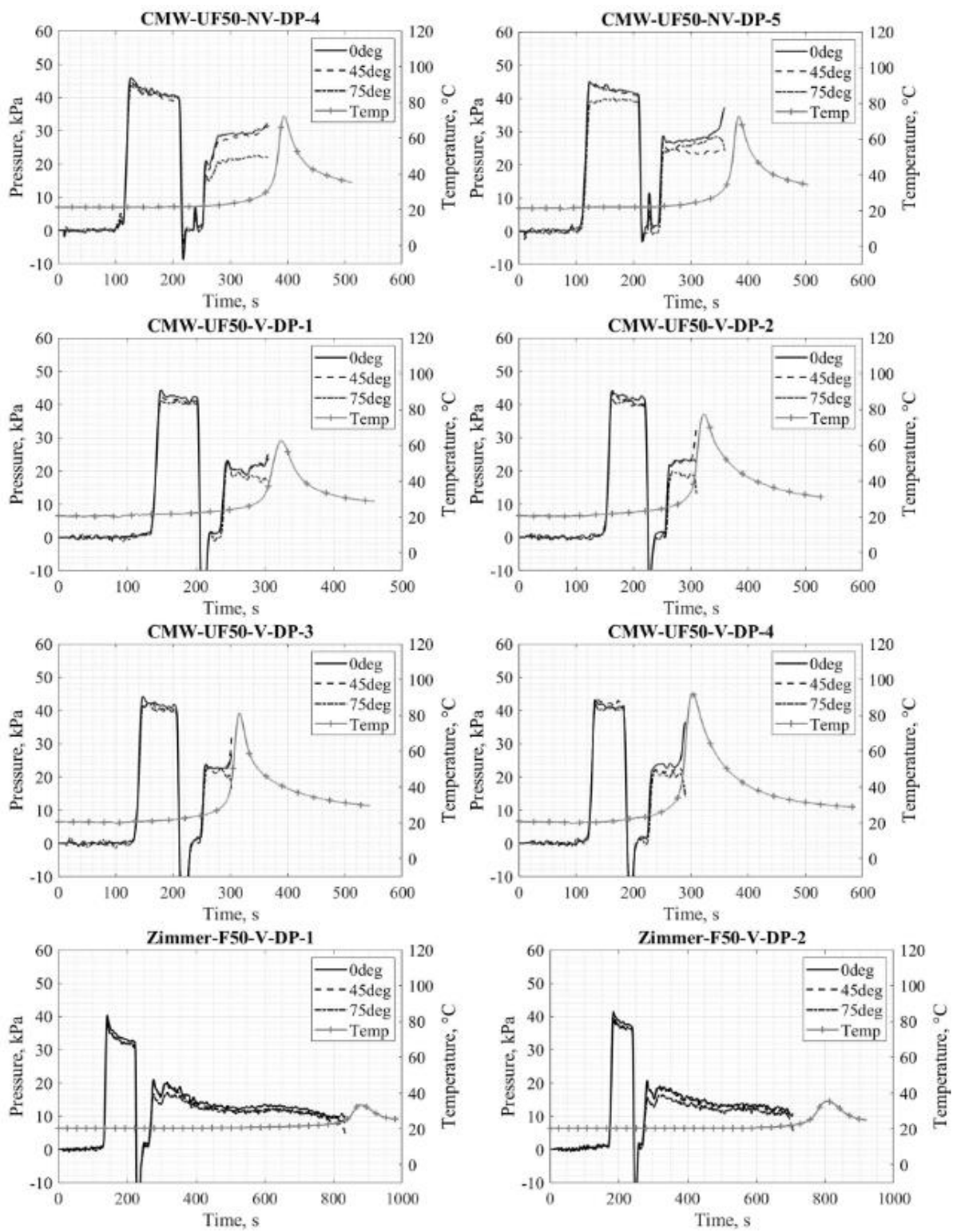
```

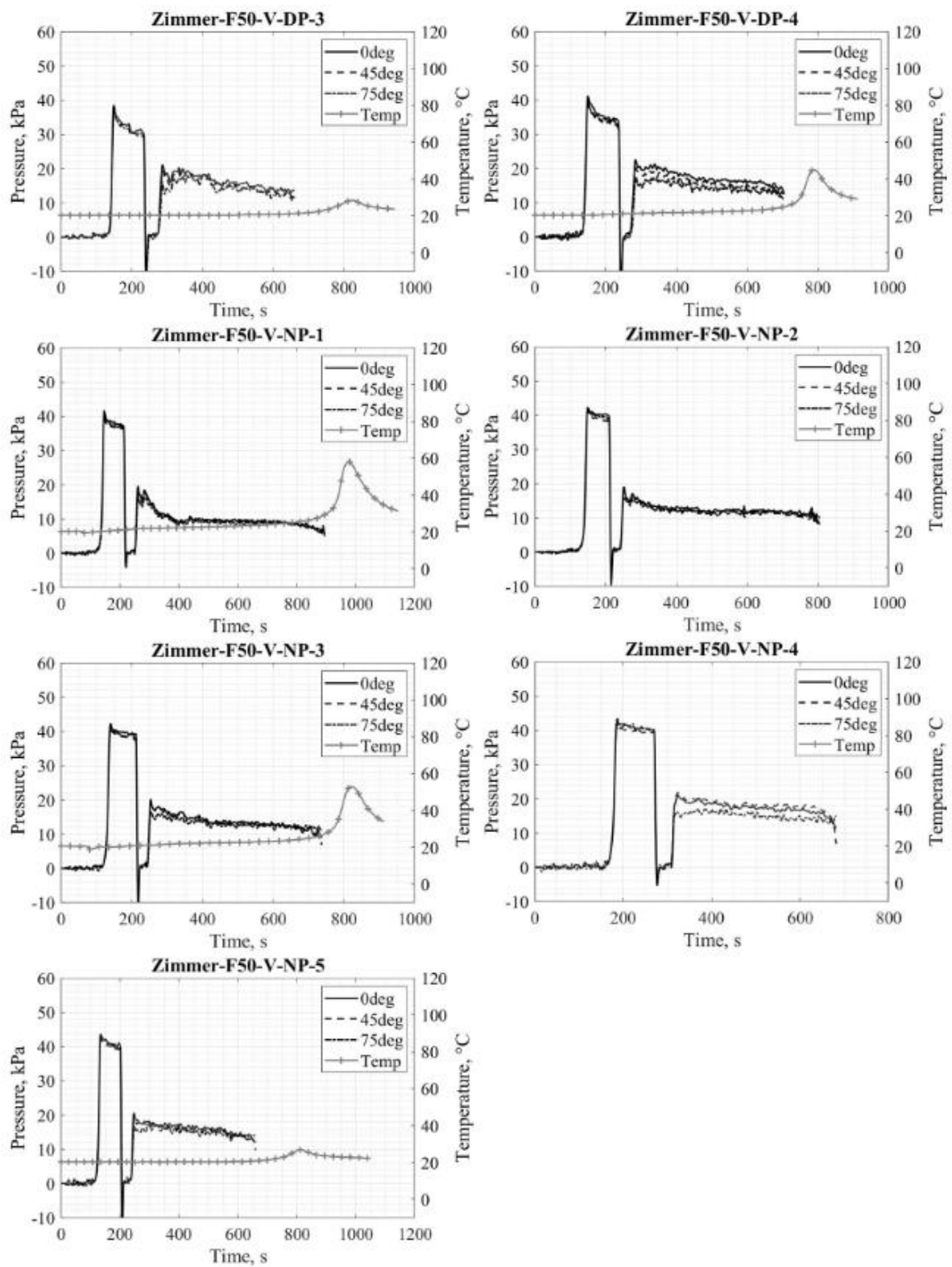
## Appendix I. Pressure and Temperature-Time Plots for Each of the Mock Implantation Experiments

Code: Z = Zimmer, CMW = CMW 2 Bone Cement, F50 = 50mm diameter flanged acetabular cup, UF50 = 50mm diameter unflanged acetabular cup, V = Vacuum mixed cement, NV = Non-vacuum mixed cement, DP = Depuy pressuriser, NP = Novel pressuriser and the number refers to the number of the sample.









#### Appendix J – Copyright Statements

National Joint Registry Annual Report: Figures 1.4 - Data available for public use.